

IAEA-TECDOC-221

# **CURRENT STATUS OF NEUTRON SPECTRUM UNFOLDING**

PROCEEDINGS OF A  
TECHNICAL COMMITTEE MEETING ON  
CURRENT STATUS OF NEUTRON SPECTRUM UNFOLDING  
ORGANIZED BY THE  
INTERNATIONAL ATOMIC ENERGY AGENCY  
HELD IN OAK RIDGE, 10-12 OCTOBER 1977



A TECHNICAL DOCUMENT ISSUED BY THE  
INTERNATIONAL ATOMIC ENERGY AGENCY, VIENNA, 1979

CURRENT STATUS OF NEUTRON SPECTRUM UNFOLDING  
IAEA, VIENNA, 1979

Printed by the IAEA in Austria  
August 1979

**PLEASE BE AWARE THAT  
ALL OF THE MISSING PAGES IN THIS DOCUMENT  
WERE ORIGINALLY BLANK**

The IAEA does not maintain stocks of reports in this series. However, microfiche copies of these reports can be obtained from

**INIS Microfiche Clearinghouse**  
International Atomic Energy Agency  
Kärntner Ring 11  
P.O. Box 590  
A-1011 Vienna, Austria

on prepayment of US \$1.00 or against one IAEA microfiche service coupon.

## FOREWORD

According to the recommendation of the International Working Group on Reactor Radiation Measurements (IWGRRM) and within the frame of the IAEA programme on standardization of reactor radiation measurements, the technical committee meeting on "Current Status of Neutron Spectrum Unfolding" was held by the IAEA. The meeting took place at Oak Ridge, Tennessee, USA, from 10 to 12 October 1977, hosted by the Oak Ridge National Laboratory, with Betty F. Maskewitz, Radiation Shielding Information Center, as general chairman and F. B. K. Kam, Operations Division, as technical programme chairman. The meeting was attended by 27 participants from 5 countries.

The development of the multiple foil neutron activation technique has allowed detailed spectrum information to be obtained for the whole energy range important for reactor technology. The importance of accurate and well-documented unfolding procedures is widely recognized. The overall objective of the meeting was to permit a number of experts to discuss recent advances in the field of neutron spectrum unfolding, and then to summarize the current state-of-the-art in the form of recommendations for use by researchers and to the Agency's future programme in the field.

The participants considered and discussed the following aspects:

- Cross-section data libraries; quality and availability
- Methods for evaluation of computed spectra
- Selection of suitable foil sets

The proceedings included 14 papers submitted and discussed at the meeting in Oak Ridge, summary of this meeting, conclusions having been proposed by the participants. It is hoped that these proceedings will not only be a useful reference, but will also serve as a point for more advanced work in the field.

The Agency wishes to express its appreciation to the authors of papers, to the authorities in the host country who helped to arrange the meeting.

V. V. Chernyshev  
Scientific Secretary  
of the IWGRRM

## CONTENTS

Comparison of neutron spectrum unfolding codes .....	1
W.L. Zijp, J.H. Board, H.J. Nolthenius	
Review of unfolding methods used in the U.S. and their standardization for dosimetry .....	29
C.A. Oster	
Cross section library DOSCROSS-77 (in the SAND-II format) .....	45
H.J. Nolthenius, W.L. Zijp, N.J.C.M. van der Borg	
Shielding effect of foil covers .....	133
W.L. Zijp, H.J. Nolthenius, N.J.C.M. van der Borg	
Spectrum unfolding in the high neutron energy range; comparison of detector sets and unfolding procedures .....	139
L.J.M. Kuijpers	
The modifying factor in unfolding .....	151
W.L. Zijp, H.C. Rieffle	
The certainty parameter in unfolding .....	161
W.L. Zijp, H.C. Rieffle	
Errors in damage function analysis .....	167
E.R. Burrus	
The quadruple technique .....	169
W.L. Zijp, H.J. Nolthenius, N.J.C.M. van der Borg	
Window function and bounds in multiple foil dosimetry .....	179
F.M. Stallmann, F.B.K. Kam	
Application des methodes de la programmation lineaire au depouillement des resultats de mesures par activation .....	183
J. Dorlet	
Spectrum unfolding by the least square method .....	195
F.G. Perey	
Progress report on the IAEA activity on neutron spectra unfolding by activation technique .....	237
C. Ertek, B. Cross, M. Vlasov	
Preparation of cross section files and corrections in neutron spectrum unfolding .....	259
M. Matzke	
Summary and Conclusions .....	269
List of Participants .....	275

PAPERS PRESENTED

# COMPARISON OF NEUTRON SPECTRUM UNFOLDING CODES

W.L. Zijp, J.H. Board, H.J. Nolthenius  
Netherlands Energy Research Foundation ECN  
Petten, Netherlands

## Abstract:

This report presents results obtained in a comparison of three promising neutron spectrum unfolding procedures based on the CRYSTAL BALL, RFSP-JÜL and SAND-II computer programs.

The calculations have been performed for three neutron spectra i.e. CFRMF, ΣΣ and STEK.

Two cross section data sets were considered based on a recent SAND-II library and the ENDF/B-IV dosimetry file.

The codes give comparable results when good input spectrum information is given. When in particular energy regions (e.g. between 1 keV and 1 MeV) there is no or poor detector response, then the three codes give there different output spectra.

RFSP-JÜL modifies the input spectrum only in those regions where there is appreciable detector response. CRYSTAL BALL and SAND-II extend the modifications also to regions with no or little response. The smoothest modification curve is obtained with CRYSTAL BALL.

## 1. INTRODUCTION

At present three computer programs (CRYSTAL BALL, RFSP-JÜL and SAND-II) seem to be most promising for the determination of neutron flux density spectra, starting from experimental reaction rates in irradiated activation and fission detectors.

In principle one has a set of equations of the following type:

$$\alpha_i = \int_0^{\infty} \sigma_i(E) \cdot \phi_E(E) \cdot dE \quad (\text{for } i=1 \dots n)$$

where:

$\alpha_i$  = the experimentally obtained reaction rate per target nucleus  
(for an activation detector this corresponds to the saturation activity) per target nucleus;

$\sigma_i(E)$  = the energy dependent activation cross section;

$\phi_E(E)$  = the flux density per unit energy interval;

$n$  = the number of detection reaction.



The unfolding programs studied have a number of energy groups larger than the number of detectors. They require à priori knowledge in the form of an input spectrum, which represents the available neutron spectrum information from physics experiments or reactor physics calculations.

The approaches and algorithms of the three unfolding programs have been reviewed elsewhere |1|.

This report describes results of an intercomparison of the three programs mentioned in selected illustrative examples. The investigation comprised:

- three unfolding codes: CRYSTAL BALL |2|, RFSP-JÛL |3| and SAND-II (|4| and |5|);
- three fast neutron flux density spectra, from the facilities CFRMF at Idaho |6|, ΣΣ at Mol |7| and STEK at Petten |8|;
- two cross section libraries, a recent SAND-II library (denoted here as SAND/L) |9| and the ENDF/B-IV dosimetry file |10|.

The input activities and the input spectra were taken from literature |11| and |12|.

Preliminary results obtained for this intercomparison were presented in two progress reports |13| and |14|. A shortened version of |13| is given in |15|.

This report presents the summary of the previous results (|13|, |14|, |15|) together with some new information.

The intercomparison was performed in such a way that as much as possible the same input data were applied for the three codes.

The computer programs which have been used for the calculations were in most cases somewhat modified without influencing the actual spectrum calculation algorithm.

The modification referred mainly to the output procedures and to the calculation of the improvement ratio |16|.

The SAND-II program was extended with a procedure which calculates an estimate of the uncertainty for each of the 620 group flux density values of the solution spectra.

This procedure is based on the Monte Carlo procedure described by Oster et al. |17|. While Oster performs the Monte Carlo procedure on the calculated activities using the output spectrum, the procedure followed in this study is to modify the input activities using the input spectrum for each Monte Carlo run. This SAND-II extension can also take into account modifications in cross section values and in input spectrum.

## 2. SPECTRUM CALCULATIONS

### 2.1. Role of input data

With the activity values presented in table 1 and the convergence criteria given in table 2, solution spectra were calculated.

The calculations were performed with cross section values obtained from either an updated SAND-II library (coded SAND/L) or the ENDF/B-IV dosimetry file.

During the calculations it turned out that in some cases the calculated activity values deviated too much from the experimental input activities. The activity values which were deleted and the reason for this deletion are indicated in table 1. It will be clear that sometimes more than one reason holds for deletion.

The shapes of the three neutron spectra are visible in figure 1. The mid line gives the SAND-II solution and the two outer lines are plotted at distances of two standard deviations from the SAND-II solutions.

The plots at the left are obtained with variations of the input activities. The variation of these activity values was based on the experimental measurement error (table 1).

The plots at the right are obtained with variations of activity values as well as of the cross section values.

The solution spectra were calculated with the updated SAND-II library (SAND/L). The influence of the cross section library on the solution is related to the responses for the applied reactions.

The responses for the three neutron spectra and the two cross section libraries are shown in figure 2. Comparison of the corresponding responses shows that there is a clear difference in these two libraries.

The consequence of these different responses for the CFRMF using the three programs and the two libraries are shown in figure 3. In this figure the ratios of output and input are presented. These results show that the ENDF/B-IV dosimetry file gives an important correction at about 130 eV in the solution spectra, and that the SAND/L file gives a more pronounced contribution at about 10 MeV.

### 2.2. Ratio of output and input spectra

The right part of figure 3 and the plots of figure 4 show the ratios of solution spectra (i.e. accepted output spectra) and input spectra.

These solution spectra are calculated with aid of the data from the ENDF/B-IV dosimetry file. From these plots the following observations can be made:

- The modification which have to be made in the input spectrum to obtain the solution are the smallest for the CFRMF while the STEK spectrum needs the largest corrections. This may be due to a less correct input spectrum at the low energy side where we had to perform some extrapolations.

An indication therefore is the difference in response for the CFRMF compared with the responses of the  $\Sigma\Sigma$  and the STEK (fig. 2);

- The modifications by CRYSTAL BALL are rather smooth;
- The modifications by RFSP-JÜL show sharp peaks which also may be related to the coarse group structure;
- The modifications by SAND-II show in most cases sharp peaks in the resonance region;
- In most cases the modifications obtained with all three programs have the same overall shape but the smoothness of the solution is different;
- In the regions with a relative small detector response (10 keV - 0.5 MeV) some important deviations are visible (fig. 2 and fig. 4).

### 2.3. The improvement ratio

Plots for the improvement ratios of the three programs and the three spectra are presented in figure 5 and 6. These figures show that the CRYSTAL BALL and the SAND-II improvement ratio curves have some structure.

The structure in the CRYSTAL BALL results is probably due to a rounding procedure during data transfer (allowing too few digits) while the structure in the SAND-II data reflects some response peaks.

Both SAND-II and CRYSTAL BALL improvement ratio curves show low values for the energy regions between about  $10^{-2}$  and 1 MeV.

The program SAND-II and CRYSTAL BALL give clearly values smaller than 1. In general the best improvement ratio curve is obtained with the program CRYSTAL BALL. Both with respect to the neutron spectra of the CFRMF and the  $\Sigma\Sigma$  one can observe that the program RFSP-JÜL gives clearly better improvement in the energy region between  $10^{-2}$  and 1 MeV than the two other programs.

## 3. THE ROLE OF CONVERGENCE

### 3.1. Convergence criteria

The three unfolding codes have different methods to check whether the spectrum results after an iteration step fulfil the required agreement with the input data.

In the program CRYSTAL BALL the iteration procedure is ended if the "aver-

age relative deviation" is smaller than a specified number. This average relative deviation (ARD) is defined by the relation:

$$ARD = \left( \frac{1}{n} \sum_{i=1}^n \left( \frac{A_i^m - A_i^c}{s_i^m} \right)^2 \right)^{\frac{1}{2}}$$

with:

- n = number of input activity values;
- $A_i^m$  = measured activity (input value);
- $A_i^c$  = calculated activity at the last iteration step;
- $s_i^m$  = estimated uncertainty of the input activity.

If the input values for  $s_i^m$  have the correct size, then a value of 1 for the ARD looks reasonable. In this case the average deviation of measured and calculated activity will be equal to the uncertainty in the input activity values.

In the program RFSP-JUL the iteration procedure is ended, if the "mean activity error limit" (ERRE) is smaller than a given number.

This ERRE value is defined by the relation:

$$ERRE = \frac{1}{n} \sum_{i=1}^n \left| \frac{A_i^c - A_i^m}{A_i^m} \right|$$

It will be clear that in this case the choice of ERRE is somewhat difficult, but a value equal to the average of the estimated uncertainties of the input activities seems reasonable.

In the program SAND-II the iteration procedure is ended if the "deviation" parameter is smaller than a given number. This deviation (DEV) is defined by the relation:

$$DEV = S = \left[ \frac{1}{(n-1)} \sum_{i=1}^n \left\{ \left( \frac{A_i^m}{A_i^c} \right) - 1 \right\}^2 \right]^{\frac{1}{2}}$$

A suitable choice for the value of DEV can be obtained for instance as the average of the estimated uncertainties of the input activities.

The three convergence criteria of the programs have no simple relationships. For a very large number of detectors one has the asymptotic relation:

$$DEV = 0.8431 ERRE$$

To facilitate a comparison the DEV values (as used in the SAND-II program) were also calculated for the CRYSTAL BALL and the RFSP-JUL solutions.

### 3.2. The convergence parameter in CRYSTAL BALL

Several runs have been performed with CRYSTAL BALL to calculate the neutron spectrum of the STEK-4000 facility. The input activities (for 15 reactions) and the best available information for the input spectrum were the same as for the other runs.

In these calculations a SAND-II cross section library modified for neutron selfshielding was applied. The errors in the activities which had to be specified, were chosen equal to 4% for all activities.

The  $\gamma_0$  and decrement and increment factors which are input parameters for the convergence, were chosen in such a way that the number of iterations (k) became  $>$ ; the maximum number of iterations in this series was 6. The S and ARD values and the number of iterations obtained and the ratios of output and input spectra are shown in figure 7. From these plots the influence of the choice of the convergence criterium can be seen.

A high value for ARD gives small modifications, while a low value gives appreciable corrections and often a smooth structure in the solution spectrum.

If the uncertainties in the activity values are given correctly and not arbitrarily as in these calculations, then the value 1 for the ARD will give a good solution, from the point of view of counting errors.

In figure 7c the normalized ratio of the output spectra which are obtained with ARD=1.08 and 0.926 is presented. The normalization in this plot is based on 10 values at the low energy side of the spectrum. This plot shows that the ARD=1 value has to be reached rather accurately to obtain a well defined solution. The deviation of the output spectra which are obtained for these two ARD values has a maximum of roughly 10% in these runs.

### 3.3. The speed of convergence

The speed of convergence of CRYSTAL BALL and RFSP-JÜL can be influenced by the experimenter, while the speed of convergence of the SAND-II is always fixed.

An advantage of the adjustment of the speed of convergence is that the convergence criterium can be reached in a reasonable number of iterations. The CRYSTAL BALL and RFSP-JÜL code however can both yield rather easily "too good" output spectra.

The qualification "too good" refers to those spectra for which the S-value is appreciably smaller than the value of the deviation parameter specified in the input.

If in that case the speed of convergence is decreased, a more realistic S-value can be obtained.

In practice often more iteration steps are required to reach the solution with the decreased speed of convergence.

The number of iterations is of interest since it is directly related to the computer time required to finish a job. This holds especially for CRYSTAL BALL.

For these reasons one should try to make an appropriate choice of the speed of convergence. The speed of convergence is adjusted with the parameter  $\gamma_0$  in CRYSTAL BALL, and with the parameter  $\omega$  in RFSP-JÜL.

When the parameters  $\omega$  and  $\gamma_0$  are decreasing, the convergence speed will in general increase.

The actual value of  $\gamma_0$  in CRYSTAL BALL is also determined by the "DECREMENT" and "INCREMENT" factors to be specified in the input information. The first factor prescribes the maximum change of the  $\gamma_0$  value in each iteration step (after the first step, which is a spectrum normalization step).

The second factor corrects the  $\gamma_0$ , if a negative flux density value in the output spectrum is detected; a new output spectrum without negative values is then calculated for the  $\gamma_0$  value multiplied with the increment factor.

#### 3.4. The convergence speed for RFSP-JÜL

The RFSP program was used with a 50 group structure. The input spectrum made by SAND-II (620 groups) was converted to this 50 groups structure. The other input data for the STEK were the same as mentioned previously. The uncertainties in the activities were 1% for these calculations.

In the calculations various values of  $\omega$  were applied.

The results for the improvement ratio and spectrum ratio are shown in figure 8.

The number of iterations varied from 1 to 21 in this series of calculations.

The results show that the improvement ratio and the flux density ratio are rather independent of the  $\omega$  value. For the smallest  $\omega$  value, however, we observed a lower improvement ratio, while the general shape of the flux density ratio curve remains unchanged. The reason for the change of the improvement ratio for low values of  $\omega$  is not yet known.

#### 4. PERFORMANCE FOR 2 OR 3 REACTIONS

Several calculations have been performed with a rather small set of input activities. The neutron spectrum for the STEK-4000 facility is calculated with the three programs of interest.

The activity errors needed in CRYSTAL BALL and RFSP-JÜL were chosen as 4% and 1% respectively. Runs with two and three input activities were done. These series of runs were aimed to obtain some characteristics of the programs for simple input activity sets.

The results for these calculations are presented in figure 9 and 10.

##### 4.1. Two reactions

The results for activities of the reaction  $^{58}\text{Ni}(n,p)$  and  $^{59}\text{Co}(n,\gamma)$  are given in figure 9.

The improvement ratios obtained with the different programs show different shapes. The programs CRYSTAL BALL and SAND-II have both improvement ratios which in some energy regions become smaller than 1.

These small values are obtained for energies smaller than  $10^{-7}$  MeV and in the region from  $10^{-2}$  to 1 MeV.

The improvement ratio for RFSP-JÜL is small and in most energy regions equal to 1.

A value somewhat larger than one is obtained at the resonance energy of  $^{59}\text{Co}(n,\gamma)$  at  $0.132 \times 10^{-3}$  MeV and in the response region of the  $^{58}\text{Co}(n,p)$  reaction (e.g. above 0.920 MeV).

The influence of the sharp resonances of  $^{59}\text{Co}(n,\gamma)$  can also be seen in the improvement ratios calculated with the programs CRYSTAL BALL and SAND-II.

A comparison of the flux density ratios obtained in figure 9 shows the difference in modifying properties of the three programs. In fig. 9 the most important response is obtained at the resonance of  $^{59}\text{Co}(n,\gamma)^{60}\text{Co}$  and above about 1 MeV. Between these energy values the response is rather small.

In the flux density ratios these points are clearly visible in the CRYSTAL BALL and RFSP-JÜL flux density ratio plots.

The type of modification of the input is different for the three programs.

##### CRYSTAL BALL:

The modification between the points with clear detector response is a smooth function and in this case more or less linear. The  $\text{Co}(n,\gamma)$  resonances at higher energies seem to have no influence ( $10^{-3}$  to  $10^{-2}$  MeV). Below and above these energy values the modification remains constant.

#### RFSP-JÜL:

The modifications are only present at the energy values where detector response is available.

Furthermore the modification seems to be proportional with the detector response; e.g. in the energy regions where only information from one detector is present energy dependent modifications are performed.

In the energy regions with rather small detector response no modifications are found (neglecting the normalization).

#### SAND-II:

The modifications in the spectrum are for this case a step function. The step is found at the threshold energy of the fast reaction.

The magnitude of the overall modification difference between the points with important detector response is the highest for RFSP-JÜL and the smallest for CRYSTAL BALL.

This effect is probably due to the influence of the spectrum modifications which may be performed in the energy regions with small response.

#### 4.2. Three reactions

The results obtained for three activity values in the input of the program are presented in figure 10.

The input activities were chosen in such a way that two reactions with intermediate response were used i.e.  $^{59}\text{Co}(n,\gamma)$  and  $^{235}\text{U}(n,f)$  and one reaction with a fast response.

The main resonance of  $^{59}\text{Co}(n,\gamma)$  has an energy of  $1.32 \times 10^{-4}$  MeV and the resonances with the highest cross section of  $^{235}\text{U}$  are found between  $10^{-5}$  and  $10^{-4}$  MeV.

The improvement ratios presented in figure 10 have the same general shape as these ratios obtained for two activity values.

Remarkable are the low improvement ratios obtained with RFSP-JÜL.

Especially the improvement ratio of the SAND-II shows clearly the contribution of the two activities i.e. a sharp peak due to the main resonance of  $^{59}\text{Co}(n,\gamma)$ .

The flux density ratios shown in figure 10 show the same characteristics as the corresponding results for two activity values.

The correction in the region between the points with large responses is in this case not strictly linear in the results of CRYSTAL BALL.

It can also be seen that the resonance of  $^{59}\text{Co}(n,\gamma)$  at  $1.32 \times 10^{-4}$  MeV determines the sharp change in modification, while the resonance region of  $^{235}\text{U}$  seems less important in this case.



The solution of SAND-II shows a peculiar effect; some valleys are present in the flux density ratio. The energy values corresponding with these valleys are the same as the resonance energies of  $^{59}\text{Co}(n,\gamma)$ . The valleys are nearly equally deep, while the cross section value accompanying the higher resonances are about a factor 100 and 1000 lower than those of the main resonance.

This effect can be explained by looking at the definition of the modifying factor  $M$ , in which the fractional response of reaction  $i$  in group  $j$  plays an important role. The algorithm shows that for each energy group the modification factor for reaction  $i$  is not dependent on its group cross section value, but on the normalized local response as fraction of the summed normalized responses in that group due to all reactions.

#### 4.3. Smoothing in SAND-II

The results for three foils for the SAND-II program (Fig. 10) indicate that smoothing may be necessary. For this reason some runs have been done with the same input data but with the use of the smoothing procedure of the SAND-II program.

The results are presented in figure 11. These results show that the small structure which is present in the results of fig. 10 disappears rather fast.

The strong peaks of  $^{60}\text{Co}$  become more pronounced and wider.

In general the solutions seem to become worse when stronger smoothing is applied. The smoothing procedure removes small fluctuations, but broadens pronounced hills and valleys.

### 5. DISCUSSION

#### 5.1. Input data for unfolding

From the results for the responses of the detector sets (fig. 2) it follows that the lower and the higher energy regions of the neutron spectra show the largest responses.

For two spectra (i.e.  $\Sigma\Sigma$  and STEK) no calculation results were available for the low energy side of the input spectra. For this reason extrapolation procedures had to be performed which may have introduced some errors. When in the extrapolation region large errors in the relatively small flux densities are made, while the cross section there are relatively large, then one may expect unjustified spectrum modification in the other energy regions.

The experimentally determined reaction rates which have been kept for the unfolding are in general accurate enough. This can be seen in the results of the Monte Carlo calculations (fig. 1).

Of course this does not hold for the reactions which had to be deleted in the unfolding but in these cases it is not possible to judge whether the too large deviations are due to deviations in the activity and/or cross section values.

### 5.2. Cross section libraries

The responses of the detector sets, which are presented in figure 2 indicate that the SAND/L file and the ENDF/B-IV dosimetry file are not exactly the same.

Application of these 2 files yielded also differences of the solution spectra.(fig. 3).

In table 1 one may observe that in a few cases the cross section set from one library is used in the unfolding while the corresponding cross section set from the other library gives results which make it necessary to delete the reaction from the unfolding.

The influence of the error of the cross section data on the unfolding results is shown in figure 1. From these results for changes of activity and cross section data it follows that especially for the two softer neutron spectra relative important uncertainties due to the cross section values are introduced. The smallest uncertainty is found for the CFRMF.

### 5.3. Unfolding results

From the ratios of output and input spectra presented for the three spectra and the three unfolding codes in figure 3 and figure 4 it follows that the modifications of the input spectrum are the smallest for the CFRMF.

For the other two neutron spectra modifications of about a factor two are sometimes found for some regions of the spectra.

The magnitude of modification is strongly dependent on the convergence, which is applied in the calculations. This is shown in figure 7 for results obtained with CRYSTAL BALL, using different values for the ARD convergence parameter. Even a small change in the value of the ARD parameter, when this is about 1, can give changes in the output spectrum of about 10%.

At this moment there is no reason to assume that in this respect the other programs will behave in a different way.

In order to reach the convergence criterium in the appropriate way, it is convenient that the speed of convergence can be adapted. The results which were obtained with different speeds of convergence for the program RFSP-JÜL are shown in figure 8. From this figure it follows that the results are nearly the same for the different speeds.

It is assumed that CRYSTAL BALL will show comparable results. These three spectra show two regions with good detector response and between these two one region with poor detector response.

The characteristic modification pattern of the unfolding code is important in this energy region. This characteristic modification pattern is demonstrated in figures 9 and 10 for unfolding with two and three input activities respectively.

The characteristic pattern is shown between about  $10^{-3}$  and 1 MeV (between intermediate and fast response). The improvement ratios are also small for the programs (smaller than 1 for CRYSTAL BALL and SAND-II).

The modifications in this energy region for the final results given in figures 3 and 4 will mainly be determined by this characteristic modification pattern.

The difficulties for the unfolding codes in this energy region are also clearly shown in the improvement ratios (fig. 5 and 6). Low values between  $10^{-3}$  and 1 MeV for all programs but RFSP-JÜL seems to give somewhat better results compared with the other programs.

Figures 9 and 10 show also a peculiar property of RFSP-JÜL, i.e. it performs energy dependent spectrum modifications only in those regions where detector response is available. This peculiarity is related to the minimization of the least squares expression which includes a term with spectrum deviations.

The SAND-II solution for the  $\Sigma\Sigma$  and the STEK gives rather much structure (fig. 4). This effect can also be seen in the improvement ratios.

Some calculations were done with the smoothing procedure of SAND-II with the intention to decrease this structure. Some results of these calculations are presented in figure 11. From these results it follows that this smoothing procedure cannot successfully be applied to prevent this type of structure.

## 6. CONCLUSION

In this comparison it was found that the three unfolding programs give comparable results for the three spectra under consideration if the modifications are only small.

When appreciable changes have to be applied to the input spectrum, the three unfolding codes show different behaviour of the ratio between output and input spectrum in the energy region between about  $10^{-3}$  and 1 MeV, where normally the detectors give very poor response.

RFSP-JÜL shows localized spectrum changes in energy regions with appreciable response, but negligible changes in energy regions with no or poor response.

The programs CRYSTAL BALL and SAND-II extend the modifications also to regions with no or little response. The smoothest modification curve is obtained with CRYSTAL BALL.

The improvement ratio is a means to indicate the energy regions with a bad modification. The main problem at this moment and for this type of spectra seems to be the lack of response in the energy region between  $10^{-3}$  and 1 MeV and the small number of detectors which can be used in the other energy regions.

The inconsistencies due to cross section uncertainties and activity inaccuracies as well as input spectrum problems are at this moment the limiting factor to obtain better results.

## 7. REFERENCES

- |1| Zijp, W.L.: "Review of activation methods for the determination of neutron flux density spectra"  
Report RCN-241 (Reactor Centrum Nederland, Petten, 1976); See also Proc. 1st ASTM-Euratom Symposium on Reactor Dosimetry, held at Petten, 22-26 September 1975. Report EUR 5667 e/f, Part I, p.233-299 (C.E.C., Luxembourg, 1977).
  
- |2| Kam, F.B.K.; Stallmann, F.W.: "CRYSTAL BALL - A computer program for determining neutron spectra from activation measurements"  
Report ORNL-TM-4601 (Oak Ridge National Laboratory, Tennessee, June 1974).
  
- |3a| Фишер А. и Тури Л., "RFSP: Программа для определения спектра нейтронов из активационных данных" КФКИ-71-22 (1971).
  
- |3b| Fischer, A.; Turi, L.: "The RFSP programme for unfolding neutron spectra from activation data"  
INDC(HUN)-8/u (IAEA, Vienna, 1972).
  
- |4| McElroy, W.N. et al.: "A computer automated iterative method for neutron flux spectra determination by foil activation"  
Vol I - IV. Report AFWL-TR-67-41 (1967).

- |5| Berg, S.: "Modifications of SAND-II"  
BNWL-855 (1968).
- |6| Rogers, J.W.; Millsap, D.A.; Harker, Y.D.: "CFRME neutron field  
flux spectral characterization"  
Nuclear Technology 25 (1975), p. 330.
- |7| Fabry, A.; De Leeuw, G.; De Leeuw, S.: "The secondary intermediate  
energy standard neutron field at the Mol  $\Sigma\Sigma$  facility"  
Nuclear Technology 25 (1975), p 349.
- |8| Bustraan, M. et al.: "STEK. The fast thermal coupled facility of  
RCN at Petten"  
RCN-122 (Reactor Centrum Nederland, Petten, 1970).
- |9| Eisenhauer, C.; Fabry, A.: "DETAN-74: Computer code for calculating  
detector responses in reactor neutron spectra"  
Private communication (October 1974).
- |10| Magurno, B.A.; Ozer, O.: "ENDF/B file for dosimetry applications"  
Nuclear Technology 25 (1975), p 376.
- |11| McElroy, W.N.; Kellogg, L.S.: "Fuels and materials fast reactor  
dosimetry data development and testing"  
Nuclear Technology 25 (1975), p 180.
- |12| Zijp, W.L., et al.: "Neutron spectra in the STEK facility determined  
with the SAND-II activation technique"  
RCN-232 (Reactor Centrum Nederland, Petten, September 1975).
- |13| Zijp, W.L.; Nolthenius, H.J.: "Comparison of neutron spectrum un-  
folding codes (First progress report, June 1976)"  
ECN-76-109 (E.C.N., Petten, August 1976).
- |14| Zijp, W.L., et al.: "Comparison of neutron spectrum unfolding codes  
(Second progress report)"  
ECN-76-135 (E.C.N., Petten, November 1976).
- |15| Zijp, W.L.; Nolthenius, H.J.: "Progress Report: Intercomparison of  
unfolding procedures (programs and libraries)"  
ORNL/RSIC-40 (page 223-234) (Radiation Shielding Information Centre,  
Oak Ridge, October 1976).

- [16] Fischer, A. et al.: "Comparison of SAND-II and RFSP-JUL spectrum unfolding codes for several neutron spectra of the STEK facility" RCN-245 (Reactor Centrum Nederland, Petten, April 1976).
- [17] Oster, C.A.; McElroy, W.N.; Marr, J.M.: " A Monte Carlo program for SAND-II error analysis" HEDL-TME-73-20 (Hanford Engineering Development Lab., Washington, 1974).

Table 1: Relative experimental saturation activities

reaction	neutron spectrum					
	CFRMF		SIGMA-SIGMA		STEK-4000	
$^{235}\text{U}(n,f)\text{FP}$	1.000	-	1.0	3.5%	1.000	2.9%
$^{239}\text{Pu}(n,f)\text{FP}$	1.145	1.5%	1.18	3.5%	-	-
$^{237}\text{Np}(n,f)\text{FP}$	0.354	2.3%	0.399	4.0%	-	-
$^{232}\text{Th}(n,f)\text{FP}$	-	-	0.0132	6 %	-	-
$^{238}\text{U}(n,f)\text{FP}$	0.0485	1.4%	0.0550	3.5%	0.0180	8.7%
$^{238}\text{U}(n,\gamma)^{239}\text{U}$	0.118	2.8% <sup>3)4)</sup>	0.122	5 %	0.370	2.1%
$^{23}\text{Na}(n,\gamma)^{24}\text{Na}$	-	-	-	-	0.00131	2.6% <sup>6)</sup>
$^{45}\text{Sc}(n,\gamma)^{46}\text{Sc}$	0.01507	2.3% <sup>1)6)</sup>	-	-	0.02396	2.2% <sup>1)2)</sup>
$^{55}\text{Mn}(n,\gamma)^{56}\text{Mn}$	-	-	0.0250	4.5% <sup>10)</sup>	0.0747	2.3% <sup>10)</sup>
$^{58}\text{Fe}(n,\gamma)^{59}\text{Fe}$	0.00393	2.1% <sup>3)</sup>	-	-	0.00775	3.6%
$^{59}\text{Co}(n,\gamma)^{60}\text{Co}$	0.0588	2.7% <sup>7)</sup>	-	-	0.255	2.1%
$^{63}\text{Cu}(n,\gamma)^{64}\text{Cu}$	0.0292	4.7% <sup>7)</sup>	0.0252	6 %	-	-
$^{115}\text{In}(n,\gamma)^{116}\text{In}^m$	0.181	2.9% <sup>6)</sup>	0.164	5 %	0.460	2.1% <sup>1)4)</sup>
$^{151}\text{Eu}(n,\gamma)^{152}\text{Eu}^{s+m}$	-	-	-	-	5.640	7.7% <sup>9)10)</sup>
$^{164}\text{Dy}(n,\gamma)^{165}\text{Dy}$	-	-	-	-	0.372	4.9% <sup>9)10)</sup>
$^{197}\text{Au}(n,\gamma)^{198}\text{Au}$	0.273	1.7%	0.278	3.5%	0.391	2.2% <sup>2)</sup>
$^{27}\text{Al}(n,p)^{27}\text{Mg}$	0.000561	2.4% <sup>3)</sup>	0.00065	10 %	-	-
$^{27}\text{Al}(n,\alpha)^{24}\text{Na}$	0.0001038	1.8% <sup>2)</sup>	0.000114	4.5%	0.0000156	4.4% <sup>3)4)</sup>
$^{46}\text{Ti}(n,p)^{46}\text{Sc}$	0.001675	2.4% <sup>2)</sup>	-	-	0.000505	13.7% <sup>2)</sup>
$^{47}\text{Ti}(n,p)^{47}\text{Sc}$	0.00268	4.2% <sup>1)4)</sup>	-	-	0.000910	2.2% <sup>4)</sup>
$^{48}\text{Ti}(n,p)^{48}\text{Sc}$	0.0000442	2.4% <sup>2)</sup>	-	-	0.0000105	2.6% <sup>2)</sup>
$^{54}\text{Fe}(n,p)^{54}\text{Mn}$	0.01120	1.7%	-	-	0.00377	2.6%
$^{56}\text{Fe}(n,p)^{56}\text{Mn}$	-	-	0.000172	5 %	0.0000402	2.8%
$^{58}\text{Ni}(n,p)^{58}\text{Co}$	0.01544	1.7% <sup>7)6)</sup>	0.0181	4 %	0.00503	2.2%
$^{115}\text{In}(n,n')^{115}\text{In}^m$	0.03194	4.6% <sup>7)6)</sup>	0.0369	3.5%	0.0122	2.3%

For SAND/L.	not applied activity values	For ENDF/B-IV
1)	Ratio $A_{exp}/A_{calc}$ at 0-th iteration too large	2)
3)	Ratio $A_{exp}/A_{calc}$ at 0-th iteration too small	4)
5)	Structure in solution spectrum	6)
7)	Standard deviation in activity value too large	8)
9)	Cross section data not available	10)

Table 2: Convergence criteria

parameter	unfolding program		
	CRYSTAL BALL**	RFSP	SAND-II
<u>for CFRMF:</u>			
relative deviation	1.1%	-	-
average deviation	-	3%	-
deviation	-	-	3%
max. number of iterations	10	10	10
number of Monte Carlo cases	-	-	40
number of $\alpha$ runs	10	10	10
number of iterations*:			
for SAND/L	2	1( $\omega=15$ )	1
for ENDF/B-IV	2	1( $\omega=15$ )	2
<u>for SIGMA-SIGMA:</u>			
relative deviation	1.0%	-	-
average deviation	-	3%	-
deviation	-	-	5%
max. number of iterations	10	10	10
number of Monte Carlo cases	-	-	40
number of $\alpha$ runs	10	10	10
number of iterations*:			
for SAND/L	3	2( $\omega=30$ )	3
for ENDF/B-IV	3	2( $\omega=30$ )	3
<u>for STEK-4000:</u>			
relative deviation	1.0%	-	-
average deviation	-	3%	-
deviation	-	-	4.5%
max. number of iterations	10	10	10
number of Monte Carlo cases	-	-	40
number of $\alpha$ runs	10	10	
number of iterations*:			
for SAND/L	3	2( $\omega=30$ )	2
for ENDF/B-IV	3	3( $\omega=30$ )	2

\* number of iterations required to obtain solution;

\*\* for all calculations:  $\gamma_0=100$ , increment factor 3 and decrement factor 0.3.

# VARIATIONS

In A

In A and  $\sigma$

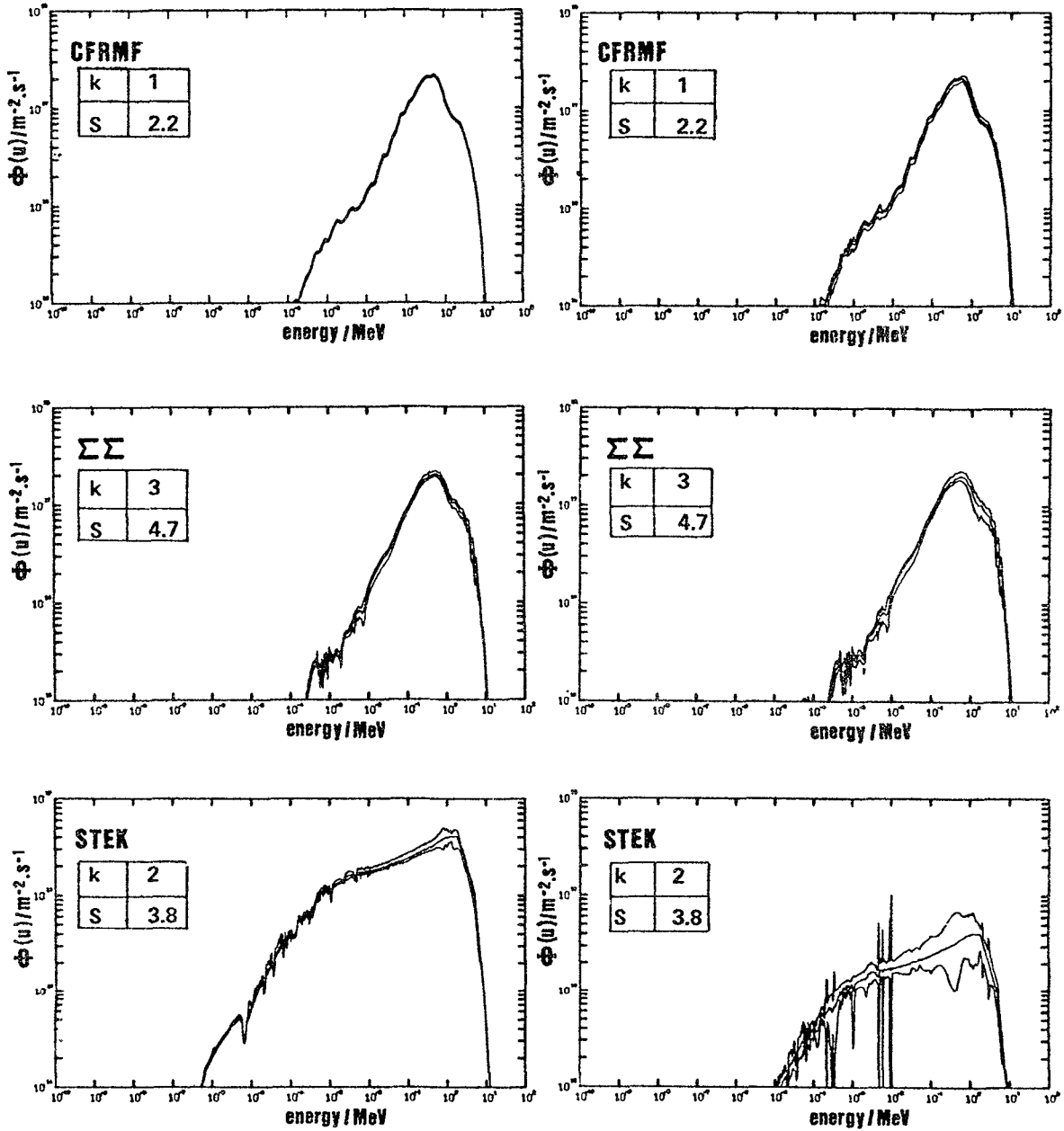


Fig. 1: SAND SPECTRA USING SAND/L



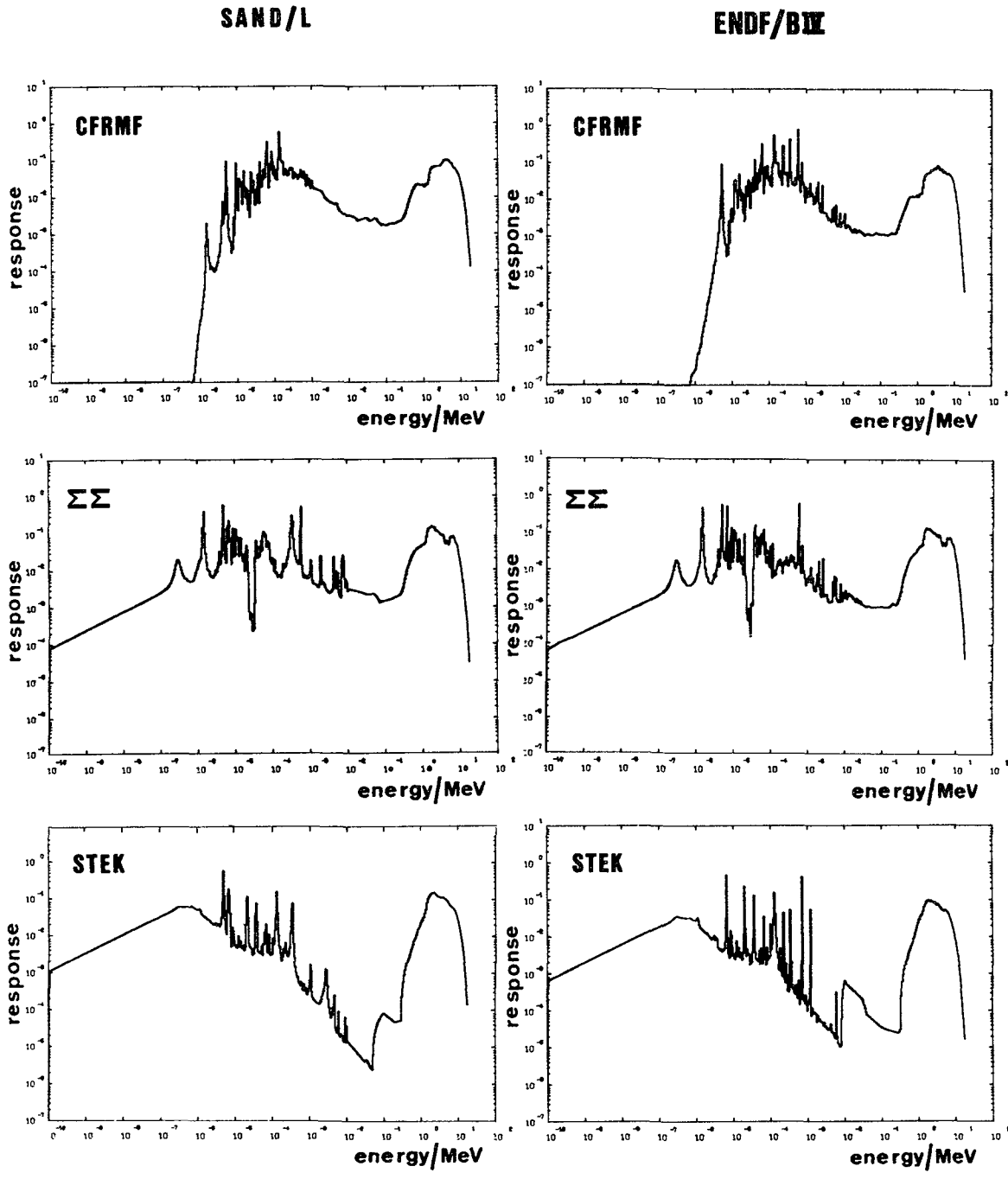


Fig. 2: DETECTOR SET RESPONSE

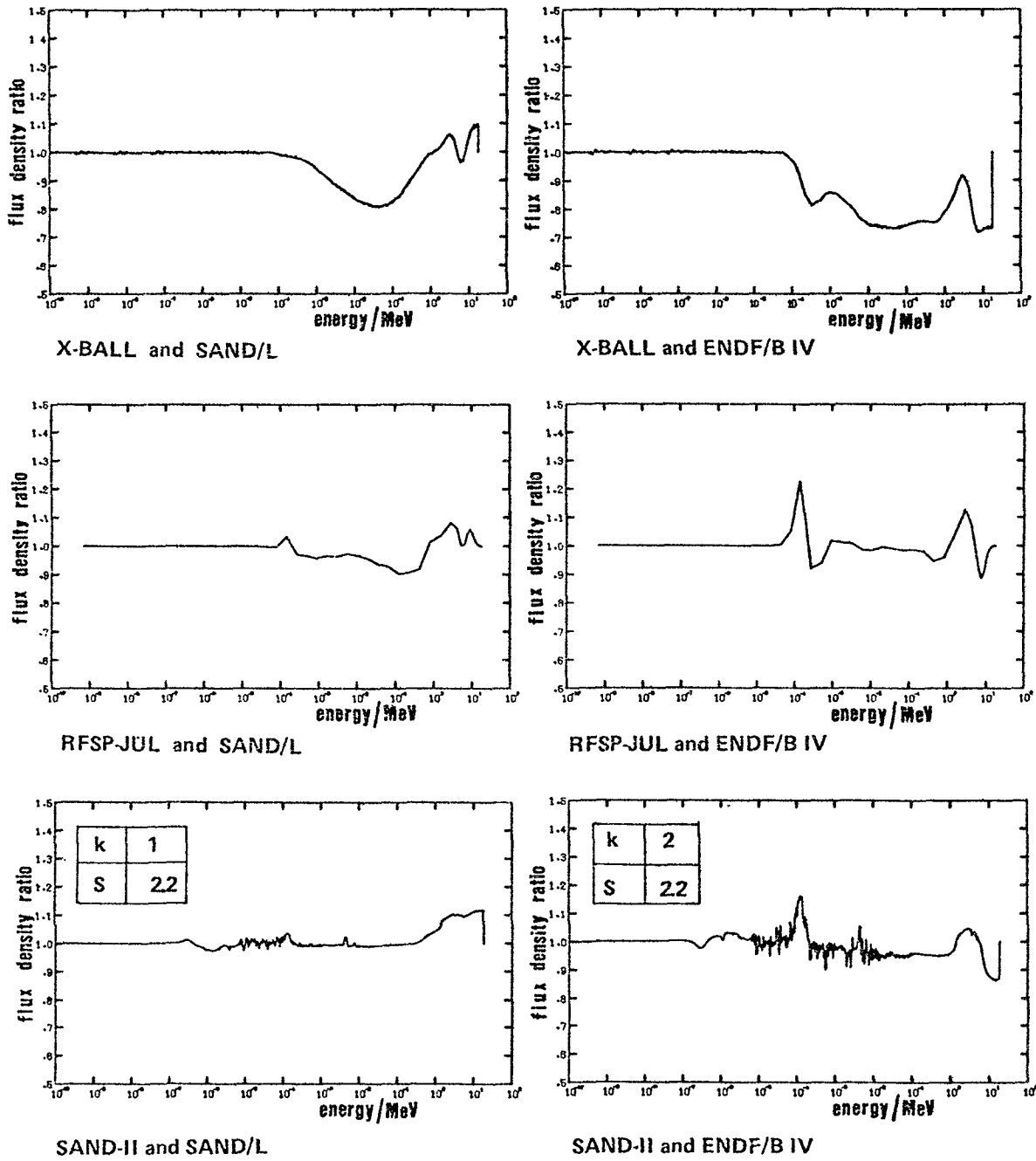
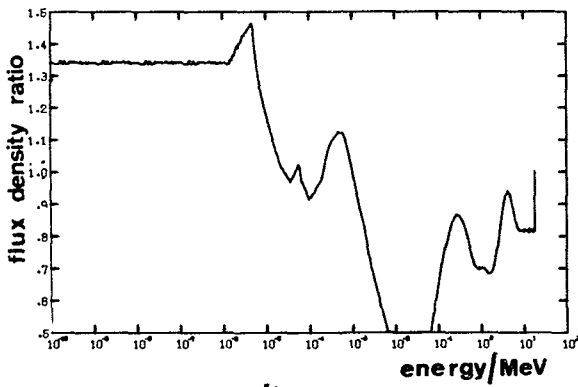
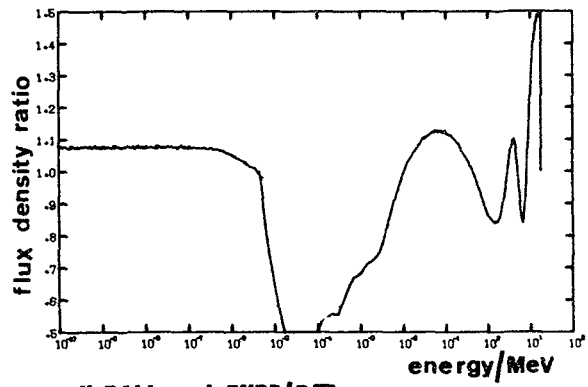


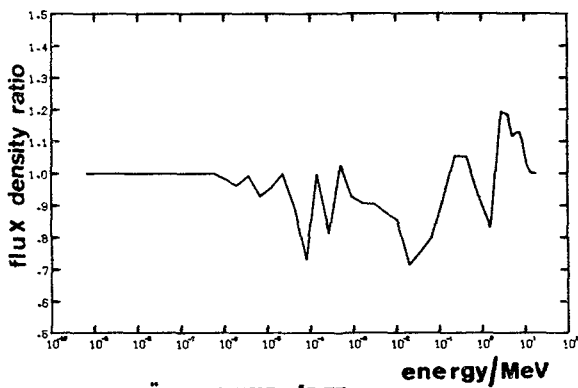
Fig. 3: RATIOS OF OUTPUT AND INPUT SPECTRA FOR THE CFRMF



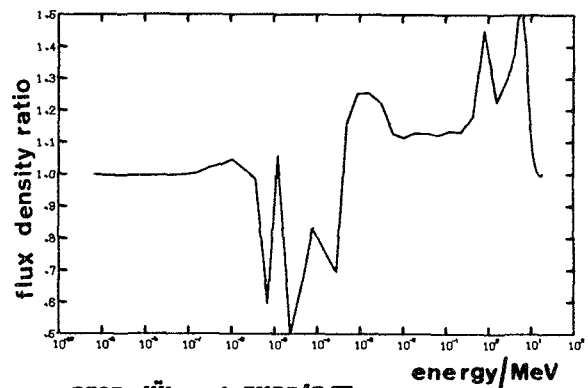
**X-BALL and ENDF/B IX**



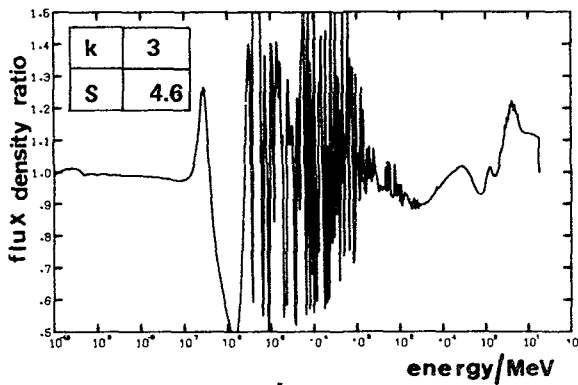
**X-BALL and ENDF/B IX**



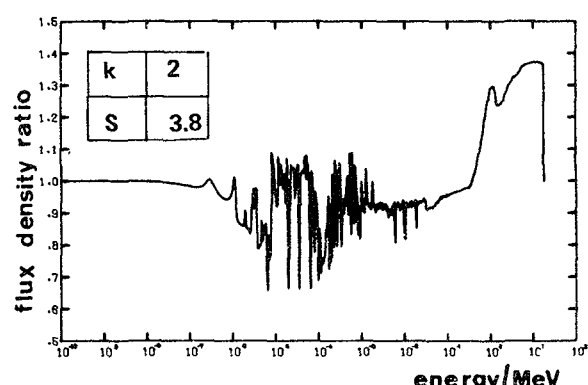
**RFSP-JÜL and ENDF/B IX**



**RFSP-JÜL and ENDF/B IX**



**SAND-II and ENDF/B IX**



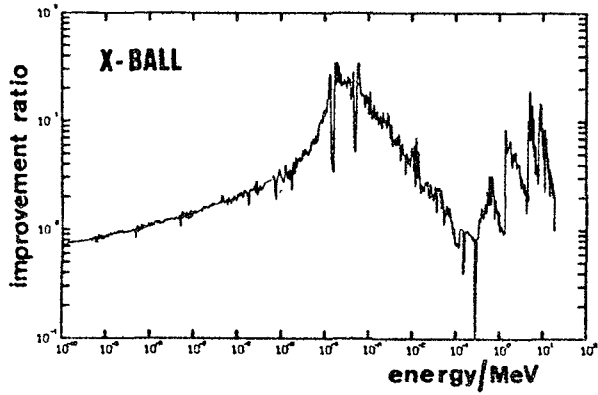
**SAND-II and ENDF/B IX**

**ΣΣ**

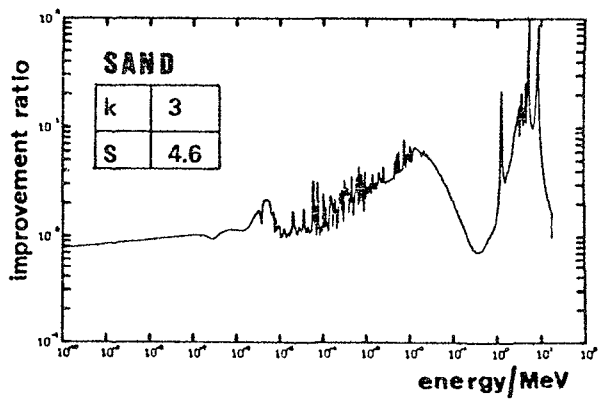
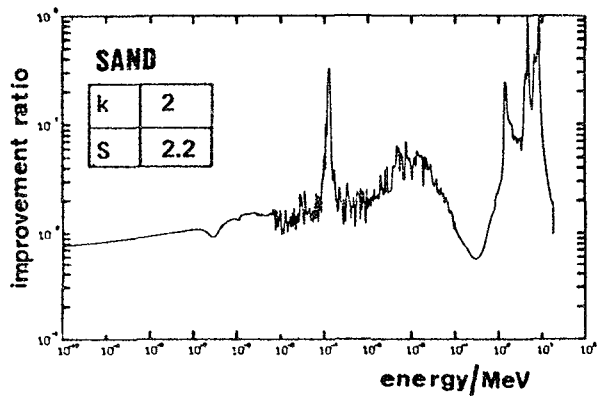
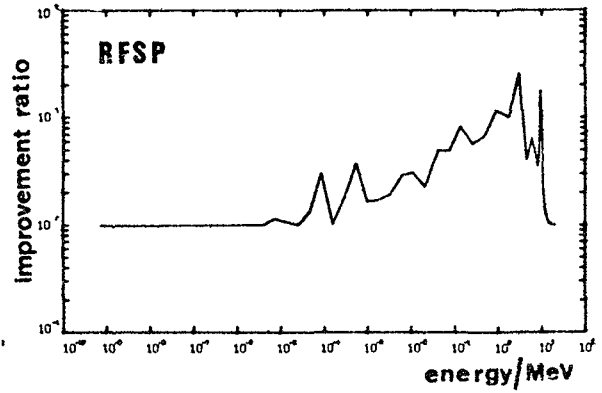
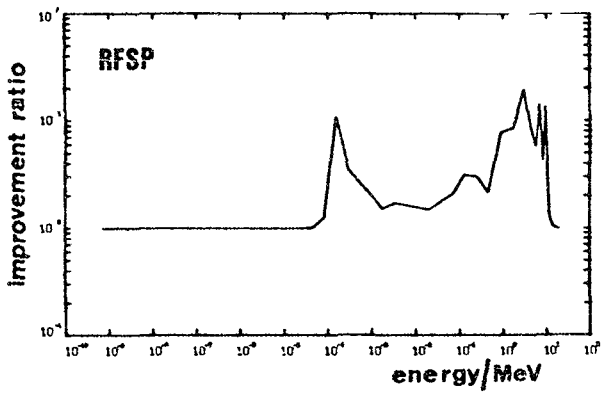
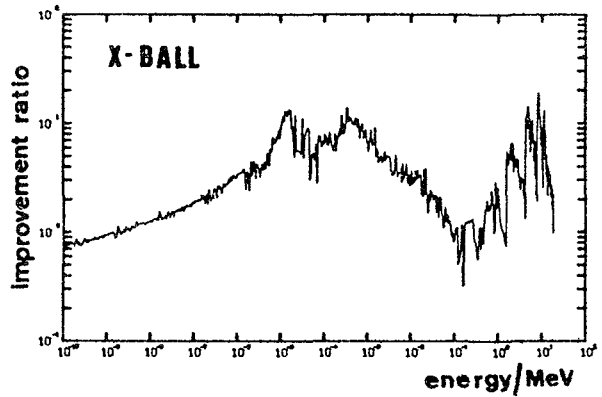
**STEK-4000**

**Fig. 4: RATIO OF OUTPUT AND INPUT SPECTRA**

ENDF/B IV



ENDF/B IV

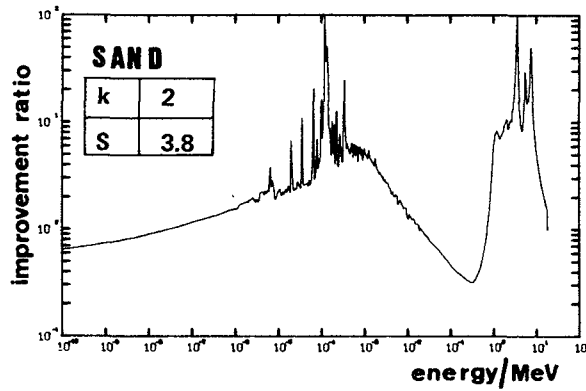
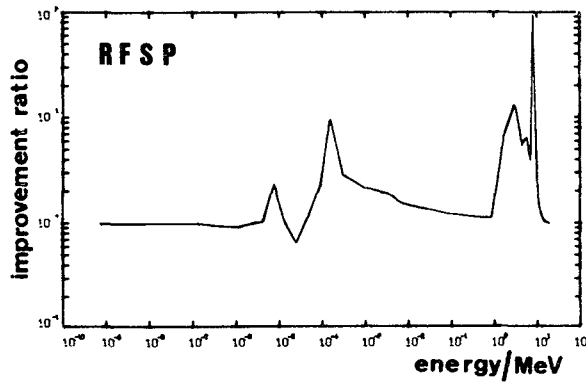
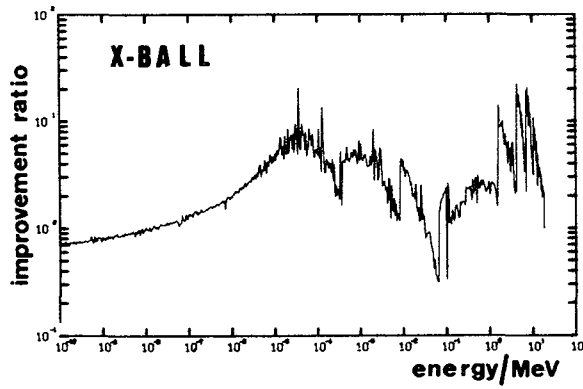


CFRME

ΣΣ

Fig. 5: IMPROVEMENT RATIOS

# ENDF/BIV



# STEK-4000

Fig. 6: IMPROVEMENT RATIOS

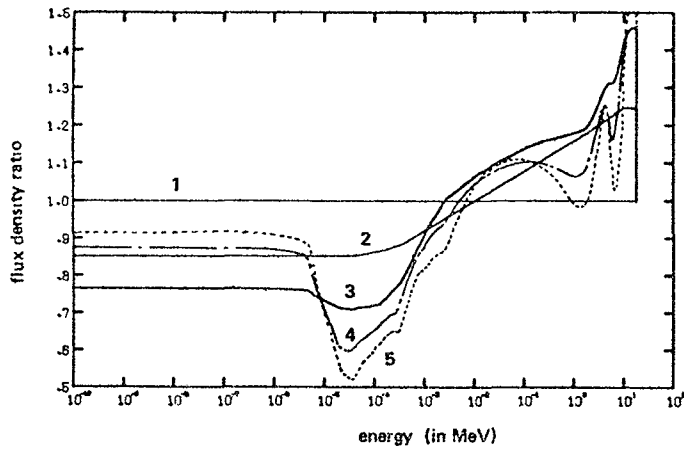


Fig. 7a. Ratio of output and input spectrum.

plot	1*	2	3	4	5
k	1	3	3	2	2
ARD	5.7	2.4	1.0	0.71	0.47
S( $\omega$ )	25.5	10.0	4.2	2.9	1.9

\* No modifications

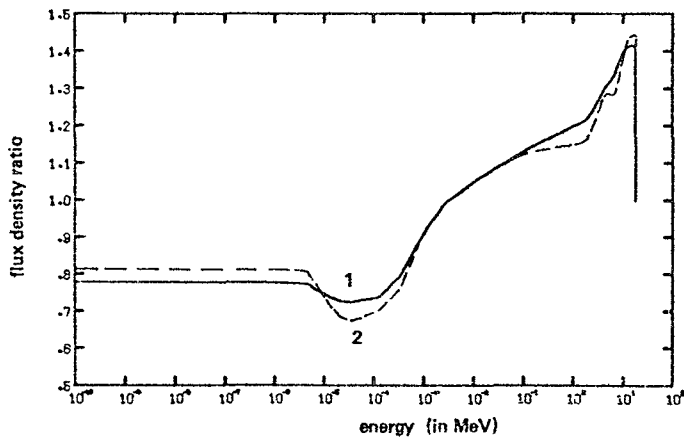


Fig. 7b. Ratio of output and input spectrum.

plot	1	2
k	6	2
ARD	1.1	0.93
S( $\omega$ )	4.5	3.8

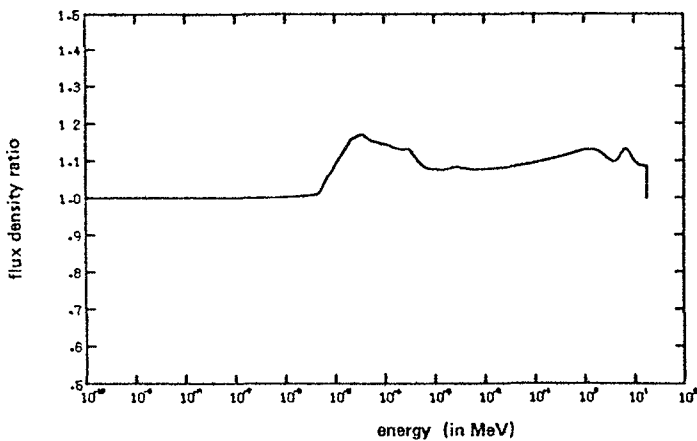


Fig. 7c. Ratio of solution spectra for ARD is 1.1 and 0.93.

Fig. 7: INFLUENCE CONVERGENCE VALUE FOR CRYSTAL BALL.

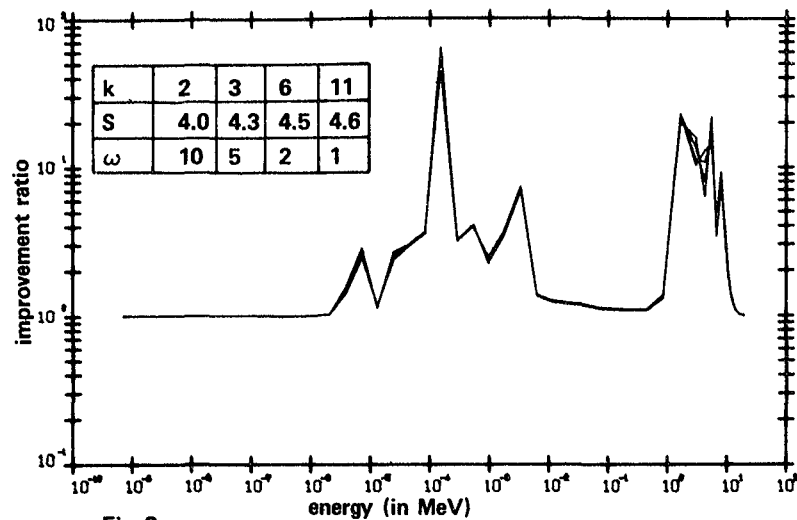


Fig. 8a.

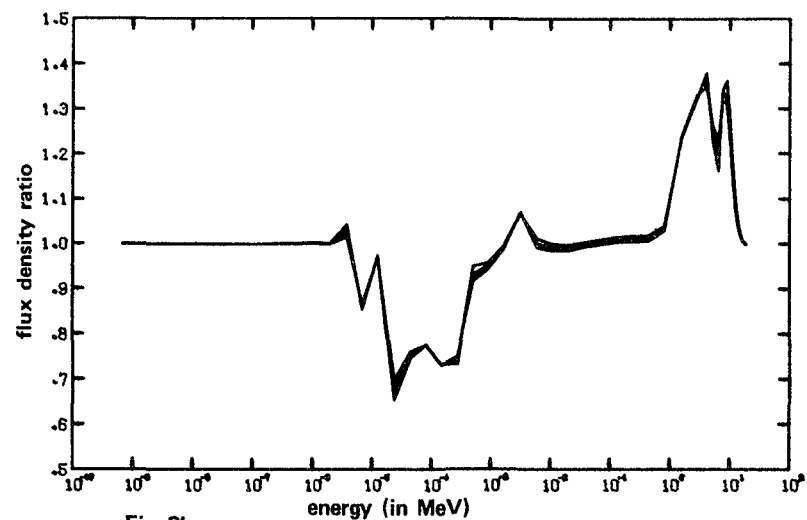


Fig. 8b.

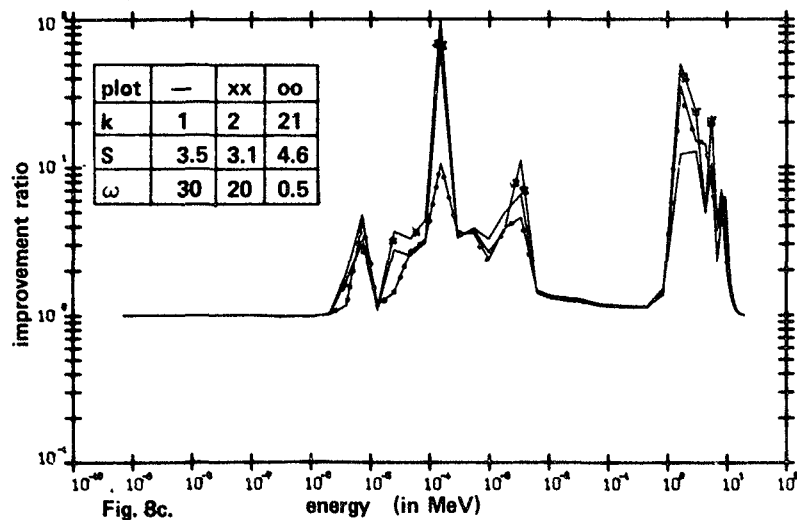


Fig. 8c.

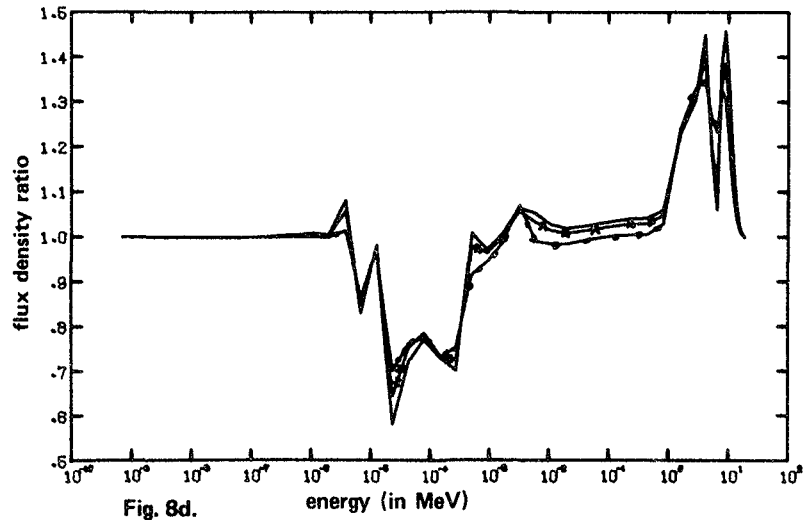


Fig. 8d.

Fig. 8a and 8c present the improvement ratios for different values of  $\omega$ . Fig. 8b and 8d present the  $\phi^{\text{out}}(E)/\phi^{\text{in}}(E)$  for the different values of  $\omega$ .

Fig. 8: IMPROVEMENT RATIOS AND SPECTRUM RATIOS FOR RFSP (15 detectors)

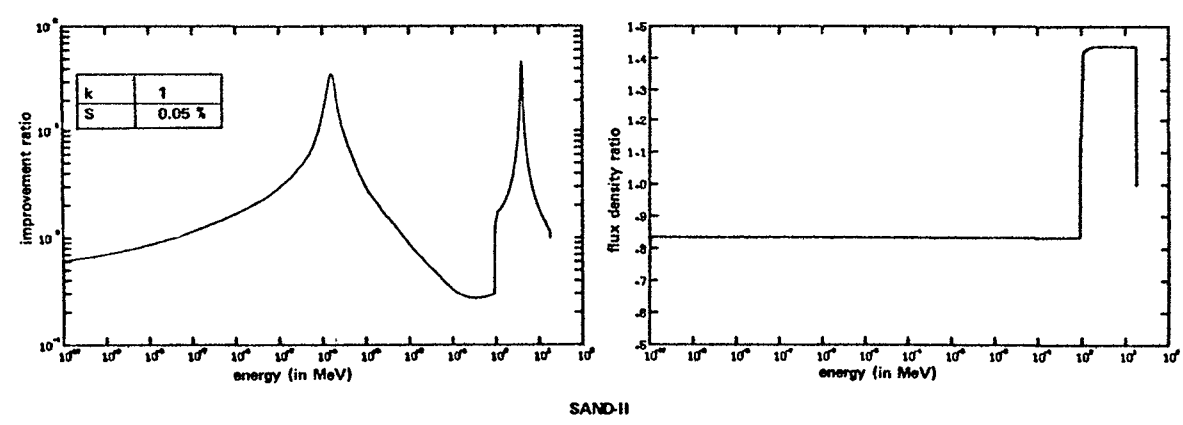
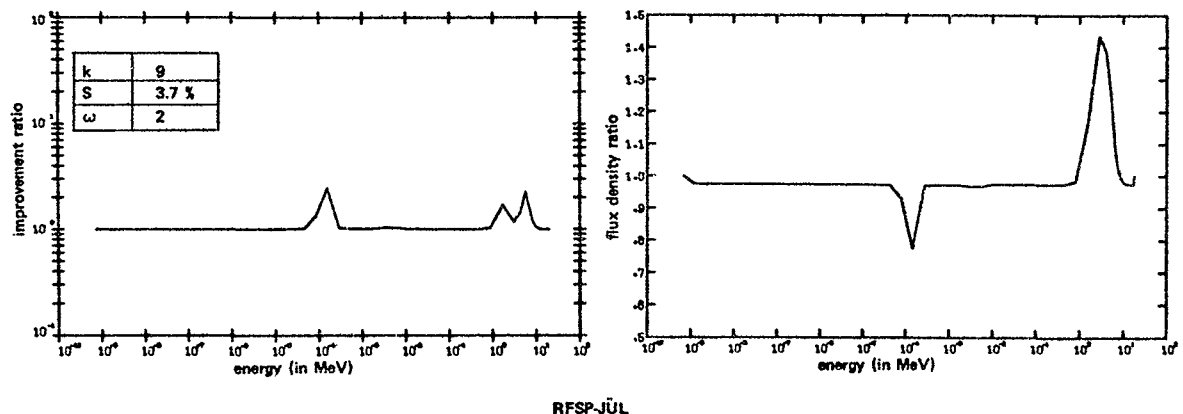
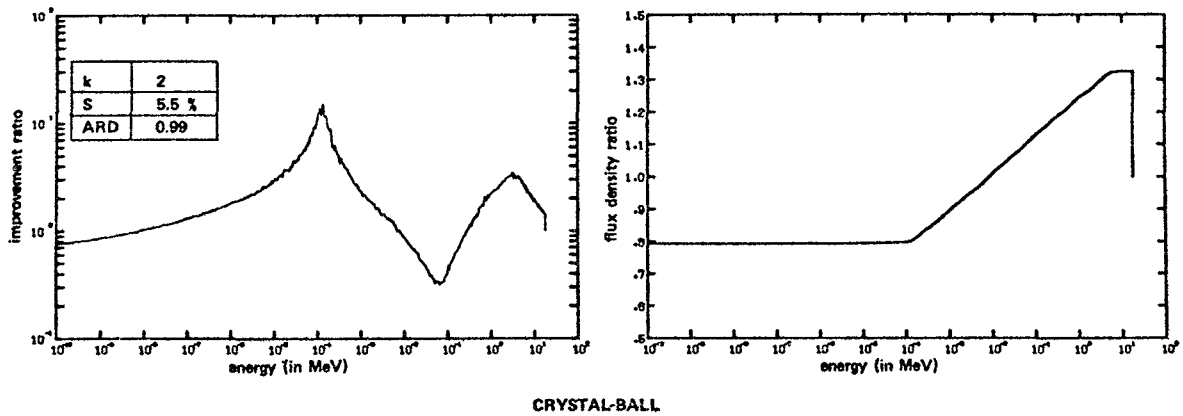
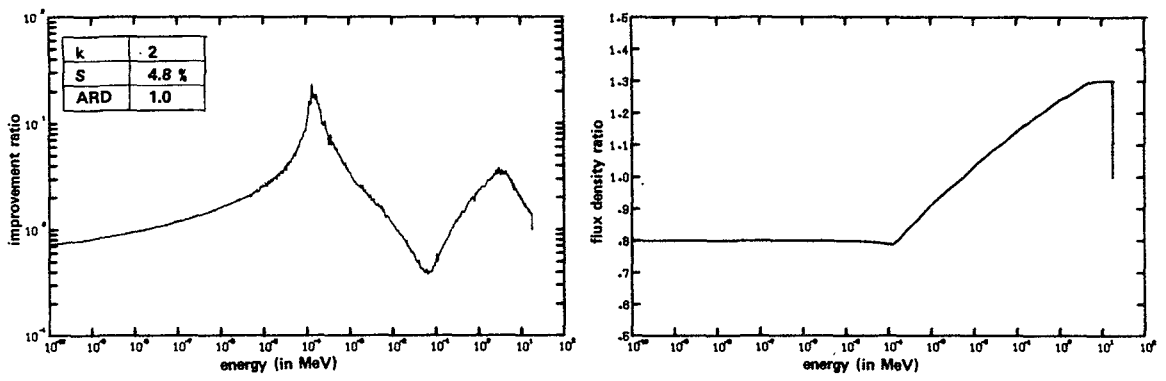
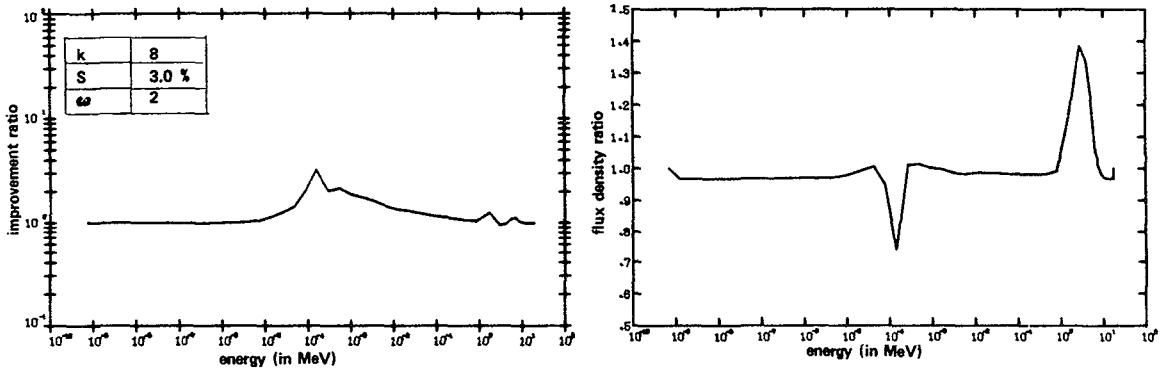


Fig. 9: RESULTS FOR THE Co AND Ni SET

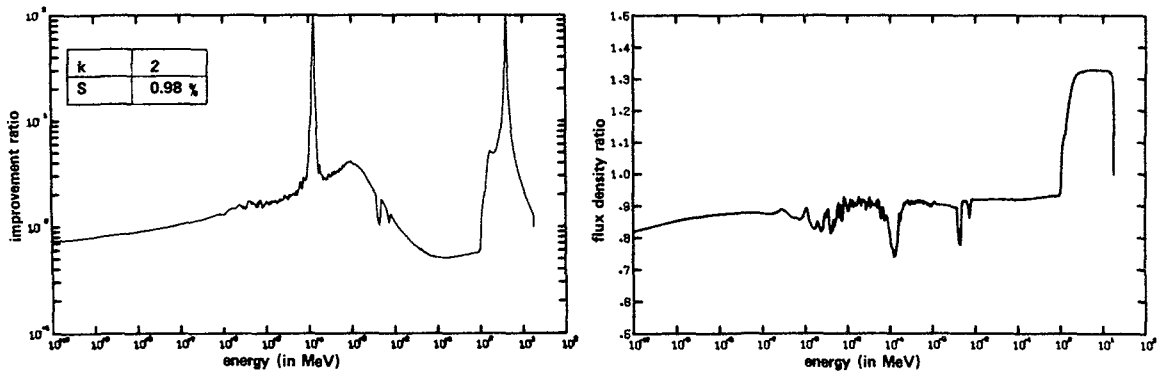




CRYSTAL-BALL



RFSP-JÜL



SAND-II

Fig. 10: RESULTS FOR THE U, Ni AND Co SET

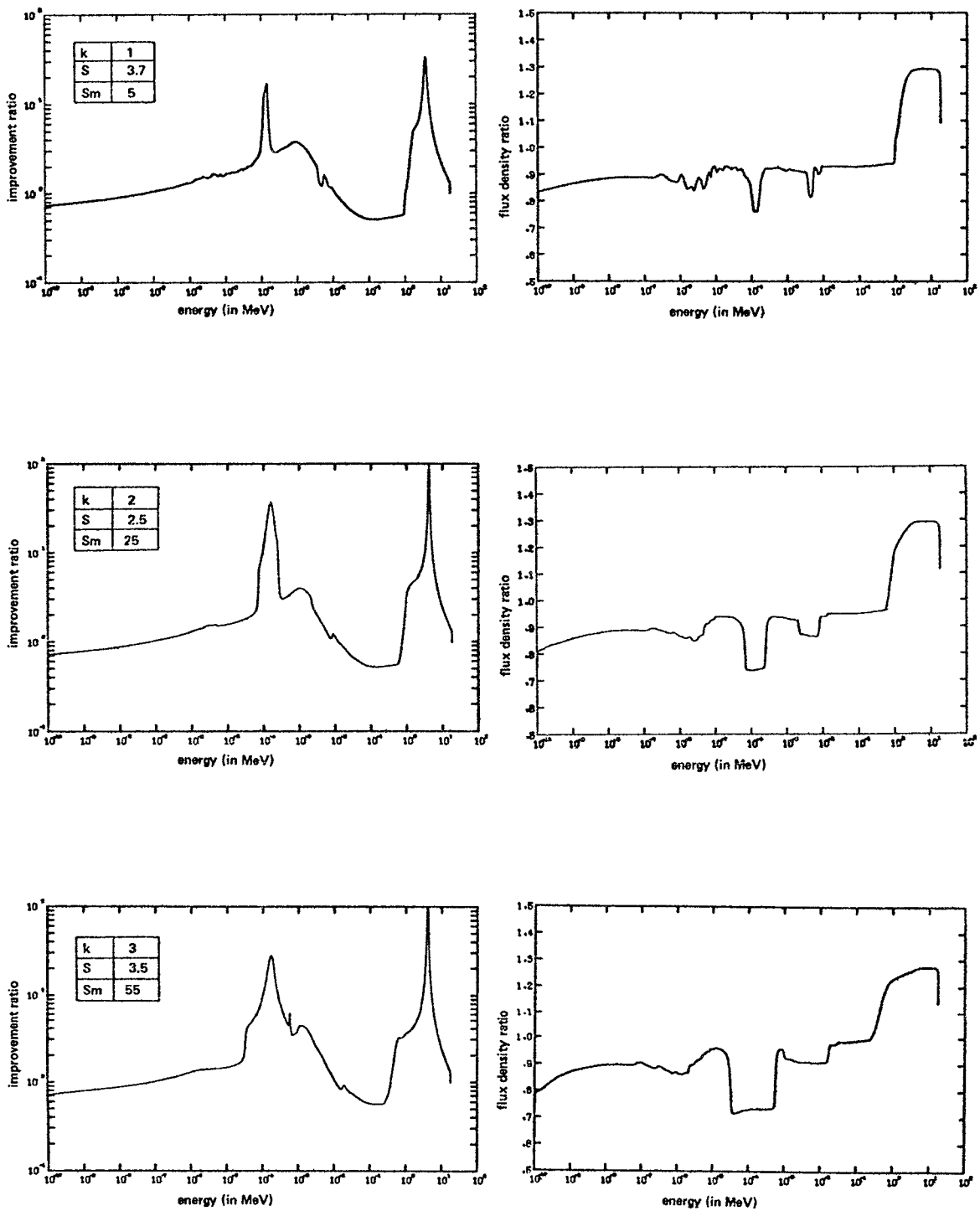


Fig. 11: INFLUENCE OF SMOOTHING IN SAND-II

# REVIEW OF UNFOLDING METHODS USED IN THE U.S. AND THEIR STANDARDIZATION FOR DOSIMETRY

C. A. Oster  
Battelle, Pacific Northwest Laboratories  
Richland, Washington 99352

## Abstract

A summary of the methods used in the U.S. to unfold radiation spectra is given. For discussion purposes, the methods studied are placed in groups, based on the algorithm used for unfolding and/or treatment of data uncertainties. Specific codes from each group are selected and examined for their role in dosimetry standardization. Finally, the preparation of the ASTM recommended practices and use of benchmark problems in the standardization process are discussed.

## Introduction

The measurement of radioactivity induced by neutrons provides information on the neutron flux. By studying activation reactions, each having a different energy-dependent response function, one can obtain knowledge about the energy-dependent neutron flux distribution. Let  $A_i$  denote the saturation activity of the  $i$ th detector. We then seek a solution for the neutron spectrum  $\phi(E)$  from the set of activation equations

$$A_i = \int_{E_{\min}}^{E_{\max}} \sigma_i(E) \phi(E) dE \quad i=1,2,\dots,m; \quad (1)$$

where  $\sigma_i(E)$  is the energy-dependent response function, or cross section, associated with the  $i$ th detector.  $E_{\min}$  and  $E_{\max}$  define the energy range of the neutron spectrum. Equation (1) is a discretized form of the Fredholm integral equation of the first kind

$$A(E') = \int_{a(E')}^{b(E')} \sigma(E',E) \phi(E) dE. \quad (2)$$

The problem of obtaining  $\phi(E)$  from this equation is frequently called the unfolding problem.

Unfolding procedures have been widely used to compute neutron and gamma ray spectra from experimental data. The problem is quite complex, which is one factor in the proliferation of computer codes. Unfortunately, even within specific categories, computer codes do not all yield the same solution spectra.<sup>1</sup> Any serious practitioner must face the question of determining which solution, if any, is correct. Work has begun on developing standards to enable the practitioner to answer this question.<sup>2,3</sup> Meyer and Miller<sup>3</sup> view the radiation spectra standardization problem as two separate problems: standardizing the measuring system and standardizing the unfolding procedures. These authors describe a number of publications wherein the germ of standardization was present but no coordinated effort developed.

It is primarily the second problem we wish to address here, although some time will be given to the first problem.

The unfolding standardization process begins with defining benchmark problems. The term benchmark is used in many contexts. Here we shall consider benchmark problems as carefully and sensibly stated problems which can be used to gage the performance of unfolding procedures. In fact, one view of the standardization process is that, given a properly stated benchmark problem, all unfolding methods applied should yield the same solution, with, perhaps, differing efficiencies of calculation and accuracies.<sup>4</sup> Fig. 1 shows the relationship of the unfolding procedure to the benchmark problems. The benchmark problem encompasses the function boxes above and on either side of the central box, which is designated the unfolding procedure.

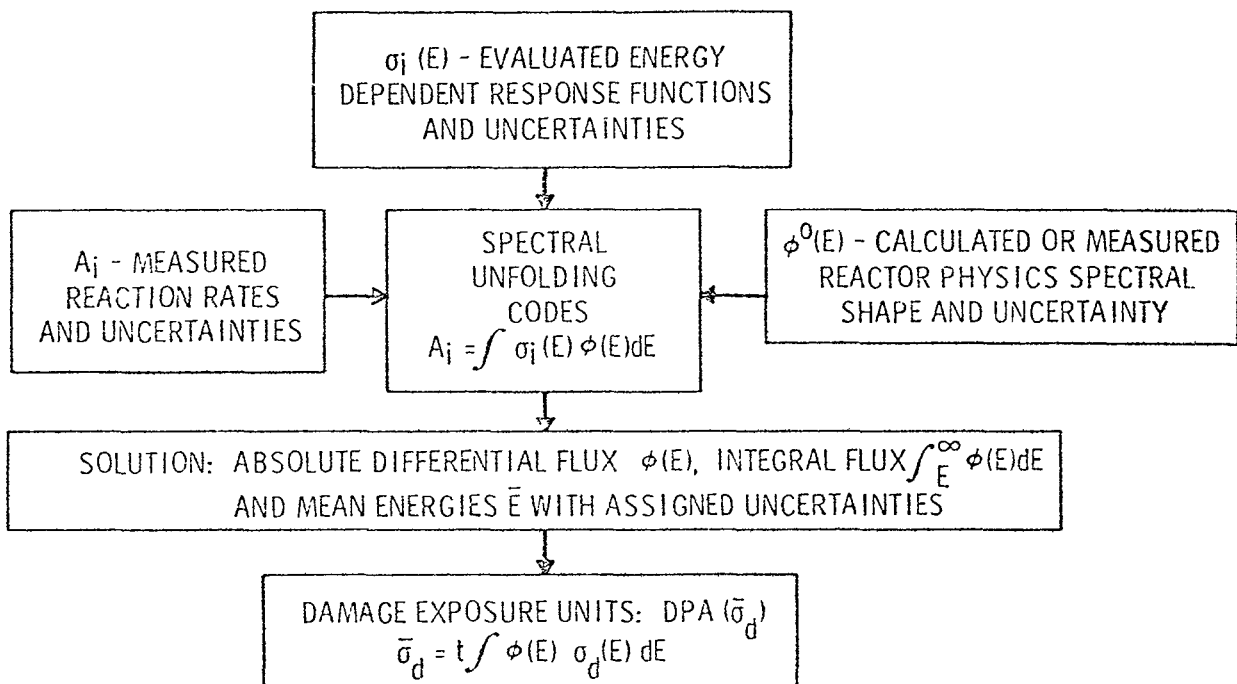


Figure 1. Components of a Reactor Dosimetry Problem

Several groups are currently active in standards work. Of note here are the ASTM E10.05 Subcommittee on Dosimetry and the American Nuclear Society's ANS-6 Standards Group. Details of a workshop on unfolding benchmarks are contained in Ref. 3. This workshop resulted in the formation of two working groups, operating under the auspices of the Radiation Shielding Information Center (RSIC) and the ANS-6 Standards Group. One group is studying the many-channel gamma ray and neutron spectroscopy problems; the other is investigating the few-channel neutron spectroscopy problem. (More will be said later about the many- and few-channel problems.) The general objectives of these two working groups are:<sup>3</sup>

1. A comprehensive set of well-defined goals of the benchmarking effort must be set out and agreed upon by consensus.
2. The goals will be compatible with, and useful in standardizing, realistic problems.
3. All terms must be clearly defined and agreed upon.

4. For particular applications, the data will be agreed upon and frozen to eliminate calibration problems in the benchmarking effort.

With these objectives in mind, the working groups are well on the way toward establishing a workable benchmark procedure.

### Benchmark Procedures

The objectives of the working groups listed in the previous section also include the development of benchmark problems and adequate data reporting forms. Benchmark problem development is seen as a long process requiring good documentation and wide acceptance by the scientific community.

A benchmark problem is a well-defined problem which can be used to measure one unfolding code against other unfolding codes. It is, in essence, a standard. A good benchmark problem should, except for the unfolding process itself, leave no room for ambiguity. This means that the response functions  $\sigma_i(E)$  and measured activities  $A_i$  of Equation (1) and Fig. 1 must be specified. If there is to be a unified use of the problem, then these quantities must remain as invariant as possible when transferred from one computer to another. In addition, the reference spectra and any available uncertainty data for it should be part of the benchmark specification. The reference spectra should be the best (in some well-defined sense) available solution to the benchmark problem.

It is highly desirable that an unfolding code permit the use of uncertainty or error data, not only for dosimeter activity measurements but for the response functions as well. Any error correlations which might exist between these input quantities must also be included. These uncertainties must be precisely defined.

The key item in the standardization process being considered here is the unfolding procedure. Before turning our attention to the unfolding procedures themselves, let us consider the response functions.

### Response Functions

To be included in a benchmark problem, the response functions must be critically examined by the scientific community. This examination must be comparable to that required for the benchmark problem itself. Factors to consider in establishing standardized response functions include 1) the energy range covered by the detectors and 2) the end use of the data. Two groups of scientists interested in unfolding procedures are the dosimetrists and the material investigators. The dosimetrist is primarily interested in the flux distribution while the material scientist is concerned mainly with comparing radiation effects on a wide variety of materials irradiated at different reactor sites. The material scientist must determine the neutron flux as one step in satisfying his primary interest.<sup>5,6</sup> See, for example, the bottom box of Fig. 1. Thus it is important to know the appropriate energy range for any given benchmark problem.

Radiation spectroscopy problems are generally placed in one of two broad categories, referred to as the few-channel problems and the many-channel problems. These category labels designate the activity detectors used in the typical laboratory procedure, i.e.,  $m$  in Equation (1). Gamma

ray and some neutron spectroscopy problems are treated as many-channel problems. Other neutron spectroscopy problems are treated as few-channel problems.

For some applications there is a lack of adequate  $(n,\gamma)$ -reaction response function data for energies below 20 MeV and adequate data is virtually absent for energies above 20 MeV.<sup>7</sup> The quality of response function data has prompted work in this area. Two sets of response function data are widely used. One is the response matrix distributed by RSIC with the FERD/FERDOR and COOLC codes and generally known as the Verbinski response matrix.<sup>8</sup> The second set consists of the ENDF/B cross section data.<sup>9,10</sup> The Verbinski data is specified for energy in the range of 0.20 to 22 MeV. Several workers have been actively engaged in improving the data but the energy range has remained the same.<sup>11-13</sup> These data have been specifically designed for the FERD/FERDOR and COOLC codes and must be altered, usually minimally, to obtain a consistent set for other codes.

The ENDF/B cross section data have been standardized, but some slight modifications may be necessary for other data sets for adaptation to different codes. For example, no standard exists for energy groupings within codes; hence, interpolation may be needed to achieve compatibility. At the other extreme, it may be desirable to collapse or reduce the amount of data used in a code. One code examined here does, in fact, take such actions.<sup>14</sup> In either case, it is essential that acceptable procedures for each operation--interpolation or collapsing--should be spelled out in the standards documentation.

### Spectra Unfolding Methods

The unfolding methods upon which codes are based may be classified into four broad categories. These categories are displayed in Fig. 2, showing the relationships of specific codes. The specific codes included in this study are listed below the terminal boxes. There are undoubtedly codes in existence which have not been included in this study.

The first category, designated Monte Carlo, is intended to contain codes in which a candidate spectrum is randomly selected from specific distributions. The selected spectrum is then folded into the given response function to produce a calculated activity response. If this computed activity is in sufficient agreement with measured activity values, the candidate spectrum is accepted as adequate for use in computing an average spectrum. If the agreement between the calculated and measured activity values is too large, the spectrum is rejected and another selected. Only one code, known as SWIFT,<sup>15,16</sup> is considered in the Monte Carlo category. Including only the SWIFT code is not intended to indicate the nonexistence of other codes which should be grouped here. Rather, it is the only one found. Also some codes have the words Monte Carlo associated with them, yet are not considered here.

The next category is labeled parametric representation and contains procedures which may be used when a functional representation of the neutron spectrum is available, e.g., the fission spectrum. This functional form must be based on either theoretical or previous experimental results. The user then determines the parameters by matching measured responses. This procedure severely limits the form which the computed spectrum may take and is used only when these restrictions can be justified or when insufficient

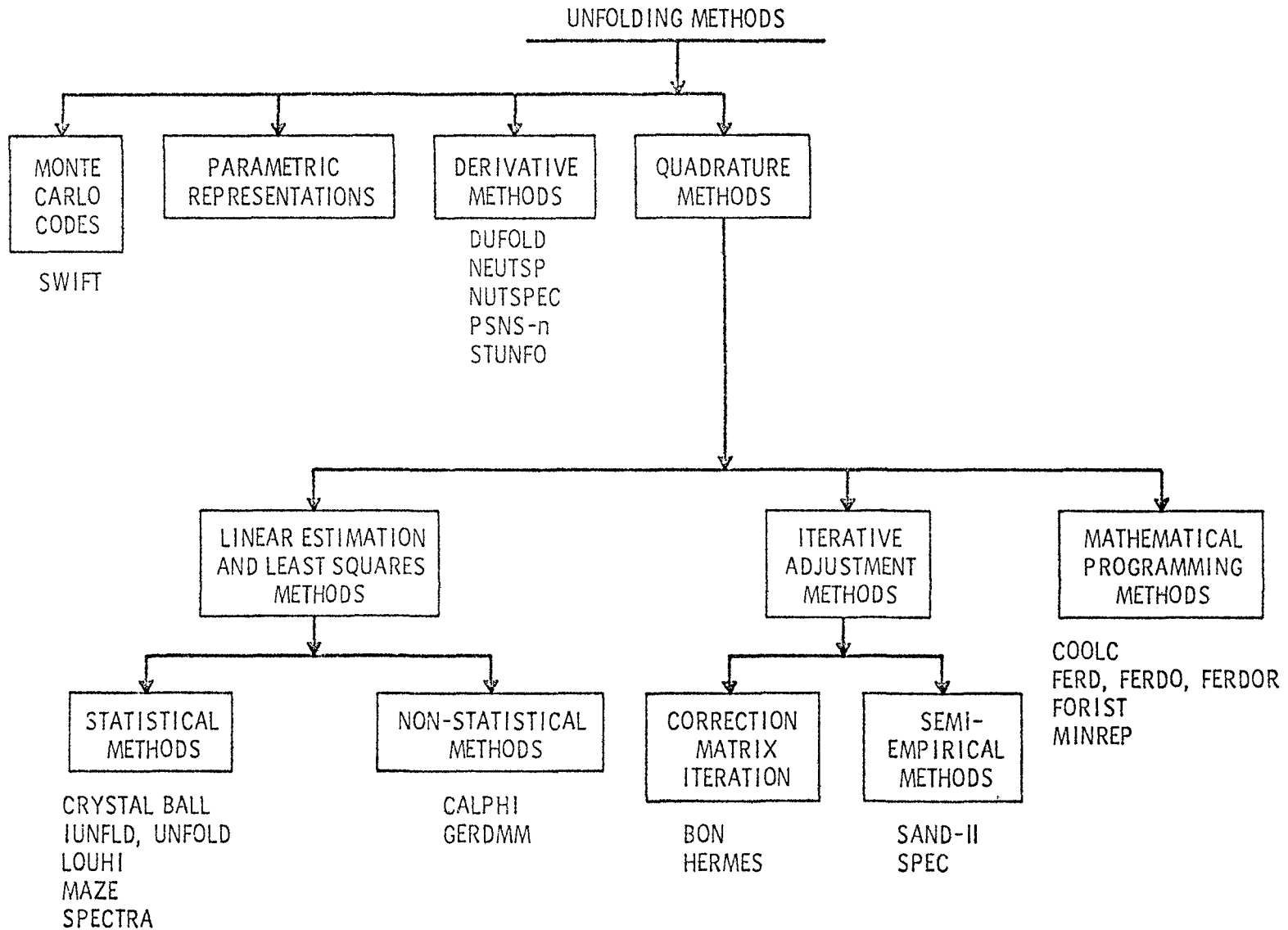


Figure 2. Classification Relationships of Unfolding Methods and Codes

experimental information is available for other methods. The one positive aspect to this method is that most of the computational complications peculiar to other methods are avoided.<sup>17</sup> Parametric representation has been successfully applied to high-energy neutron spectroscopy.<sup>18-20</sup>

The other two categories used to derive algorithms for solving the unfolding problem stated by Equation (1) contain the derivative methods, which we shall consider next, and the quadrature methods. These two categories are similar in that both require knowledge of the response function. The response function must be either measured experimentally for the particular system or calculated using some appropriate model. The two categories differ in that the derivative methods use an approximation to cause the neutron spectrum to become a readily determined explicit function of the measured response. This avoids the computational problems associated with the numerical solution of the equation system obtained by replacing the integral in Equation (1) with a quadrature formula.

In the derivative method, by assuming the system's response to a monoenergetic source to be a step function, one may write

$$\sigma(E', E) = H(E' - E) \frac{\epsilon(E)}{F}$$

where  $H(E' - E)$  is the Heavyside function defined as 0 for negative arguments and 1 otherwise, and  $\epsilon(E)$  is the efficiency of the detector at  $E$ . Now if  $a(E') = 0$  and  $b(E') = \infty$ , then the derivative of Equation (2) with respect to  $E'$  reduces to

$$\frac{dA}{dE} = - \frac{\epsilon(E)}{E} \phi(E)$$

where the primes have been dropped from the  $E$ s. This expression may be readily solved for  $\phi(E)$ . In Ref. 21, O'Brien et al. provide an excellent discussion of the assumption used in developing this expression for the recoil-proton distribution. They point out that the assumption does not remain valid for  $E$  above about 10 MeV. This method is extensively discussed by Coolbough et al.<sup>22</sup> and Slaughter.<sup>23</sup> If  $\epsilon(E)$  is known, then the original unfolding problem is replaced with approximating  $dA/dE$ . This is the method used by the derivative codes DUFOLD,<sup>22</sup> NUTSPEC,<sup>23</sup> PSNS-n,<sup>24</sup> NEUTSP<sup>25</sup> and STUNFO.<sup>26</sup>

Now let us consider the fourth class of unfolding methods in Fig. 1, the quadrature methods. One does not solve the integral Equation (1) directly but rather approximates the integral with a quadrature formula yielding

$$A_i = \sum_{j=1}^m \sigma_{ij} \phi_j \Delta E_j \quad i=1,2,\dots,m. \quad (3)$$

If the spacings  $\Delta E_j$  are taken too small, the system of linear equations becomes unstable, that is, the solution becomes very sensitive to small changes in the coefficient matrix.

A second source of ill conditioning is any linear dependence of the response function, i.e., detector cross sections. For example, most available detector cross sections are affected by linear dependence in the thermal and epithermal energy ranges from below  $0.50 \times 10^{-6}$  to 1 MeV.<sup>27</sup>



There are three major classes of methods in the quadrature category: the linear estimation methods, the mathematical programming methods and the iterative improvement methods. In the linear estimation methods the system of Equation (3) is solved directly. This solution may then be improved by an iterative process.<sup>5</sup> Included here are the constrained linear least squares methods and least structure methods.<sup>28</sup> The linear estimation methods may be further subdivided into those which utilize statistical methods and those which do not. The statistical methods may be viewed as those wherein one assigns probabilities to all possible spectra, assuming some probability distribution function. Then, from all spectra consistent with the measured activations data, the one with the highest probability is selected. This approach readily permits use of uncertainty data in the activation data as well as the response functions.<sup>29</sup> Examples of this method are the CRYSTAL BALL<sup>30</sup> and SPECTRA<sup>31</sup> codes.

The next class of unfolding methods under the category of quadrature methods is the iterative adjustment. Many codes in other classes also use iterative adjustment modes to ensure smoothness and nonnegativity for the solution. SPECTRA,<sup>31</sup> CRYSTAL BALL,<sup>30</sup> and LOUHI<sup>17</sup> are examples. Such codes are primarily designed around a different procedure, however. The codes in this class are based essentially on the iterative adjustment policy. Two types of codes fall within this class: the correction matrix iterative and the semiempirical types. The codes examined in this study, which are included in the correction matrix iteration type, were all based on the method attributed to Scofield<sup>32</sup> and Gold.<sup>33</sup> This method finds a nonnegative solution by minimizing the difference between the measured and computed activities through the iterative procedure.<sup>17</sup> Variations to incorporate smoothing procedures into the original method have been included in some instances. Sanna has used the Scofield-Gold method to obtain solutions for energies extending up to 400 MeV.<sup>34</sup>

The semiempirical type is generally exemplified by the algorithm in the SAND II code.<sup>35,36</sup> A second method, simpler but relatively unpublicized, is given by Schmotzer and Levine.<sup>37</sup> Beginning with a starting initial spectrum, these methods apply a nonlinear adjustment repeatedly until specific convergence criteria are satisfied. These methods have been used for neutron energies ranging from  $10^{-10}$  to 18 MeV.

The final class of unfolding methods examined under the quadrature category is the mathematical programming methods. Perhaps the best known methods here are based on the Burrus techniques.<sup>38,39</sup> These methods result from a precise mathematical formulation restricting the statistical distributions of the spectra to those spectra with nonnegative flux values. The Burrus procedure uses a linear estimation technique to produce the spectrum and mathematical programming to provide upper and lower bounds (probabilistic) for the solution values.

The work of Kirmser, Hu and Meyer<sup>40,41</sup> is also included in this class. It is based on the precise definition of the unfolding problem in terms of absolute upper and lower bounds.<sup>14</sup> When refolded with the response matrix the solution produces the minimum distance between the measured and calculated responses. Another interesting feature employed in MINREP is the use of a minimum number of columns from the initial response matrix.

Table I lists most of the unfolding codes readily available in this country today. Each code listed is assigned a classification key, consisting of three parts separated by hyphens. The left-most part is the category key, the middle part is the class key, and the right-most part is the type

Table I. Summary of Unfolding Codes Used in  
the United States for Dosimetry

Code Name (a)	Code Classification Key (b)	Effective Energy Range (c)	Problem Type (d)	Comments and References
BON	Q-IA-CMI	Thermal $\leq E \leq 400$ MeV	M	Scofield-Gold Iterative Technique (References 32 and 42)
CALPHI	Q-LE-NS		M	Laguerre Polynomial Expansion Designed for well-thermalized spectra (References 43 and 44)
COOLC	Q-MP-QP	$0.2 \leq E \leq 22$ MeV	M	Uses Verbinski response matrix IBM 360 version of FERDOR-RSIC Program No. PSR-017 (References 8, 38, 39, 45, 46, and 47)
CRYSTAL BALL	Q-LE-S		F	Minimize deviation in shape using Lagrange multiplier method. RSIC Program No. CCC-233 (References 5 and 30)
DUFOLD	D	$E < 10$ MeV	M	Uses a differentiated least square quadratic polynomial to estimate $dA/dE$ . RSIC Program No. PSR-042 (Reference 22)
FERD, FERDO, FERDOR	Q-MP-QP	$0.2 \leq E \leq 22$ MeV	M	Linear estimation method used to produce spectrum and mathematical programming used to obtain error analysis. Uses Verbinski's response matrix. RSIC Program Nos.: FERDO/FERD - PSR-102; FERDOR - PSR-017 (References 8, 38, 39, 45, 46, 47)
FORIST	Q-MP-QP	$0.2 \leq E \leq 22$ MeV	M	Computes optimum windows. FORIST $\equiv$ FERDOR with Optimized Resolution using an Iterative Smoothing Technique. RSIC Program No. PSR-092 (References 13 and 48)
GERDMM	Q-LE-NS	$10^{-10} \leq E \leq 15$ MeV	F	General Electric proprietary version of the Ispra code RDMM (RDMM $\equiv$ Relative Deviation Minimization Method). Uses Laguerre polynomial expansion, extensive library of starting spectra (References 27, 49, 50, and 51)
Harker	PR	$10 \text{ eV} \leq E \leq 15$ MeV	F	Predefined functional form non-linear least squares used to fit parameters (Reference 20)
HERMES	Q-IA-CMI	$1 \leq E \leq 40$ MeV	M	Scofield-Gold Iterative Technique (References 32 and 42)
IUNFLD, UNFOLD	Q-LE-S		M	Constrained weighted linear least squares code using 3-splines basis functions (Reference 52)
LOUHI	Q-LE-S		F, M	Generalized constrained least squares program (References 17, 53, and 54)
MAZE	Q-LE-S		F	Maximum entropy method. RSIC Program No. PSR-041 (References 55 and 56)
MINREP	Q-MP	$0.2 \leq E \leq 22$ MeV	M	Uses modified Verbinski response matrix, using a minimum of the data columns. Gradient methods are used in the search to minimize the distance between the measured to calculated response (References 11, 40, and 41)
NEUTSP	D	$E < 10$ MeV	M	Reference 25.

(a) Code names in upper case if known, otherwise the originator's name is used.

(b) See Table II.

(c) Effective energy range is based on assumptions and usage appearing in publications.

(d) F denotes few-channel problem; M denotes many-channel problems based on published usage.

Table I. (cont)

<u>Code Name</u> <sup>(a)</sup>	<u>Code Classification Key</u> <sup>(b)</sup>	<u>Effective Energy Range</u> <sup>(c)</sup>	<u>Problem Type</u> <sup>(d)</sup>	<u>Comments and References</u>
NUTSPEC	D	E < 10 MeV	M	Similar to DUFOLD but uses B-splines to approximate derivatives of scintillator light output function (Reference 23)
PSNS-n	D	1 keV - 2 MeV	M	Mini-computer code (Reference 24)
SAND II	Q-IA-SEM		F	An early version is RSIC Program No. CCC-112. The Monte Carlo version has been submitted to RSIC (References 35, 36, 57, 58, 59 and 60)
Schmotzer	Q-IA-SEM		F	Schmotzer-Levine variation on Fortney-Levine method (References 37 and 61)
SPECTRA	Q-LE-S		F	Minimizes deviation in magnitude under determined systems. RSIC Program No. CCC-108 (References 31, 60, and 62)
SPEC	Q-IA-SEM		F	Linear least squares method applied to minimizing the deviation between the measured and computed spectral indices (References 63, 64, 65, and 66)
SPEC4			F, M	Code for calculating recoil proton energy distribution from monoenergetic and continuous spectrum neutrons. RSIC Program No. PSR-99 (References 45 and 67)
STUNFO	D	1 - 20 MeV	M	Time series analysis and Fourier analysis used to smooth the spectrum (Reference 26)
SWIFT	MC		F	Monte Carlo method. RSIC Program No. PSR-031 (References 15, 16, and 42)

(a) Code names in upper case if known, otherwise the originator's name is used.

(b) See Table II.

(c) Effective energy range is based on assumptions and usage appearing in publications.

(d) F denotes few-channel problem; M denotes many-channel problems based on published usage.

key. The values for these keys are given in Table II. These values are coordinated with Fig. 2. It should be noted that all combinations of the various keys do not occur. Some classification keys do not have three parts. The missing parts are the type key or both the class and type keys. In one instance, SPEC4, no classification code was assigned due to lack of sufficient information about the code.

### Recommendations

The development of ASTM recommended practices for radiation dosimetry is based on the establishment of standards. These standards must include a means of upgrading the benchmark problems and codes. The standardization procedure is seen as a sequence of stages and has been discussed by Meyer et al.<sup>2</sup> and Meyer and Miller.<sup>3</sup> No one benchmark problem is going to adequately satisfy all standardization needs; hence several categories of benchmark problems are needed. Within each category a sequence of problems with graduated levels of complexity is needed. At the simple end of this sequence could be a problem consisting of artificial data designed to point out any gross difficulties a code might encounter. This problem should be little more complex than one used during the developmental stage of a code.

Table II. Code Classification Keys<sup>(a)</sup>

Category	{	PR	Parametric Representation
		D	Derivative
		Q	Quadrature
		MC	Monte Carlo
Class	{	LE	Linear Estimation
		IA	Iterative Adjustment
		MP	Mathematical Programming
Type	{	S	Statistical
		NS	Nonstatistical
		CMI	Correction Matrix Iteration
		SEM	Semiempirical
		LP	Linear Programming
		QP	Quadratic Programming

(a) Each key has the form category-class-type.

At the highly complex level would be problems selected from actual test data so as to severely test any method. A graduated set of benchmark problems would provide the user with a systematic means for upgrading a standard code. Weaknesses would be identified in an orderly sequence.

The general objectives of the two working groups emerging from the 1976 RSIC meeting and listed earlier here should be kept in mind.<sup>3</sup> Kam and Stallman<sup>5</sup> list the following items as worthy of consideration for the real data benchmark problems.

1. The choice of the monitor set is essential in obtaining a good approximation to a radiation spectra. In selecting the set, attention should be directed to the properties of coverage and resolution. Finally, the number of detectors is important to the extent that more coverage and resolution are possible with more detectors.
2. The trial spectrum (if needed) probably influences the outcome of the unfolding in regions where the monitor set coverage is weak or even non-existent. A good trial spectrum can considerably reduce the number of iterations needed to produce a solution.

Item 2 should be included in the computational complexity decisions noted above.

At least three questions must be confronted by the standardization process. These questions are:

1. What quantities are to be used to compare codes?
2. How are the comparison quantities defined precisely?
3. How does one judge the quality of the comparison quantities?

Some of these questions may not be pertinent for all benchmark problems. For example, if the problem is designed around a monoenergetic source, questions about results for energies far removed from the source need not be seriously considered.

In establishing standardized response matrices and cross sections, consideration should be given to include accuracy information for any interpolation used. For example, Ref. 68 lists, for each column of tabulated data, both the maximum error incurred for linear interpolation and the number of points needed to achieve full accuracy within the column. Additional techniques useful in constructing and using tabular data are contained in Ref. 69.

So far we have discussed the procedures for developing benchmarks-- i.e., methods for testing unfolding codes. The final question to be addressed here is "How does the practitioner utilize the benchmark information for dosimetry work?" The following steps are a tentative answer:

1. Determine the dosimeter type used.
2. Determine any a priori data available.
3. Determine any a posteriori data available.
4. Determine any intuitive data applicable.<sup>38</sup>
5. Select the response functions needed for the dosimeter used.
6. Choose an unfolding method which has been found acceptable through appropriate benchmark tests. These tests must be compatible with Steps 1 through 5.
7. Use the chosen unfolding method to unfold the data of Steps 2 through 5.
8. Subject the unfolded solution to appropriate validity checks, e.g., is the solution consistent with Steps 2 through 4?
9. If the checks in Step 8 fail, revise the data in Steps 2 through 5 and repeat Steps 6 through 8.

#### References

1. A. Fischer, International Intercomparison of Neutron Spectra Evaluating Methods Using Activation Detectors, JUL-1196, Kernforschungsanlage Julich, Federal Republic of Germany, (June 1975).
2. Walter Meyer, William H. Miller, P. G. Kirmser and K. K. Hu, "Defining a Methodology for Benchmarking Spectrum Unfolding Codes," in A Review of Radiation Energy Spectra Unfolding, compiled by D. K. Trubey, ORNL/RSIC-40, pp. 235-245 (October 1976).
3. Walter Meyer and William H. Miller, editors, "The Benchmark Problem Proposal," in A Review of Radiation Energy Spectra Unfolding, compiled by D. K. Trubey, ORNL/RSIC-40, pp. 247-254 (October 1976).
4. Philip G. Kirmser, Personal Communication, Letter (April 8, 1977).

5. F. B. K. Kam and F. W. Stallmann, "Neutron Spectrum Analysis from Dosimetry Experiments," Journal of Testing and Evaluation, JTEVA, Vol. 3, No. 3, pp. 211-216 (May 1975).
6. A. H. Kazi, E. D. McGarry and D. M. Gilliam, "Standardization of Fast Pulse Reactor Dosimetry," presented at the International Specialists Symposium on Neutron Standards and Applications, National Bureau of Standards (March 28-31, 1977).
7. William Quam, Personal Communication, Letter (April 18, 1977).
8. V. V. Verbinski, W. R. Burrus, T. A. Love, W. Zobel, N. W. Hill and R. Textor, "Calibration of an Organic Scintillator for Neutron Spectrometry," Nuclear Instruments and Methods, Vol. 65, pp. 8-25 (1968).
9. B. A. Magurno and O. Ozer, "ENDF/B File for Dosimetry Applications," Nuclear Technology, Vol. 25, pp. 376-380 (February 1975).
10. P. B. Hemmig, "Development of the ENDF/B System," Proc. of 3rd Conference on Neutron Cross Sections and Technology, Knoxville, TN, March 15-17, 1971, CONF-710301, Vol. 1, pp. 348-353.
11. Philip Kirmser, Kuo-Kuang Hu and Walter Meyer, "Effects of Smoothness of Response Matrices on Unfolding Radiation Data," Transactions of the American Nuclear Society, Vol. 21, pp. 536-537 (1975).
12. R. H. Johnson, B. W. Wehring and J. J. Dorning, "NE-213 Neutron Spectrometry System for Measurements to 15 MeV," Proceedings of the Conference on Nuclear Cross Sections and Technology, held at Washington, DC, March 3-7, 1975, NBS Special Publication 425, p. 62 (1975).
13. R. H. Johnson, D. T. Ingersoll, B. W. Wehring and J. J. Dorning, "NE-213 Neutron Spectrometry System for Measurements from 1.0 to 20 MeV," Nuclear Instruments and Methods (1977).
14. P. G. Kirmser, K. K. Hu and W. Meyer, "A Mathematically Precise Statement of the Unfolding Problem," in A Review of Radiation Energy Spectra Unfolding, compiled by D. K. Trubey, ORNL/RSIC-40, pp. 83-91 (October 1976).
15. R. Sanna and K. O'Brien, "Monte-Carlo Unfolding of Neutron Spectra," Nuclear Instruments and Methods, Vol. 91, pp. 573-576 (1971).
16. Robert S. Sanna, "A User's Guide to SWIFT, a Monte-Carlo Technique for Unfolding Neutron Spectra," U.S. Atomic Energy Commission Document No. HASL-224 (July 1971).
17. J. T. Routti, "Mathematical Considerations of Determining Neutron Spectra from Activation Measurements," in Proceedings of 2nd International Symposium on Accelerator Dosimetry and Experience, Stanford University, November 5-7, 1969, Paper No. Conf 691101, pp. 494-415.
18. Ronald P. Omberg and H. Wade Patterson, "Applications of the Stars Produced in a Nuclear Emulsion to Determine a High-Neutron Energy Spectrum," Lawrence Radiation Laboratory Report UCRL-17063 (February 1967).

19. H. Wade Patterson, Harry H. Heckman, Jr., and Jorma T. Routti, "New Measurements of Star Production in Nuclear Emulsions and Applications to High-Energy Neutron Spectroscopy," Lawrence Radiation Laboratory Report UCRL-19389 (October 1969).
20. Y. D. Harker, "An Application of Semi-Empirical Modeling and Non-Linear Regression to Unfolding Fast Neutron Spectra from Integral Reaction Rate Data," in A Review of Radiation Energy Spectra Unfolding, compiled by D. K. Trubey, ORNL/RSIC-40, pp. 164-176 (October 1976).
21. K. O'Brien, R. Sanna, M. Alberg, J. E. McLaughlin and S. Rothenberg, "Nuclear-Track Emulsion Spectrometry at Low and Intermediate Neutron Energies," Nuovo Cimento Suppl., Vol. 3, pp. 409-421 (1965).
22. M. J. Coolbaugh, R. E. Faw and W. Meyer, "Fast Neutron Spectroscopy in Aqueous Media Using an NE-213 Proton Recoil Neutron Spectrometer System," Nuclear Engineering Department, Manhattan, KA, COO-2049-7 (1971).
23. D. R. Slaughter, "A Simple Method to Unfold NE-213 and Stilbene Neutron Spectral Data," in A Review of Radiation Energy Spectra Unfolding, compiled by D. K. Trubey, ORNL/RSIC-40, pp. 65-77 (October 1976).
24. E. F. Bennett and T. J. Yule, "Techniques and Analysis of Fast-Reactor Neutron Spectroscopy with Proton-Recoil Proportional Counters," Argonne National Laboratory, ANL-7763 (1971).
25. M. E. Toms, "A Computer Analysis to Obtain Neutron Spectra from an Organic Scintillator," Nucl. Instr. Methods, Vol. 92, pp. 61-70 (1971).
26. G. A. Mutone and W. Meyer, "Neutron Spectra Estimation from Proton Recoil Data," Nucl. Instr. Meth., Vol. 106, p. 445 (1973).
27. "Discussion of Computer Codes for Determining Neutron Flux Spectra by Multiple Foil Measurements," American Society of Testing and Measurements (1974 Annual), pp. 851-856.
28. Carl S. Young, "Least-Structure Techniques in Unfolding," Transactions of the American Nuclear Society, Vol. 14, p. 388 (1971).
29. F. W. Stallman and F. K. K. Kam, "Review of Unfolding Methods for Neutron Flux Dosimetry," presented at the First ASTM-EURATOM Symposium on Reactor Dosimetry, Petten, The Netherlands (September 22-26, 1975).
30. F. B. K. Kam and F. W. Stallman, "CRYSTAL BALL: A Computer Program for Determining Neutron Spectra from Activation Measurements," ORNL-TM-4601 (June 1974).
31. C. R. Greer, J. A. Halbleib and J. V. Walker, "A Technique for Unfolding Neutron Spectra from Activation Measurements," SC-RR-67-746 (1967).
32. N. E. Scofield, "Technique for Unfolding Gamma-Ray Scintillation Spectrometer Pulse Height Distributions," USNRDL-TD-447 (1960).
33. Raymond Gold, "An Iterative Unfolding Method for Response Matrices," Argonne National Laboratory ANL-6984 (December 1964).

34. Robert S. Sanna, "Modification of an Iterative Code for Unfolding Neutron Spectra from Multisphere Data," US-ERDA Report HASL-311 (October 1976).
35. W. N. McElroy, S. Berg, T. Crockett and R. Hawkins, "A Computer-Automated Iterative Method for Neutron Flux Spectra Determination by Foil Activation," AFWL-TR-67-41, Vol. I (1967).
36. C. A. Oster, W. N. McElroy, R. L. Simons, E. P. Lippincott, G. R. Odette, "Solution Weighting for the Sand-II Monte Carlo Code," in A Review of Radiation Energy Spectra Unfolding, compiled by D. K. Trubey, ORNL/RSIC-40, pp. 148-161 (October 1976).
37. J. K. Schmotzer and S. H. Levine, "An Improved Technique for Unfolding Foil Activation Data," Trans. Amer. Nuc. Soc., Vol. 18, pp. 370-371 (1974).
38. Walter R. Burrus, "FERD and FERDOR Type Unfolding Codes," in A Review of Radiation Energy Spectra Unfolding, compiled by D. K. Trubey, ORNL/RSIC-40, pp. 1-22 (October 1976).
39. Burt W. Rust, "Mathematical Foundations of the Burrus Techniques for Spectral Unfolding," in A Review of Radiation Energy Spectra Unfolding, compiled by D. K. Trubey, ORNL/RSIC-40, pp. 23-32 (October 1976).
40. Philip G. Kirmser, Kuo-Kuang Hu, and Walter Meyer, "A Method for Unfolding Bounded Radiation Data," Transactions of the American Nuclear Society, Vol. 15, pp. 541-543 (1972).
41. P. G. Kirmser, K. K. Hu and W. Meyer, "A New Method for Solving the Unfolding Problem for Bounded, Inaccurate Radiation Data," in A Review of Radiation Energy Spectra Unfolding, compiled by D. K. Trubey, ORNL/RSIC-40, pp. 107-116 (October 1976).
42. Robert S. Sanna, "Neutron Spectral Unfolding at ERDA's Health and Safety Laboratory" (June 2, 1977).
43. Jacek Jedruch, "An Activation Experiment to Determine the Coefficient in the Laguerre Expansion of Perturbed Thermal-Neutron Spectra," Nuclear Science and Engineering, Vol. 31, pp. 377-387 (1968).
44. J. Jedruch, "Unfolding of Neutron Spectra Perturbed by Resonance Absorbers," in A Review of Radiation Energy Spectra Unfolding, compiled by D. K. Trubey, ORNL/RSIC-40, pp. 139-146 (October 1976).
45. R. W. Peelle, "Techniques Used at Oak Ridge National Laboratory for Unfolding Neutron and Gamma-Ray Pulse-Height Spectra," Transactions of the American Nuclear Society, Vol. 14, pp. 389-390 (1971).
46. V. V. Verbinski, H. Wever, R. E. Sund, "Measurement of Fission Fragment Isomers with Ge(Li) Detectors: Unfolding Spectra with Discrete and Continuum Components," Transactions of the American Nuclear Society, Vol. 14, pp. 391-392 (1971).
47. Burt W. Rust and Walter R. Burrus, Mathematical Programming and the Numerical Solution of Linear Equations, American Elsevier Publishing Company, Inc., New York (1972).



48. D. T. Ingersoll and B. W. Wehring, "Gamma-Ray Pulse-Height Response of an NE-213 Scintillation Detector," submitted to Nuclear Instruments and Methods, May 1977.
49. G. DiCola and A. Rota, "Analysis and Development of the Series Expansion Methods in Threshold Detector Activation Data Handling," presented at the Symposium on Fast and Epithermal Neutron Spectra in Reactors, Harwell, Didcot (Great Britain), December 11-13, 1963, Document No. EUR 588.e (1964).
50. G. DiCola and A. Rota, "Calculation of Differential Fast-Neutron Spectra from Threshold-Foil Activation Data by Least-Squares Series Expansion Methods," Nuclear Science and Engineering, Vol. 23, pp. 344-353 (1965).
51. G. DiCola and A. Rota, "RDMM - A Code for Fast Neutron Spectra Determination by Activation Analysis," Joint Nuclear Research Center, Ispra Establishment, Italy, Document No. EUR 2985.e (1966).
52. Frank Biggs and Donald E. Amos, "Numerical Solutions of Integral Equations and Curve Fitting," Sandia Laboratories, Albuquerque, NM, Document No. SC-RR-710212 (September 1971).
53. Jorma Tapio Routti, "High Energy Neutron Spectroscopy with Activation Detectors Incorporating New Methods for Analysis of Ge(Li) Gamma-Ray Spectra and the Solution of Fredholm Integral Equations," PhD Thesis, Document No. UCRL-18514 (April 1969).
54. R. V. Griffith, "Progress in Multisphere Neutron Spectrometry," in Hazards Control Progress Report No. 45, January through April 1973, Lawrence Livermore Laboratory, UCRL-50007-73-1, pp. 18-19, 24.
55. H. Kendrick and L. Harris, Jr., "Experimental Studies of Unfolding," Transactions of the American Nuclear Society, Vol. 14, pp. 390-391 (1971).
56. S. M. Sperling, "Structural Survey of Unfolding," Transactions of the American Nuclear Society, Vol. 14, p. 387 (1971).
57. C. A. Oster, W. N. McElroy and J. M. Marr, "A Monte Carlo Program for SAND-II Error Analysis," Hanford Engineering Development Laboratory, Document No. HEDL-TME 73-20 (February 1973).
58. W. N. McElroy, "Fast Reactor Flux-Spectral Characterization," Proceedings American Nuclear Society Topical Meeting on "Irradiation Experimentation in Fast Reactors," Jackson Lake Lodge, Wyoming, September 10-12, 1973, Document No. HEDL-SA-556.
59. W. N. McElroy and L. S. Kellog, "Fuels and Materials Fast-Reactor Dosimetry Data Development and Testing," Nuclear Technology, Vol. 25, pp. 180-223 (February 1975).
60. "Standard Method for Measuring Neutron Flux by Radioactivation Techniques," E261-70, American Society of Testing and Measurements, pp. 776-786 (1976 Annual).
61. R. E. Fortney and S. H. Levine, "A New Iterative Method for Unfolding Multiple Foil Activation Data," Trans. Am. Nuc. Soc., Vol. 13, No. 1, p. 432 (June-July 1970).

62. J. A. Halbleib, J. V. Walker and C. L. Greer, "Neutron Spectroscopy by Foil Activation in Radiation Effects Studies," SC-DC-67-1572, Sandia Corporation (July 1967).
63. James A. Grundl, "A Study of Fission-Neutron Spectra with High-Energy Activation Detectors--Part I. Detector Development and Excitation Measurements," Nuclear Science and Engineering, Vol. 30, pp. 39-53 (1967).
64. James A. Grundl, "A Study of Fission-Neutron Spectra with High-Energy Activation Detectors. Part II: Fission Spectra," Nuclear Science and Engineering, Vol. 31, pp. 191-206 (1968).
65. J. Grundl, "Spectral Index Measurements and the Extraction of Spectra," unpublished, July 22, 1971.
66. J. A. Grundl, D. M. Gilliam, N. D. Dudey and R. J. Popek, "Measurement of Absolute Fission Rates," Nuclear Technology, Vol. 25, pp. 237-257 (February 1975).
67. P. W. Benjamin, C. D. Kemshall and A. Brickstock, Analysis of Recoil Proton Spectra, Atomic Weapons Research Establishment, Aldermaston, England, Doc. No. AWRE-0-9/68 (March 1968).
68. Milton Abramowitz and Irene A. Stegun, Handbook of Mathematical Functions with Functions, Graphs, and Mathematical Tables, National Bureau of Standards No. 55, U.S. Government Printing Office, Washington, DC (1964).
69. L. Fox, The Use and Construction of Mathematical Tables, Vol. 1, National Physical Laboratory, Her Majesty's Stationery Office, London, England (1956).

CROSS SECTION LIBRARY DOSCROSS 77  
(IN THE SAND-II FORMAT)

W.L. Zijp, H.J. Nolthenius, N.J.C.M. van der Borg  
Netherlands Energy Research Foundation ECN  
Petten, Netherlands

Abstract:

In this report the dosimetry cross section library DOSCROSS77 is documented with tables, plots and cross section values averaged over a few reference spectra.

This library is based on the ENDF/B-IV dosimetry file, supplemented with some other evaluations.

The total number of reaction cross section sets incorporated in this library is 49 (+3 cover cross section sets).

The cross section data are available in a format which is suitable for the program SAND-II.

Keywords:

CROSS SECTIONS

NUCLEAR DATA COLLECTIONS

NEUTRON DOSIMETRY

NEUTRON REACTIONS

DATA COMPILATION

1. INTRODUCTION

The cross section library DOSCROSS77 is a combination of several cross section libraries which are available in the 620 groups SAND-II format [1]. The new library comprises 49 detector cross section sets and 3 cover cross section sets.

The basic content of this library is the ENDF/B-IV dosimetry file [2]. The cross section data sets of  $^{46}\text{Ti}(n,p)$ ,  $^{47}\text{Ti}(n,p)$ ,  $^{48}\text{Ti}(n,p)$  and  $^{115}\text{In}(n,n')$  of the ENDF/B-IV file have been replaced by more recent data in the DOSCROSS77.

Furthermore the ENDF/B-IV dosimetry file is supplemented with data from SAND-II (DETAN74), LAPENAS and from CESNEF cross section libraries. The origin of the cross section sets is given in table 51. The references refer to RCN and ECN reports, which give the numerical data and the plots of the cross section data sets in the same way as presented in this report. The three cover cross section sets originate from an older SAND-II library [1]. These cross section sets are required in the SAND-II program

for taking into account the influence of special detector surroundings such as cadmium, boron or/and gold.

## 2. NEW CROSS SECTION SETS

A new evaluation for the reaction  $^{115}\text{In}(n,n')$  is presented in [7]. This new data set is intended to be a part of the ENDF/B-V dosimetry file. The data are available in the form of point cross section values. The interpolation scheme is also given in [7]. With a small program point cross section values were calculated for all energy values of the SAND-II groups between the lowest and highest energy value of the input cross section data.

The point cross section data were calculated with the indicated interpolation scheme. With these data and the original data the average cross section was calculated for all successive energy intervals.

The average cross section was obtained by dividing the area by the energy width of the interval. The area was determined by linear or an exponential interpolation (according to input specification) between the boundary values of the interval.

If a SAND-II interval comprises more subintervals then the groups cross section is calculated as the weighted average of the subgroups. The weight factor is proportional with the energy widths of the subgroups.

The evaluation of the reactions  $^{46}\text{Ti}$ ,  $^{47}\text{Ti}$  and  $^{48}\text{Ti}$  [8] were converted with the same program. The interpolation scheme was not presented in this report. For this reason the scheme as presented in table 50 has been applied [9].

The output of the conversion program was used as input for the program CSTAPE of the SAND-II package [1].

## 3. COMBINATION OF THE CROSS SECTION SETS

A small program was applied to write the various group cross section sets on one file. This was performed in such a way that the file could be used as a SAND-II library.

## 4. PRESENTATION OF THE DATA

### 4.1. Cross section values

The cross section values of all sets are given in the tables 1 to 49.

These values are also shown as plots in the figures 1 to 49.

The numbers of the tables and plots which correspond to the different sets are given in table 51.

## 4.2. Characterization of the cross sections

In order to obtain some data for a quick comparison of the various cross section data sets the spectrum averaged cross sections are calculated for three theoretical spectral distributions:

- The Maxwell spectrum function at a temperature of 293 K:

$$\chi_M(E) = 1.5918 \times 10^{15} E \exp(-3.987 \times 10^7 E)$$

- The 1/E spectrum:

$$\chi_{1/E}(E) = 1/E \text{ between } 0.55 \times 10^{-6} \text{ and } 1 \text{ MeV;}$$

$$\chi_{1/E}(E) = 0 \text{ outside this energy interval.}$$

- The Watt fission neutron spectrum:

$$\chi_W(E) = 0.484 \sinh(\sqrt{2E}) \cdot e^{-E}.$$

In the expressions above E is expressed in MeV.

The average cross section values are presented in table 51. Furthermore this table presents the values for  $g \cdot \sigma_0$ . This value is calculated by multiplying the averaged cross section in the Maxwell spectrum by 1.128. This value is the ratio of the cross section at the averaged and the most probable speed in a Maxwell spectrum for a  $1/v$  cross section. When the value  $g \cdot \sigma_0$  is the same as  $\sigma_0$  (i.e. the cross section at 0.255 meV) (see tables 1...49), the cross section under consideration has a pure  $1/v$  shape.

## 6. REFERENCES

- |1| McElroy, W.N. et al.: "SAND-II neutron flux spectra determinations by multiple foil activation iterative method"  
RSIC Computer code collection CCC-112 (Oak Ridge National Laboratory, Radiation Shielding Centre, May 1969).
- |2| Magurno, B.A.: "ENDF/B-IV dosimetry file"  
BNL-NCS-50446 (National Neutron Cross Section Centre, New York, April 1975).
- |3| Rieffe, H.Ch.; H.J. Nolthenius: "Cross section library ENDF/B-IV BNL (in the SAND-II format)"  
RCN-75-157 (Reactor Centrum Nederland, Petten, December 1975).

- |4| Rieffe, H.Ch.; H.J. Nolthenius: "Cross section library DETAN74 (in the SAND-II format)"  
RCN-75-139 (Reactor Centrum Nederland, Petten, October 1975).
- |5| Kramer, L.G.A.; H.J. Nolthenius; W.L. Zijp: "Cross section library LAPENAS (presented in the SAND-II format)"  
RCN-76-020 (Reactor Centrum Nederland, Petten, January 1976).
- |6| Kramer, L.G.A.; H.J. Nolthenius: "Cross section library CESNEF (presented in the SAND-II format)"  
RCN-76-019 (Reactor Centrum Nederland, Petten, February 1976).
- |7| Smith, D.L.: "Evaluation of the IN-115(N,N')IN-115M reaction for the ENDF/B-IV dosimetry file"  
ANL/NDM-26 and erratum (Argonne National Laboratory, Argonne, December 1976).
- |8| Philis, C. et al.: "Evaluated (n,p) cross sections of  $^{46}\text{Ti}$ ,  $^{47}\text{Ti}$  and  $^{48}\text{Ti}^*$ "  
ANL/NDM-27 (Argonne National Laboratory, Argonne, January 1977).
- |9| Smith, D.L.: Private communication (1977-05-03).











Table 7:

REACTION	P31P	P31(N,P)SI31		REACTION	P31P	P31(N,P)SI31		REACTION	P31P	P31(N,P)SI31	
ENERGY	CROSSSECTION	ENERGY	CROSSSECTION	ENERGY	CROSSSECTION	ENERGY	CROSSSECTION	ENERGY	CROSSSECTION	ENERGY	CROSSSECTION
/MEV	/M**2	/MEV	/M**2	/MEV	/M**2	/MEV	/M**2	/MEV	/M**2	/MEV	/M**2
.150E+01	.112E-30	.160E+01	.337E-30	.170E+01	.562E-30	.180E+01	.787E-30	.190E+01	.118E-29	.200E+01	.146E-29
.200E+01	.175E-29	.210E+01	.242E-29	.220E+01	.317E-29	.230E+01	.391E-29	.240E+01	.463E-29	.250E+01	.546E-29
.250E+01	.567E-29	.260E+01	.704E-29	.270E+01	.763E-29	.280E+01	.743E-29	.290E+01	.799E-29	.300E+01	.868E-29
.300E+01	.931E-29	.310E+01	.963E-29	.320E+01	.895E-29	.330E+01	.863E-29	.340E+01	.868E-29	.350E+01	.987E-29
.400E+01	.932E-29	.410E+01	.962E-29	.420E+01	.108E-28	.430E+01	.116E-28	.440E+01	.121E-28	.450E+01	.118E-28
.500E+01	.111E-28	.510E+01	.111E-28	.520E+01	.118E-28	.530E+01	.123E-28	.540E+01	.126E-28	.550E+01	.134E-28
.600E+01	.134E-28	.610E+01	.135E-28	.620E+01	.135E-28	.630E+01	.135E-28	.640E+01	.135E-28	.650E+01	.134E-28
.700E+01	.134E-28	.710E+01	.133E-28	.720E+01	.133E-28	.730E+01	.133E-28	.740E+01	.132E-28	.750E+01	.132E-28
.800E+01	.132E-28	.810E+01	.132E-28	.820E+01	.132E-28	.830E+01	.132E-28	.840E+01	.132E-28	.850E+01	.135E-28
.900E+01	.137E-28	.910E+01	.138E-28	.920E+01	.140E-28	.930E+01	.140E-28	.940E+01	.140E-28	.950E+01	.138E-28
.100E+02	.130E-28	.101E+02	.137E-28	.102E+02	.136E-28	.103E+02	.135E-28	.104E+02	.134E-28	.105E+02	.129E-28
.110E+02	.126E-28	.111E+02	.125E-28	.112E+02	.123E-28	.113E+02	.122E-28	.114E+02	.120E-28	.115E+02	.117E-28
.120E+02	.112E-28	.121E+02	.110E-28	.122E+02	.109E-28	.123E+02	.108E-28	.124E+02	.106E-28	.125E+02	.967E-28
.130E+02	.984E-29	.131E+02	.971E-29	.132E+02	.957E-29	.133E+02	.944E-29	.134E+02	.931E-29	.135E+02	.879E-29
.140E+02	.857E-29	.141E+02	.845E-29	.142E+02	.833E-29	.143E+02	.821E-29	.144E+02	.809E-29	.145E+02	.753E-29
.150E+02	.742E-29	.151E+02	.731E-29	.152E+02	.720E-29	.153E+02	.709E-29	.154E+02	.698E-29	.155E+02	.643E-29
.160E+02	.633E-29	.161E+02	.622E-29	.162E+02	.611E-29	.163E+02	.600E-29	.164E+02	.569E-29	.165E+02	.532E-29
.170E+02	.520E-29	.171E+02	.509E-29	.172E+02	.497E-29	.173E+02	.485E-29	.174E+02	.474E-29	.175E+02	.416E-29

Table 8:

REACTION	S32P4	S32(N,P)P32		REACTION	S32P4	S32(N,P)P32		REACTION	S32P4	S32(N,P)P32	
ENERGY	CROSSSECTION	ENERGY	CROSSSECTION	ENERGY	CROSSSECTION	ENERGY	CROSSSECTION	ENERGY	CROSSSECTION	ENERGY	CROSSSECTION
/MEV	/M**2	/MEV	/M**2	/MEV	/M**2	/MEV	/M**2	/MEV	/M**2	/MEV	/M**2
.800E+00	0.	.840E+00	0.	.880E+00	0.	.920E+00	.335E-35	.960E+00	.685E-33	.100E+01	.350E-31
.150E+01	.189E-32	.160E+01	.137E-30	.170E+01	.290E-30	.180E+01	.590E-30	.190E+01	.111E-29	.200E+01	.179E-29
.250E+01	.220E-29	.260E+01	.407E-29	.270E+01	.630E-29	.280E+01	.896E-29	.290E+01	.111E-28	.300E+01	.111E-28
.350E+01	.760E-29	.360E+01	.725E-29	.370E+01	.975E-29	.380E+01	.111E-28	.390E+01	.290E+01	.400E+01	.203E-28
.400E+01	.155E-28	.410E+01	.161E-28	.420E+01	.150E-28	.430E+01	.211E-28	.440E+01	.340E+01	.450E+01	.227E-28
.450E+01	.220E-28	.460E+01	.224E-28	.470E+01	.188E-28	.480E+01	.175E-28	.490E+01	.390E+01	.500E+01	.306E-28
.500E+01	.287E-28	.510E+01	.319E-28	.520E+01	.341E-28	.530E+01	.336E-28	.540E+01	.440E+01	.550E+01	.235E-28
.550E+01	.271E-28	.560E+01	.249E-28	.570E+01	.240E-28	.580E+01	.236E-28	.590E+01	.239E-28	.600E+01	.249E-28
.650E+01	.268E-28	.660E+01	.283E-28	.670E+01	.296E-28	.680E+01	.305E-28	.690E+01	.309E-28	.700E+01	.309E-28
.750E+01	.311E-28	.760E+01	.312E-28	.770E+01	.312E-28	.780E+01	.313E-28	.790E+01	.314E-28	.800E+01	.314E-28
.800E+01	.314E-28	.810E+01	.315E-28	.820E+01	.315E-28	.830E+01	.315E-28	.840E+01	.315E-28	.850E+01	.316E-28
.850E+01	.316E-28	.860E+01	.317E-28	.870E+01	.318E-28	.880E+01	.318E-28	.890E+01	.319E-28	.900E+01	.320E-28
.900E+01	.320E-28	.910E+01	.321E-28	.920E+01	.322E-28	.930E+01	.323E-28	.940E+01	.324E-28	.950E+01	.324E-28
.950E+01	.325E-28	.960E+01	.326E-28	.970E+01	.327E-28	.980E+01	.328E-28	.990E+01	.329E-28	.100E+02	.330E-28
.100E+02	.331E-28	.101E+02	.333E-28	.102E+02	.335E-28	.103E+02	.337E-28	.104E+02	.339E-28	.105E+02	.343E-28
.110E+02	.341E-28	.111E+02	.344E-28	.112E+02	.347E-28	.113E+02	.350E-28	.114E+02	.353E-28	.115E+02	.353E-28
.120E+02	.356E-28	.121E+02	.359E-28	.122E+02	.362E-28	.123E+02	.365E-28	.124E+02	.368E-28	.125E+02	.368E-28
.130E+02	.371E-28	.131E+02	.374E-28	.132E+02	.376E-28	.133E+02	.378E-28	.134E+02	.381E-28	.135E+02	.381E-28
.140E+02	.382E-28	.141E+02	.383E-28	.142E+02	.383E-28	.143E+02	.384E-28	.144E+02	.385E-28	.145E+02	.385E-28
.150E+02	.385E-28	.151E+02	.385E-28	.152E+02	.384E-28	.153E+02	.384E-28	.154E+02	.384E-28	.155E+02	.384E-28
.160E+02	.382E-28	.161E+02	.379E-28	.162E+02	.375E-28	.163E+02	.371E-28	.164E+02	.368E-28	.165E+02	.368E-28
.170E+02	.362E-28	.171E+02	.355E-28	.172E+02	.347E-28	.173E+02	.339E-28	.174E+02	.332E-28	.175E+02	.332E-28
.180E+02	.326E-28	.181E+02	.322E-28	.182E+02	.318E-28	.183E+02	.314E-28	.184E+02	.310E-28	.185E+02	.310E-28
.190E+02	.305E-28	.191E+02	.300E-28	.192E+02	.294E-28	.193E+02	.288E-28	.194E+02	.283E-28	.195E+02	.283E-28
.200E+02	.277E-28	.201E+02	.272E-28	.202E+02	.266E-28	.203E+02	.261E-28	.204E+02	.256E-28	.205E+02	.256E-28
.210E+02	.250E-28	.211E+02	.245E-28	.212E+02	.239E-28	.213E+02	.233E-28	.214E+02	.228E-28	.215E+02	.228E-28
.220E+02	.223E-28	.221E+02	.220E-28	.222E+02	.217E-28	.223E+02	.214E-28	.224E+02	.211E-28	.225E+02	.211E-28
.230E+02	.208E-28	.231E+02	.203E-28	.232E+02	.198E-28	.233E+02	.194E-28	.234E+02	.189E-28	.235E+02	.189E-28
.240E+02	.185E-28	.241E+02	.180E-28	.242E+02	.175E-28	.243E+02	.171E-28	.244E+02	.166E-28	.245E+02	.166E-28
.250E+02	.162E-28	.251E+02	.158E-28	.252E+02	.155E-28	.253E+02	.151E-28	.254E+02	.147E-28	.255E+02	.147E-28
.260E+02	.144E-28	.261E+02	.140E-28	.262E+02	.136E-28	.263E+02	.132E-28	.264E+02	.129E-28	.265E+02	.129E-28
.270E+02	.126E-28	.271E+02	.123E-28	.272E+02	.120E-28	.273E+02	.118E-28	.274E+02	.115E-28	.275E+02	.115E-28
.280E+02	.113E-28	.281E+02	.110E-28	.282E+02	.107E-28	.283E+02	.105E-28	.284E+02	.102E-28	.285E+02	.102E-28



Table 10:

REACTION	ENERGY /MEV	CROSSSECTION /M**2	ENERGY /MEV	CROSSSECTION /M**2	ENERGY /MEV	CROSSSECTION /M**2	ENERGY /MEV	CROSSSECTION /M**2	ENERGY /MEV	CROSSSECTION /M**2
II46P5	II46(N,P)SC46									
	0.									
	•150E+01	•160E+01	•147-118	•170E+01	•106-106	•180E+01	•761E-95	•190E+01	•548E-83	
	•200E+01	•210E+01	•283E-59	•220E+01	•204E-47	•230E+01	•147E-35	•240E+01	•676E-34	
	•250E+01	•260E+01	•472E-33	•270E+01	•144E-32	•280E+01	•799E-32	•290E+01	•469E-31	
	•300E+01	•310E+01	•207E-30	•320E+01	•327E-30	•330E+01	•473E-30	•340E+01	•674E-30	
	•350E+01	•360E+01	•114E-29	•370E+01	•145E-29	•380E+01	•183E-29	•390E+01	•232E-29	
	•400E+01	•410E+01	•313E-29	•420E+01	•353E-29	•430E+01	•400E-29	•440E+01	•452E-29	
	•450E+01	•460E+01	•544E-29	•470E+01	•592E-29	•480E+01	•644E-29	•490E+01	•700E-29	
	•500E+01	•510E+01	•800E-29	•520E+01	•850E-29	•530E+01	•904E-29	•540E+01	•960E-29	
	•550E+01	•560E+01	•106E-28	•570E+01	•111E-28	•580E+01	•116E-28	•590E+01	•121E-28	
	•600E+01	•610E+01	•131E-28	•620E+01	•136E-28	•630E+01	•142E-28	•640E+01	•147E-28	
	•650E+01	•660E+01	•157E-28	•670E+01	•161E-28	•680E+01	•166E-28	•690E+01	•171E-28	
	•700E+01	•710E+01	•178E-28	•720E+01	•181E-28	•730E+01	•185E-28	•740E+01	•188E-28	
	•750E+01	•760E+01	•195E-28	•770E+01	•199E-28	•780E+01	•202E-28	•790E+01	•206E-28	
	•800E+01	•810E+01	•212E-28	•820E+01	•214E-28	•830E+01	•216E-28	•840E+01	•219E-28	
	•850E+01	•860E+01	•224E-28	•870E+01	•226E-28	•880E+01	•228E-28	•890E+01	•231E-28	
	•900E+01	•910E+01	•235E-28	•920E+01	•237E-28	•930E+01	•239E-28	•940E+01	•241E-28	
	•950E+01	•960E+01	•245E-28	•970E+01	•247E-28	•980E+01	•249E-28	•990E+01	•251E-28	
	•100E+02	•101E+02	•254E-28	•102E+02	•255E-28	•103E+02	•256E-28	•104E+02	•257E-28	
	•105E+02	•106E+02	•260E-28	•107E+02	•261E-28	•108E+02	•262E-28	•109E+02	•263E-28	
	•110E+02	•111E+02	•265E-28	•112E+02	•265E-28	•113E+02	•266E-28	•114E+02	•267E-28	
	•115E+02	•116E+02	•268E-28	•117E+02	•268E-28	•118E+02	•269E-28	•119E+02	•270E-28	
	•120E+02	•121E+02	•270E-28	•122E+02	•270E-28	•123E+02	•269E-28	•124E+02	•269E-28	
	•125E+02	•126E+02	•269E-28	•127E+02	•269E-28	•128E+02	•268E-28	•129E+02	•268E-28	
	•130E+02	•131E+02	•267E-28	•132E+02	•266E-28	•133E+02	•265E-28	•134E+02	•264E-28	
	•135E+02	•136E+02	•263E-28	•137E+02	•262E-28	•138E+02	•261E-28	•139E+02	•260E-28	
	•140E+02	•141E+02	•258E-28	•142E+02	•256E-28	•143E+02	•255E-28	•144E+02	•253E-28	
	•145E+02	•146E+02	•250E-28	•147E+02	•249E-28	•148E+02	•247E-28	•149E+02	•246E-28	
	•150E+02	•151E+02	•242E-28	•152E+02	•241E-28	•153E+02	•239E-28	•154E+02	•237E-28	
	•155E+02	•156E+02	•234E-28	•157E+02	•232E-28	•158E+02	•230E-28	•159E+02	•228E-28	
	•160E+02	•161E+02	•225E-28	•162E+02	•223E-28	•163E+02	•221E-28	•164E+02	•220E-28	
	•165E+02	•166E+02	•216E-28	•167E+02	•214E-28	•168E+02	•213E-28	•169E+02	•211E-28	
	•170E+02	•171E+02	•207E-28	•172E+02	•205E-28	•173E+02	•203E-28	•174E+02	•201E-28	
	•175E+02	•176E+02	•198E-28	•177E+02	•196E-28	•178E+02	•194E-28	•179E+02	•192E-28	









Table 17:

REACTION	MN53 24	MN55 (N, 2N)	MN54	REACTION	MN53 24	MN55 (N, 2N)	MN54	REACTION	MN53 24	MN55 (N, 2N)	MN54
ENERGY /MEV	CROSSSECTION /M**2	ENERGY /MEV	CROSSSECTION /M**2	ENERGY /MEV	CROSSSECTION /M**2	ENERGY /MEV	CROSSSECTION /M**2	ENERGY /MEV	CROSSSECTION /M**2	ENERGY /MEV	CROSSSECTION /M**2
.100E+02	0.	.101E+02	0.	.102E+02	0.	.103E+02	0.	.104E+02	.339E-30	.105E+02	.783E-29
.105E+02	.122E-29	.106E+02	.238E-29	.107E+02	.389E-29	.108E+02	.570E-29	.109E+02	.114E+02	.114E+02	.225E-28
.110E+02	.103E-28	.111E+02	.132E-28	.112E+02	.161E-28	.113E+02	.191E-28	.114E+02	.119E+02	.119E+02	.391E-28
.115E+02	.250E-28	.116E+02	.292E-28	.117E+02	.325E-28	.118E+02	.358E-28	.119E+02	.124E+02	.124E+02	.526E-28
.120E+02	.422E-28	.121E+02	.449E-28	.122E+02	.477E-28	.123E+02	.503E-28	.124E+02	.129E+02	.129E+02	.627E-28
.125E+02	.548E-28	.126E+02	.570E-28	.127E+02	.590E-28	.128E+02	.608E-28	.129E+02	.134E+02	.134E+02	.704E-28
.130E+02	.644E-28	.131E+02	.659E-28	.132E+02	.675E-28	.133E+02	.690E-28	.134E+02	.139E+02	.139E+02	.763E-28
.135E+02	.717E-28	.136E+02	.730E-28	.137E+02	.741E-28	.138E+02	.752E-28	.139E+02	.144E+02	.144E+02	.807E-28
.140E+02	.773E-28	.141E+02	.782E-28	.142E+02	.791E-28	.143E+02	.800E-28	.144E+02	.149E+02	.149E+02	.839E-28
.145E+02	.814E-28	.146E+02	.821E-28	.147E+02	.827E-28	.148E+02	.833E-28	.149E+02	.154E+02	.154E+02	.862E-28
.150E+02	.844E-28	.151E+02	.849E-28	.152E+02	.854E-28	.153E+02	.858E-28	.154E+02	.159E+02	.159E+02	.878E-28
.155E+02	.866E-28	.156E+02	.869E-28	.157E+02	.872E-28	.158E+02	.875E-28	.159E+02	.164E+02	.164E+02	.889E-28
.160E+02	.881E-28	.161E+02	.883E-28	.162E+02	.885E-28	.163E+02	.887E-28	.164E+02	.169E+02	.169E+02	.897E-28
.165E+02	.891E-28	.166E+02	.893E-28	.167E+02	.895E-28	.168E+02	.896E-28	.169E+02	.174E+02	.174E+02	.908E-28
.170E+02	.898E-28	.171E+02	.899E-28	.172E+02	.900E-28	.173E+02	.900E-28	.174E+02	.179E+02	.179E+02	.908E-28
.175E+02	.900E-28	.176E+02	.900E-28	.177E+02	.900E-28	.178E+02	.900E-28	.179E+02			

Table 18:

REACTION	FE56 P4	FE56 (N,P)	MN56	REACTION	FE56 P4	FE56 (N,P)	MN56	REACTION	FE56 P4	FE56 (N,P)	MN56
ENERGY /MEV	CROSSSECTION /M**2	ENERGY /MEV	CROSSSECTION /M**2	ENERGY /MEV	CROSSSECTION /M**2	ENERGY /MEV	CROSSSECTION /M**2	ENERGY /MEV	CROSSSECTION /M**2	ENERGY /MEV	CROSSSECTION /M**2
.250E+01	0.	.260E+01	0.	.270E+01	0.	.280E+01	0.	.290E+01	.165E-35	.300E+01	.520E-34
.300E+01	.130E-34	.310E+01	.180E-34	.320E+01	.252E-34	.330E+01	.357E-34	.340E+01	.390E+01	.390E+01	.620E-33
.350E+01	.800E-34	.360E+01	.124E-33	.370E+01	.200E-33	.380E+01	.345E-33	.390E+01	.440E+01	.440E+01	.121E-31
.400E+01	.100E-32	.410E+01	.205E-32	.420E+01	.425E-32	.430E+01	.745E-32	.440E+01	.490E+01	.490E+01	.105E-30
.450E+01	.194E-31	.460E+01	.306E-31	.470E+01	.465E-31	.480E+01	.717E-31	.490E+01	.540E+01	.540E+01	.515E-30
.500E+01	.146E-30	.510E+01	.192E-30	.520E+01	.271E-30	.530E+01	.389E-30	.540E+01	.109E-29	.109E-29	.124E-29
.550E+01	.548E-30	.560E+01	.789E-30	.570E+01	.936E-30	.580E+01	.109E-29	.590E+01	.640E+01	.640E+01	.206E-29
.600E+01	.140E-29	.610E+01	.156E-29	.620E+01	.172E-29	.630E+01	.189E-29	.640E+01	.690E+01	.690E+01	.288E-29
.650E+01	.223E-29	.660E+01	.239E-29	.670E+01	.256E-29	.680E+01	.272E-29	.690E+01	.740E+01	.740E+01	.364E-29
.700E+01	.304E-29	.710E+01	.319E-29	.720E+01	.334E-29	.730E+01	.349E-29	.740E+01	.420E-29	.420E-29	.433E-29
.750E+01	.379E-29	.760E+01	.392E-29	.770E+01	.406E-29	.780E+01	.420E-29	.790E+01	.485E-29	.485E-29	.498E-29
.800E+01	.446E-29	.810E+01	.459E-29	.820E+01	.472E-29	.830E+01	.485E-29	.840E+01	.548E-29	.548E-29	.561E-29
.850E+01	.510E-29	.860E+01	.523E-29	.870E+01	.535E-29	.880E+01	.548E-29	.890E+01	.613E-29	.613E-29	.626E-29
.900E+01	.574E-29	.910E+01	.587E-29	.920E+01	.600E-29	.930E+01	.613E-29	.940E+01	.684E-29	.684E-29	.699E-29
.950E+01	.640E-29	.960E+01	.655E-29	.970E+01	.669E-29	.980E+01	.684E-29	.990E+01	.763E-29	.763E-29	.779E-29
.100E+02	.714E-29	.101E+02	.730E-29	.102E+02	.746E-29	.103E+02	.763E-29	.104E+02	.846E-29	.846E-29	.863E-29
.105E+02	.795E-29	.106E+02	.812E-29	.107E+02	.829E-29	.108E+02	.846E-29	.109E+02	.931E-29	.931E-29	.948E-29
.110E+02	.880E-29	.111E+02	.897E-29	.112E+02	.914E-29	.113E+02	.931E-29	.114E+02	.101E-28	.101E-28	.102E-28
.115E+02	.963E-29	.116E+02	.978E-29	.117E+02	.993E-29	.118E+02	.101E-28	.119E+02	.107E-28	.107E-28	.108E-28
.120E+02	.104E-28	.121E+02	.105E-28	.122E+02	.106E-28	.123E+02	.107E-28	.124E+02	.114E-28	.114E-28	.114E-28
.125E+02	.109E-28	.126E+02	.110E-28	.127E+02	.111E-28	.128E+02	.112E-28	.129E+02	.114E-28	.114E-28	.114E-28
.130E+02	.113E-28	.131E+02	.113E-28	.132E+02	.114E-28	.133E+02	.114E-28	.134E+02	.112E-28	.112E-28	.112E-28
.135E+02	.113E-28	.136E+02	.113E-28	.137E+02	.113E-28	.138E+02	.112E-28	.139E+02	.108E-28	.108E-28	.107E-28
.140E+02	.111E-28	.141E+02	.110E-28	.142E+02	.109E-28	.143E+02	.108E-28	.144E+02	.102E-28	.102E-28	.100E-28
.145E+02	.105E-28	.146E+02	.104E-28	.147E+02	.103E-28	.148E+02	.102E-28	.149E+02	.933E-29	.933E-29	.916E-29
.150E+02	.985E-29	.151E+02	.968E-29	.152E+02	.950E-29	.153E+02	.933E-29	.154E+02	.845E-29	.845E-29	.827E-29
.155E+02	.898E-29	.156E+02	.880E-29	.157E+02	.862E-29	.158E+02	.845E-29	.159E+02	.779E-29	.779E-29	.768E-29
.160E+02	.812E-29	.161E+02	.801E-29	.162E+02	.790E-29	.163E+02	.779E-29	.164E+02	.713E-29	.713E-29	.699E-29
.165E+02	.755E-29	.166E+02	.741E-29	.167E+02	.727E-29	.168E+02	.713E-29	.169E+02	.652E-29	.652E-29	.641E-29
.170E+02	.686E-29	.171E+02	.675E-29	.172E+02	.663E-29	.173E+02	.652E-29	.174E+02	.603E-29	.603E-29	.594E-29
.175E+02	.630E-29	.176E+02	.621E-29	.177E+02	.612E-29	.178E+02	.603E-29	.179E+02			

Table 19:

REACTION	FE58G4	FE58 UN	G1FE59								
ENERGY	CROSSSECTION	ENERGY	CROSSSECTION	ENERGY	CROSSSECTION	ENERGY	CROSSSECTION	ENERGY	CROSSSECTION	ENERGY	CROSSSECTION
/MEV	/M**2	/MEV	/M**2	/MEV	/M**2	/MEV	/M**2	/MEV	/M**2	/MEV	/M**2
100E-09	1.88E-26	1.05E-09	1.81E-26	1.10E-09	1.177E-26	1.15E-09	1.173E-26	1.20E-09	1.163E-26	1.16E-09	1.166E-26
120E-09	1.64E-26	1.35E-09	1.49E-26	1.43E-09	1.55E-26	1.50E-09	1.50E-26	1.60E-09	1.46E-26	1.46E-09	1.46E-26
170E-09	1.10E-26	1.00E-09	1.10E-26	1.90E-09	1.10E-26	1.90E-09	1.11E-26	2.10E-09	1.13E-26	2.10E-09	1.13E-26
230E-09	1.25E-26	2.30E-09	1.22E-26	2.40E-09	1.19E-26	2.55E-09	1.16E-26	2.70E-09	1.13E-26	2.70E-09	1.13E-26
280E-09	1.10E-26	3.00E-09	1.06E-26	3.20E-09	1.03E-26	3.40E-09	1.00E-26	3.60E-09	9.74E-27	3.60E-09	9.74E-27
380E-09	9.49E-27	4.00E-09	9.23E-27	4.25E-09	8.97E-27	4.50E-09	8.72E-27	4.75E-09	8.45E-27	4.75E-09	8.45E-27
500E-09	8.29E-27	5.25E-09	8.09E-27	5.50E-09	7.91E-27	5.75E-09	7.73E-27	6.00E-09	7.56E-27	6.00E-09	7.56E-27
630E-09	7.38E-27	6.60E-09	7.22E-27	6.90E-09	7.06E-27	7.20E-09	6.89E-27	7.40E-09	6.71E-27	7.40E-09	6.71E-27
800E-09	6.55E-27	8.40E-09	6.39E-27	8.80E-09	6.25E-27	9.20E-09	6.12E-27	9.60E-09	5.99E-27	9.60E-09	5.99E-27
100E-08	5.86E-27	1.05E-08	5.72E-27	1.10E-08	5.59E-27	1.15E-08	5.47E-27	1.20E-08	5.33E-27	1.20E-08	5.33E-27
128E-08	5.18E-27	1.35E-08	5.03E-27	1.43E-08	4.90E-27	1.50E-08	4.76E-27	1.60E-08	4.62E-27	1.60E-08	4.62E-27
170E-08	4.49E-27	1.80E-08	4.36E-27	1.90E-08	4.25E-27	2.00E-08	4.14E-27	2.10E-08	4.05E-27	2.10E-08	4.05E-27
220E-08	3.95E-27	2.30E-08	3.82E-27	2.40E-08	3.71E-27	2.55E-08	3.66E-27	2.70E-08	3.58E-27	2.70E-08	3.58E-27
280E-08	3.41E-27	3.00E-08	3.32E-27	3.20E-08	3.27E-27	3.40E-08	3.17E-27	3.60E-08	3.08E-27	3.60E-08	3.08E-27
380E-08	3.01E-27	4.00E-08	2.92E-27	4.25E-08	2.84E-27	4.50E-08	2.76E-27	4.75E-08	2.69E-27	4.75E-08	2.69E-27
500E-08	2.62E-27	5.25E-08	2.56E-27	5.50E-08	2.50E-27	5.75E-08	2.45E-27	6.00E-08	2.39E-27	6.00E-08	2.39E-27
630E-08	2.34E-27	6.60E-08	2.29E-27	6.90E-08	2.23E-27	7.20E-08	2.18E-27	7.40E-08	2.13E-27	7.40E-08	2.13E-27
800E-08	2.07E-27	8.40E-08	2.02E-27	8.80E-08	1.98E-27	9.20E-08	1.94E-27	9.60E-08	1.90E-27	9.60E-08	1.90E-27
100E-07	1.86E-27	1.05E-07	1.81E-27	1.10E-07	1.77E-27	1.15E-07	1.73E-27	1.20E-07	1.69E-27	1.20E-07	1.69E-27
128E-07	1.64E-27	1.35E-07	1.59E-27	1.43E-07	1.55E-27	1.50E-07	1.51E-27	1.60E-07	1.46E-27	1.60E-07	1.46E-27
170E-07	1.42E-27	1.80E-07	1.38E-27	1.90E-07	1.35E-27	2.00E-07	1.31E-27	2.10E-07	1.28E-27	2.10E-07	1.28E-27
220E-07	1.25E-27	2.30E-07	1.23E-27	2.40E-07	1.19E-27	2.55E-07	1.16E-27	2.70E-07	1.13E-27	2.70E-07	1.13E-27
280E-07	1.10E-27	3.00E-07	1.07E-27	3.20E-07	1.04E-27	3.40E-07	1.00E-27	3.60E-07	9.77E-28	3.60E-07	9.77E-28
380E-07	9.52E-28	4.00E-07	9.25E-28	4.25E-07	8.95E-28	4.50E-07	8.74E-28	4.75E-07	8.50E-28	4.75E-07	8.50E-28
500E-07	8.29E-28	5.25E-07	8.10E-28	5.50E-07	7.91E-28	5.75E-07	7.75E-28	6.00E-07	7.59E-28	6.00E-07	7.59E-28
630E-07	7.41E-28	6.60E-07	7.23E-28	6.90E-07	7.06E-28	7.20E-07	6.91E-28	7.40E-07	6.73E-28	7.40E-07	6.73E-28
800E-07	6.55E-28	8.40E-07	6.40E-28	8.80E-07	6.28E-28	9.20E-07	6.15E-28	9.60E-07	6.03E-28	9.60E-07	6.03E-28
100E-06	5.89E-28	1.05E-06	5.74E-28	1.10E-06	5.59E-28	1.15E-06	5.48E-28	1.20E-06	5.35E-28	1.20E-06	5.35E-28
128E-06	5.19E-28	1.35E-06	5.03E-28	1.43E-06	4.90E-28	1.50E-06	4.77E-28	1.60E-06	4.61E-28	1.60E-06	4.61E-28
170E-06	4.49E-28	1.80E-06	4.38E-28	1.90E-06	4.27E-28	2.00E-06	4.17E-28	2.10E-06	4.05E-28	2.10E-06	4.05E-28
220E-06	3.95E-28	2.30E-06	3.87E-28	2.40E-06	3.77E-28	2.55E-06	3.66E-28	2.70E-06	3.57E-28	2.70E-06	3.57E-28
280E-06	3.41E-28	3.00E-06	3.37E-28	3.20E-06	3.26E-28	3.40E-06	3.17E-28	3.60E-06	3.09E-28	3.60E-06	3.09E-28
380E-06	3.01E-28	4.00E-06	2.93E-28	4.25E-06	2.83E-28	4.50E-06	2.75E-28	4.75E-06	2.69E-28	4.75E-06	2.69E-28
500E-06	2.62E-28	5.25E-06	2.56E-28	5.50E-06	2.52E-28	5.75E-06	2.47E-28	6.00E-06	2.42E-28	6.00E-06	2.42E-28
630E-06	2.34E-28	6.60E-06	2.29E-28	6.90E-06	2.23E-28	7.20E-06	2.18E-28	7.40E-06	2.13E-28	7.40E-06	2.13E-28
800E-06	2.07E-28	8.40E-06	2.01E-28	8.80E-06	1.95E-28	9.20E-06	1.92E-28	9.60E-06	1.88E-28	9.60E-06	1.88E-28
100E-05	1.86E-28	1.05E-05	1.81E-28	1.10E-05	1.77E-28	1.15E-05	1.73E-28	1.20E-05	1.69E-28	1.20E-05	1.69E-28
128E-05	1.62E-28	1.35E-05	1.57E-28	1.43E-05	1.54E-28	1.50E-05	1.49E-28	1.60E-05	1.44E-28	1.60E-05	1.44E-28
170E-05	1.40E-28	1.80E-05	1.36E-28	1.90E-05	1.33E-28	2.00E-05	1.30E-28	2.10E-05	1.27E-28	2.10E-05	1.27E-28
220E-05	1.24E-28	2.30E-05	1.21E-28	2.40E-05	1.18E-28	2.55E-05	1.13E-28	2.70E-05	1.10E-28	2.70E-05	1.10E-28
280E-05	1.04E-28	3.00E-05	1.04E-28	3.20E-05	1.01E-28	3.40E-05	9.71E-29	3.60E-05	9.45E-29	3.60E-05	9.45E-29
380E-05	9.29E-29	4.00E-05	9.10E-29	4.25E-05	8.89E-29	4.50E-05	8.68E-29	4.75E-05	8.47E-29	4.75E-05	8.47E-29
500E-05	8.26E-29	5.25E-05	8.05E-29	5.50E-05	7.84E-29	5.75E-05	7.63E-29	6.00E-05	7.40E-29	6.00E-05	7.40E-29
630E-05	7.45E-29	6.60E-05	7.25E-29	6.90E-05	7.04E-29	7.20E-05	6.86E-29	7.40E-05	6.64E-29	7.40E-05	6.64E-29
800E-05	6.55E-29	8.40E-05	6.39E-29	8.80E-05	6.19E-29	9.20E-05	6.00E-29	9.60E-05	5.79E-29	9.60E-05	5.79E-29
100E-04	5.95E-29	1.05E-04	5.80E-29	1.10E-04	5.62E-29	1.15E-04	5.43E-29	1.20E-04	5.24E-29	1.20E-04	5.24E-29
128E-04	5.25E-29	1.35E-04	5.10E-29	1.43E-04	4.93E-29	1.50E-04	4.74E-29	1.60E-04	4.55E-29	1.60E-04	4.55E-29
170E-04	4.49E-29	1.80E-04	4.38E-29	1.90E-04	4.27E-29	2.00E-04	4.17E-29	2.10E-04	4.05E-29	2.10E-04	4.05E-29
220E-04	3.95E-29	2.30E-04	3.87E-29	2.40E-04	3.77E-29	2.55E-04	3.66E-29	2.70E-04	3.57E-29	2.70E-04	3.57E-29
280E-04	3.41E-29	3.00E-04	3.37E-29	3.20E-04	3.26E-29	3.40E-04	3.17E-29	3.60E-04	3.09E-29	3.60E-04	3.09E-29
380E-04	3.01E-29	4.00E-04	2.93E-29	4.25E-04	2.83E-29	4.50E-04	2.75E-29	4.75E-04	2.69E-29	4.75E-04	2.69E-29
500E-04	2.62E-29	5.25E-04	2.56E-29	5.50E-04	2.50E-29	5.75E-04	2.45E-29	6.00E-04	2.39E-29	6.00E-04	2.39E-29
630E-04	2.34E-29	6.60E-04	2.29E-29	6.90E-04	2.23E-29	7.20E-04	2.18E-29	7.40E-04	2.13E-29	7.40E-04	2.13E-29
800E-04	2.07E-29	8.40E-04	2.01E-29	8.80E-04	1.95E-29	9.20E-04	1.92E-29	9.60E-04	1.88E-29	9.60E-04	1.88E-29
100E-03	1.86E-29	1.05E-03	1.81E-29	1.10E-03	1.77E-29	1.15E-03	1.73E-29	1.20E-03	1.69E-29	1.20E-03	1.69E-29
128E-03	1.62E-29	1.35E-03	1.57E-29	1.43E-03	1.54E-29	1.50E-03	1.49E-29	1.60E-03	1.44E-29	1.60E-03	1.44E-29
170E-03	1.40E-29	1.80E-03	1.36E-29	1.90E-03	1.33E-29	2.00E-03	1.30E-29	2.10E-03	1.27E-29	2.10E-03	1.27E-29
220E-03	1.24E-29	2.30E-03	1.21E-29	2.40E-03	1.18E-29	2.55E-03	1.13E-29	2.70E-03	1.10E-29	2.70E-03	1.10E-29
280E-03	1.04E-29	3.00E-03	1.04E-29	3.20E-03	1.01E-29	3.40E-03	9.71E-30	3.60E-03	9.45E-30	3.60E-03	9.45E-30
380E-03	9.29E-30	4.00E-03	9.10E-30	4.25E-03	8.89E-30	4.50E-03	8.68E-30	4.75E-03	8.47E-30	4.75E-03	8.47E-30
500E-03	8.26E-30	5.25E-03	8.05E-30	5.50E-03	7.84E-30	5.75E-03	7.63E-30	6.00E-03	7.40E-30	6.00E-03	7.40E-30
630E-03	7.45E-30	6.60E-03	7.25E-30	6.90E-03	7.04E-30	7.20E-03	6.86E-30	7.40E-03	6.64E-30	7.40E-03	6.64E-30
800E-03	6.55E-30	8.40E-03	6.39E-30	8.80E-03	6.19E-30	9.20E-03	6.00E-30	9.60E-03	5.79E-30	9.60E-03	5.79E-30
100E-02	5.95E-30	1.05E-02	5.80E-30	1.10E-02	5.62E-30	1.15E-02	5.43E-30	1.20E-02	5.24E-30	1.20E-02	5.24E-30
128E-02	5.25E-30	1.35E-02	5.10E-30	1.43E-02	4.93E-30	1.50E-02	4.74E-30	1.60E-02	4.55E-30	1.60E-02	4.55E-30
170E-02	4.49E-30	1.80E-02	4.38E-30	1.90E-02	4.27E-30	2.00E-02	4.17E-30	2.10E-02	4.05E-30	2.10E-02	4.05E-30
220E-02	3.95E-30	2.30E-02	3.87E-30	2.40E-02	3.77E-30	2.55E-02	3.66E-30	2.70E-02	3.57E-30	2.70E-02	3.57E-30
280E-02	3.41E-30	3.00E-02	3.37E-30	3.20E-02	3.26E-30	3.40E-02	3.17E-30	3.60E-02	3.09E-30	3.60E-02	3.09E-30
380E-02	3.01E-30	4.00E-02	2.93E-30	4.25E-02	2.83E-30	4.50E-02	2.75E-30	4.75E-02	2.69E-30	4.75E-02	2.69E-30
500E-02	2.62E-30	5.25E-02	2.56E-30	5.50E-02	2.50E-30	5.75E-02	2.45E-30	6.00E-02	2.39E-30	6.00E-02	2.39E-30
630E-02	2.34E-30	6.60E-02	2.29E-30	6.90E-02	2.23E-30	7.20E-02	2.18E-30	7.40E-02	2.13E-30	7.40E-02	2.13E-30
800E-02	2.07E-30	8.40E-02	2.01E-30	8.80E-02	1.95E-30	9.20E-02	1.92E-30	9.60E-02	1.88E-30	9.60E-02	1.88E-30
100E-01	1.86E-30	1.05E-01	1.81E-30	1.10E-01	1.77E-30	1.15E-01	1.73E-30	1.20E-01	1.69E-30	1.20E-01	1.69E-30
128E-01	1.62E-30	1.35E-01	1.57E-30	1.43E-01	1.54E-30	1.50E-01	1.49E-30	1.60E-01	1.44E-30	1.60E-01	1.44E-30
170E-01	1.40E-30	1.80E-01	1.36E-30	1.90E-01	1.33E-30	2.00E-01	1.30E-30	2.10E-01	1.27E-30	2.10E-01	1.27E-30

Table 20:

REACTION	NI58 2%	NI58 (N,2N) NI57	REACTION	NI58 2%	NI58 (N,2N) NI57	REACTION	NI58 2%	NI58 (N,2N) NI57	REACTION	NI58 2%	NI58 (N,2N) NI57
ENERGY /MEV	CROSSSECTION /M**2	ENERGY /MEV	CROSSSECTION /M**2	ENERGY /MEV	CROSSSECTION /M**2	ENERGY /MEV	CROSSSECTION /M**2	ENERGY /MEV	CROSSSECTION /M**2	ENERGY /MEV	CROSSSECTION /M**2
.120E+02	0.	.121E+02	0.	.122E+02	0.	.123E+02	0.	.124E+02	0.	.125E+02	0.
.125E+02	.406E-31	.126E+02	.771E-31	.127E+02	.114E-30	.128E+02	.128E-30	.129E+02	.129E-30	.130E+02	.130E-30
.130E+02	.334E-30	.131E+02	.593E-30	.132E+02	.852E-30	.133E+02	.111E-29	.134E+02	.134E-29	.135E+02	.135E-29
.135E+02	.159E-29	.136E+02	.177E-29	.137E+02	.195E-29	.138E+02	.213E-29	.139E+02	.231E-29	.140E+02	.249E-29
.140E+02	.247E-29	.141E+02	.262E-29	.142E+02	.277E-29	.143E+02	.292E-29	.144E+02	.307E-29	.145E+02	.322E-29
.145E+02	.321E-29	.146E+02	.335E-29	.147E+02	.345E-29	.148E+02	.357E-29	.149E+02	.369E-29	.150E+02	.381E-29
.150E+02	.380E-29	.151E+02	.389E-29	.152E+02	.398E-29	.153E+02	.408E-29	.154E+02	.417E-29	.155E+02	.426E-29
.155E+02	.426E-29	.156E+02	.433E-29	.157E+02	.441E-29	.158E+02	.448E-29	.159E+02	.456E-29	.160E+02	.464E-29
.160E+02	.463E-29	.161E+02	.469E-29	.162E+02	.475E-29	.163E+02	.481E-29	.164E+02	.487E-29	.165E+02	.492E-29
.165E+02	.492E-29	.166E+02	.496E-29	.167E+02	.500E-29	.168E+02	.504E-29	.169E+02	.508E-29	.170E+02	.512E-29
.170E+02	.512E-29	.171E+02	.516E-29	.172E+02	.520E-29	.173E+02	.524E-29	.174E+02	.528E-29	.175E+02	.532E-29
.175E+02	.531E-29	.176E+02	.534E-29	.177E+02	.537E-29	.178E+02	.540E-29	.179E+02	.543E-29	.180E+02	.546E-29

Table 21:

REACTION	NI58 P4	NI58 (N,P) O58	REACTION	NI58 P4	NI58 (N,P) O58	REACTION	NI58 P4	NI58 (N,P) O58	REACTION	NI58 P4	NI58 (N,P) O58
ENERGY /MEV	CROSSSECTION /M**2	ENERGY /MEV	CROSSSECTION /M**2	ENERGY /MEV	CROSSSECTION /M**2	ENERGY /MEV	CROSSSECTION /M**2	ENERGY /MEV	CROSSSECTION /M**2	ENERGY /MEV	CROSSSECTION /M**2
.200E+00	.586E-34	.300E+00	.151E-35	.320E+00	.370E-35	.340E+00	.420E-35	.360E+00	.450E-35	.380E+00	.550E-35
.300E+00	.366E-33	.400E+00	.549E-33	.420E+00	.590E-33	.440E+00	.640E-33	.460E+00	.690E-33	.480E+00	.750E-33
.500E+00	.279E-32	.600E+00	.420E-32	.690E+00	.644E-32	.720E+00	.700E-32	.760E+00	.760E-32	.800E+00	.820E-32
.630E+00	.252E-31	.840E+00	.308E-31	.880E+00	.420E-31	.920E+00	.480E-31	.960E+00	.540E-31	.100E+01	.600E-31
.100E+01	.139E-30	.110E+01	.359E-30	.120E+01	.516E-30	.130E+01	.700E-30	.140E+01	.900E-30	.150E+01	.110E-29
.150E+01	.443E-29	.160E+01	.190E-29	.170E+01	.250E-29	.180E+01	.320E-29	.190E+01	.400E-29	.200E+01	.490E-29
.200E+01	.114E-28	.210E+01	.494E-28	.220E+01	.745E-28	.230E+01	.100E-28	.240E+01	.130E-28	.250E+01	.160E-28
.250E+01	.109E-28	.260E+01	.119E-28	.270E+01	.146E-28	.280E+01	.180E-28	.290E+01	.220E-28	.300E+01	.260E-28
.300E+01	.184E-28	.310E+01	.199E-28	.320E+01	.242E-28	.330E+01	.290E-28	.340E+01	.340E-28	.350E+01	.390E-28
.350E+01	.284E-28	.360E+01	.294E-28	.370E+01	.313E-28	.380E+01	.340E-28	.390E+01	.370E-28	.400E+01	.400E-28
.400E+01	.348E-28	.410E+01	.357E-28	.420E+01	.403E-28	.430E+01	.440E-28	.440E+01	.480E-28	.450E+01	.520E-28
.450E+01	.409E-28	.460E+01	.407E-28	.470E+01	.440E-28	.480E+01	.480E-28	.490E+01	.520E-28	.500E+01	.560E-28
.500E+01	.460E-28	.510E+01	.465E-28	.520E+01	.481E-28	.530E+01	.510E-28	.540E+01	.540E-28	.550E+01	.570E-28
.550E+01	.542E-28	.560E+01	.582E-28	.570E+01	.616E-28	.580E+01	.650E-28	.590E+01	.690E-28	.600E+01	.730E-28
.600E+01	.512E-28	.610E+01	.615E-28	.620E+01	.618E-28	.630E+01	.620E-28	.640E+01	.622E-28	.650E+01	.626E-28
.650E+01	.624E-28	.660E+01	.627E-28	.670E+01	.630E-28	.680E+01	.633E-28	.690E+01	.636E-28	.700E+01	.639E-28
.700E+01	.638E-28	.710E+01	.641E-28	.720E+01	.643E-28	.730E+01	.645E-28	.740E+01	.647E-28	.750E+01	.649E-28
.750E+01	.650E-28	.760E+01	.651E-28	.770E+01	.652E-28	.780E+01	.653E-28	.790E+01	.654E-28	.800E+01	.655E-28
.800E+01	.657E-28	.810E+01	.658E-28	.820E+01	.659E-28	.830E+01	.660E-28	.840E+01	.661E-28	.850E+01	.662E-28
.850E+01	.660E-28	.860E+01	.661E-28	.870E+01	.662E-28	.880E+01	.663E-28	.890E+01	.664E-28	.900E+01	.665E-28
.900E+01	.662E-28	.910E+01	.661E-28	.920E+01	.661E-28	.930E+01	.660E-28	.940E+01	.659E-28	.950E+01	.658E-28
.950E+01	.658E-28	.960E+01	.657E-28	.970E+01	.655E-28	.980E+01	.653E-28	.990E+01	.651E-28	.100E+02	.649E-28
.100E+02	.650E-28	.101E+02	.649E-28	.102E+02	.648E-28	.103E+02	.647E-28	.104E+02	.646E-28	.105E+02	.645E-28
.105E+02	.637E-28	.106E+02	.634E-28	.107E+02	.630E-28	.108E+02	.626E-28	.109E+02	.623E-28	.110E+02	.620E-28
.110E+02	.618E-28	.111E+02	.613E-28	.112E+02	.608E-28	.113E+02	.602E-28	.114E+02	.596E-28	.115E+02	.590E-28
.115E+02	.590E-28	.116E+02	.583E-28	.117E+02	.576E-28	.118E+02	.569E-28	.119E+02	.562E-28	.120E+02	.555E-28
.120E+02	.554E-28	.121E+02	.546E-28	.122E+02	.538E-28	.123E+02	.530E-28	.124E+02	.522E-28	.125E+02	.514E-28
.125E+02	.514E-28	.126E+02	.506E-28	.127E+02	.498E-28	.128E+02	.489E-28	.129E+02	.480E-28	.130E+02	.471E-28
.130E+02	.470E-28	.131E+02	.460E-28	.132E+02	.450E-28	.133E+02	.440E-28	.134E+02	.430E-28	.135E+02	.420E-28
.135E+02	.421E-28	.136E+02	.413E-28	.137E+02	.405E-28	.138E+02	.396E-28	.139E+02	.387E-28	.140E+02	.378E-28
.140E+02	.378E-28	.141E+02	.372E-28	.142E+02	.365E-28	.143E+02	.358E-28	.144E+02	.350E-28	.145E+02	.342E-28
.145E+02	.344E-28	.146E+02	.338E-28	.147E+02	.332E-28	.148E+02	.325E-28	.149E+02	.319E-28	.150E+02	.312E-28
.150E+02	.313E-28	.151E+02	.307E-28	.152E+02	.302E-28	.153E+02	.296E-28	.154E+02	.291E-28	.155E+02	.286E-28
.155E+02	.286E-28	.156E+02	.281E-28	.157E+02	.276E-28	.158E+02	.271E-28	.159E+02	.266E-28	.160E+02	.261E-28
.160E+02	.262E-28	.161E+02	.257E-28	.162E+02	.253E-28	.163E+02	.249E-28	.164E+02	.245E-28	.165E+02	.241E-28
.165E+02	.241E-28	.166E+02	.236E-28	.167E+02	.234E-28	.168E+02	.231E-28	.169E+02	.228E-28	.170E+02	.225E-28
.170E+02	.225E-28	.171E+02	.222E-28	.172E+02	.219E-28	.173E+02	.217E-28	.174E+02	.214E-28	.175E+02	.212E-28
.175E+02	.211E-28	.176E+02	.209E-28	.177E+02	.207E-28	.178E+02	.205E-28	.179E+02	.203E-28	.180E+02	.201E-28

Table 22:

REACTION	C059 A4	C059 (N,4) MN56	REACTION	C059 A4	C059 (N,4) MN56	REACTION	C059 A4	C059 (N,4) MN56	REACTION	C059 A4	C059 (N,4) MN56
ENERGY /MEV	CROSSSECTION /M**2	ENERGY /MEV	CROSSSECTION /M**2	ENERGY /MEV	CROSSSECTION /M**2	ENERGY /MEV	CROSSSECTION /M**2	ENERGY /MEV	CROSSSECTION /M**2	ENERGY /MEV	CROSSSECTION /M**2
.500E+01	.400E-32	.510E+01	.120E-31	.520E+01	.200E-31	.530E+01	.280E-31	.540E+01	.360E-31	.550E+01	.440E-31
.550E+01	.460E-31	.560E+01	.580E-31	.570E+01	.700E-31	.580E+01	.820E-31	.590E+01	.940E-31	.600E+01	.110E-30
.600E+01	.110E-30	.610E+01	.130E-30	.620E+01	.150E-30	.630E+01	.170E-30	.640E+01	.190E-30	.650E+01	.210E-30
.650E+01	.215E-30	.660E+01	.245E-30	.670E+01	.275E-30	.680E+01	.305E-30	.690E+01	.335E-30	.700E+01	.365E-30
.700E+01	.367E-30	.710E+01	.402E-30	.720E+01	.437E-30	.730E+01	.472E-30	.740E+01	.507E-30	.750E+01	.542E-30
.750E+01	.546E-30	.760E+01	.589E-30	.770E+01	.632E-30	.780E+01	.675E-30	.790E+01	.718E-30	.800E+01	.761E-30
.800E+01	.765E-30	.810E+01	.820E-30	.820E+01	.865E-30	.830E+01	.910E-30	.840E+01	.955E-30	.850E+01	.100E-29
.850E+01	.101E-29	.860E+01	.106E-29	.870E+01	.110E-29	.880E+01	.114E-29	.890E+01	.118E-29	.900E+01	.122E-29
.900E+01	.123E-29	.910E+01	.126E-29	.920E+01	.130E-29	.930E+01	.134E-29	.940E+01	.137E-29	.950E+01	.140E-29
.950E+01	.141E-29	.960E+01	.145E-29	.970E+01	.148E-29	.980E+01	.152E-29	.990E+01	.155E-29	.100E+02	.158E-29
.100E+02	.159E-29	.101E+02	.163E-29	.102E+02	.167E-29	.103E+02	.170E-29	.104E+02	.174E-29	.105E+02	.178E-29
.105E+02	.178E-29	.106E+02	.181E-29	.107E+02	.185E-29	.108E+02	.189E-29	.109E+02	.192E-29	.110E+02	.196E-29
.110E+02	.196E-29	.111E+02	.200E-29	.112E+02	.203E-29	.113E+02	.207E-29	.114E+02	.210E-29	.115E+02	.214E-29
.115E+02	.214E-29	.116E+02	.219E-29	.117E+02	.224E-29	.118E+02	.229E-29	.119E+02	.234E-29	.120E+02	.239E-29
.120E+02	.239E-29	.121E+02	.245E-29	.122E+02	.250E-29	.123E+02	.255E-29	.124E+02	.260E-29	.125E+02	.265E-29
.125E+02	.264E-29	.126E+02	.267E-29	.127E+02	.270E-29	.128E+02	.273E-29	.129E+02	.276E-29	.130E+02	.279E-29
.130E+02	.278E-29	.131E+02	.280E-29	.132E+02	.283E-29	.133E+02	.285E-29	.134E+02	.288E-29	.135E+02	.291E-29
.135E+02	.289E-29	.136E+02	.290E-29	.137E+02	.290E-29	.138E+02	.291E-29	.139E+02	.291E-29	.140E+02	.291E-29
.140E+02	.291E-29	.141E+02	.291E-29	.142E+02	.291E-29	.143E+02	.290E-29	.144E+02	.289E-29	.145E+02	.288E-29
.145E+02	.288E-29	.146E+02	.286E-29	.147E+02	.284E-29	.148E+02	.283E-29	.149E+02	.281E-29	.150E+02	.279E-29
.150E+02	.278E-29	.151E+02	.275E-29	.152E+02	.272E-29	.153E+02	.269E-29	.154E+02	.266E-29	.155E+02	.263E-29
.155E+02	.262E-29	.156E+02	.259E-29	.157E+02	.256E-29	.158E+02	.253E-29	.159E+02	.250E-29	.160E+02	.247E-29
.160E+02	.246E-29	.161E+02	.243E-29	.162E+02	.239E-29	.163E+02	.235E-29	.164E+02	.232E-29	.165E+02	.228E-29
.165E+02	.228E-29	.166E+02	.225E-29	.167E+02	.221E-29	.168E+02	.217E-29	.169E+02	.214E-29	.170E+02	.210E-29
.170E+02	.210E-29	.171E+02	.205E-29	.172E+02	.200E-29	.173E+02	.195E-29	.174E+02	.190E-29	.175E+02	.185E-29
.175E+02	.186E-29	.176E+02	.181E-29	.177E+02	.177E-29	.178E+02	.174E-29	.1			

Table 24:

REACTION ENERGY /MEV	C059 G4 CROSSSECTION /M**2	C059 (N,G)C060 ENERGY /MEV	CROSSSECTION /M**2	ENERGY /MEV	CROSSSECTION /M**2	ENERGY /MEV	CROSSSECTION /M**2	ENERGY /MEV	CROSSSECTION /M**2	ENERGY /MEV	CROSSSECTION /M**2
.100E-09	.585E-25	.105E-09	.571E-25	.110E-09	.558E-25	.115E-09	.546E-25	.120E-09	.537E-25	.125E-09	.528E-25
.128E-09	.517E-25	.135E-09	.503E-25	.143E-09	.490E-25	.150E-09	.476E-25	.160E-09	.461E-25	.168E-09	.448E-25
.170E-09	.448E-25	.180E-09	.435E-25	.190E-09	.424E-25	.200E-09	.414E-25	.210E-09	.405E-25	.220E-09	.397E-25
.220E-09	.397E-25	.230E-09	.386E-25	.240E-09	.376E-25	.250E-09	.366E-25	.270E-09	.357E-25	.280E-09	.348E-25
.300E-09	.340E-25	.300E-09	.340E-25	.320E-09	.326E-25	.340E-09	.314E-25	.360E-09	.303E-25	.380E-09	.293E-25
.500E-09	.261E-25	.525E-09	.255E-25	.550E-09	.250E-25	.575E-09	.244E-25	.600E-09	.239E-25	.630E-09	.233E-25
.630E-09	.233E-25	.660E-09	.228E-25	.690E-09	.223E-25	.720E-09	.218E-25	.760E-09	.212E-25	.800E-09	.207E-25
.800E-09	.207E-25	.840E-09	.202E-25	.880E-09	.197E-25	.920E-09	.193E-25	.960E-09	.189E-25	.100E+00	.185E-25
.100E+00	.185E-25	.105E+00	.181E-25	.110E+00	.176E-25	.115E+00	.173E-25	.120E+00	.168E-25	.125E+00	.164E-25
.128E+00	.163E-25	.135E+00	.159E-25	.143E+00	.155E-25	.150E+00	.150E-25	.160E+00	.146E-25	.170E+00	.142E-25
.170E+00	.142E-25	.180E+00	.138E-25	.190E+00	.134E-25	.200E+00	.130E-25	.210E+00	.126E-25	.220E+00	.122E-25
.220E+00	.122E-25	.230E+00	.118E-25	.240E+00	.114E-25	.250E+00	.110E-25	.260E+00	.106E-25	.280E+00	.102E-25
.300E+00	.102E-25	.300E+00	.102E-25	.320E+00	.976E-26	.340E+00	.930E-26	.360E+00	.884E-26	.380E+00	.837E-26
.500E+00	.726E-26	.525E+00	.712E-26	.550E+00	.698E-26	.575E+00	.674E-26	.600E+00	.650E-26	.630E+00	.626E-26
.630E+00	.626E-26	.660E+00	.602E-26	.690E+00	.578E-26	.720E+00	.534E-26	.760E+00	.490E-26	.800E+00	.446E-26
.800E+00	.446E-26	.840E+00	.422E-26	.880E+00	.408E-26	.920E+00	.384E-26	.960E+00	.360E-26	.100E+00	.336E-26
.100E+00	.336E-26	.105E+00	.332E-26	.110E+00	.328E-26	.115E+00	.324E-26	.120E+00	.320E-26	.125E+00	.316E-26
.128E+00	.316E-26	.135E+00	.312E-26	.143E+00	.308E-26	.150E+00	.304E-26	.160E+00	.300E-26	.170E+00	.296E-26
.170E+00	.296E-26	.180E+00	.292E-26	.190E+00	.288E-26	.200E+00	.284E-26	.210E+00	.280E-26	.220E+00	.276E-26
.220E+00	.276E-26	.230E+00	.272E-26	.240E+00	.268E-26	.250E+00	.264E-26	.260E+00	.260E-26	.280E+00	.256E-26
.300E+00	.256E-26	.300E+00	.256E-26	.320E+00	.252E-26	.340E+00	.248E-26	.360E+00	.244E-26	.380E+00	.240E-26
.500E+00	.240E-26	.525E+00	.236E-26	.550E+00	.232E-26	.575E+00	.228E-26	.600E+00	.224E-26	.630E+00	.220E-26
.630E+00	.220E-26	.660E+00	.216E-26	.690E+00	.212E-26	.720E+00	.208E-26	.760E+00	.204E-26	.800E+00	.200E-26
.800E+00	.200E-26	.840E+00	.196E-26	.880E+00	.192E-26	.920E+00	.188E-26	.960E+00	.184E-26	.100E+00	.180E-26
.100E+00	.180E-26	.105E+00	.176E-26	.110E+00	.172E-26	.115E+00	.168E-26	.120E+00	.164E-26	.125E+00	.160E-26
.128E+00	.160E-26	.135E+00	.156E-26	.143E+00	.152E-26	.150E+00	.148E-26	.160E+00	.144E-26	.170E+00	.140E-26
.170E+00	.140E-26	.180E+00	.136E-26	.190E+00	.132E-26	.200E+00	.128E-26	.210E+00	.124E-26	.220E+00	.120E-26
.220E+00	.120E-26	.230E+00	.116E-26	.240E+00	.112E-26	.250E+00	.108E-26	.260E+00	.104E-26	.280E+00	.100E-26
.300E+00	.100E-26	.300E+00	.100E-26	.320E+00	.956E-27	.340E+00	.912E-27	.360E+00	.868E-27	.380E+00	.824E-27
.500E+00	.824E-27	.525E+00	.800E-27	.550E+00	.776E-27	.575E+00	.732E-27	.600E+00	.688E-27	.630E+00	.644E-27
.630E+00	.644E-27	.660E+00	.620E-27	.690E+00	.576E-27	.720E+00	.532E-27	.760E+00	.488E-27	.800E+00	.444E-27
.800E+00	.444E-27	.840E+00	.420E-27	.880E+00	.384E-27	.920E+00	.340E-27	.960E+00	.300E-27	.100E+00	.260E-27
.100E+00	.260E-27	.105E+00	.256E-27	.110E+00	.252E-27	.115E+00	.248E-27	.120E+00	.244E-27	.125E+00	.240E-27
.128E+00	.240E-27	.135E+00	.236E-27	.143E+00	.232E-27	.150E+00	.228E-27	.160E+00	.224E-27	.170E+00	.220E-27
.170E+00	.220E-27	.180E+00	.216E-27	.190E+00	.212E-27	.200E+00	.208E-27	.210E+00	.204E-27	.220E+00	.200E-27
.220E+00	.200E-27	.230E+00	.196E-27	.240E+00	.192E-27	.250E+00	.188E-27	.260E+00	.184E-27	.280E+00	.180E-27
.300E+00	.180E-27	.300E+00	.180E-27	.320E+00	.176E-27	.340E+00	.172E-27	.360E+00	.168E-27	.380E+00	.164E-27
.500E+00	.164E-27	.525E+00	.160E-27	.550E+00	.156E-27	.575E+00	.152E-27	.600E+00	.148E-27	.630E+00	.144E-27
.630E+00	.144E-27	.660E+00	.140E-27	.690E+00	.136E-27	.720E+00	.132E-27	.760E+00	.128E-27	.800E+00	.124E-27
.800E+00	.124E-27	.840E+00	.120E-27	.880E+00	.116E-27	.920E+00	.112E-27	.960E+00	.108E-27	.100E+00	.104E-27
.100E+00	.104E-27	.105E+00	.100E-27	.110E+00	.956E-28	.115E+00	.912E-28	.120E+00	.868E-28	.125E+00	.824E-28
.128E+00	.824E-28	.135E+00	.800E-28	.143E+00	.756E-28	.150E+00	.712E-28	.160E+00	.668E-28	.170E+00	.624E-28
.170E+00	.624E-28	.180E+00	.600E-28	.190E+00	.552E-28	.200E+00	.508E-28	.210E+00	.464E-28	.220E+00	.420E-28
.220E+00	.420E-28	.230E+00	.400E-28	.240E+00	.356E-28	.250E+00	.312E-28	.260E+00	.268E-28	.280E+00	.224E-28
.300E+00	.224E-28	.300E+00	.224E-28	.320E+00	.200E-28	.340E+00	.176E-28	.360E+00	.152E-28	.380E+00	.128E-28
.500E+00	.128E-28	.525E+00	.124E-28	.550E+00	.120E-28	.575E+00	.116E-28	.600E+00	.112E-28	.630E+00	.108E-28
.630E+00	.108E-28	.660E+00	.104E-28	.690E+00	.96E-29	.720E+00	.92E-29	.760E+00	.88E-29	.800E+00	.84E-29
.800E+00	.84E-29	.840E+00	.80E-29	.880E+00	.72E-29	.920E+00	.68E-29	.960E+00	.64E-29	.100E+00	.60E-29
.100E+00	.60E-29	.105E+00	.58E-29	.110E+00	.56E-29	.115E+00	.54E-29	.120E+00	.52E-29	.125E+00	.50E-29
.128E+00	.50E-29	.135E+00	.48E-29	.143E+00	.46E-29	.150E+00	.44E-29	.160E+00	.42E-29	.170E+00	.40E-29
.170E+00	.40E-29	.180E+00	.38E-29	.190E+00	.36E-29	.200E+00	.34E-29	.210E+00	.32E-29	.220E+00	.30E-29
.220E+00	.30E-29	.230E+00	.28E-29	.240E+00	.26E-29	.250E+00	.24E-29	.260E+00	.22E-29	.280E+00	.20E-29
.300E+00	.20E-29	.300E+00	.20E-29	.320E+00	.18E-29	.340E+00	.16E-29	.360E+00	.14E-29	.380E+00	.12E-29
.500E+00	.12E-29	.525E+00	.116E-29	.550E+00	.110E-29	.575E+00	.104E-29	.600E+00	.98E-30	.630E+00	.92E-30
.630E+00	.92E-30	.660E+00	.88E-30	.690E+00	.84E-30	.720E+00	.80E-30	.760E+00	.76E-30	.800E+00	.72E-30
.800E+00	.72E-30	.840E+00	.68E-30	.880E+00	.64E-30	.920E+00	.60E-30	.960E+00	.56E-30	.100E+00	.52E-30
.100E+00	.52E-30	.105E+00	.50E-30	.110E+00	.48E-30	.115E+00	.46E-30	.120E+00	.44E-30	.125E+00	.42E-30
.128E+00	.42E-30	.135E+00	.40E-30	.143E+00	.38E-30	.150E+00	.36E-30	.160E+00	.34E-30	.170E+00	.32E-30
.170E+00	.32E-30	.180E+00	.30E-30	.190E+00	.28E-30	.200E+00	.26E-30	.210E+00	.24E-30	.220E+00	.22E-30
.220E+00	.22E-30	.230E+00	.20E-30	.240E+00	.18E-30	.250E+00	.16E-30	.260E+00	.14E-30	.280E+00	.12E-30
.300E+00	.12E-30	.300E+00	.12E-30	.320E+00	.10E-30	.340E+00	.8E-31	.360E+00	.6E-31	.380E+00	.4E-31
.500E+00	.4E-31	.525E+00	.36E-31	.550E+00	.32E-31	.575E+00	.28E-31	.600E+00	.24E-31	.630E+00	.20E-31
.630E+00	.20E-31	.660E+00	.18E-31	.690E+00	.16E-31	.720E+00	.14E-31	.760E+00	.12E-31	.800E+00	.10E-31
.800E+00	.10E-31	.840E+00	.96E-32	.880E+00	.92E-32	.920E+00	.88E-32	.960E+00	.84E-32	.100E+00	.80E-32
.100E+00	.80E-32	.105E+00	.76E-32	.110E+00	.72E-32	.115E+00	.68E-32	.120E+00	.64E-32	.125E+00	.60E-32
.128E+00	.60E-32	.135E+00	.56E-32	.143E+00	.52E-32	.150E+00	.48E-32	.160E+00	.44E-32	.170E+00	.40E-32
.170E+00	.40E-32	.180E+00	.36E-32	.190E+00	.32E-32	.200E+00	.28E-32	.210E+00	.24E-32	.220E+00	.20E-32
.220E+00	.20E-32	.230E+00	.18E-32	.240E+00	.16E-32	.250E+00	.14E-32	.260E+00	.12E-32	.280E+00	.10E-32
.300E+00	.10E-32	.300E+00	.10E-32	.320E+00	.88E-33	.340E+00	.84E-33	.360E+00	.80E-33	.380E+00	.76E-33
.500E+00	.76E-33	.525E+00	.72E-33	.550E+00	.68E-33	.575E+00	.64E-33	.600E+00	.60E-33	.630E+00	.56E-33
.630E+00	.56E-33	.660E+00	.52E-33	.690E+00	.48E-33	.720E+00	.44E-33	.760E+00	.40E-33	.800E+00	.36E-33
.800E+00	.36E-33	.840E+00	.32E-33	.880E+00	.28E-33	.920E+00	.24E-33	.960E+00	.20E-33	.100E+00	.16E-33
.100E+00	.16E-33	.105E+00	.152E-33	.110E+00	.148E-33	.115E+00	.144E-33	.120E+00	.140E-33	.125E+00	.136E-33
.128E+00	.136E-33	.135E+00	.132E-33	.143E+00	.128E-33	.150E+00	.124E-33	.160E+00	.120E-33	.170E+00	.116E-33
.170E+00	.116E-33	.180E+00	.112E-33	.190E+00	.108E-33	.200E+00	.104E-33	.210E+00	.100E-33	.220E+00	.96E-34
.220E+00	.96E-34	.230E+00	.92E-34	.240E+00	.88E-34	.250E+00	.84E-34	.260E+00	.80E-34	.280E+00	.76E-34
.300E+00	.76E-34	.300E+00	.76E-34	.320E+00	.72E-34	.340E+00	.68E-34	.360E+00	.64E-34	.380E+00	.60E-34
.500E+00	.60E-34	.525E+00	.56E-34	.550E+00	.52E-34	.575E+00	.48E-34	.600E+00	.44E-34	.630E+00	.40E-34
.630E+00	.40E-34	.660E+00	.36E-34	.690E+00	.32E-34	.720E+00	.28E-34	.760E+00	.24E-34	.800E+00	.20E-34
.800E+00	.20E-34	.840E+00	.18E-34	.880E+00	.16E-34	.920E+00	.14E-34	.960E+00	.12E-34	.100E+00	.10E-34
.100E+00	.10E-34	.105E+00	.96E-35	.110E+00	.92E-35	.115E+00	.88E-35	.120E+00	.84E-35	.125E+00	.80E-35
.128E+00	.80E-35	.135E+00	.76E-35	.143E+00	.72E-35	.150E+00	.68E-35	.160E+00	.64E-35	.170E+00	.60E-35
.170E+00	.60E-35	.180E+00	.56E-35	.190E+00	.52E-35	.200E+00	.48E-35	.210E+00	.44E-35	.	

Table 25:

REACTION	NI60P4	NI60 (N,P)C060	ENERGY	CROSSSECTION	ENERGY	CROSSSECTION	ENERGY	CROSSSECTION	ENERGY	CROSSSECTION	ENERGY	CROSSSECTION	
/MEV	/M**2	/MEV	/M**2	/MEV	/M**2	/MEV	/M**2	/MEV	/M**2	/MEV	/M**2	/MEV	/M**2
.200E+01	0.	.210E+01	0.	.220E+01	0.	.230E+01	.558E-34	.240E+01	.309E-32				
.250E+01	.782E-32	.260E+01	.125E-31	.270E+01	.173E-31	.280E+01	.220E-31	.290E+01	.267E-31				
.300E+01	.314E-31	.310E+01	.362E-31	.320E+01	.409E-31	.330E+01	.456E-31	.340E+01	.504E-31				
.350E+01	.551E-31	.360E+01	.598E-31	.370E+01	.645E-31	.380E+01	.693E-31	.390E+01	.740E-31				
.400E+01	.787E-31	.410E+01	.834E-31	.420E+01	.882E-31	.430E+01	.929E-31	.440E+01	.976E-31				
.450E+01	.138E-30	.460E+01	.1214E-30	.470E+01	.290E-30	.480E+01	.366E-30	.490E+01	.442E-30				
.500E+01	.582E-30	.510E+01	.786E-30	.520E+01	.990E-30	.530E+01	.119E-29	.540E+01	.140E-29				
.550E+01	.166E-29	.560E+01	.199E-29	.570E+01	.232E-29	.580E+01	.265E-29	.590E+01	.298E-29				
.600E+01	.328E-29	.610E+01	.355E-29	.620E+01	.382E-29	.630E+01	.409E-29	.640E+01	.436E-29				
.650E+01	.468E-29	.660E+01	.504E-29	.670E+01	.540E-29	.680E+01	.576E-29	.690E+01	.612E-29				
.700E+01	.646E-29	.710E+01	.678E-29	.720E+01	.710E-29	.730E+01	.742E-29	.740E+01	.774E-29				
.750E+01	.805E-29	.760E+01	.835E-29	.770E+01	.865E-29	.780E+01	.895E-29	.790E+01	.925E-29				
.800E+01	.963E-29	.810E+01	.101E-28	.820E+01	.105E-28	.830E+01	.110E-28	.840E+01	.115E-28				
.850E+01	.119E-28	.860E+01	.122E-28	.870E+01	.126E-28	.880E+01	.130E-28	.890E+01	.133E-28				
.900E+01	.136E-28	.910E+01	.139E-28	.920E+01	.142E-28	.930E+01	.145E-28	.940E+01	.148E-28				
.950E+01	.151E-28	.960E+01	.153E-28	.970E+01	.155E-28	.980E+01	.157E-28	.990E+01	.159E-28				
.100E+02	.161E-28	.101E+02	.162E-28	.102E+02	.163E-28	.103E+02	.164E-28	.104E+02	.165E-28				
.105E+02	.166E-28	.106E+02	.165E-28	.107E+02	.165E-28	.108E+02	.165E-28	.109E+02	.164E-28				
.110E+02	.163E-28	.111E+02	.162E-28	.112E+02	.160E-28	.113E+02	.159E-28	.114E+02	.158E-28				
.115E+02	.156E-28	.116E+02	.154E-28	.117E+02	.152E-28	.118E+02	.150E-28	.119E+02	.148E-28				
.120E+02	.146E-28	.121E+02	.145E-28	.122E+02	.144E-28	.123E+02	.143E-28	.124E+02	.142E-28				
.125E+02	.142E-28	.126E+02	.141E-28	.127E+02	.141E-28	.128E+02	.141E-28	.129E+02	.140E-28				
.130E+02	.139E-28	.131E+02	.138E-28	.132E+02	.137E-28	.133E+02	.136E-28	.134E+02	.135E-28				
.135E+02	.134E-28	.136E+02	.133E-28	.137E+02	.132E-28	.138E+02	.131E-28	.139E+02	.130E-28				
.140E+02	.129E-28	.141E+02	.127E-28	.142E+02	.125E-28	.143E+02	.124E-28	.144E+02	.122E-28				
.145E+02	.120E-28	.146E+02	.118E-28	.147E+02	.115E-28	.148E+02	.113E-28	.149E+02	.111E-28				
.150E+02	.109E-28	.151E+02	.107E-28	.152E+02	.105E-28	.153E+02	.103E-28	.154E+02	.101E-28				
.155E+02	.993E-29	.156E+02	.979E-29	.157E+02	.965E-29	.158E+02	.951E-29	.159E+02	.937E-29				
.160E+02	.923E-29	.161E+02	.909E-29	.162E+02	.895E-29	.163E+02	.881E-29	.164E+02	.867E-29				
.165E+02	.855E-29	.166E+02	.845E-29	.167E+02	.835E-29	.168E+02	.825E-29	.169E+02	.815E-29				
.170E+02	.805E-29	.171E+02	.795E-29	.172E+02	.785E-29	.173E+02	.775E-29	.174E+02	.765E-29				
.175E+02	.756E-29	.176E+02	.748E-29	.177E+02	.740E-29	.178E+02	.732E-29	.179E+02	.724E-29				

Table 26:

REACTION	CU63A4	CU63 (N,A)C060	ENERGY	CROSSSECTION	ENERGY	CROSSSECTION	ENERGY	CROSSSECTION	ENERGY	CROSSSECTION	ENERGY	CROSSSECTION	
/MEV	/M**2	/MEV	/M**2	/MEV	/M**2	/MEV	/M**2	/MEV	/M**2	/MEV	/M**2	/MEV	/M**2
.550E+01	.220E-31	.560E+01	.459E-31	.570E+01	.757E-31	.580E+01	.136E-30	.590E+01	.203E-30				
.600E+01	.277E-30	.610E+01	.360E-30	.620E+01	.442E-30	.630E+01	.528E-30	.640E+01	.614E-30				
.650E+01	.698E-30	.660E+01	.779E-30	.670E+01	.859E-30	.680E+01	.928E-30	.690E+01	.995E-30				
.700E+01	.105E-29	.710E+01	.110E-29	.720E+01	.115E-29	.730E+01	.120E-29	.740E+01	.124E-29				
.750E+01	.129E-29	.760E+01	.135E-29	.770E+01	.141E-29	.780E+01	.150E-29	.790E+01	.159E-29				
.800E+01	.170E-29	.810E+01	.183E-29	.820E+01	.196E-29	.830E+01	.211E-29	.840E+01	.227E-29				
.850E+01	.243E-29	.860E+01	.259E-29	.870E+01	.275E-29	.880E+01	.289E-29	.890E+01	.303E-29				
.900E+01	.315E-29	.910E+01	.326E-29	.920E+01	.336E-29	.930E+01	.344E-29	.940E+01	.352E-29				
.950E+01	.359E-29	.960E+01	.365E-29	.970E+01	.372E-29	.980E+01	.378E-29	.990E+01	.384E-29				
.100E+02	.391E-29	.101E+02	.399E-29	.102E+02	.407E-29	.103E+02	.415E-29	.104E+02	.423E-29				
.105E+02	.431E-29	.106E+02	.438E-29	.107E+02	.445E-29	.108E+02	.452E-29	.109E+02	.458E-29				
.110E+02	.462E-29	.111E+02	.466E-29	.112E+02	.468E-29	.113E+02	.466E-29	.114E+02	.464E-29				
.115E+02	.458E-29	.116E+02	.449E-29	.117E+02	.440E-29	.118E+02	.429E-29	.119E+02	.419E-29				
.120E+02	.410E-29	.121E+02	.404E-29	.122E+02	.397E-29	.123E+02	.394E-29	.124E+02	.391E-29				
.125E+02	.390E-29	.126E+02	.389E-29	.127E+02	.389E-29	.128E+02	.389E-29	.129E+02	.389E-29				
.130E+02	.389E-29	.131E+02	.388E-29	.132E+02	.387E-29	.133E+02	.386E-29	.134E+02	.385E-29				
.135E+02	.383E-29	.136E+02	.380E-29	.137E+02	.378E-29	.138E+02	.377E-29	.139E+02	.376E-29				
.140E+02	.373E-29	.141E+02	.367E-29	.142E+02	.362E-29	.143E+02	.357E-29	.144E+02	.353E-29				
.145E+02	.348E-29	.146E+02	.343E-29	.147E+02	.339E-29	.148E+02	.333E-29	.149E+02	.328E-29				
.150E+02	.323E-29	.151E+02	.317E-29	.152E+02	.312E-29	.153E+02	.306E-29	.154E+02	.300E-29				
.155E+02	.294E-29	.156E+02	.288E-29	.157E+02	.282E-29	.158E+02	.276E-29	.159E+02	.270E-29				
.160E+02	.264E-29	.161E+02	.258E-29	.162E+02	.252E-29	.163E+02	.246E-29	.164E+02	.240E-29				
.165E+02	.234E-29	.166E+02	.228E-29	.167E+02	.223E-29	.168E+02	.217E-29	.169E+02	.212E-29				
.170E+02	.207E-29	.171E+02	.202E-29	.172E+02	.197E-29	.173E+02	.192E-29	.174E+02	.188E-29				
.175E+02	.183E-29	.176E+02	.179E-29	.177E+02	.175E-29	.178E+02	.171E-29	.179E+02	.167E-29				

Table 27:

REACTION	CU63G	CU63 (M,G)CU64	ENERGY /MEV	CROSSSECTION /#*#2	ENERGY /MEV	CROSSSECTION /#*#2	ENERGY /MEV	CROSSSECTION /#*#2	ENERGY /MEV	CROSSSECTION /#*#2
.110E+09	.170E+26	.110E+09	.650E+26	.110E+09	.674E+26	.115E+09	.659E+26	.120E+09	.643E+26	
.120E+09	.180E+26	.120E+09	.667E+26	.120E+09	.691E+26	.125E+09	.674E+26	.130E+09	.658E+26	
.170E+09	.240E+26	.180E+09	.525E+26	.190E+09	.512E+26	.200E+09	.499E+26	.210E+09	.487E+26	
.230E+09	.310E+26	.230E+09	.466E+26	.240E+09	.454E+26	.255E+09	.444E+26	.270E+09	.438E+26	
.280E+09	.361E+26	.300E+09	.405E+26	.320E+09	.393E+26	.340E+09	.381E+26	.360E+09	.371E+26	
.380E+09	.431E+26	.400E+09	.351E+26	.425E+09	.341E+26	.450E+09	.332E+26	.475E+09	.323E+26	
.500E+09	.515E+26	.525E+09	.308E+26	.550E+09	.301E+26	.575E+09	.294E+26	.600E+09	.288E+26	
.630E+09	.601E+26	.660E+09	.275E+26	.690E+09	.269E+26	.720E+09	.263E+26	.760E+09	.256E+26	
.800E+09	.720E+26	.840E+09	.244E+26	.880E+09	.238E+26	.920E+09	.233E+26	.960E+09	.228E+26	
.100E+09	.870E+26	.105E+09	.218E+26	.110E+09	.213E+26	.115E+09	.209E+26	.120E+09	.205E+26	
.120E+09	.100E+27	.135E+09	.192E+26	.143E+09	.187E+26	.150E+09	.182E+26	.160E+09	.176E+26	
.170E+09	.130E+27	.180E+09	.166E+26	.190E+09	.162E+26	.200E+09	.158E+26	.210E+09	.154E+26	
.220E+09	.160E+27	.230E+09	.148E+26	.240E+09	.144E+26	.255E+09	.140E+26	.270E+09	.136E+26	
.280E+09	.190E+27	.300E+09	.128E+26	.320E+09	.125E+26	.340E+09	.121E+26	.360E+09	.118E+26	
.380E+09	.230E+27	.400E+09	.111E+26	.425E+09	.108E+26	.450E+09	.105E+26	.475E+09	.102E+26	
.500E+09	.280E+27	.525E+09	.976E+27	.550E+09	.954E+27	.575E+09	.933E+27	.600E+09	.912E+27	
.630E+09	.340E+27	.660E+09	.871E+27	.690E+09	.852E+27	.720E+09	.832E+27	.760E+09	.810E+27	
.800E+09	.420E+27	.840E+09	.771E+27	.880E+09	.754E+27	.920E+09	.738E+27	.960E+09	.723E+27	
.100E+07	.500E+27	.105E+07	.690E+27	.110E+07	.675E+27	.115E+07	.660E+27	.120E+07	.644E+27	
.120E+07	.560E+27	.135E+07	.600E+27	.143E+07	.592E+27	.150E+07	.575E+27	.160E+07	.557E+27	
.170E+07	.640E+27	.180E+07	.526E+27	.190E+07	.512E+27	.200E+07	.500E+27	.210E+07	.488E+27	
.230E+07	.750E+27	.240E+07	.465E+27	.250E+07	.452E+27	.260E+07	.440E+27	.270E+07	.431E+27	
.280E+07	.870E+27	.300E+07	.406E+27	.320E+07	.394E+27	.340E+07	.382E+27	.360E+07	.370E+27	
.380E+07	.100E+28	.400E+07	.352E+27	.425E+07	.342E+27	.450E+07	.332E+27	.475E+07	.322E+27	
.500E+07	.120E+28	.525E+07	.308E+27	.550E+07	.301E+27	.575E+07	.295E+27	.600E+07	.288E+27	
.630E+07	.140E+28	.660E+07	.275E+27	.690E+07	.269E+27	.720E+07	.263E+27	.760E+07	.256E+27	
.800E+07	.170E+28	.840E+07	.244E+27	.880E+07	.238E+27	.920E+07	.233E+27	.960E+07	.228E+27	
.100E+06	.200E+28	.105E+06	.218E+27	.110E+06	.213E+27	.115E+06	.208E+27	.120E+06	.203E+27	
.120E+06	.230E+28	.135E+06	.192E+27	.143E+06	.187E+27	.150E+06	.181E+27	.160E+06	.176E+27	
.170E+06	.280E+28	.180E+06	.166E+27	.190E+06	.162E+27	.200E+06	.158E+27	.210E+06	.154E+27	
.220E+06	.330E+28	.230E+06	.147E+27	.240E+06	.143E+27	.255E+06	.139E+27	.270E+06	.136E+27	
.280E+06	.390E+28	.300E+06	.126E+27	.320E+06	.124E+27	.340E+06	.121E+27	.360E+06	.118E+27	
.380E+06	.470E+28	.400E+06	.111E+27	.425E+06	.108E+27	.450E+06	.105E+27	.475E+06	.102E+27	
.500E+06	.570E+28	.525E+06	.976E+28	.550E+06	.954E+28	.575E+06	.933E+28	.600E+06	.912E+28	
.630E+06	.680E+28	.660E+06	.871E+28	.690E+06	.852E+28	.720E+06	.832E+28	.760E+06	.810E+28	
.800E+06	.820E+28	.840E+06	.776E+28	.880E+06	.754E+28	.920E+06	.738E+28	.960E+06	.723E+28	
.100E+05	.100E+29	.105E+05	.867E+28	.110E+05	.849E+28	.115E+05	.828E+28	.120E+05	.805E+28	
.120E+05	.110E+29	.135E+05	.768E+28	.140E+05	.750E+28	.150E+05	.734E+28	.160E+05	.719E+28	
.170E+05	.140E+29	.180E+05	.686E+28	.190E+05	.670E+28	.200E+05	.655E+28	.210E+05	.638E+28	
.220E+05	.170E+29	.230E+05	.601E+28	.240E+05	.585E+28	.255E+05	.568E+28	.270E+05	.550E+28	
.280E+05	.210E+29	.300E+05	.518E+28	.320E+05	.505E+28	.340E+05	.492E+28	.360E+05	.479E+28	
.380E+05	.260E+29	.400E+05	.458E+28	.420E+05	.446E+28	.450E+05	.433E+28	.470E+05	.423E+28	
.500E+05	.320E+29	.525E+05	.397E+28	.550E+05	.385E+28	.575E+05	.373E+28	.600E+05	.363E+28	
.630E+05	.390E+29	.660E+05	.343E+28	.690E+05	.333E+28	.720E+05	.323E+28	.760E+05	.315E+28	
.800E+05	.470E+29	.840E+05	.299E+28	.880E+05	.292E+28	.920E+05	.285E+28	.960E+05	.279E+28	
.100E+04	.570E+29	.105E+04	.265E+28	.110E+04	.259E+28	.115E+04	.252E+28	.120E+04	.246E+28	
.120E+04	.640E+29	.135E+04	.232E+28	.140E+04	.227E+28	.150E+04	.221E+28	.160E+04	.215E+28	
.170E+04	.780E+29	.180E+04	.211E+28	.190E+04	.207E+28	.200E+04	.202E+28	.210E+04	.197E+28	
.220E+04	.940E+29	.230E+04	.184E+28	.240E+04	.178E+28	.255E+04	.173E+28	.270E+04	.167E+28	
.280E+04	.110E+30	.300E+04	.156E+28	.320E+04	.152E+28	.340E+04	.148E+28	.360E+04	.145E+28	
.380E+04	.130E+30	.400E+04	.138E+28	.420E+04	.134E+28	.450E+04	.129E+28	.470E+04	.125E+28	
.500E+04	.160E+30	.525E+04	.118E+28	.550E+04	.115E+28	.575E+04	.111E+28	.600E+04	.108E+28	
.630E+04	.190E+30	.660E+04	.100E+28	.690E+04	.97E+28	.720E+04	.920E+28	.760E+04	.89E+28	
.800E+04	.230E+30	.840E+04	.850E+28	.880E+04	.82E+28	.920E+04	.79E+28	.960E+04	.77E+28	
.100E+03	.280E+30	.105E+03	.737E+28	.110E+03	.719E+28	.115E+03	.699E+28	.120E+03	.676E+28	
.120E+03	.320E+30	.135E+03	.646E+28	.140E+03	.629E+28	.150E+03	.616E+28	.160E+03	.602E+28	
.170E+03	.390E+30	.180E+03	.576E+28	.190E+03	.559E+28	.200E+03	.543E+28	.210E+03	.527E+28	
.220E+03	.470E+30	.230E+03	.500E+28	.240E+03	.486E+28	.255E+03	.473E+28	.270E+03	.463E+28	
.280E+03	.570E+30	.300E+03	.444E+28	.320E+03	.437E+28	.340E+03	.432E+28	.360E+03	.427E+28	
.380E+03	.680E+30	.400E+03	.422E+28	.420E+03	.421E+28	.450E+03	.420E+28	.470E+03	.419E+28	
.500E+03	.810E+30	.525E+03	.425E+28	.550E+03	.424E+28	.575E+03	.423E+28	.600E+03	.422E+28	
.630E+03	.960E+30	.660E+03	.400E+28	.690E+03	.400E+28	.720E+03	.400E+28	.760E+03	.400E+28	
.800E+03	.110E+31	.840E+03	.373E+28	.880E+03	.373E+28	.920E+03	.373E+28	.960E+03	.373E+28	
.100E+02	.130E+31	.105E+02	.345E+28	.110E+02	.345E+28	.115E+02	.345E+28	.120E+02	.345E+28	
.120E+02	.150E+31	.135E+02	.319E+28	.140E+02	.319E+28	.150E+02	.319E+28	.160E+02	.319E+28	
.170E+02	.190E+31	.180E+02	.286E+28	.190E+02	.286E+28	.200E+02	.286E+28	.210E+02	.286E+28	
.220E+02	.230E+31	.230E+02	.266E+28	.240E+02	.266E+28	.255E+02	.266E+28	.270E+02	.266E+28	
.280E+02	.280E+31	.300E+02	.242E+28	.320E+02	.242E+28	.340E+02	.242E+28	.360E+02	.242E+28	
.380E+02	.340E+31	.400E+02	.220E+28	.420E+02	.220E+28	.450E+02	.220E+28	.470E+02	.220E+28	
.500E+02	.410E+31	.525E+02	.200E+28	.550E+02	.200E+28	.575E+02	.200E+28	.600E+02	.200E+28	
.630E+02	.490E+31	.660E+02	.180E+28	.690E+02	.180E+28	.720E+02	.180E+28	.760E+02	.180E+28	
.800E+02	.580E+31	.840E+02	.160E+28	.880E+02	.160E+28	.920E+02	.160E+28	.960E+02	.160E+28	
.100E+01	.690E+31	.105E+01	.140E+28	.110E+01	.140E+28	.115E+01	.140E+28	.120E+01	.140E+28	
.120E+01	.810E+31	.135E+01	.120E+28	.140E+01	.120E+28	.150E+01	.120E+28	.160E+01	.120E+28	
.170E+01	.970E+31	.180E+01	.100E+28	.190E+01	.100E+28	.200E+01	.100E+28	.210E+01	.100E+28	
.220E+01	.110E+32	.230E+01	.80E+28	.240E+01	.80E+28	.255E+01	.80E+28	.270E+01	.80E+28	
.280E+01	.130E+32	.300E+01	.64E+28	.320E+01	.64E+28	.340E+01	.64E+28	.360E+01	.64E+28	
.380E+01	.160E+32	.400E+01	.50E+28	.420E+01	.50E+28	.450E+01	.50E+28	.470E+01	.50E+28	
.500E+01	.190E+32	.525E+01	.40E+28	.550E+01	.40E+28	.575E+01	.40E+28	.600E+01	.40E+28	
.630E+01	.230E+32	.660E+01	.32E+28	.690E+01	.32E+28	.720E+01	.32E+28	.760E+01	.32E+28	
.800E+01	.280E+32	.840E+01	.26E+28	.880E+01	.26E+28	.920E+01	.26E+28	.960E+01	.26E+28	
.100E+00	.340E+32	.105E+00	.21E+28	.110E+00	.21E+28	.115E+00	.21E+28	.120E+00	.21E+28	
.120E+00	.410E+32	.135E+00	.17E+28	.140E+00	.17E+28	.150E+00	.17E+28	.160E+00	.17E+28	
.170E+00	.490E+32	.180E+00	.14E+28	.190E+00	.14E+28	.200E+00	.14E+28	.210E+00	.14E+28	
.220E+00	.590E+32	.230E+00	.11E+28	.240E+00	.11E+28	.255E+00	.11E+28	.270E+00	.11E+28	
.280E+00	.710E+32	.300E+00	.90E+28	.320E+00	.90E+28	.340E+00	.90E+28	.360E+00	.90E+28	
.380E+00	.850E+32	.400E+00	.72E+28	.420E+00	.72E+28	.450E+00	.72E+28	.470E+00	.72E+28	
.500E+00	.100E+33	.525E+00	.58E+28	.550E+00	.58E+28	.575E+00	.58E+28	.600E+00	.58E+28	
.630E+00	.120E+33	.660E+00	.47E+28	.690E+00	.47E+28	.720E+00	.47E+28	.760E+00	.47E+28	
.800E+00	.150E+33	.840E+00	.38E+28	.880E+00	.38E+28	.920E+00	.38E+28	.960E+00	.38E+28	
.100E+00	.180E+33	.105E+00	.30E+28	.110E+00	.30E+28	.115E+00	.30E+28	.120E+00	.30E+28	
.120E+00	.210E+33	.135E+00	.24E+28	.140E+00	.24E+28	.150E+00	.24E+28	.160E+00	.24E+28	
.170E+00	.260E+33	.180E+00	.19E+28	.190E+00	.19E+28	.200E+00	.19E+28	.210E+00	.19E+28	
.220E+00	.320E+33	.230E+00	.15E+28	.240E+00	.15E+28	.255E+00	.15E+28	.270E+00	.15E+28	
.280E+00	.390E+33	.300E+00	.12E+28	.320E+00	.12E+28	.340E+00	.12E+28	.360E+00	.12E+28	
.380E+00	.470E+33	.400E+00	.90E+28	.420E+00	.90E+28	.450E+00	.90E+28	.470E+00	.90E+28	
.500E+00	.570E+33	.525E+00	.72E+28	.550E+00	.72E+28	.575E+00	.72E+28	.600E+00	.72E+28	
.630E+00	.690E+33	.660E+00	.58E+28	.690E+00	.58E+28	.720E+00	.58E+28	.760E+00	.58E+28	
.800E+										

Table 28:

REACTION	CU632	CU63(N,2N)CU62	REACTION	CU632	CU63(N,2N)CU62	REACTION	CU632	CU63(N,2N)CU62	REACTION	CU632	CU63(N,2N)CU62
ENERGY /MEV	CROSSSECTION /M**2	ENERGY /MEV	CROSSSECTION /M**2	ENERGY /MEV	CROSSSECTION /M**2	ENERGY /MEV	CROSSSECTION /M**2	ENERGY /MEV	CROSSSECTION /M**2	ENERGY /MEV	CROSSSECTION /M**2
.105E+02	0.	.106E+02	0.	.107E+02	.750E-32	.108E+02	.600E-31	.109E+02	.120E-30	.110E+02	.111E+02
.110E+02	.180E-30	.111E+02	.240E-30	.112E+02	.360E-30	.113E+02	.840E-30	.114E+02	.138E-29	.115E+02	.246E-29
.115E+02	.192E-29	.116E+02	.246E-29	.117E+02	.318E-29	.118E+02	.495E-29	.119E+02	.689E-29	.120E+02	.884E-29
.120E+02	.884E-29	.121E+02	.108E-28	.122E+02	.127E-28	.123E+02	.147E-28	.124E+02	.166E-28	.125E+02	.188E-28
.125E+02	.188E-28	.126E+02	.214E-28	.127E+02	.239E-28	.128E+02	.264E-28	.129E+02	.299E-28	.130E+02	.314E-28
.130E+02	.314E-28	.131E+02	.339E-28	.132E+02	.364E-28	.133E+02	.389E-28	.134E+02	.414E-28	.135E+02	.436E-28
.135E+02	.436E-28	.136E+02	.454E-28	.137E+02	.472E-28	.138E+02	.490E-28	.139E+02	.507E-28	.140E+02	.525E-28
.140E+02	.525E-28	.141E+02	.543E-28	.142E+02	.561E-28	.143E+02	.579E-28	.144E+02	.597E-28	.145E+02	.612E-28
.145E+02	.612E-28	.146E+02	.624E-28	.147E+02	.636E-28	.148E+02	.649E-28	.149E+02	.661E-28	.150E+02	.673E-28
.150E+02	.673E-28	.151E+02	.685E-28	.152E+02	.697E-28	.153E+02	.710E-28	.154E+02	.722E-28	.155E+02	.732E-28
.155E+02	.732E-28	.156E+02	.741E-28	.157E+02	.749E-28	.158E+02	.758E-28	.159E+02	.766E-28	.160E+02	.775E-28
.160E+02	.775E-28	.161E+02	.783E-28	.162E+02	.792E-28	.163E+02	.800E-28	.164E+02	.809E-28	.165E+02	.815E-28
.165E+02	.815E-28	.166E+02	.820E-28	.167E+02	.825E-28	.168E+02	.830E-28	.169E+02	.835E-28	.170E+02	.840E-28
.170E+02	.840E-28	.171E+02	.845E-28	.172E+02	.850E-28	.173E+02	.855E-28	.174E+02	.859E-28	.175E+02	.865E-28
.175E+02	.865E-28	.176E+02	.871E-28	.177E+02	.877E-28	.178E+02	.883E-28	.179E+02	.889E-28		

Table 29:

REACTION	ZN64P	64ZN(N,P)64CU	REACTION	ZN64P	64ZN(N,P)64CU	REACTION	ZN64P	64ZN(N,P)64CU	REACTION	ZN64P	64ZN(N,P)64CU
ENERGY /MEV	CROSSSECTION /M**2	ENERGY /MEV	CROSSSECTION /M**2	ENERGY /MEV	CROSSSECTION /M**2	ENERGY /MEV	CROSSSECTION /M**2	ENERGY /MEV	CROSSSECTION /M**2	ENERGY /MEV	CROSSSECTION /M**2
.150E+01	0.	.160E+01	.890E-31	.170E+01	.309E-30	.180E+01	.610E-30	.190E+01	.102E-29	.200E+01	.159E-29
.200E+01	.159E-29	.210E+01	.229E-29	.220E+01	.302E-29	.230E+01	.374E-29	.240E+01	.445E-29	.250E+01	.514E-29
.250E+01	.514E-29	.260E+01	.583E-29	.270E+01	.651E-29	.280E+01	.750E-29	.290E+01	.844E-29	.300E+01	.986E-29
.300E+01	.986E-29	.310E+01	.104E-28	.320E+01	.110E-28	.330E+01	.115E-28	.340E+01	.120E-28	.350E+01	.125E-28
.350E+01	.125E-28	.360E+01	.130E-28	.370E+01	.135E-28	.380E+01	.140E-28	.390E+01	.144E-28	.400E+01	.149E-28
.400E+01	.149E-28	.410E+01	.154E-28	.420E+01	.159E-28	.430E+01	.163E-28	.440E+01	.168E-28	.450E+01	.172E-28
.450E+01	.172E-28	.460E+01	.177E-28	.470E+01	.181E-28	.480E+01	.186E-28	.490E+01	.190E-28	.500E+01	.194E-28
.500E+01	.194E-28	.510E+01	.198E-28	.520E+01	.202E-28	.530E+01	.206E-28	.540E+01	.210E-28	.550E+01	.213E-28
.550E+01	.213E-28	.560E+01	.217E-28	.570E+01	.220E-28	.580E+01	.223E-28	.590E+01	.226E-28	.600E+01	.229E-28
.600E+01	.229E-28	.610E+01	.232E-28	.620E+01	.234E-28	.630E+01	.237E-28	.640E+01	.239E-28	.650E+01	.241E-28
.650E+01	.241E-28	.660E+01	.244E-28	.670E+01	.246E-28	.680E+01	.247E-28	.690E+01	.249E-28	.700E+01	.251E-28
.700E+01	.251E-28	.710E+01	.252E-28	.720E+01	.254E-28	.730E+01	.255E-28	.740E+01	.257E-28	.750E+01	.258E-28
.750E+01	.258E-28	.760E+01	.260E-28	.770E+01	.261E-28	.780E+01	.262E-28	.790E+01	.264E-28	.800E+01	.265E-28
.800E+01	.265E-28	.810E+01	.266E-28	.820E+01	.267E-28	.830E+01	.269E-28	.840E+01	.270E-28	.850E+01	.271E-28
.850E+01	.271E-28	.860E+01	.273E-28	.870E+01	.274E-28	.880E+01	.275E-28	.890E+01	.277E-28	.900E+01	.278E-28
.900E+01	.278E-28	.910E+01	.279E-28	.920E+01	.281E-28	.930E+01	.282E-28	.940E+01	.283E-28	.950E+01	.285E-28
.950E+01	.285E-28	.960E+01	.286E-28	.970E+01	.287E-28	.980E+01	.288E-28	.990E+01	.289E-28	.100E+02	.290E-28
.100E+02	.290E-28	.101E+02	.291E-28	.102E+02	.292E-28	.103E+02	.293E-28	.104E+02	.293E-28	.105E+02	.294E-28
.105E+02	.294E-28	.106E+02	.294E-28	.107E+02	.295E-28	.108E+02	.295E-28	.109E+02	.295E-28	.110E+02	.294E-28
.110E+02	.294E-28	.111E+02	.294E-28	.112E+02	.293E-28	.113E+02	.292E-28	.114E+02	.291E-28	.115E+02	.289E-28
.115E+02	.289E-28	.116E+02	.288E-28	.117E+02	.287E-28	.118E+02	.285E-28	.119E+02	.283E-28	.120E+02	.281E-28
.120E+02	.281E-28	.121E+02	.278E-28	.122E+02	.276E-28	.123E+02	.273E-28	.124E+02	.270E-28	.125E+02	.266E-28
.125E+02	.266E-28	.126E+02	.262E-28	.127E+02	.259E-28	.128E+02	.255E-28	.129E+02	.251E-28	.130E+02	.247E-28
.130E+02	.247E-28	.131E+02	.242E-28	.132E+02	.238E-28	.133E+02	.234E-28	.134E+02	.229E-28	.135E+02	.224E-28
.135E+02	.224E-28	.136E+02	.220E-28	.137E+02	.215E-28	.138E+02	.211E-28	.139E+02	.206E-28	.140E+02	.201E-28
.140E+02	.201E-28	.141E+02	.197E-28	.142E+02	.192E-28	.143E+02	.188E-28	.144E+02	.183E-28	.145E+02	.179E-28
.145E+02	.179E-28	.146E+02	.175E-28	.147E+02	.172E-28	.148E+02	.168E-28	.149E+02	.165E-28	.150E+02	.162E-28
.150E+02	.162E-28	.151E+02	.159E-28	.152E+02	.156E-28	.153E+02	.153E-28	.154E+02	.150E-28	.155E+02	.148E-28
.155E+02	.148E-28	.156E+02	.146E-28	.157E+02	.145E-28	.158E+02	.143E-28	.159E+02	.142E-28	.160E+02	.141E-28
.160E+02	.141E-28	.161E+02	.140E-28	.162E+02	.139E-28	.163E+02	.139E-28	.164E+02	.138E-28	.165E+02	.137E-28
.165E+02	.137E-28	.166E+02	.136E-28	.167E+02	.136E-28	.168E+02	.136E-28	.169E+02	.136E-28	.170E+02	.135E-28
.170E+02	.135E-28	.171E+02	.134E-28	.172E+02	.133E-28	.173E+02	.132E-28	.174E+02	.130E-28	.175E+02	.128E-28
.175E+02	.128E-28	.176E+02	.126E-28	.177E+02	.124E-28	.178E+02	.122E-28	.179E+02	.120E-28		

Table 30:

REACTION	ZN642N	64ZN(N,2N)63ZN	REACTION	ZN642N	64ZN(N,2N)63ZN	REACTION	ZN642N	64ZN(N,2N)63ZN	REACTION	ZN642N	64ZN(N,2N)63ZN
ENERGY /MEV	CROSSSECTION /M**2	ENERGY /MEV	CROSSSECTION /M**2	ENERGY /MEV	CROSSSECTION /M**2	ENERGY /MEV	CROSSSECTION /M**2	ENERGY /MEV	CROSSSECTION /M**2	ENERGY /MEV	CROSSSECTION /M**2
.120E+02	0.	.121E+02	.115E-30	.122E+02	.251E-30	.123E+02	.355E-30	.124E+02	.580E-30	.125E+02	.905E-30
.125E+02	.905E-30	.126E+02	.133E-29	.127E+02	.186E-29	.128E+02	.246E-29	.129E+02	.317E-29	.130E+02	.387E-29
.130E+02	.387E-29	.131E+02	.467E-29	.132E+02	.567E-29	.133E+02	.673E-29	.134E+02	.766E-29	.135E+02	.861E-29
.135E+02	.861E-29	.136E+02	.959E-29	.137E+02	.105E-28	.138E+02	.115E-28	.139E+02	.125E-28	.140E+02	.135E-28
.140E+02	.135E-28	.141E+02	.145E-28	.142E+02	.155E-28	.143E+02	.165E-28	.144E+02	.175E-28	.145E+02	.185E-28
.145E+02	.185E-28	.146E+02	.195E-28	.147E+02	.205E-28	.148E+02	.215E-28	.149E+02	.225E-28	.150E+02	.234E-28
.150E+02	.234E-28	.151E+02	.243E-28	.152E+02	.252E-28	.153E+02	.262E-28	.154E+02	.271E-28	.155E+02	.279E-28
.155E+02	.279E-28	.156E+02	.287E-28	.157E+02	.295E-28	.158E+02	.303E-28	.159E+02	.311E-28	.160E+02	.319E-28
.160E+02	.319E-28	.161E+02	.326E-28	.162E+02	.333E-28	.163E+02	.340E-28	.164E+02	.347E-28	.165E+02	.353E-28
.165E+02	.353E-28	.166E+02	.359E-28	.167E+02	.365E-28	.168E+02	.371E-28	.169E+02	.376E-28	.170E+02	.381E-28
.170E+02	.381E-28	.171E+02	.386E-28	.172E+02	.391E-28	.173E+02	.396E-28	.174E+02	.400E-28	.175E+02	.404E-28
.175E+02	.404E-28	.176E+02	.408E-28	.177E+02	.412E-28	.178E+02	.416E-28	.179E+02	.419E-28		

Table 31:

REACTION	CU6524	CU65(N,2N)CU64	REACTION	CU6524	CU65(N,2N)CU64	REACTION	CU6524	CU65(N,2N)CU64	REACTION	CU6524	CU65(N,2N)CU64
ENERGY /MEV	CROSSSECTION /M**2	ENERGY /MEV	CROSSSECTION /M**2	ENERGY /MEV	CROSSSECTION /M**2	ENERGY /MEV	CROSSSECTION /M**2	ENERGY /MEV	CROSSSECTION /M**2	ENERGY /MEV	CROSSSECTION /M**2
.100E+02	.629E-31	.101E+02	.707E-30	.102E+02	.149E-29	.103E+02	.228E-29	.104E+02	.305E-29	.105E+02	.466E-29
.105E+02	.466E-29	.106E+02	.705E-29	.107E+02	.965E-29	.108E+02	.118E-28	.109E+02	.142E-28	.110E+02	.170E-28
.110E+02	.170E-28	.111E+02	.202E-28	.112E+02	.234E-28	.113E+02	.266E-28	.114E+02	.297E-28	.115E+02	.330E-28
.115E+02	.330E-28	.116E+02	.362E-28	.117E+02	.394E-28	.118E+02	.427E-28	.119E+02	.459E-28	.120E+02	.490E-28
.120E+02	.490E-28	.121E+02	.520E-28	.122E+02	.548E-28	.123E+02	.576E-28	.124E+02	.603E-28	.125E+02	.628E-28
.125E+02	.628E-28	.126E+02	.653E-28	.127E+02	.677E-28	.128E+02	.699E-28	.129E+02	.721E-28	.130E+02	.742E-28
.130E+02	.742E-28	.131E+02	.763E-28	.132E+02	.782E-28	.133E+02	.801E-28	.134E+02	.819E-28	.135E+02	.835E-28
.135E+02	.835E-28	.136E+02	.852E-28	.137E+02	.867E-28	.138E+02	.882E-28	.139E+02	.896E-28	.140E+02	.909E-28
.140E+02	.909E-28	.141E+02	.922E-28	.142E+02	.934E-28	.143E+02	.945E-28	.144E+02	.955E-28	.145E+02	.964E-28
.145E+02	.964E-28	.146E+02	.973E-28	.147E+02	.980E-28	.148E+02	.987E-28	.149E+02	.994E-28	.150E+02	.100E-27
.150E+02	.100E-27	.151E+02	.101E-27	.152E+02	.101E-27	.153E+02	.102E-27	.154E+02	.102E-27	.155E+02	.103E-27
.155E+02	.103E-27	.156E+02	.103E-27	.157E+02	.104E-27	.158E+02	.104E-27	.159E+02	.105E-27	.160E+02	.105E-27
.160E+02	.105E-27	.161E+02	.106E-27	.162E+02	.106E-27	.163E+02	.106E-27	.164E+02	.107E-27	.165E+02	.107E-27
.165E+02	.107E-27	.166E+02									

Table 32:

REACTION	ZR90 2	ZR90 (N,2N)ZR69	ENERGY /MEV	CROSSSECTION /M**2	ENERGY /MEV	CROSSSECTION /M**2	ENERGY /MEV	CROSSSECTION /M**2	ENERGY /MEV	CROSSSECTION /M**2	ENERGY /MEV	CROSSSECTION /M**2
.120E+02	0.	.121E+02	.137E-29	.122E+02	.4 09E-29	.123E+02	.678E-29	.124E+02	.946E-29			
.125E+02	.123E-28	.126E+02	.153E-28	.127E+02	.143E-28	.128E+02	.217E-28	.129E+02	.250E-28			
.130E+02	.284E-28	.131E+02	.319E-28	.132E+02	.353E-28	.133E+02	.388E-28	.134E+02	.473E-28			
.135E+02	.458E-28	.136E+02	.495E-28	.137E+02	.532E-28	.138E+02	.566E-28	.139E+02	.600E-28			
.140E+02	.633E-28	.141E+02	.664E-28	.142E+02	.696E-28	.143E+02	.725E-28	.144E+02	.754E-28			
.145E+02	.781E-28	.146E+02	.808E-28	.147E+02	.833E-28	.148E+02	.856E-28	.149E+02	.878E-28			
.150E+02	.899E-28	.151E+02	.918E-28	.152E+02	.938E-28	.153E+02	.955E-28	.154E+02	.972E-28			
.155E+02	.989E-28	.156E+02	.100E-27	.157E+02	.102E-27	.158E+02	.103E-27	.159E+02	.105E-27			
.160E+02	.106E-27	.161E+02	.108E-27	.162E+02	.109E-27	.163E+02	.110E-27	.164E+02	.111E-27			
.165E+02	.111E-27	.166E+02	.112E-27	.167E+02	.113E-27	.168E+02	.113E-27	.169E+02	.114E-27			
.170E+02	.114E-27	.171E+02	.115E-27	.172E+02	.115E-27	.173E+02	.115E-27	.174E+02	.116E-27			
.175E+02	.116E-27	.176E+02	.116E-27	.177E+02	.117E-27	.178E+02	.117E-27	.179E+02	.117E-27			

Table 33:

REACTION	ZR90 P	90ZK(N,P)90Y	ENERGY /MEV	CROSSSECTION /M**2	ENERGY /MEV	CROSSSECTION /M**2	ENERGY /MEV	CROSSSECTION /M**2	ENERGY /MEV	CROSSSECTION /M**2	ENERGY /MEV	CROSSSECTION /M**2
.300E+01	0.	.310E+01	0.	.320E+01	0.	.330E+01	0.	.340E+01	.115E-37			
.350E+01	.350E-32	.360E+01	.615E-32	.370E+01	.935E-32	.380E+01	.132E-31	.390E+01	.178E-31			
.400E+01	.232E-31	.410E+01	.295E-31	.420E+01	.367E-31	.430E+01	.450E-31	.440E+01	.544E-31			
.450E+01	.649E-31	.460E+01	.767E-31	.470E+01	.897E-31	.480E+01	.104E-30	.490E+01	.119E-30			
.500E+01	.137E-30	.510E+01	.155E-30	.520E+01	.175E-30	.530E+01	.196E-30	.540E+01	.219E-30			
.550E+01	.243E-30	.560E+01	.269E-30	.570E+01	.296E-30	.580E+01	.325E-30	.590E+01	.355E-30			
.600E+01	.387E-30	.610E+01	.421E-30	.620E+01	.456E-30	.630E+01	.492E-30	.640E+01	.530E-30			
.650E+01	.570E-30	.660E+01	.611E-30	.670E+01	.653E-30	.680E+01	.697E-30	.690E+01	.743E-30			
.700E+01	.789E-30	.710E+01	.837E-30	.720E+01	.886E-30	.730E+01	.937E-30	.740E+01	.986E-30			
.750E+01	.104E-29	.760E+01	.109E-29	.770E+01	.115E-29	.780E+01	.121E-29	.790E+01	.126E-29			
.800E+01	.132E-29	.810E+01	.138E-29	.820E+01	.144E-29	.830E+01	.150E-29	.840E+01	.156E-29			
.850E+01	.163E-29	.860E+01	.169E-29	.870E+01	.175E-29	.880E+01	.182E-29	.890E+01	.188E-29			
.900E+01	.195E-29	.910E+01	.201E-29	.920E+01	.208E-29	.930E+01	.214E-29	.940E+01	.221E-29			
.950E+01	.228E-29	.960E+01	.234E-29	.970E+01	.241E-29	.980E+01	.248E-29	.990E+01	.254E-29			
.100E+02	.261E-29	.101E+02	.267E-29	.102E+02	.274E-29	.103E+02	.281E-29	.104E+02	.287E-29			
.105E+02	.293E-29	.106E+02	.300E-29	.107E+02	.306E-29	.108E+02	.312E-29	.109E+02	.319E-29			
.110E+02	.325E-29	.111E+02	.331E-29	.112E+02	.337E-29	.113E+02	.342E-29	.114E+02	.348E-29			
.115E+02	.354E-29	.116E+02	.359E-29	.117E+02	.364E-29	.118E+02	.370E-29	.119E+02	.375E-29			
.120E+02	.380E-29	.121E+02	.385E-29	.122E+02	.389E-29	.123E+02	.394E-29	.124E+02	.399E-29			
.125E+02	.403E-29	.126E+02	.417E-29	.127E+02	.411E-29	.128E+02	.415E-29	.129E+02	.418E-29			
.130E+02	.422E-29	.131E+02	.425E-29	.132E+02	.426E-29	.133E+02	.431E-29	.134E+02	.434E-29			
.135E+02	.437E-29	.136E+02	.439E-29	.137E+02	.442E-29	.138E+02	.444E-29	.139E+02	.446E-29			
.140E+02	.447E-29	.141E+02	.449E-29	.142E+02	.450E-29	.143E+02	.451E-29	.144E+02	.452E-29			
.145E+02	.453E-29	.146E+02	.454E-29	.147E+02	.455E-29	.148E+02	.455E-29	.149E+02	.456E-29			
.150E+02	.456E-29	.151E+02	.456E-29	.152E+02	.456E-29	.153E+02	.456E-29	.154E+02	.456E-29			
.155E+02	.455E-29	.156E+02	.454E-29	.157E+02	.453E-29	.158E+02	.452E-29	.159E+02	.452E-29			
.160E+02	.451E-29	.161E+02	.450E-29	.162E+02	.449E-29	.163E+02	.447E-29	.164E+02	.446E-29			
.165E+02	.445E-29	.166E+02	.444E-29	.167E+02	.443E-29	.168E+02	.441E-29	.169E+02	.440E-29			
.170E+02	.439E-29	.171E+02	.438E-29	.172E+02	.437E-29	.173E+02	.436E-29	.174E+02	.435E-29			
.175E+02	.434E-29	.176E+02	.433E-29	.177E+02	.432E-29	.178E+02	.431E-29	.179E+02	.430E-29			









Table 38:

REACTION	I12724	I127 (N,2N)	I126	ENERGY /MEV	CROSSSECTION /M**2	ENERGY /MEV	CROSSSECTION /M**2	ENERGY /MEV	CROSSSECTION /M**2	ENERGY /MEV	CROSSSECTION /M**2	ENERGY /MEV	CROSSSECTION /M**2
.900E+01	0.	.910E+01	0.	.920E+01	.834E-30	.930E+01	.413E-29	.940E+01	.769E-29				
.950E+01	.114E-28	.960E+01	.152E-28	.970E+01	.191E-28	.980E+01	.233E-28	.990E+01	.277E-28				
.100E+02	.324E-28	.101E+02	.374E-28	.102E+02	.425E-28	.103E+02	.479E-28	.104E+02	.533E-28				
.105E+02	.587E-28	.106E+02	.642E-28	.107E+02	.695E-28	.108E+02	.748E-28	.109E+02	.600E-28				
.110E+02	.849E-28	.111E+02	.897E-28	.112E+02	.943E-28	.113E+02	.987E-28	.114E+02	.103E-27				
.115E+02	.107E-27	.116E+02	.111E-27	.117E+02	.114E-27	.118E+02	.118E-27	.119E+02	.121E-27				
.120E+02	.124E-27	.121E+02	.128E-27	.122E+02	.130E-27	.123E+02	.133E-27	.124E+02	.136E-27				
.125E+02	.138E-27	.126E+02	.141E-27	.127E+02	.143E-27	.128E+02	.145E-27	.129E+02	.147E-27				
.130E+02	.149E-27	.131E+02	.150E-27	.132E+02	.152E-27	.133E+02	.154E-27	.134E+02	.155E-27				
.135E+02	.156E-27	.136E+02	.157E-27	.137E+02	.156E-27	.138E+02	.159E-27	.139E+02	.160E-27				
.140E+02	.161E-27	.141E+02	.162E-27	.142E+02	.163E-27	.143E+02	.164E-27	.144E+02	.165E-27				
.145E+02	.165E-27	.146E+02	.166E-27	.147E+02	.167E-27	.148E+02	.168E-27	.149E+02	.169E-27				
.150E+02	.169E-27	.151E+02	.170E-27	.152E+02	.171E-27	.153E+02	.172E-27	.154E+02	.172E-27				
.155E+02	.173E-27	.156E+02	.174E-27	.157E+02	.174E-27	.158E+02	.175E-27	.159E+02	.175E-27				
.160E+02	.175E-27	.161E+02	.175E-27	.162E+02	.175E-27	.163E+02	.174E-27	.164E+02	.173E-27				
.165E+02	.172E-27	.166E+02	.171E-27	.167E+02	.170E-27	.168E+02	.168E-27	.169E+02	.166E-27				
.170E+02	.164E-27	.171E+02	.161E-27	.172E+02	.158E-27	.173E+02	.155E-27	.174E+02	.152E-27				
.175E+02	.148E-27	.176E+02	.144E-27	.177E+02	.140E-27	.178E+02	.136E-27	.179E+02	.132E-27				





Table 41:

REACTION	TH232N	TH232(N,2N)231TH	ENERGY	CROSSSECTION	ENERGY	CROSSSECTION	ENERGY	CROSSSECTION	ENERGY	CROSSSECTION	ENERGY	CROSSSECTION
/MEV	/M**2	/MEV	/M**2	/MEV	/M**2	/MEV	/M**2	/MEV	/M**2	/MEV	/M**2	/M**2
.650E+01	.700E-30	.660E+01	.292E-29	.670E+01	.727E-29	.680E+01	.139E-28	.690E+01	.224E-28			
.700E+01	.321E-28	.710E+01	.428E-28	.720E+01	.541E-28	.730E+01	.657E-28	.740E+01	.773E-28			
.750E+01	.887E-28	.760E+01	.998E-28	.770E+01	.110E-27	.780E+01	.120E-27	.790E+01	.127E-27			
.800E+01	.134E-27	.810E+01	.140E-27	.820E+01	.146E-27	.830E+01	.151E-27	.840E+01	.156E-27			
.850E+01	.160E-27	.860E+01	.164E-27	.870E+01	.168E-27	.880E+01	.171E-27	.890E+01	.174E-27			
.900E+01	.176E-27	.910E+01	.178E-27	.920E+01	.180E-27	.930E+01	.182E-27	.940E+01	.184E-27			
.950E+01	.185E-27	.960E+01	.186E-27	.970E+01	.186E-27	.980E+01	.187E-27	.990E+01	.187E-27			
.100E+02	.188E-27	.101E+02	.188E-27	.102E+02	.188E-27	.103E+02	.187E-27	.104E+02	.187E-27			
.105E+02	.187E-27	.106E+02	.186E-27	.107E+02	.186E-27	.108E+02	.185E-27	.109E+02	.184E-27			
.110E+02	.183E-27	.111E+02	.182E-27	.112E+02	.181E-27	.113E+02	.180E-27	.114E+02	.179E-27			
.115E+02	.178E-27	.116E+02	.177E-27	.117E+02	.175E-27	.118E+02	.174E-27	.119E+02	.173E-27			
.120E+02	.172E-27	.121E+02	.170E-27	.122E+02	.169E-27	.123E+02	.168E-27	.124E+02	.166E-27			
.125E+02	.165E-27	.126E+02	.163E-27	.127E+02	.162E-27	.128E+02	.161E-27	.129E+02	.159E-27			
.130E+02	.158E-27	.131E+02	.156E-27	.132E+02	.155E-27	.133E+02	.153E-27	.134E+02	.152E-27			
.135E+02	.150E-27	.136E+02	.149E-27	.137E+02	.147E-27	.138E+02	.146E-27	.139E+02	.144E-27			
.140E+02	.143E-27	.141E+02	.141E-27	.142E+02	.139E-27	.143E+02	.138E-27	.144E+02	.136E-27			
.145E+02	.135E-27	.133E+02	.133E-27	.147E+02	.131E-27	.148E+02	.129E-27	.149E+02	.128E-27			
.150E+02	.126E-27	.151E+02	.124E-27	.152E+02	.122E-27	.153E+02	.120E-27	.154E+02	.119E-27			
.155E+02	.117E-27	.156E+02	.115E-27	.157E+02	.113E-27	.158E+02	.111E-27	.159E+02	.109E-27			
.160E+02	.106E-27	.161E+02	.104E-27	.162E+02	.102E-27	.163E+02	.999E-28	.164E+02	.977E-28			
.165E+02	.954E-28	.166E+02	.931E-28	.167E+02	.907E-28	.168E+02	.883E-28	.169E+02	.859E-28			
.170E+02	.834E-28	.171E+02	.810E-28	.172E+02	.785E-28	.173E+02	.760E-28	.174E+02	.734E-28			
.175E+02	.708E-28	.176E+02	.682E-28	.177E+02	.656E-28	.178E+02	.630E-28	.179E+02	.604E-28			

Table 42:

REACTION	TH232F4	TH232(N,F)F.P.	ENERGY	CROSSSECTION	ENERGY	CROSSSECTION	ENERGY	CROSSSECTION	ENERGY	CROSSSECTION	ENERGY	CROSSSECTION
/MEV	/M**2	/MEV	/M**2	/MEV	/M**2	/MEV	/M**2	/MEV	/M**2	/MEV	/M**2	/M**2
.100E+01	0.	.110E+01	0.	.120E+01	.500E-30	.130E+01	.275E-29	.140E+01	.667E-29			
.150E+01	.883E-29	.160E+01	.108E-28	.170E+01	.840E-29	.180E+01	.820E-29	.190E+01	.102E-28			
.200E+01	.114E-28	.210E+01	.119E-28	.220E+01	.120E-28	.230E+01	.115E-28	.240E+01	.110E-28			
.250E+01	.110E-28	.260E+01	.115E-28	.270E+01	.119E-28	.280E+01	.123E-28	.290E+01	.128E-28			
.300E+01	.131E-28	.310E+01	.132E-28	.320E+01	.134E-28	.330E+01	.136E-28	.340E+01	.137E-28			
.350E+01	.138E-28	.360E+01	.139E-28	.370E+01	.140E-28	.380E+01	.141E-28	.390E+01	.142E-28			
.400E+01	.143E-28	.410E+01	.144E-28	.420E+01	.144E-28	.430E+01	.144E-28	.440E+01	.145E-28			
.450E+01	.145E-28	.460E+01	.145E-28	.470E+01	.144E-28	.480E+01	.144E-28	.490E+01	.144E-28			
.500E+01	.144E-28	.510E+01	.143E-28	.520E+01	.142E-28	.530E+01	.141E-28	.540E+01	.140E-28			
.550E+01	.139E-28	.560E+01	.137E-28	.570E+01	.135E-28	.580E+01	.135E-28	.590E+01	.138E-28			
.600E+01	.150E-28	.610E+01	.170E-28	.620E+01	.190E-28	.630E+01	.210E-28	.640E+01	.230E-28			
.650E+01	.253E-28	.660E+01	.280E-28	.670E+01	.307E-28	.680E+01	.326E-28	.690E+01	.338E-28			
.700E+01	.350E-28	.710E+01	.362E-28	.720E+01	.364E-28	.730E+01	.357E-28	.740E+01	.349E-28			
.750E+01	.341E-28	.760E+01	.334E-28	.770E+01	.329E-28	.780E+01	.327E-28	.790E+01	.325E-28			
.800E+01	.323E-28	.810E+01	.322E-28	.820E+01	.321E-28	.830E+01	.318E-28	.840E+01	.315E-28			
.850E+01	.312E-28	.860E+01	.309E-28	.870E+01	.306E-28	.880E+01	.303E-28	.890E+01	.300E-28			
.900E+01	.297E-28	.910E+01	.296E-28	.920E+01	.294E-28	.930E+01	.293E-28	.940E+01	.291E-28			
.950E+01	.290E-28	.960E+01	.288E-28	.970E+01	.287E-28	.980E+01	.285E-28	.990E+01	.284E-28			
.100E+02	.283E-28	.101E+02	.283E-28	.102E+02	.283E-28	.103E+02	.283E-28	.104E+02	.282E-28			
.105E+02	.282E-28	.106E+02	.282E-28	.107E+02	.282E-28	.108E+02	.282E-28	.109E+02	.282E-28			
.110E+02	.282E-28	.111E+02	.283E-28	.112E+02	.284E-28	.113E+02	.285E-28	.114E+02	.285E-28			
.115E+02	.287E-28	.116E+02	.288E-28	.117E+02	.289E-28	.118E+02	.290E-28	.119E+02	.291E-28			
.120E+02	.292E-28	.121E+02	.295E-28	.122E+02	.298E-28	.123E+02	.301E-28	.124E+02	.304E-28			
.125E+02	.307E-28	.126E+02	.310E-28	.127E+02	.313E-28	.128E+02	.316E-28	.129E+02	.319E-28			
.130E+02	.322E-28	.131E+02	.326E-28	.132E+02	.330E-28	.133E+02	.334E-28	.134E+02	.338E-28			
.135E+02	.342E-28	.136E+02	.346E-28	.137E+02	.350E-28	.138E+02	.354E-28	.139E+02	.358E-28			
.140E+02	.363E-28	.141E+02	.368E-28	.142E+02	.374E-28	.143E+02	.379E-28	.144E+02	.385E-28			
.145E+02	.390E-28	.146E+02	.396E-28	.147E+02	.401E-28	.148E+02	.407E-28	.149E+02	.412E-28			
.150E+02	.416E-28	.151E+02	.418E-28	.152E+02	.421E-28	.153E+02	.423E-28	.154E+02	.425E-28			
.155E+02	.428E-28	.156E+02	.430E-28	.157E+02	.433E-28	.158E+02	.435E-28	.159E+02	.437E-28			
.160E+02	.440E-28	.161E+02	.442E-28	.162E+02	.444E-28	.163E+02	.447E-28	.164E+02	.449E-28			
.165E+02	.451E-28	.166E+02	.454E-28	.167E+02	.456E-28	.168E+02	.458E-28	.169E+02	.461E-28			
.170E+02	.463E-28	.171E+02	.465E-28	.172E+02	.468E-28	.173E+02	.470E-28	.174E+02	.472E-28			
.175E+02	.475E-28	.176E+02	.477E-28	.177E+02	.479E-28	.178E+02	.482E-28	.179E+02	.484E-28			

















Table 51: Average cross sections, key to tables and figures

reaction	code	g. $\sigma_0$ (in b)	$\langle\sigma\rangle$ (in m <sup>2</sup> )			figure number	table number	reference
			Maxwell	1/E	Watt			
${}^6\text{Li}(n,\alpha){}^3\text{H}$	LI6A4	9.437E-22	8.366E-22	4.002E-22	4.796E-25	1	1	3
${}^{10}\text{B}(n,\alpha){}^7\text{Li}$	B10A4	3.851E-21	3.414E-21	1.622E-21	5.039E-25	2	2	3
${}^{23}\text{Na}(n,\gamma){}^{24}\text{Na}$	NA23G4	5.360E-25	4.752E-25	3.315E-25	2.849E-28	3	3	3
${}^{24}\text{Mg}(n,p){}^{24}\text{Na}$	MG24P	0	0	0	1.498E-27	4	4	4
${}^{27}\text{Al}(n,\alpha){}^{24}\text{Na}$	AL27A4	0	0	0	6.844E-28	5	5	3
${}^{27}\text{Al}(n,p){}^{27}\text{Mg}$	AL27P4	0	0	0	4.101E-27	6	6	3
${}^{31}\text{P}(n,p){}^{31}\text{Si}$	P31P	0	0	0	3.301E-26	7	7	4
${}^{32}\text{S}(n,p){}^{32}\text{P}$	S32P4	0	0	1.226E-30	6.505E-26	8	8	3
${}^{45}\text{Sc}(n,\gamma){}^{46}\text{Sc}$	SC45G4	2.647E-23	2.347E-23	1.060E-23	5.716E-27	9	9	3
${}^{46}\text{Ti}(n,p){}^{46}\text{Sc}$	TI46P5	0	0	0	1.056E-26	10	10	8
${}^{47}\text{Ti}(n,p){}^{47}\text{Sc}$	TI47P5	0	0	5.700E-31	2.141E-26	11	11	8
${}^{47}\text{Ti}(n,np){}^{46}\text{Sc}$	TI47NP4	0	0	0	3.172E-30	12	12	3
${}^{48}\text{Ti}(n,p){}^{48}\text{Sc}$	TI48P5	0	0	0	2.637E-28	13	13	8
${}^{48}\text{Ti}(n,np){}^{47}\text{Sc}$	TI48NP4	0	0	0	1.820E-30	14	14	3
${}^{54}\text{Fe}(n,p){}^{54}\text{Mn}$	FE54P4	0	0	0	7.847E-26	15	15	3
${}^{55}\text{Mn}(n,\gamma){}^{56}\text{Mn}$	MN55G	1.336E-23	1.184E-23	1.560E-23	3.560E-27	16	16	4
${}^{55}\text{Mn}(n,2n){}^{54}\text{Mn}$	MN5524	0	0	0	2.321E-28	17	17	3
${}^{56}\text{Fe}(n,p){}^{56}\text{Mn}$	FE56P4	0	0	0	1.035E-27	18	18	3
${}^{58}\text{Fe}(n,\gamma){}^{59}\text{Fe}$	FE58G4	1.186E-24	1.051E-24	1.558E-24	1.676E-27	19	19	3
${}^{58}\text{Ni}(n,2n){}^{57}\text{Ni}$	NI5824	0	0	0	2.540E-30	20	20	3
${}^{58}\text{Ni}(n,p){}^{58}\text{Co}$	NI58P4	0	0	1.950E-28	1.028E-25	21	21	3
${}^{59}\text{Co}(n,\alpha){}^{56}\text{Mn}$	CO59A4	0	0	0	1.457E-28	22	22	3
${}^{59}\text{Co}(n,2n){}^{58}\text{Co}$	CO5924	0	0	0	1.624E-28	23	23	3
${}^{59}\text{Co}(n,\gamma){}^{60}\text{Co}$	CO59G4	3.739E-23	3.315E-23	7.576E-23	6.382E-27	24	24	3
${}^{60}\text{Ni}(n,p){}^{60}\text{Co}$	NI60P4	0	0	0	2.443E-27	25	25	3
${}^{63}\text{Cu}(n,\alpha){}^{60}\text{Co}$	CU63A4	0	0	0	3.472E-28	26	26	3
${}^{63}\text{Cu}(n,\gamma){}^{64}\text{Cu}$	CU63G4	4.513E-24	4.001E-24	5.386E-24	1.082E-26	27	27	3
${}^{63}\text{Cu}(n,2n){}^{62}\text{Cu}$	CU632	0	0	0	8.464E-29	28	28	4
${}^{64}\text{Zn}(n,p){}^{64}\text{Cu}$	ZN64P	0	0	0	4.294E-26	29	29	5
${}^{64}\text{Zn}(n,2n){}^{63}\text{Zn}$	ZN642N	0	0	0	1.657E-29	30	30	5
${}^{65}\text{Cu}(n,2n){}^{64}\text{Cu}$	CU6524	0	0	0	2.976E-28	31	31	3
${}^{90}\text{Zr}(n,2n){}^{89}\text{Zr}$	ZR902	0	0	0	7.953E-29	32	32	4
${}^{90}\text{Zr}(n,p){}^{90}\text{Y}$	ZR90P	0	0	0	3.567E-28	33	33	5
${}^{109}\text{Ag}(n,\gamma){}^{110}\text{Ag}^m$	AG109G	4.149E-24	3.678E-24	6.552E-23	1.151E-26	34	34	4
${}^{103}\text{Rh}(n,n'){}^{103}\text{Rh}^m$	RH103N	0	0	3.697E-25	7.135E-25	35	35	5

Table 51 (continued)

reaction	code	$g \cdot \sigma_0$ (in b)	$\langle \sigma \rangle$ (in $m^2$ )			figure number	table number	reference
			Maxwell	1/E	Watt			
$^{115}\text{In}(n, n')^{115}\text{In}^m$	IN115N5	0	0	1.924E-26	1.768E-25	36	36	7
$^{115}\text{In}(n, \gamma)^{116}\text{In}^m$	IN115G4	1.702E-22	1.509E-22	3.230E-21	1.350E-25	37	37	3
$^{127}\text{I}(n, 2n)^{126}\text{I}$	I12724	0	0	0	1.149E-27	38	38	3
$^{181}\text{Ta}(n, \gamma)^{182}\text{Ta}$	TA181G	2.103E-23	1.864E-23	7.634E-22	1.036E-25	39	39	4
$^{197}\text{Au}(n, \gamma)^{198}\text{Au}$	AU197G4	9.970E-23	8.839E-23	1.564E-21	8.306E-26	40	40	3
$^{232}\text{Th}(n, 2n)^{231}\text{Th}$	TH232N	0	0	0	1.503E-26	41	41	5
$^{232}\text{Th}(n, f)\text{FP}$	TH232F4	0	0	0	7.026E-26	42	42	3
$^{232}\text{Th}(n, \gamma)^{233}\text{Th}$	TH232G4	7.396E-24	6.557E-24	8.512E-23	1.019E-25	43	43	3
$^{235}\text{U}(n, f)\text{FP}$	U235F4	5.744E-22	5.092E-22	2.702E-22	1.241E-24	44	44	3
$^{237}\text{Np}(n, f)\text{FP}$	NP237F4	1.610E-26	1.427E-26	1.214E-24	1.337E-24	45	45	3
$^{238}\text{U}(n, f)\text{FP}$	U238F4	4.625E-33	4.100E-33	4.580E-27	3.016E-25	46	46	3
$^{238}\text{U}(n, \gamma)^{239}\text{U}$	U238G4	2.716E-24	2.408E-24	2.769E-22	7.430E-26	47	47	3
$^{239}\text{Pu}(n, f)\text{FP}$	PU239F4	7.853E-22	6.962E-22	2.919E-22	1.786E-24	48	48	3
$^{241}\text{Am}(n, p)\text{FP}$	AM241F	8.844E-32	7.840E-32	1.416E-23	1.217E-24	49	49	6



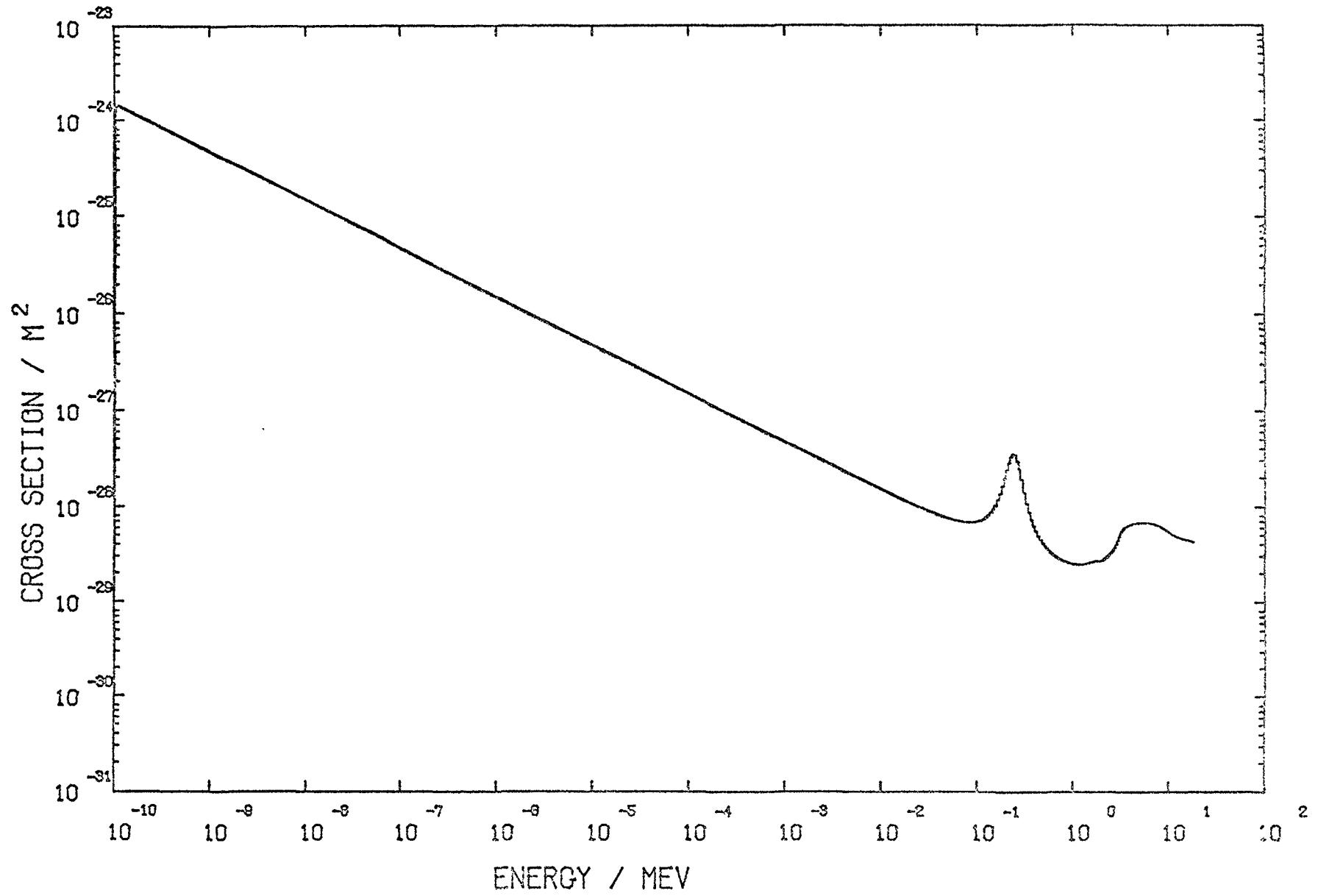


Fig. 1 Cross section curve for the reaction Li 6 (N,A) H3.

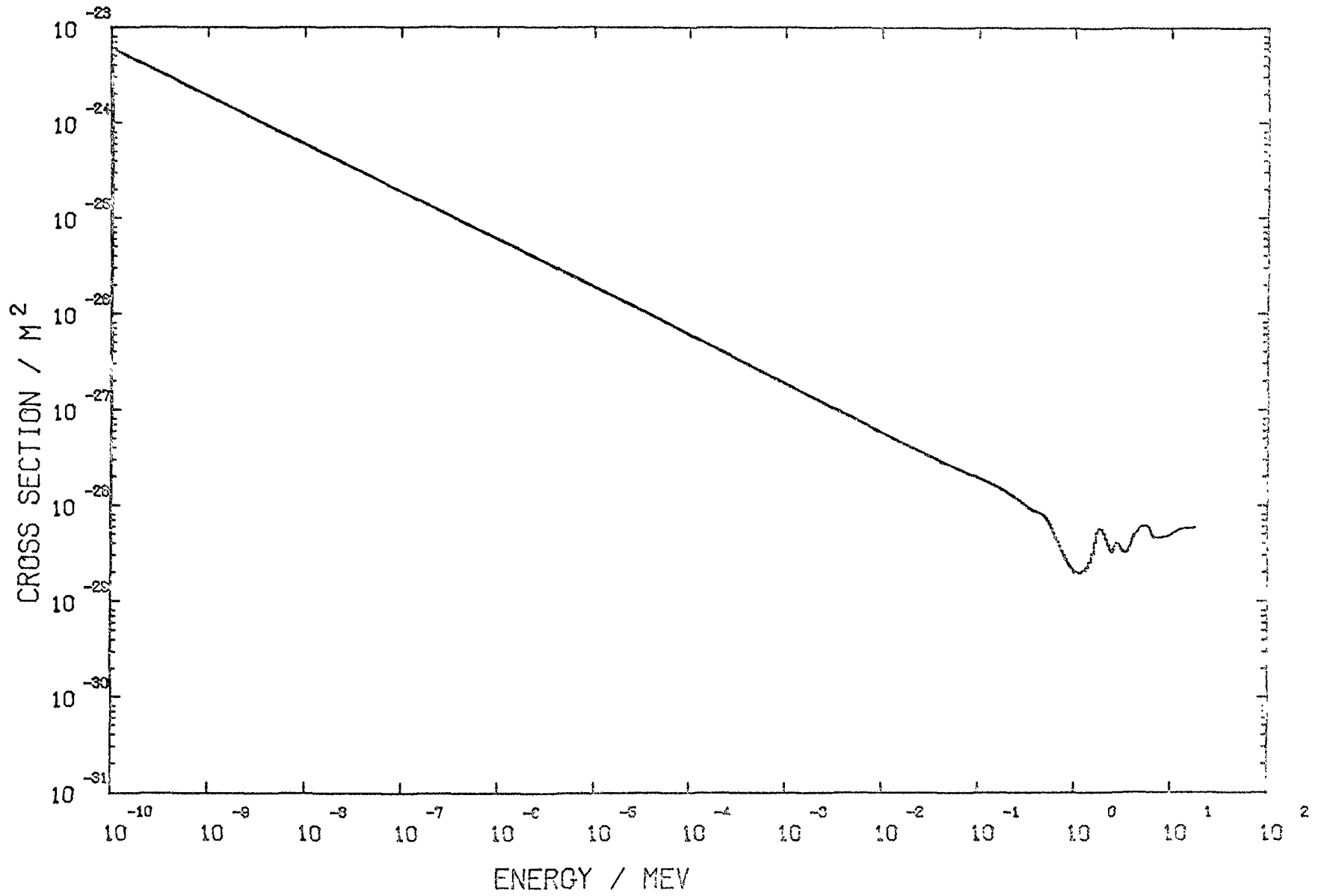


Fig. 2 Cross section curve for the reaction  $B_{10}(N,A)LI_7$ .

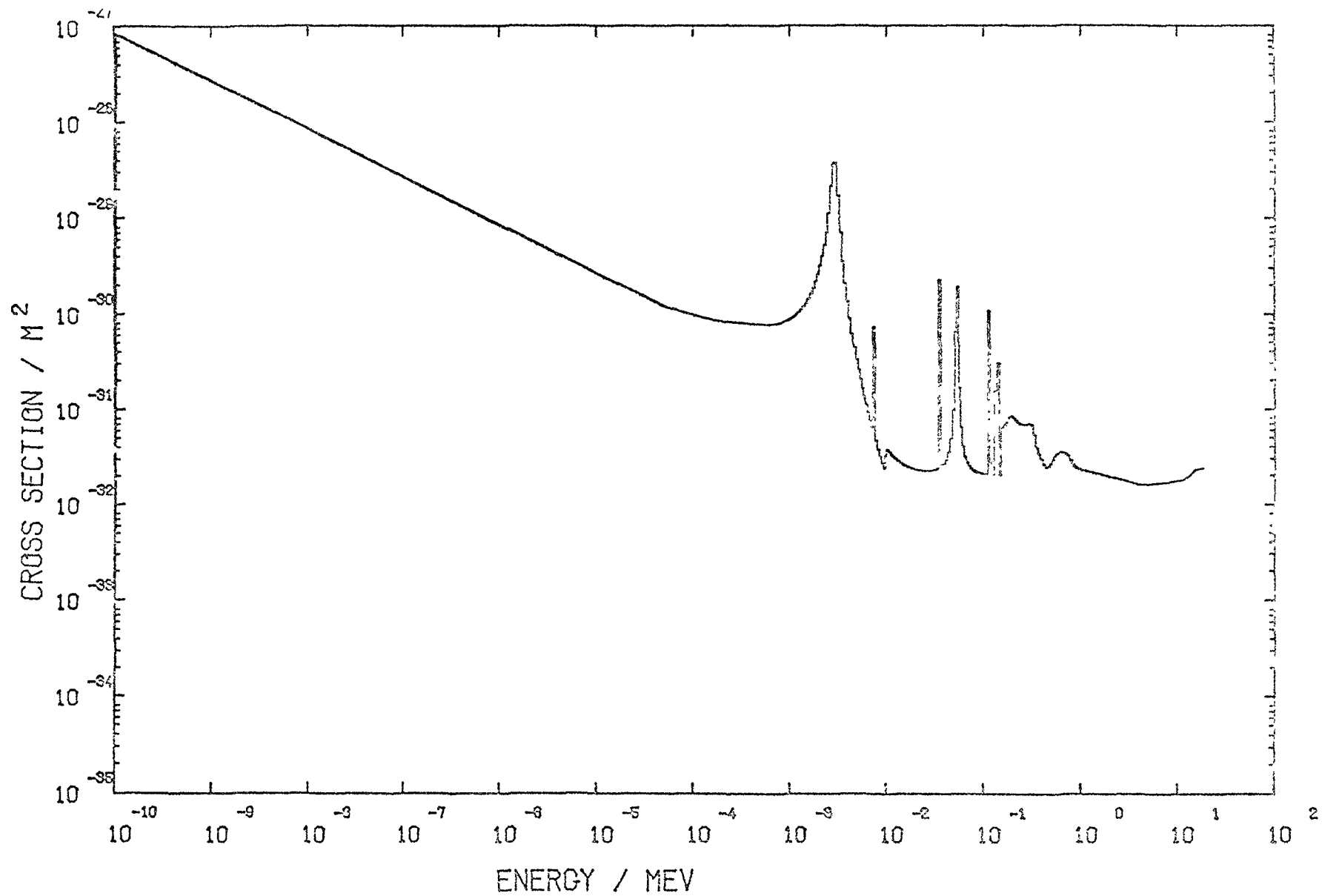


Fig. 3 Cross section curve for the reaction NA 23 (N,G) NA 24.

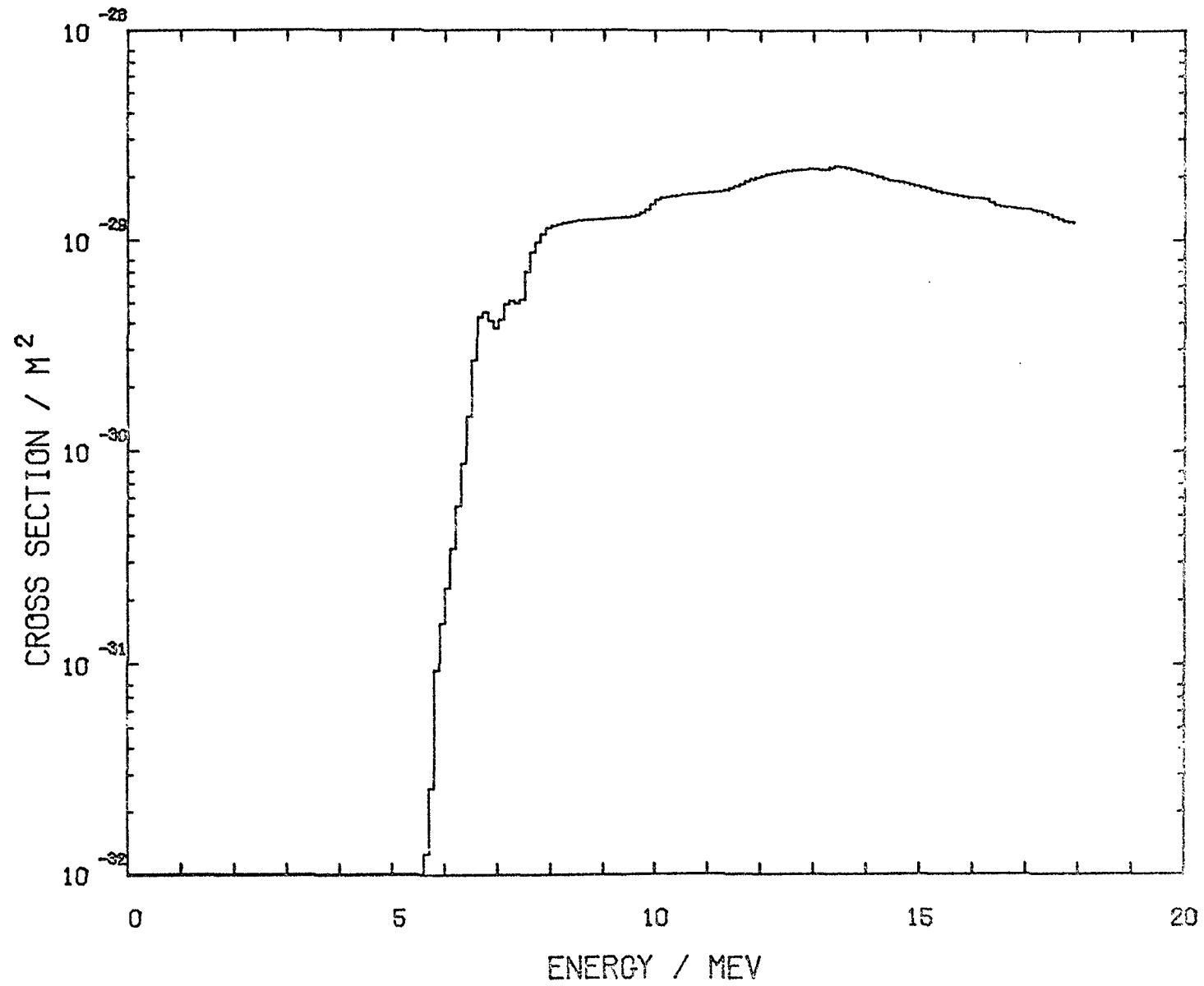


Fig. 4 Cross section curve for the reaction MG 24 (N,P) NA 24.

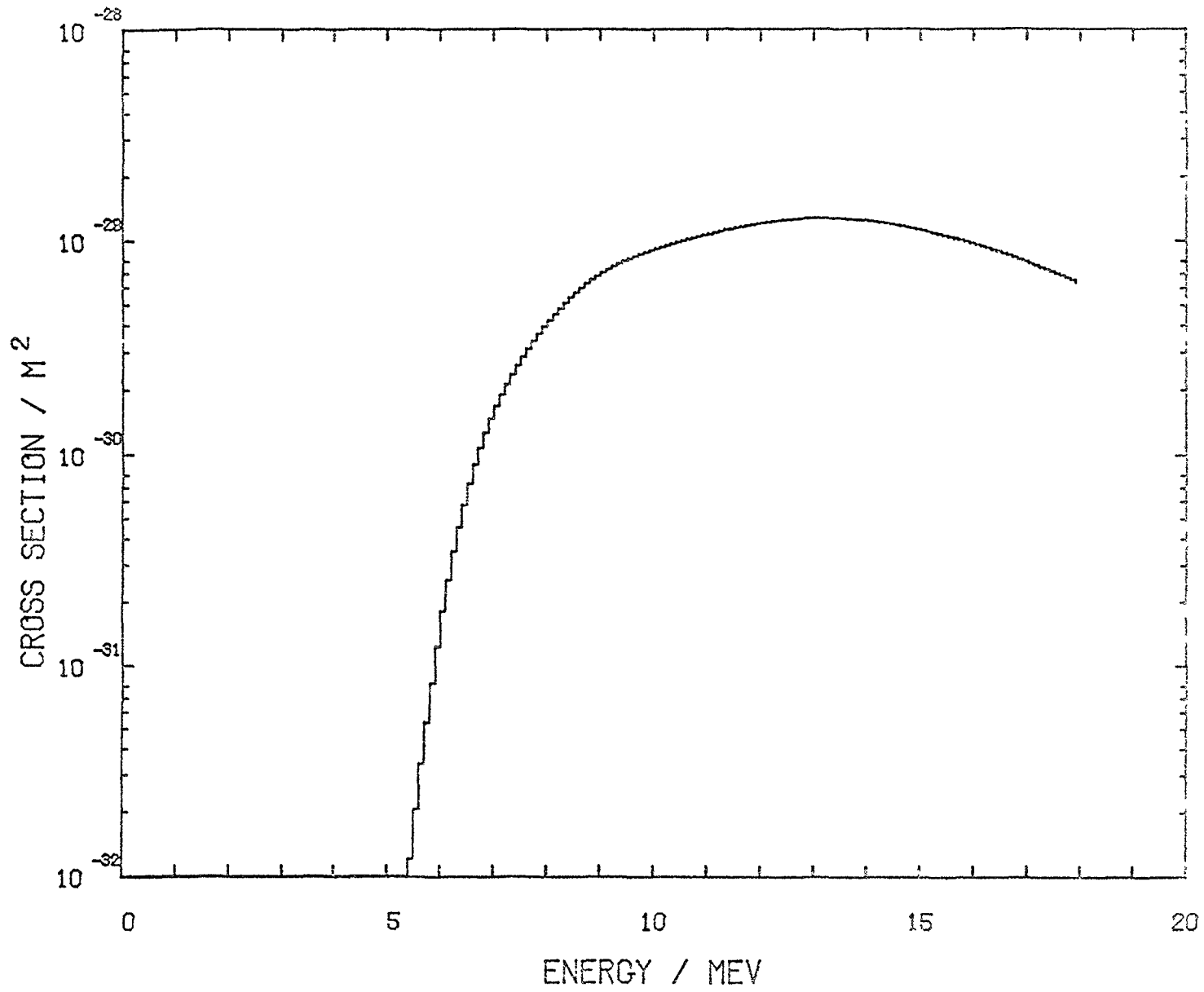


Fig. 5 Cross section curve for the reaction AL 27 (N,A) NA 24.

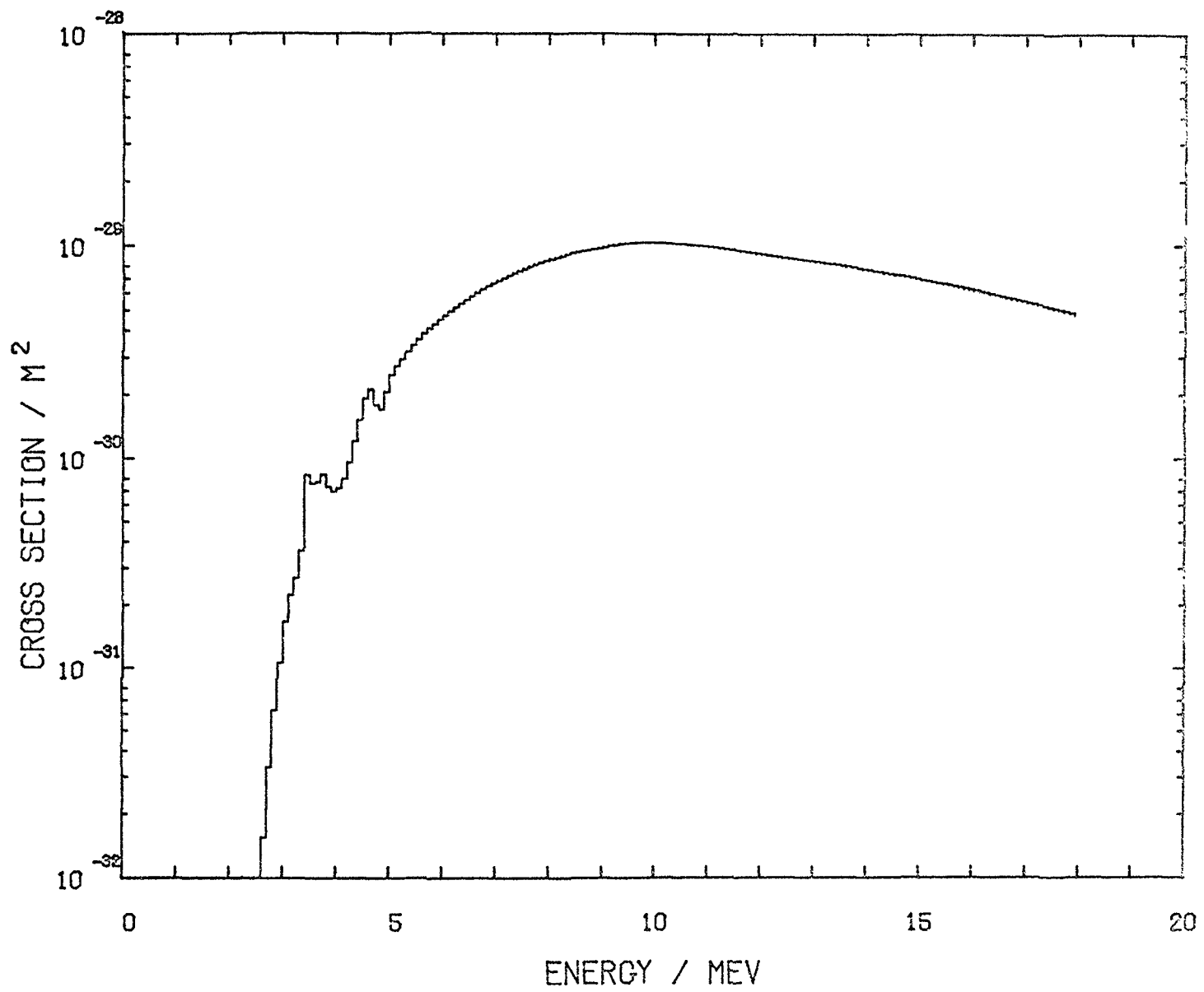


Fig. 6 Cross section curve for the reaction AL 27 (N,P) MG 27.

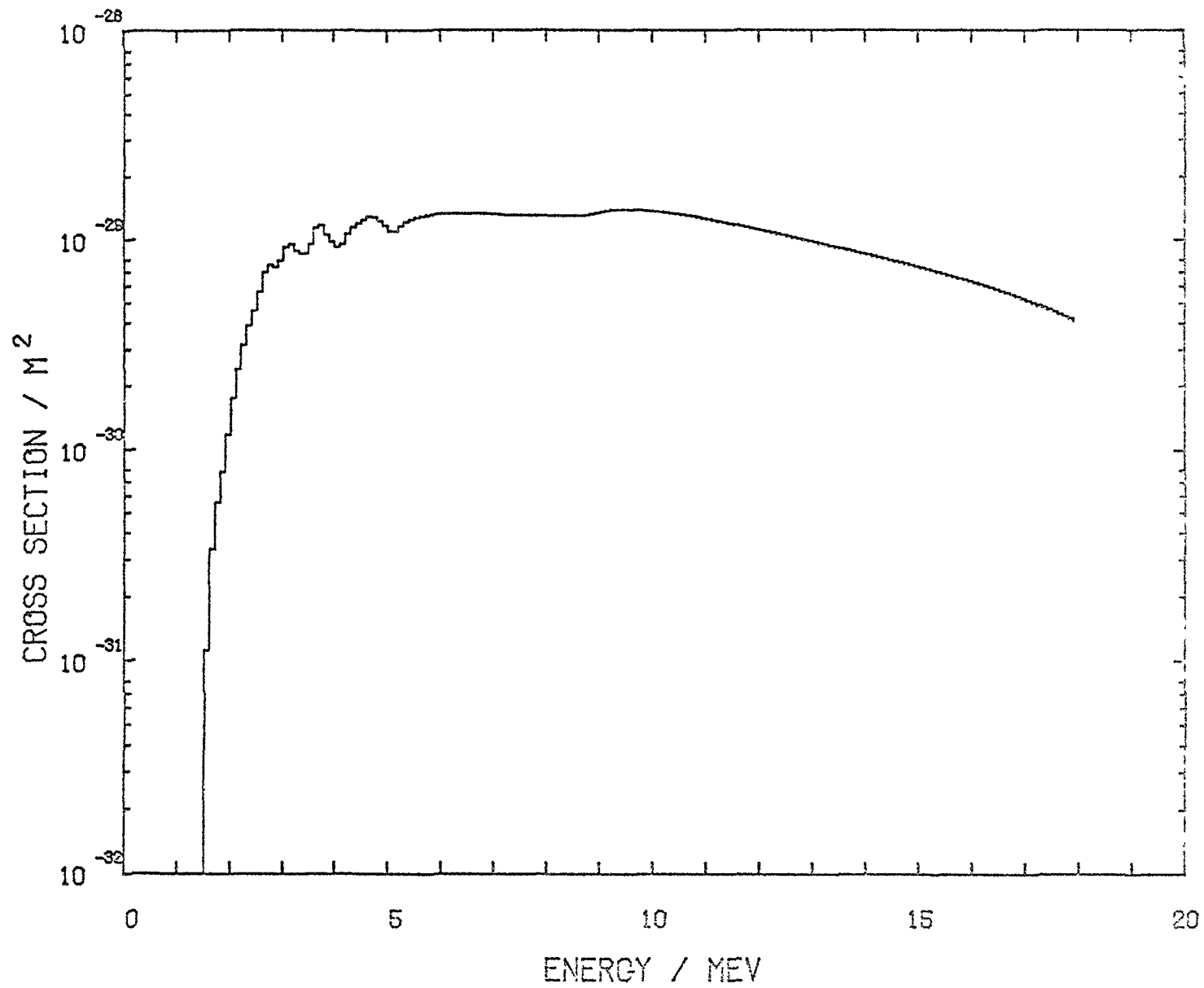


Fig. 7 Cross section curve for the reaction  $P^{31}(N,P)SI^{31}$ .

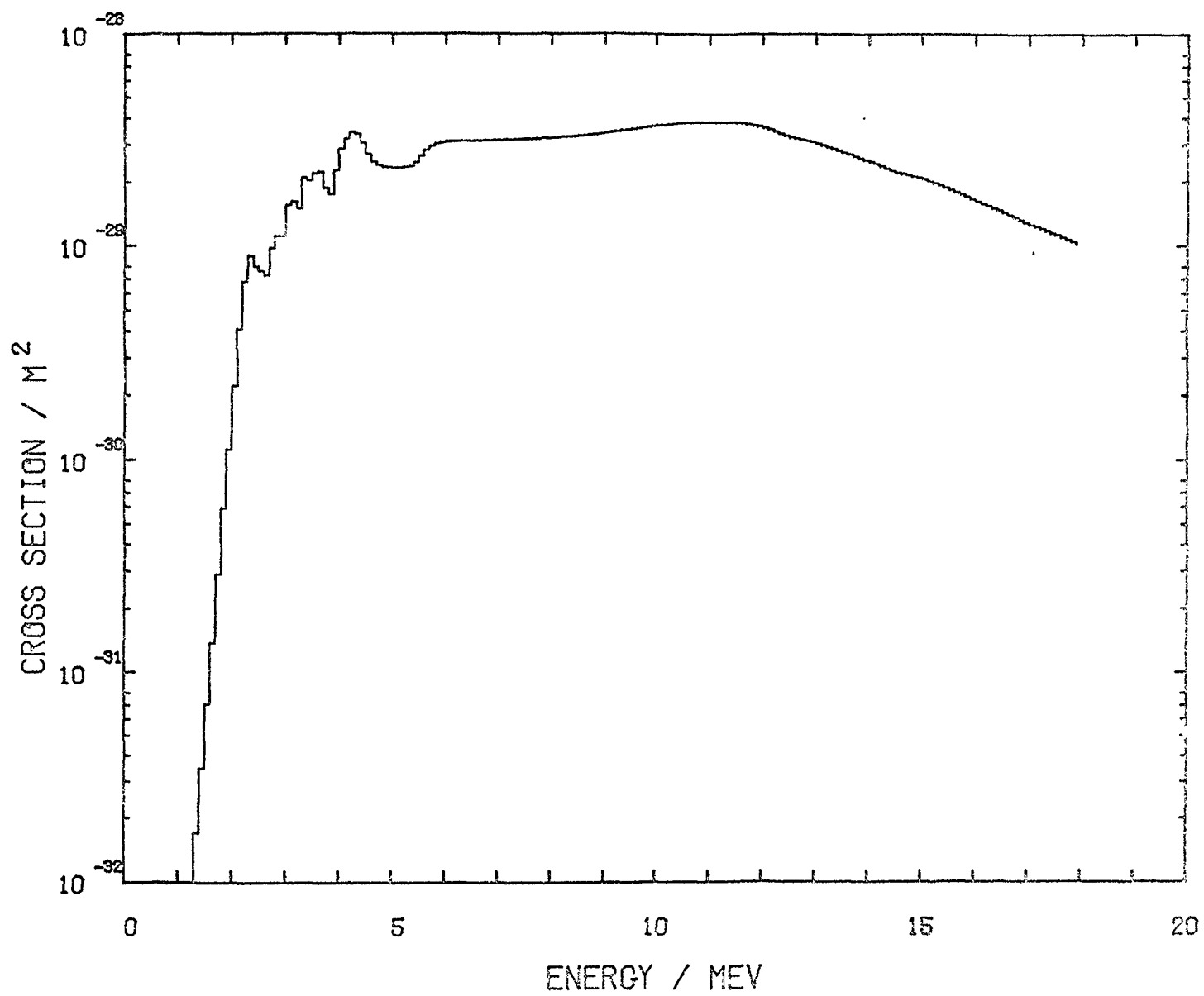


Fig. 8 Cross section curve for the reaction S 32 (N,P) P 32.



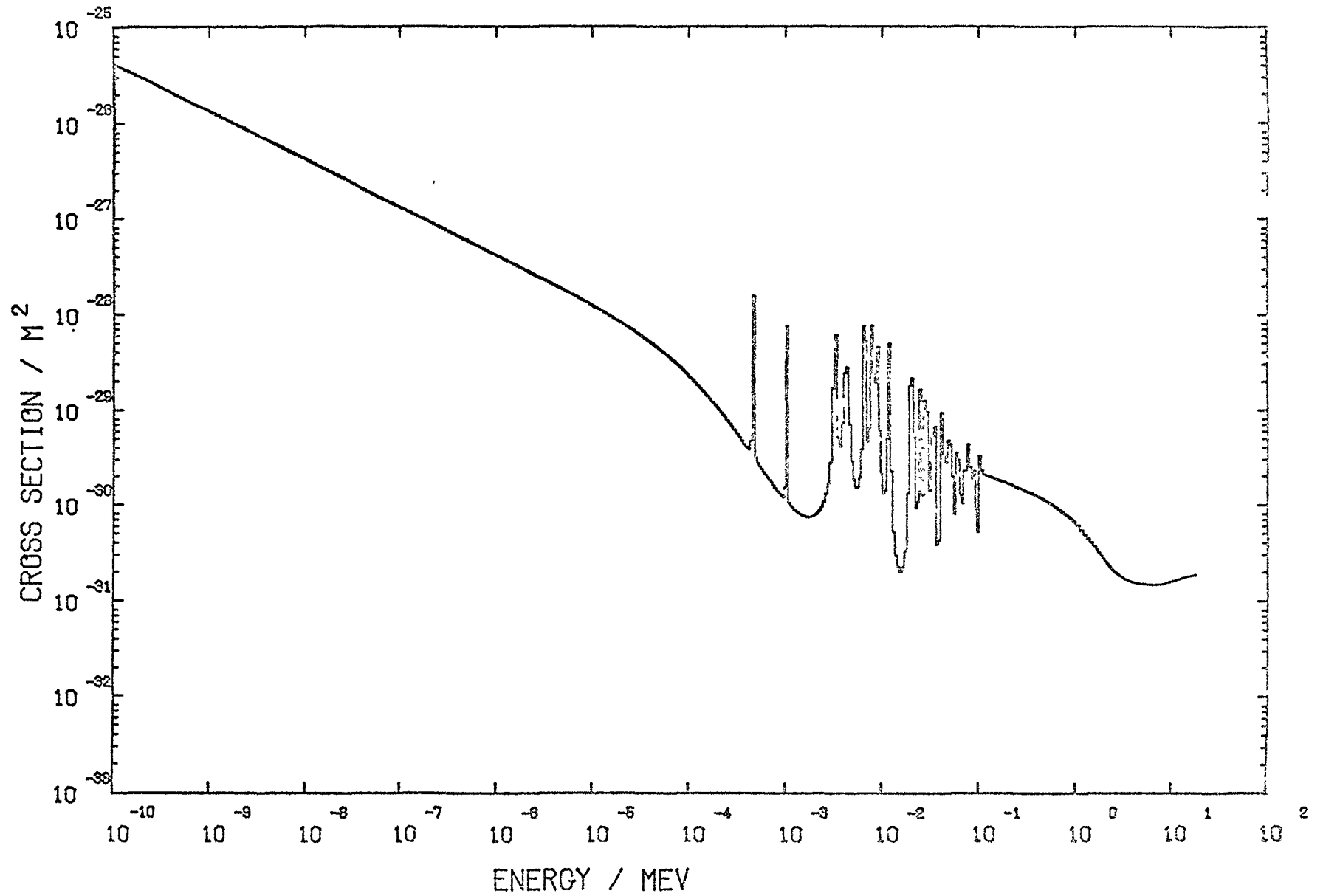


Fig. 9 Cross section curve for the reaction SC 45 (N,G) SC 46.

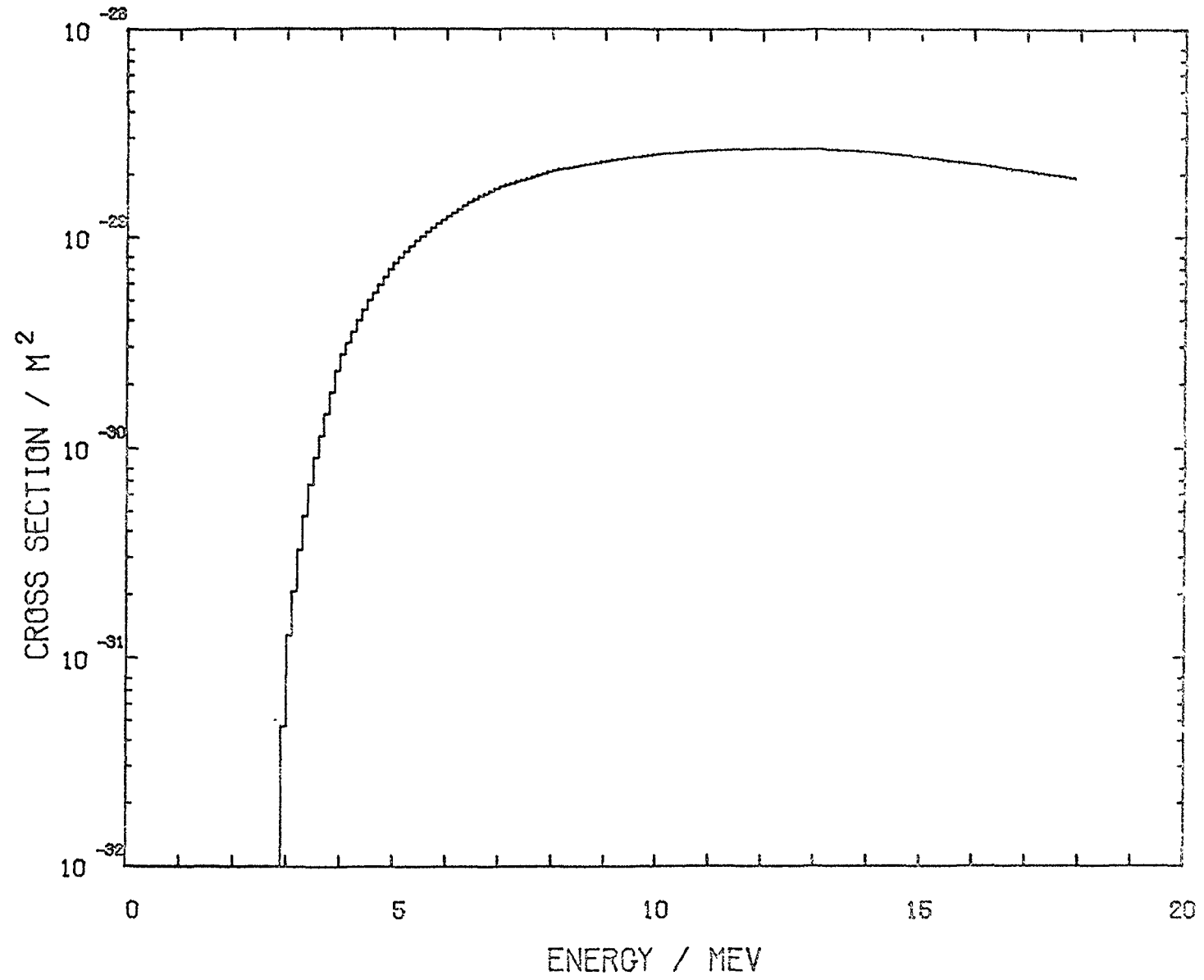


Fig. 10 Cross section curve for the reaction  $^{46}\text{Ti}(n,p)^{46}\text{Sc}$ .

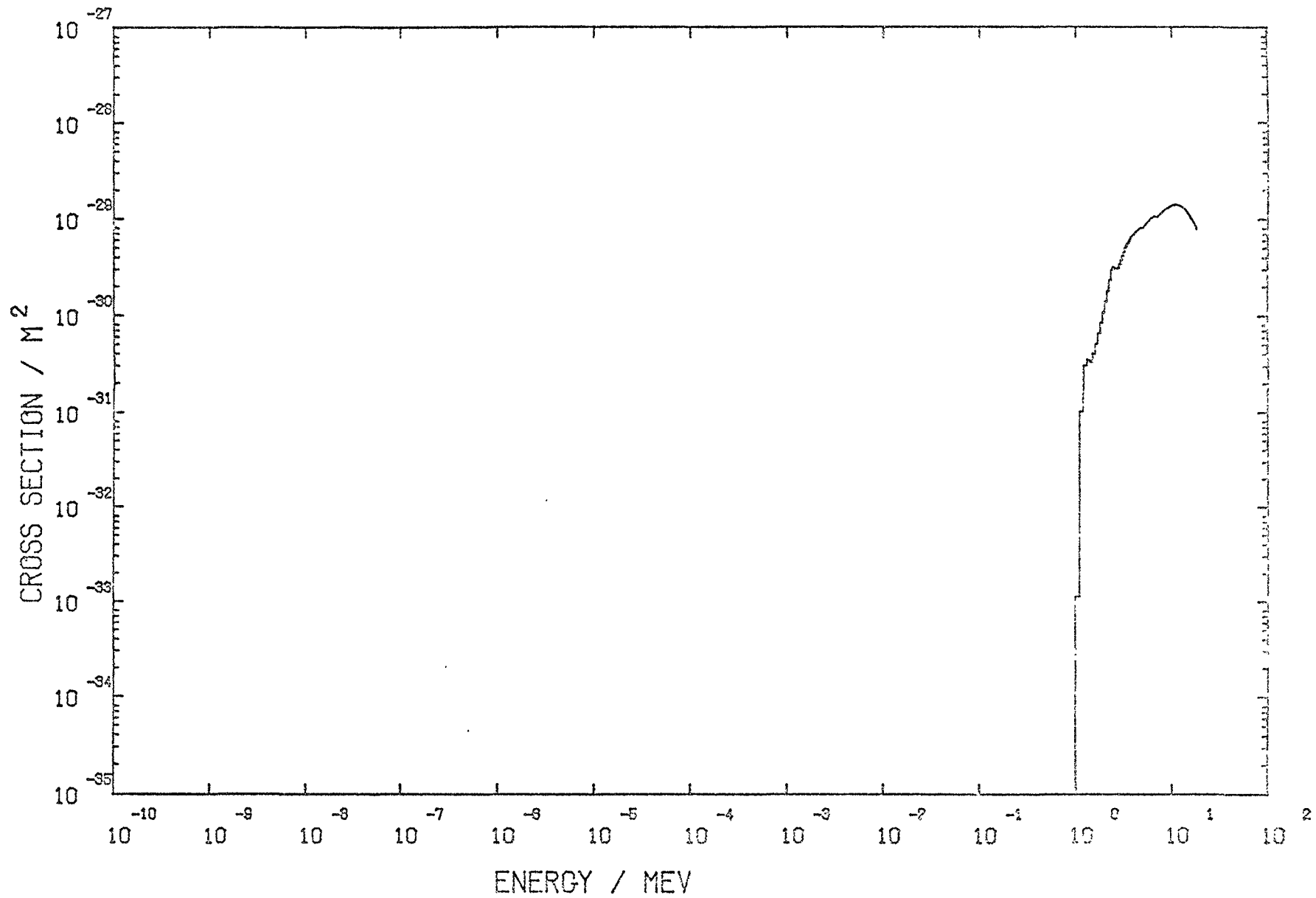


Fig. 11 Cross section curve for the reaction TI 47 (N,P) SC 47.

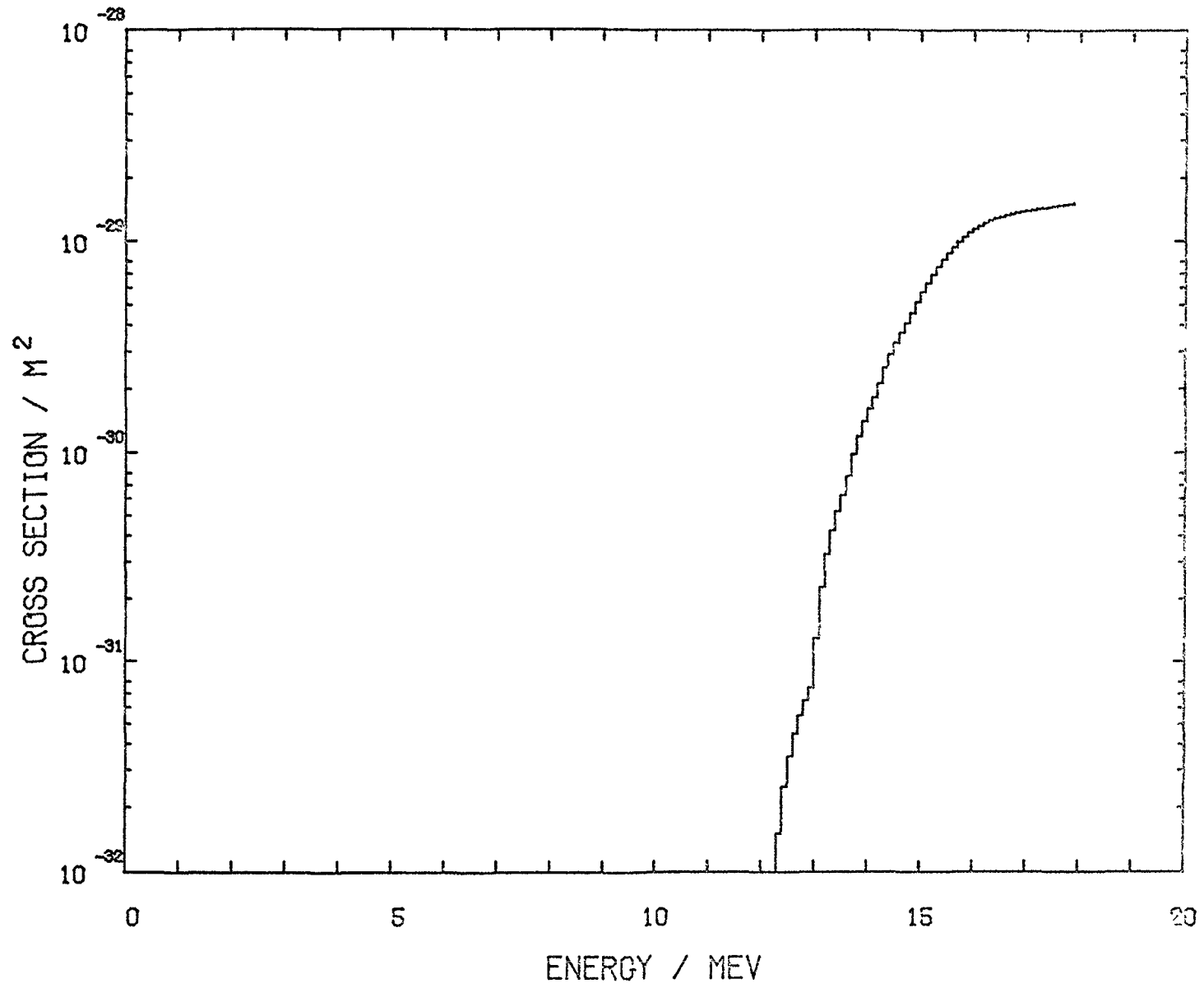


Fig. 12 Cross section curve for the reaction TI 47 (N,NP) SC 46.

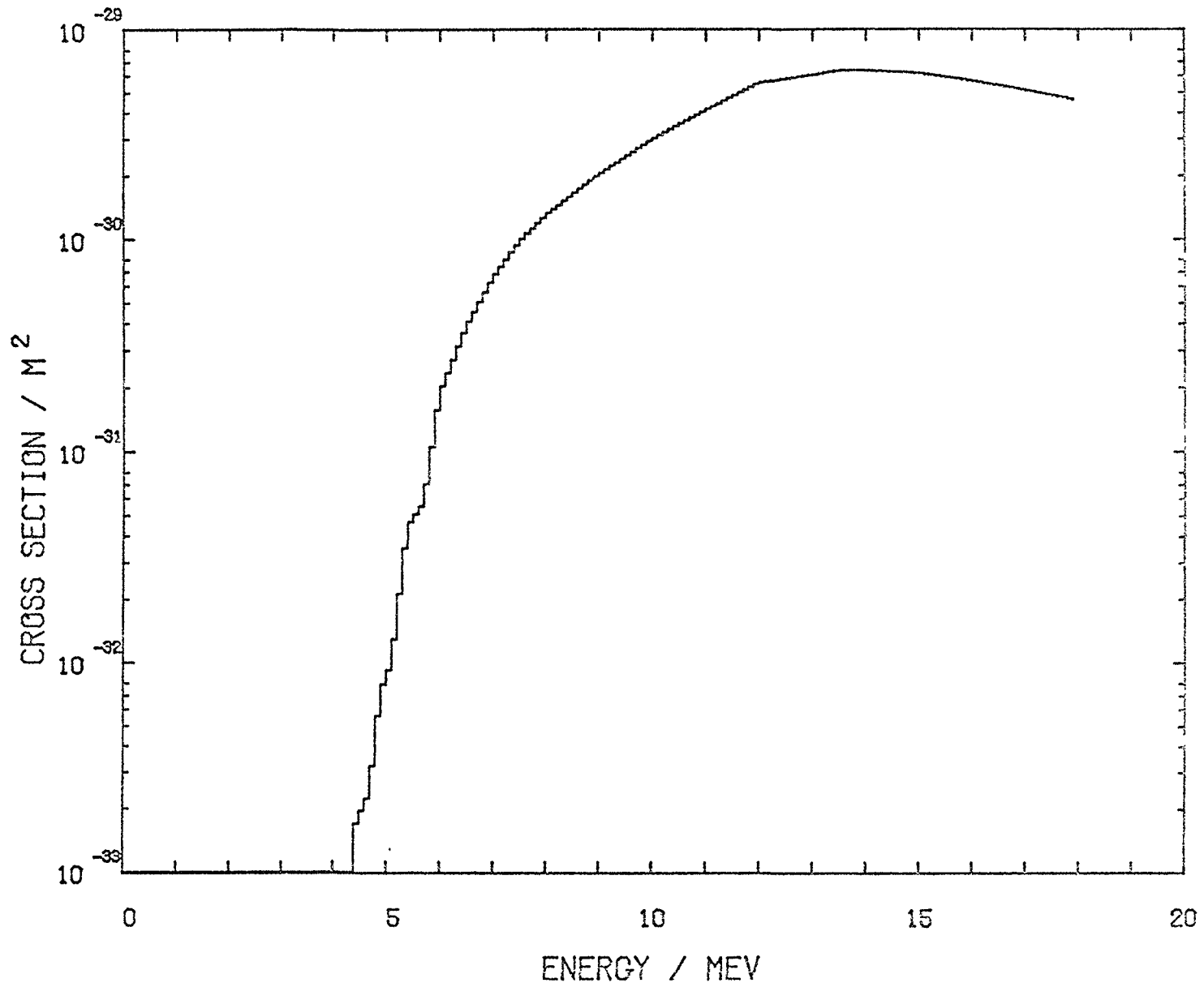


Fig. 13 Cross section curve for the reaction TI 48 (N,P) SC 48.

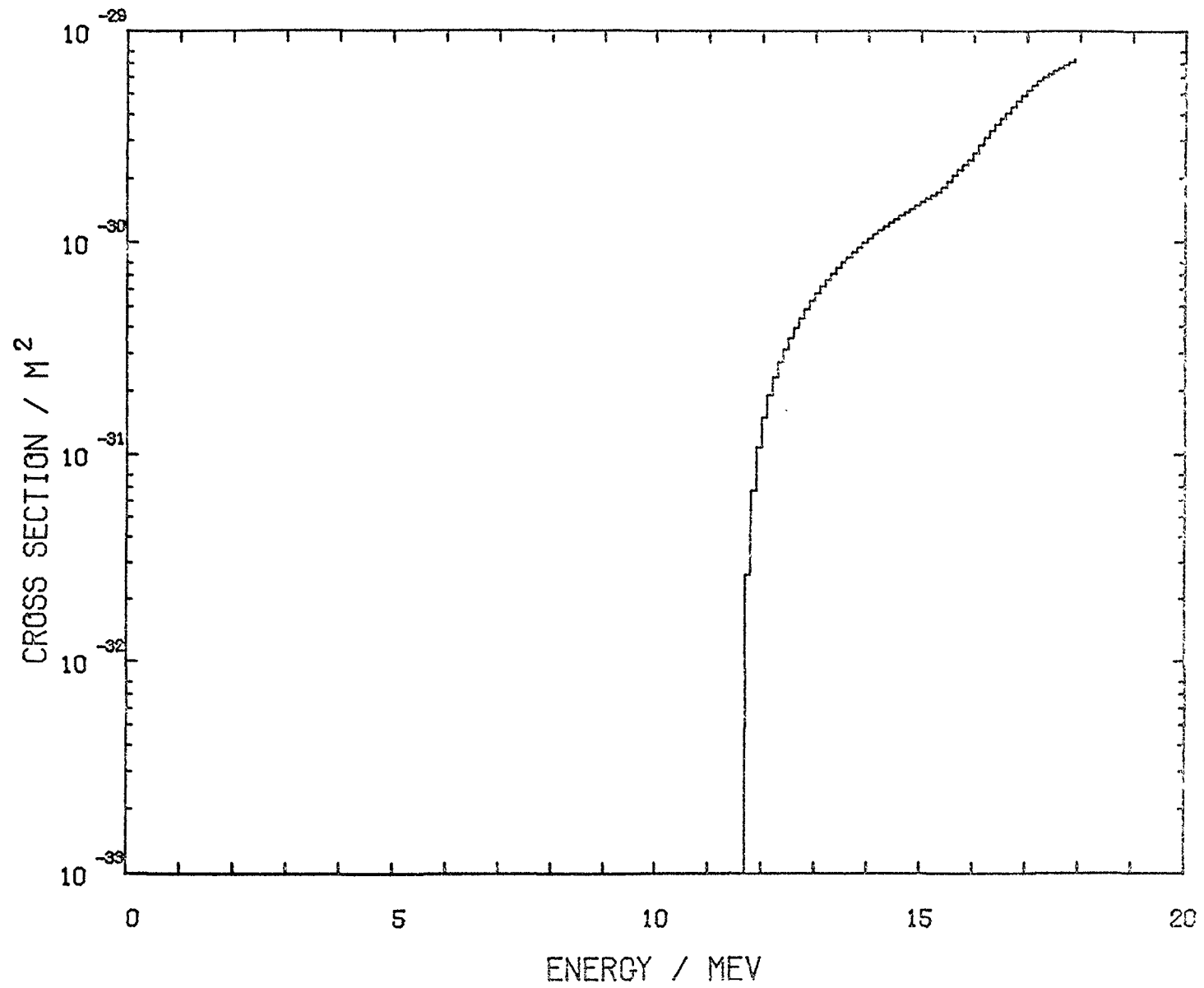


Fig. 14 Cross section curve for the reaction Tl 48 (N, NP) SC 47

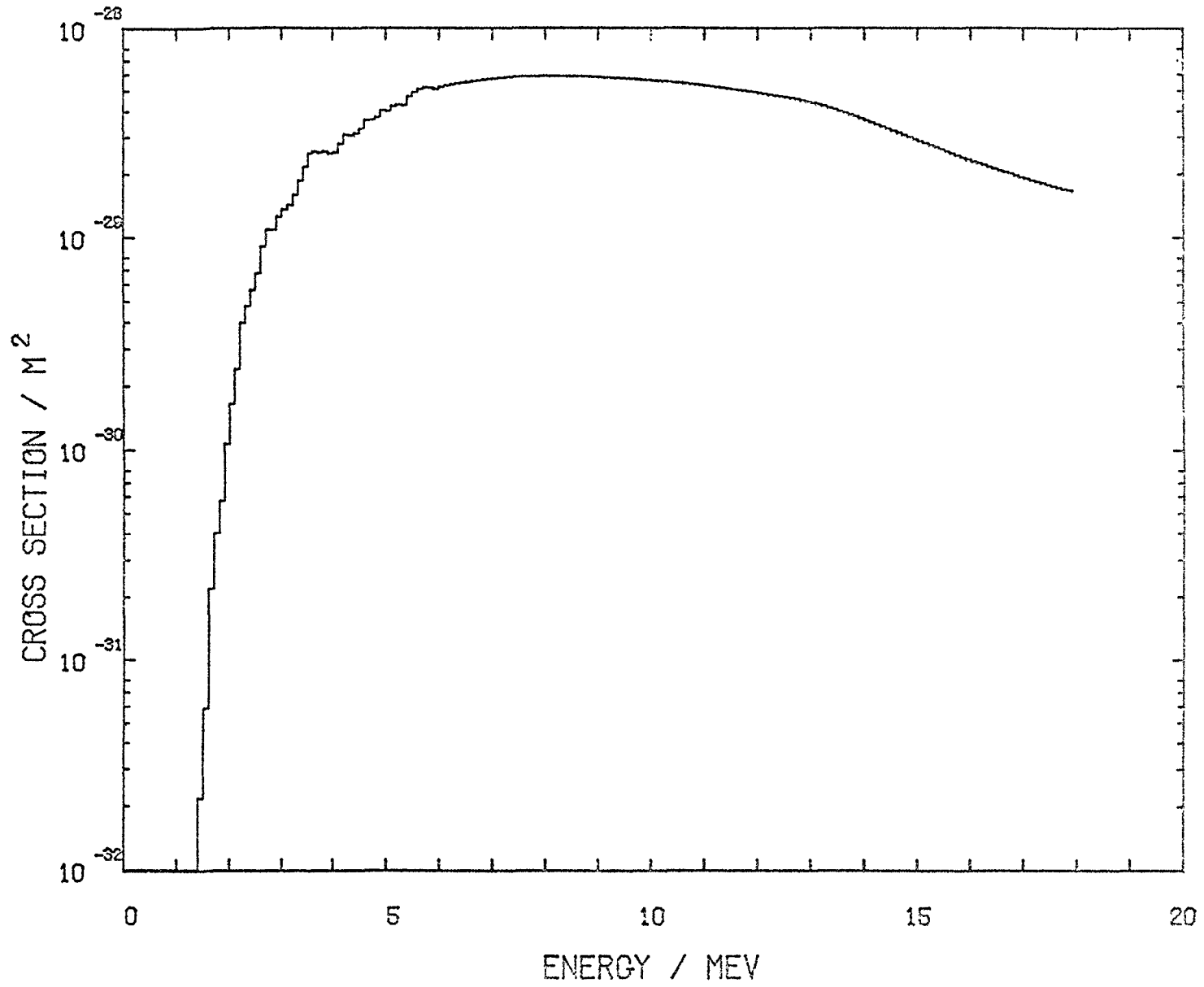


Fig. 15 Cross section curve for the reaction FE 54 (N,P) MN 54.

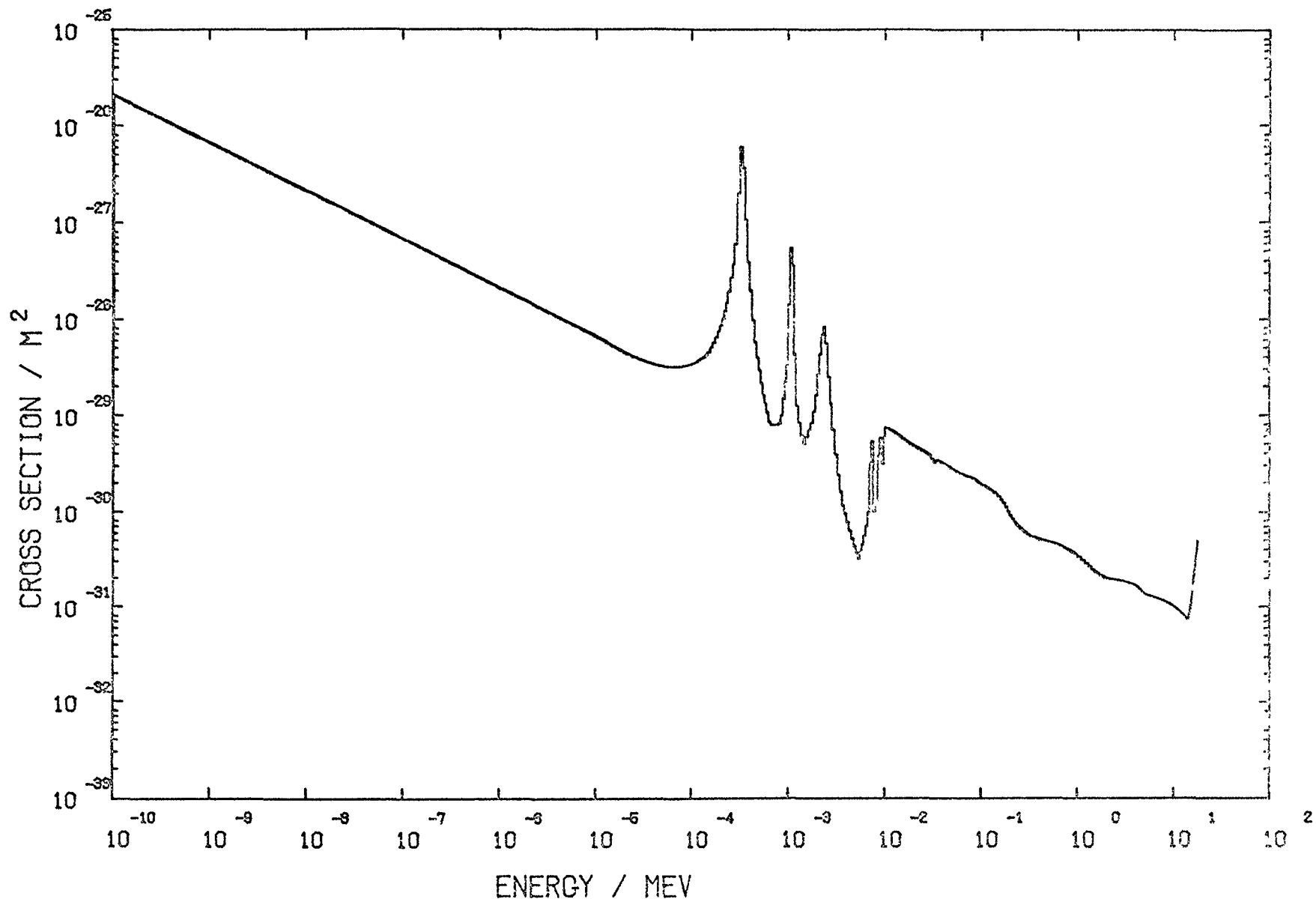


Fig. 16 Cross section curve for the reaction MN 55 (N,G) MN 56.



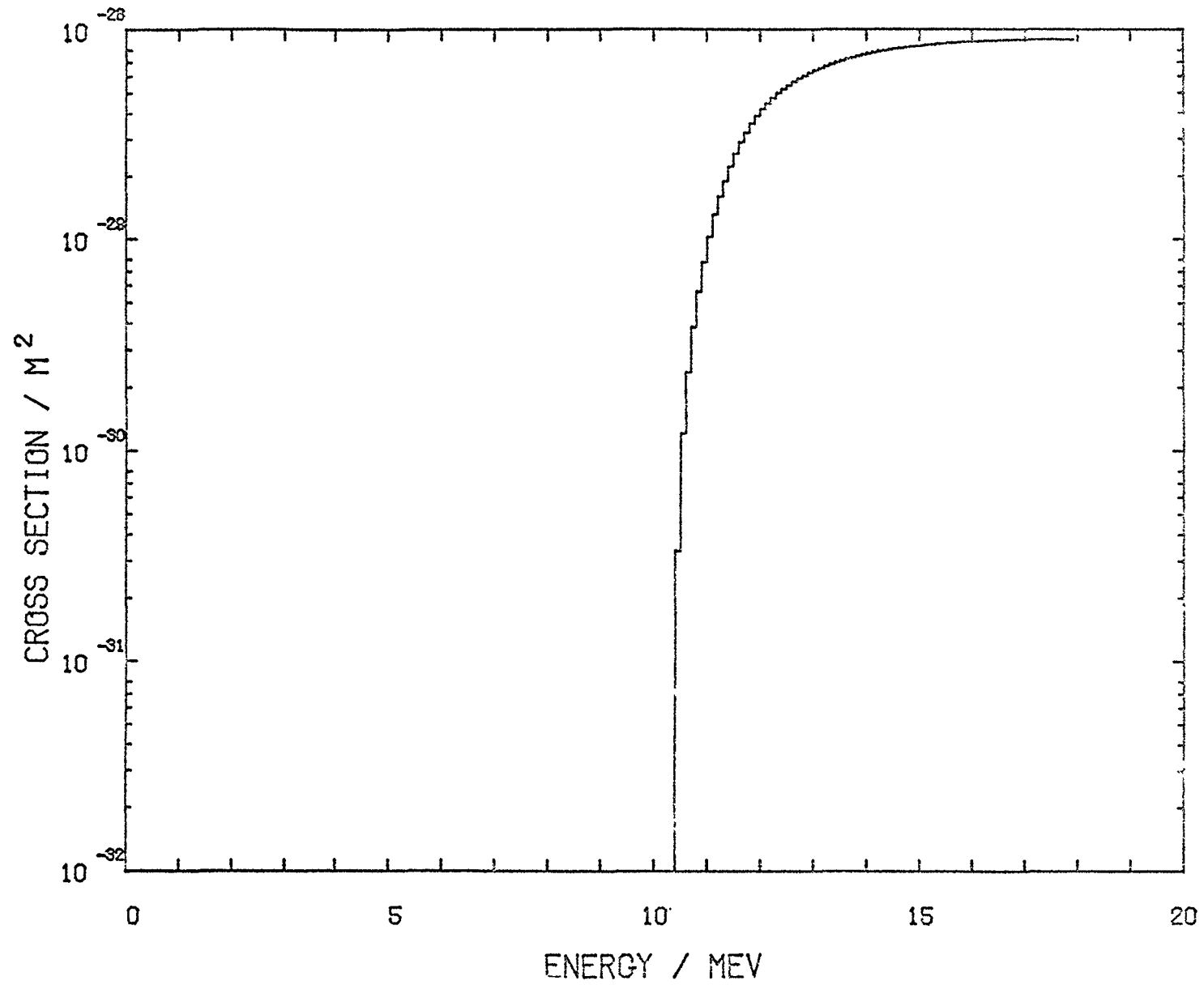


Fig. 17 Cross section curve for the reaction MN 55 (N,2N) MN 54.

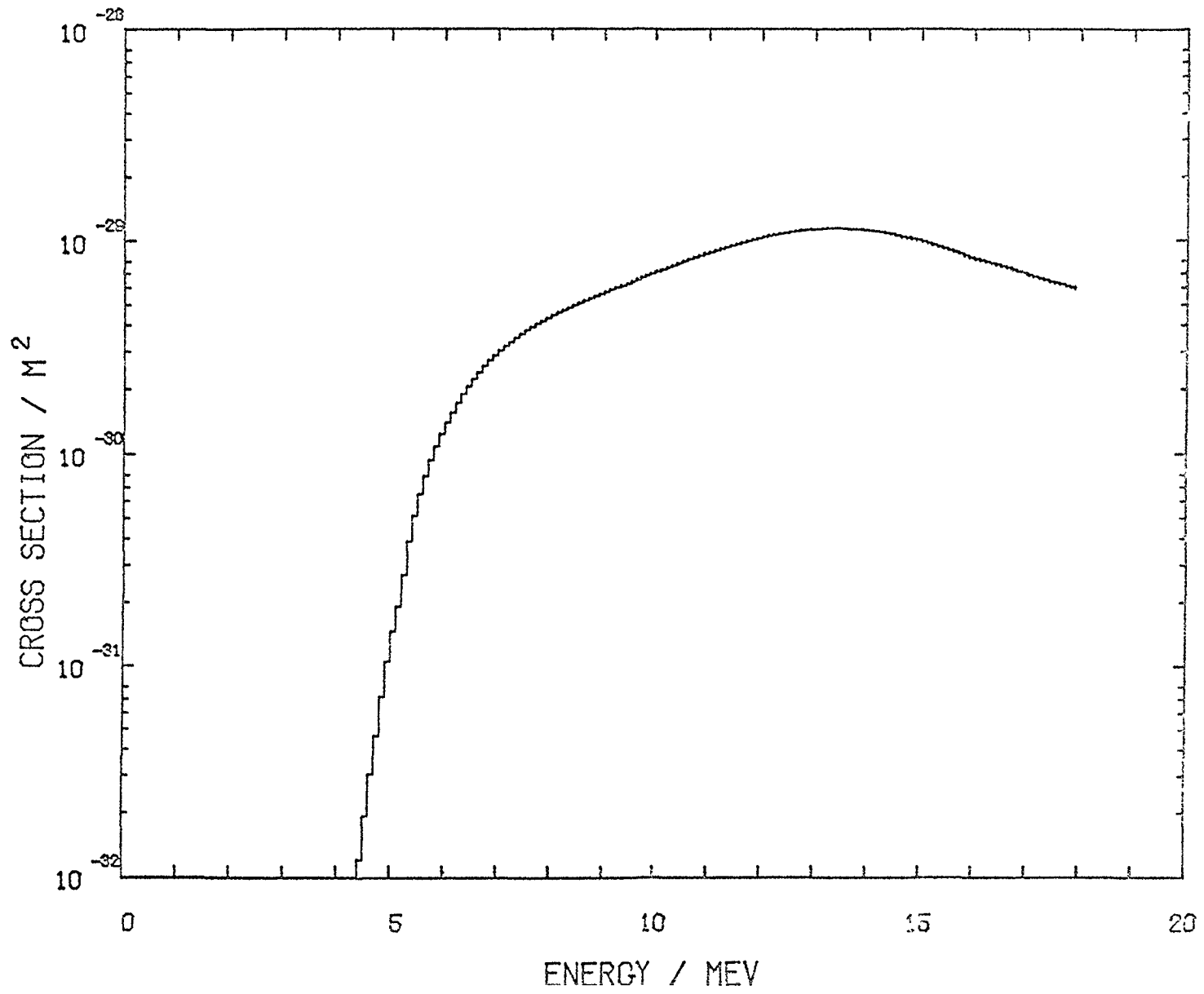


Fig. 18 Cross section curve for the reaction FE 56 (N,P) MN 56.

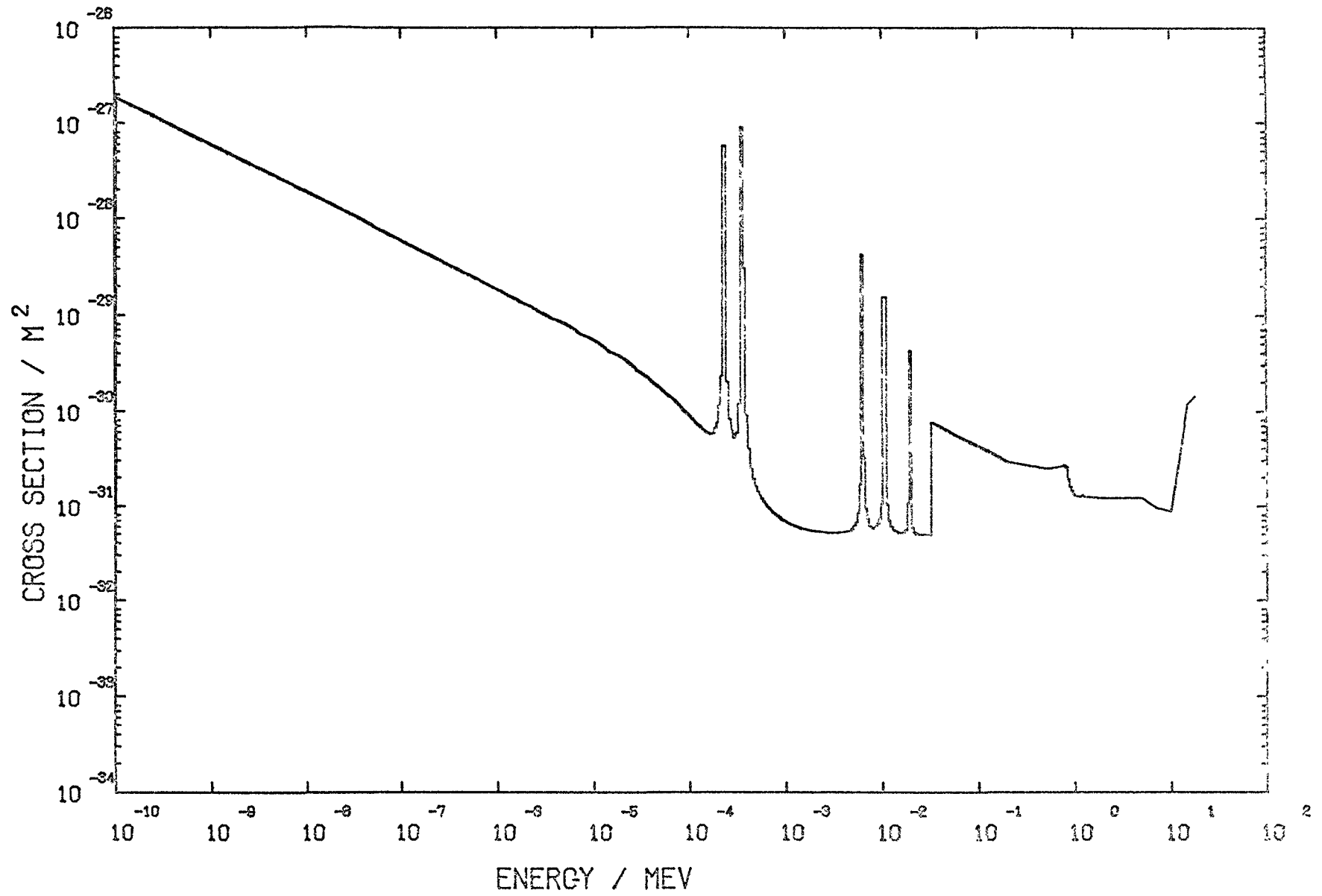


Fig. 19 Cross section curve for the reaction FE 58 (N,G) FE 59.

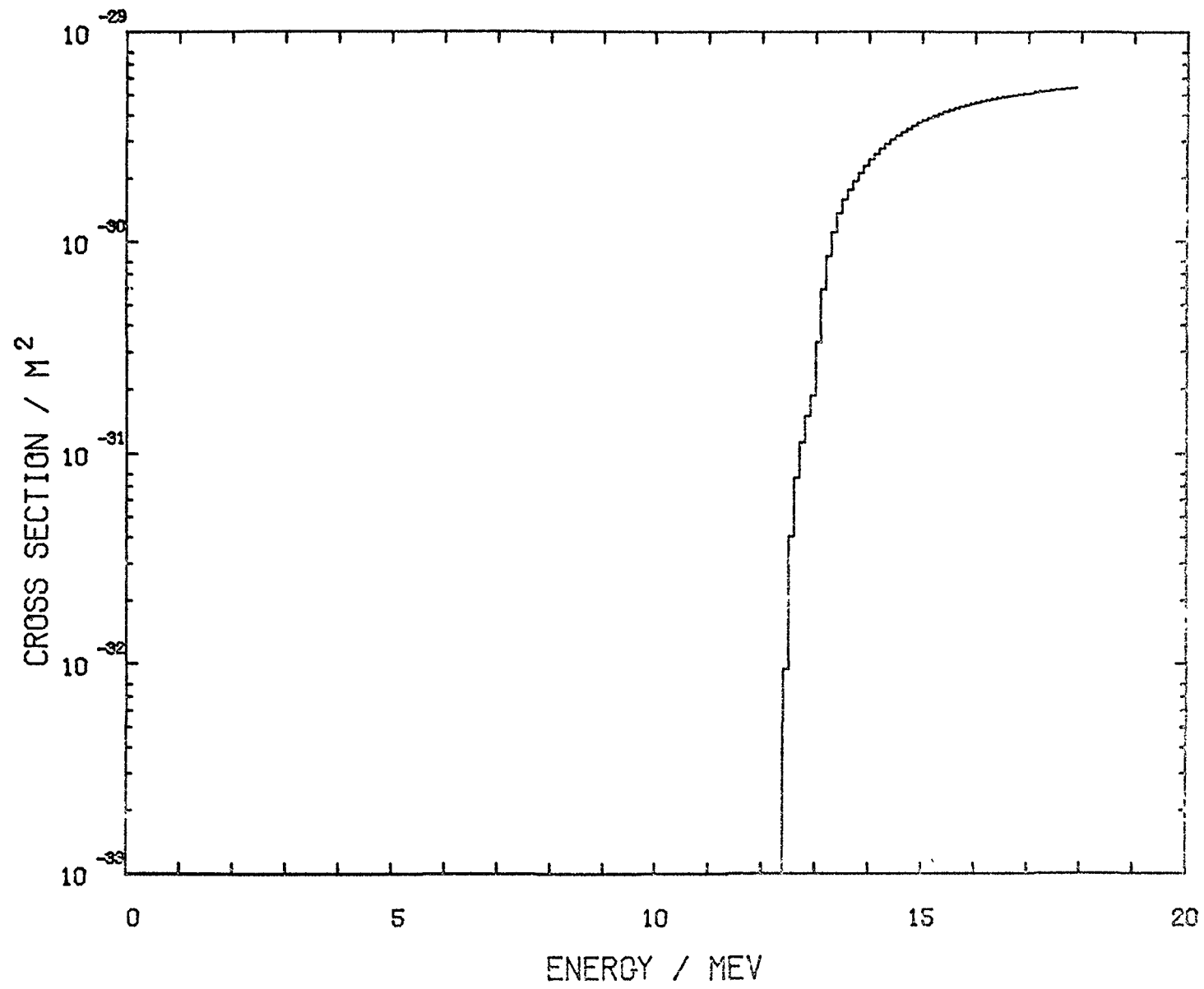


Fig. 20 Cross section curve for the reaction Ni 58 (N,2N) Ni 57.

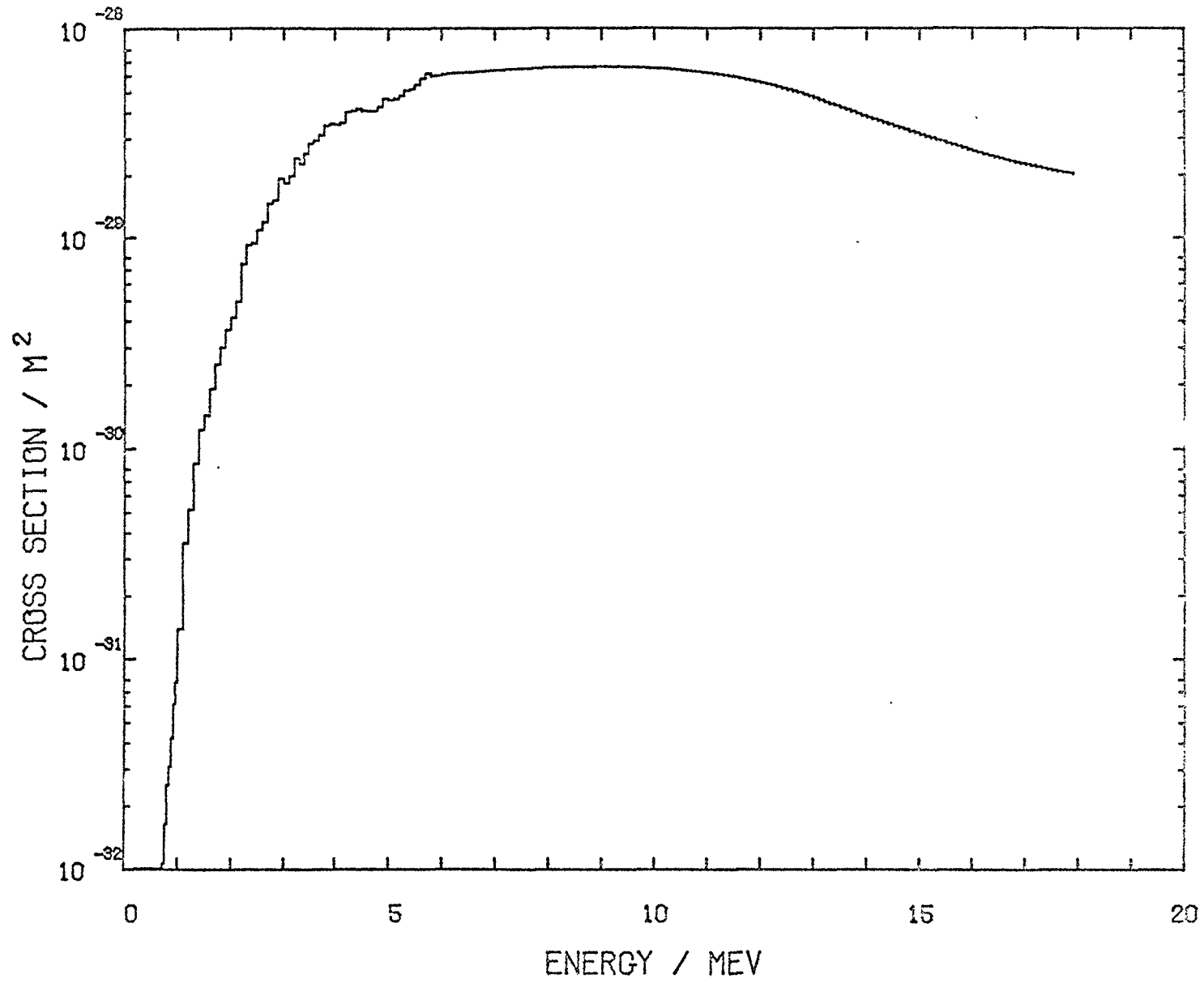


Fig. 21 Cross section curve for the reaction Ni 58 (N,P) Co 58.

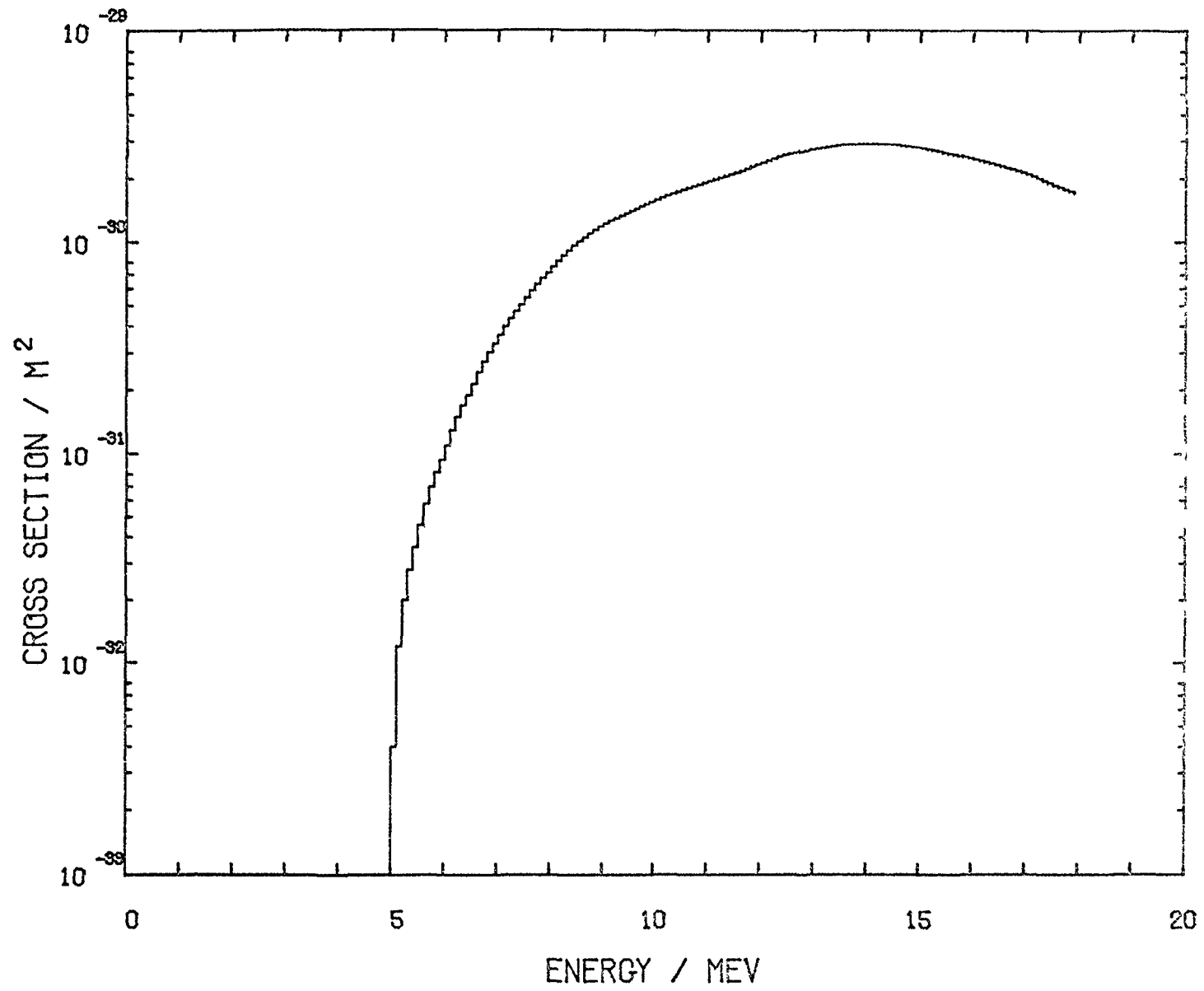


Fig. 22 Cross section curve for the reaction  $^{59}\text{Co}(n, \alpha)^{56}\text{Mn}$ .

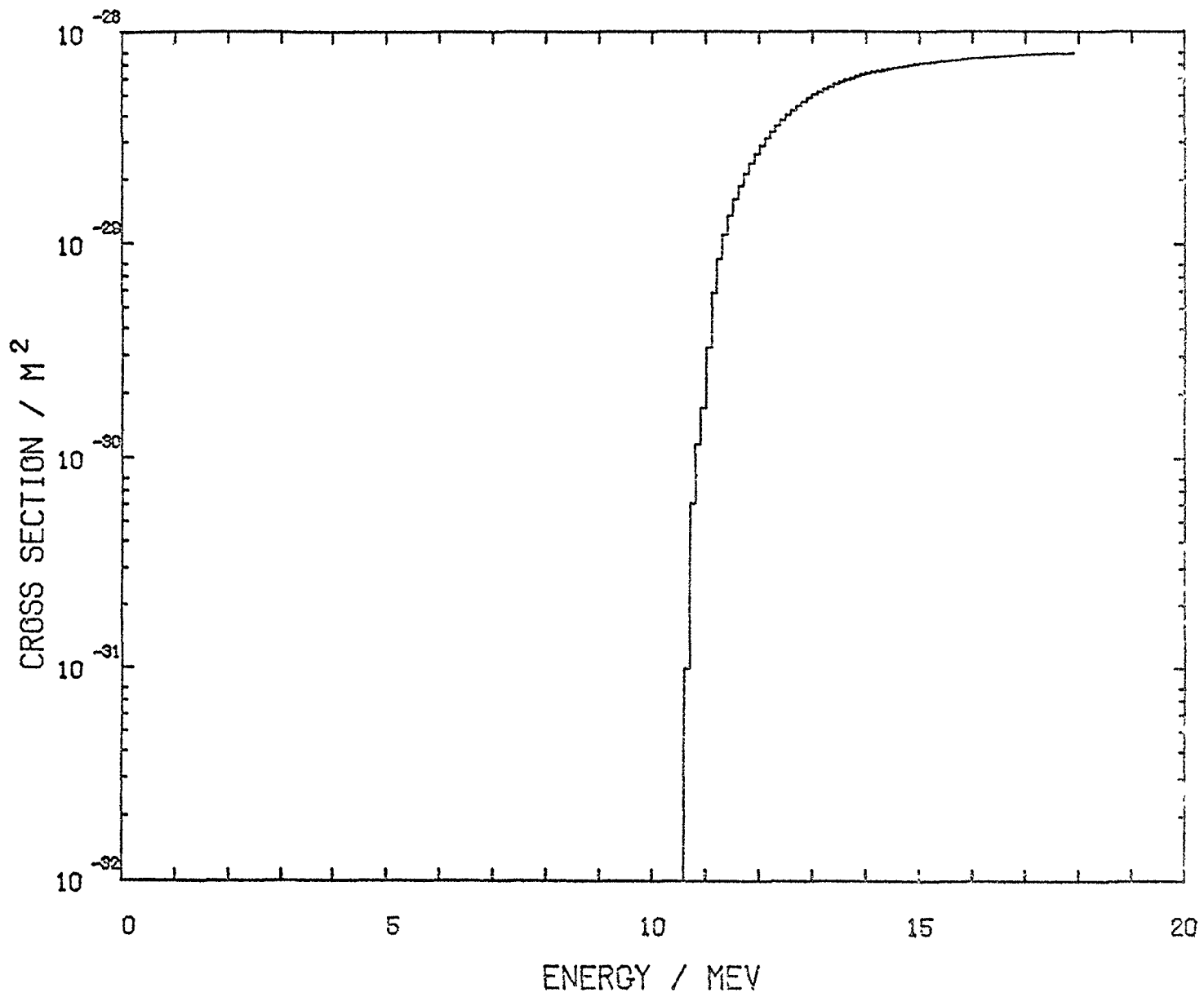


Fig. 23 Cross section curve for the reaction CO 59 (N,2N) CO 58.

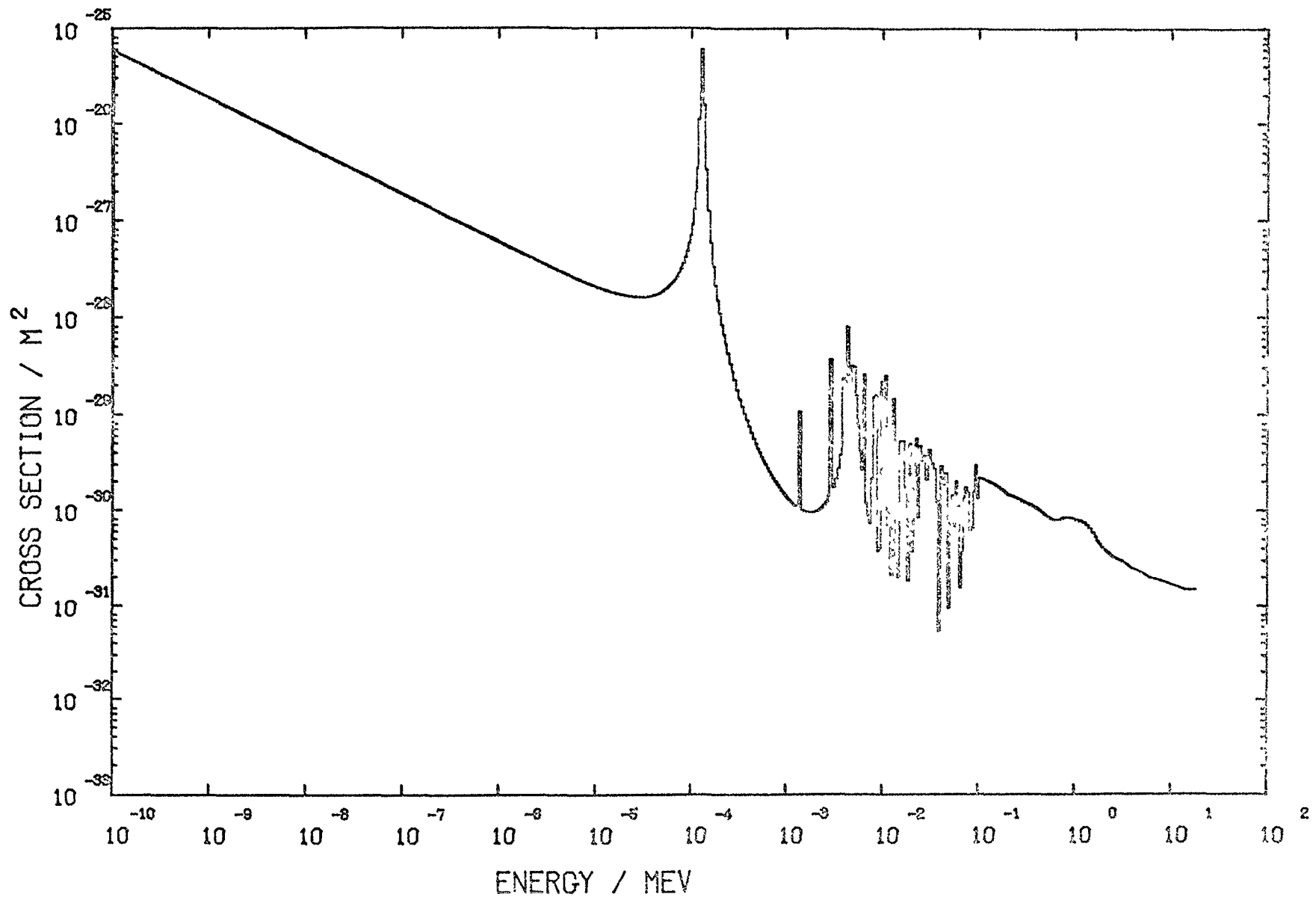


Fig. 24 Cross section curve for the reaction CO 59 (N,G) CO 60.



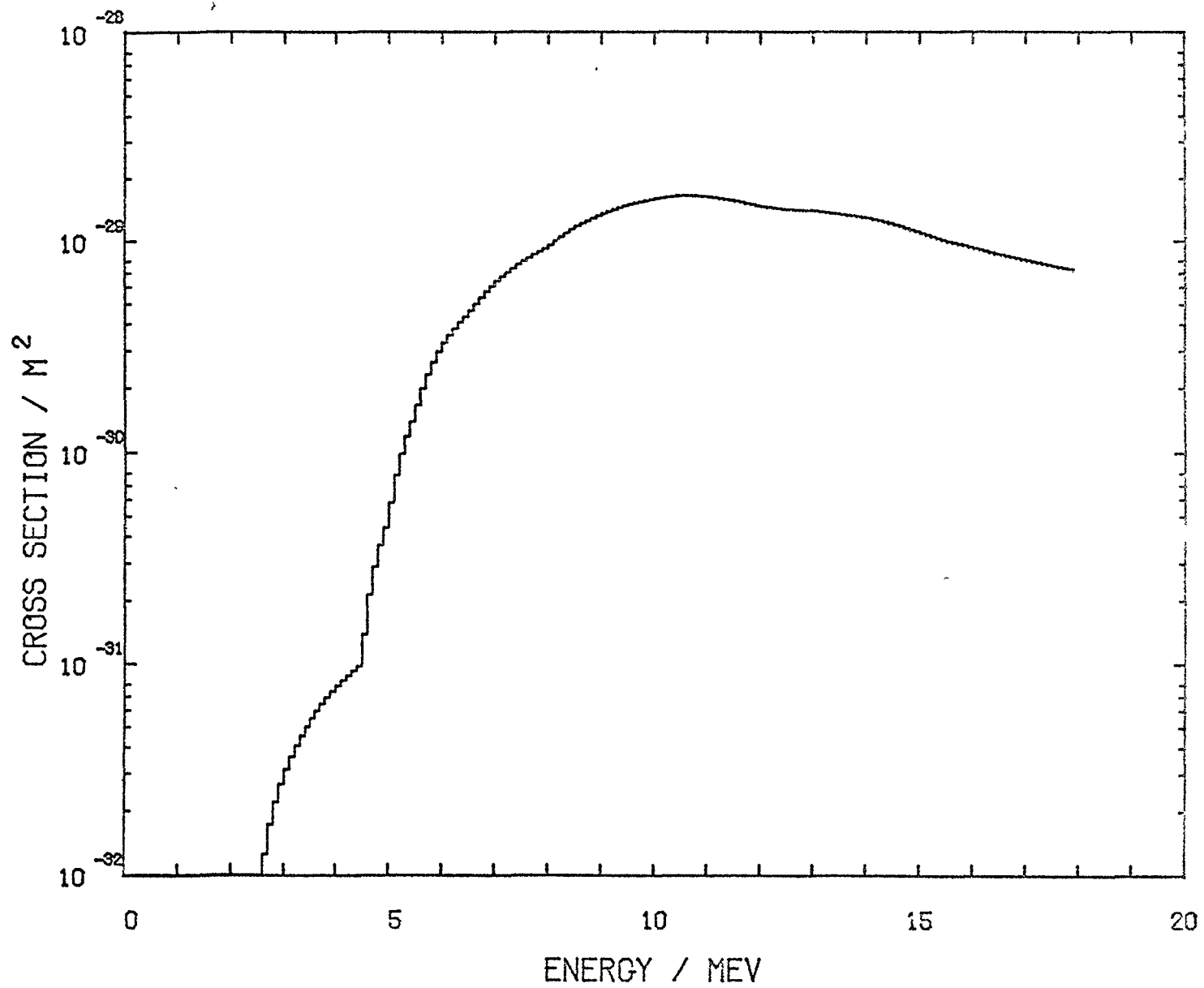


Fig. 25 Cross section curve for the reaction Ni 60 (N,P) Co 60.

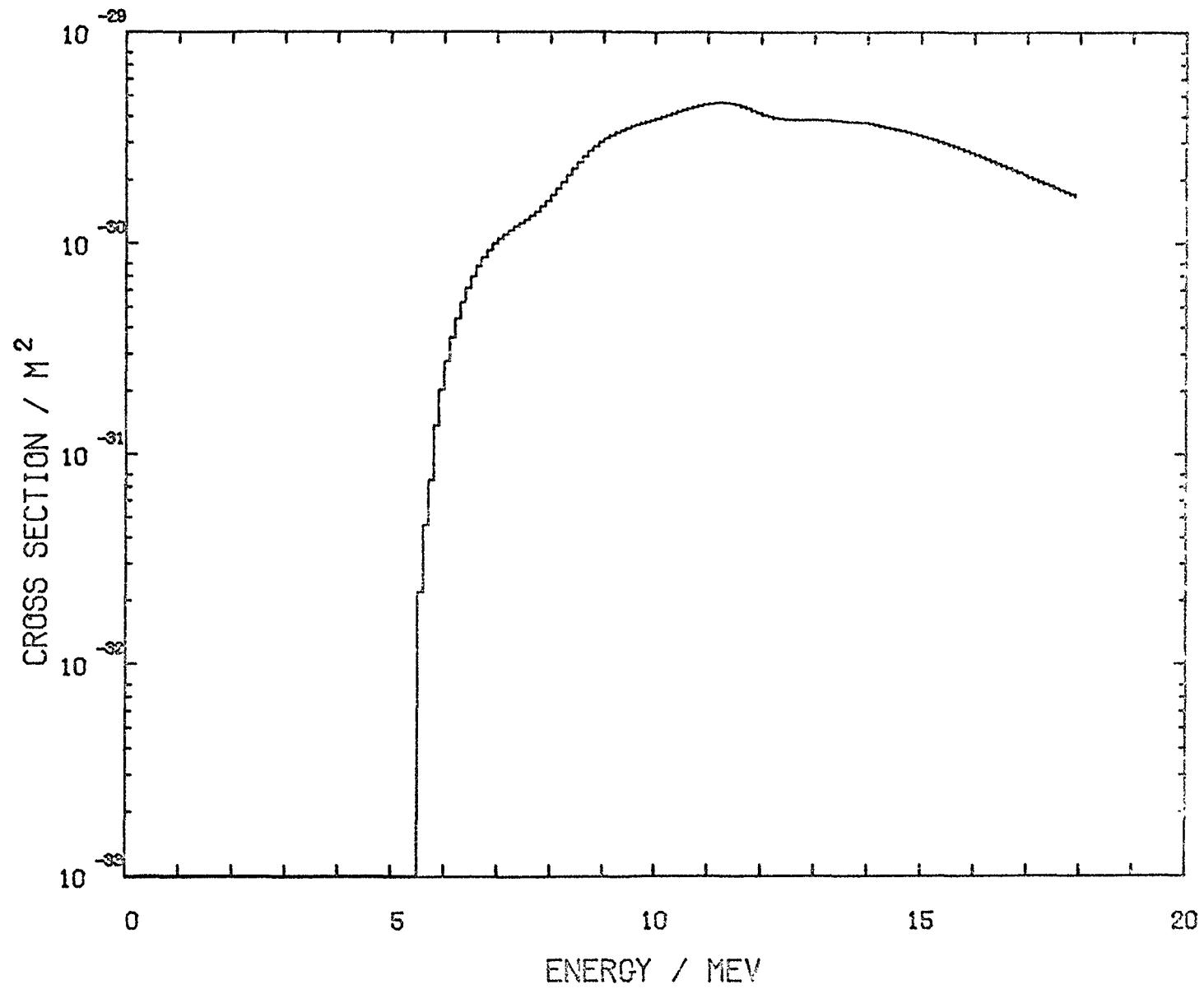


Fig. 26 Cross section curve for the reaction CU 63 (N,A) CO 60.

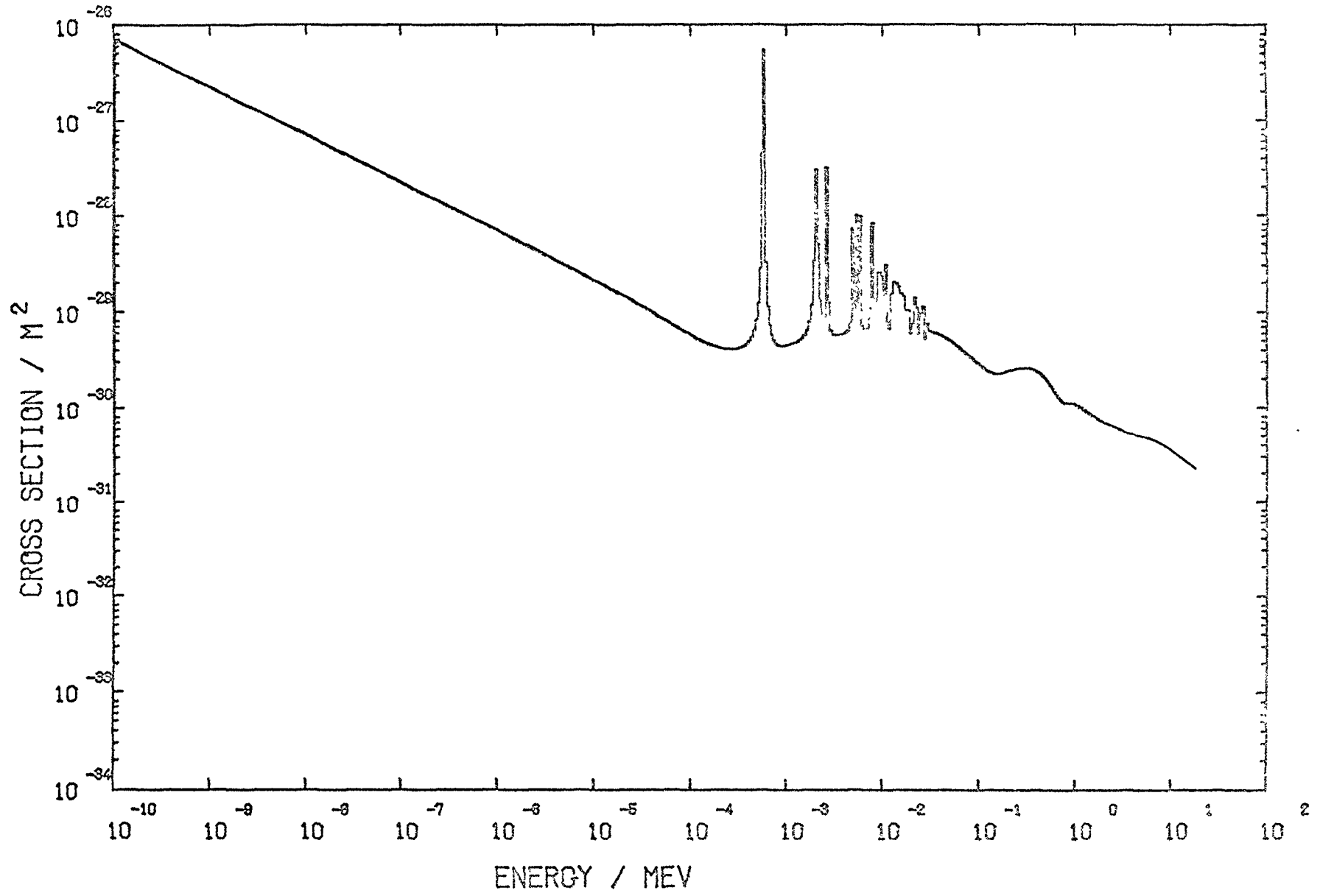


Fig. 27 Cross section curve for the reaction CU 63 (N,G) CU 64.

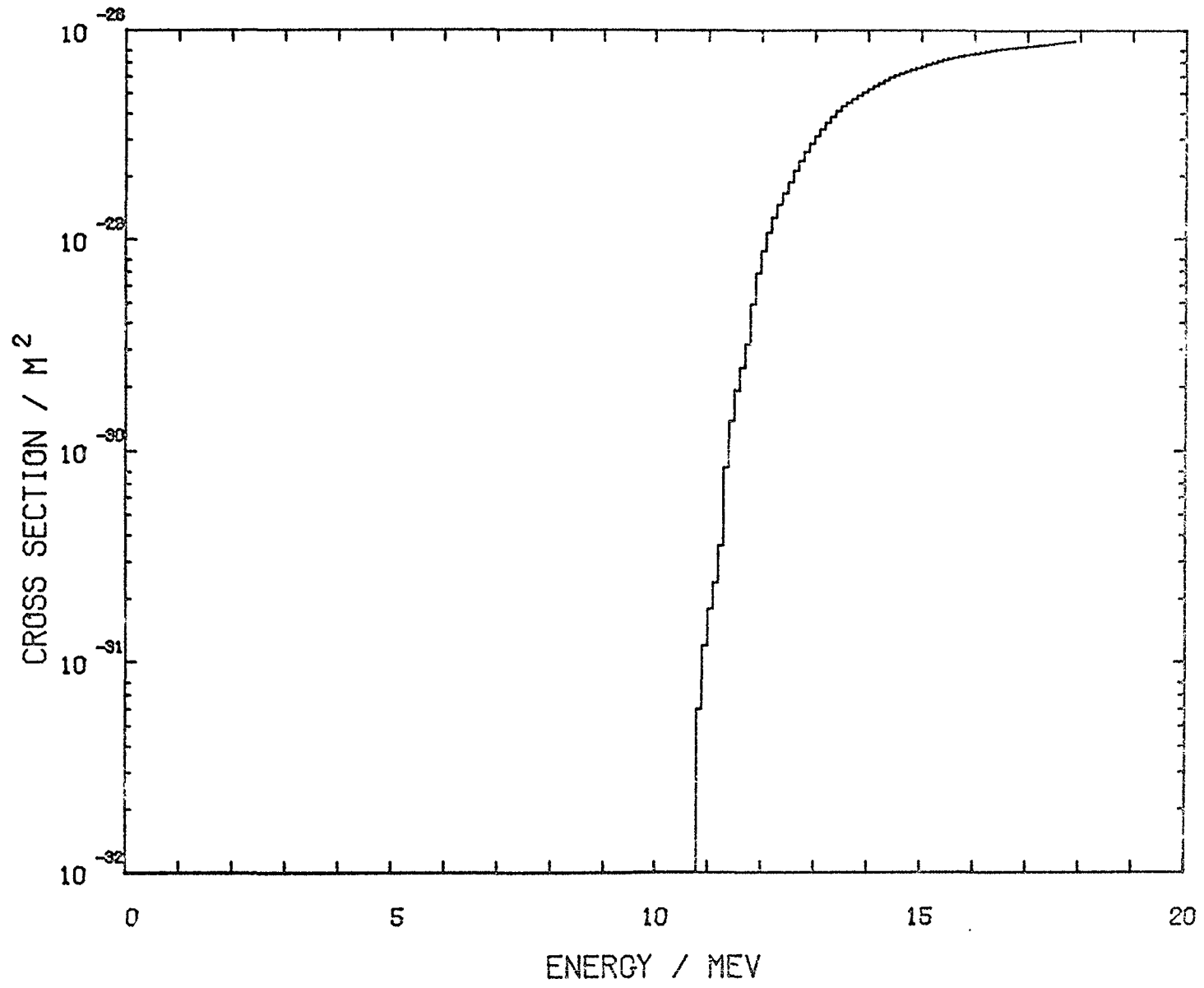


Fig. 28 Cross section curve for the reaction CU 63 (N,2N) CU 62.

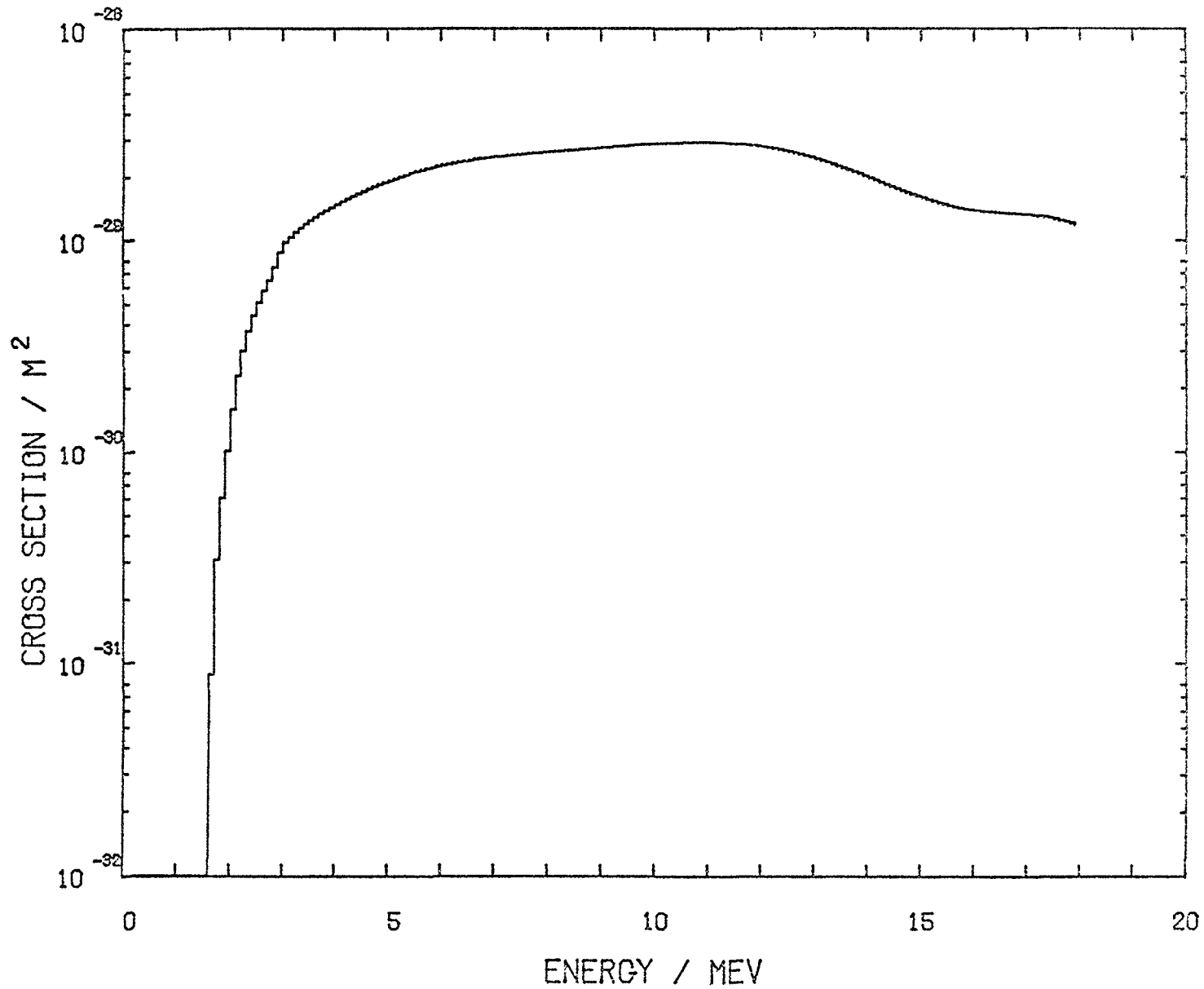


Fig. 29 Cross section curve for the reaction ZN 64 (N,P) CU 64.

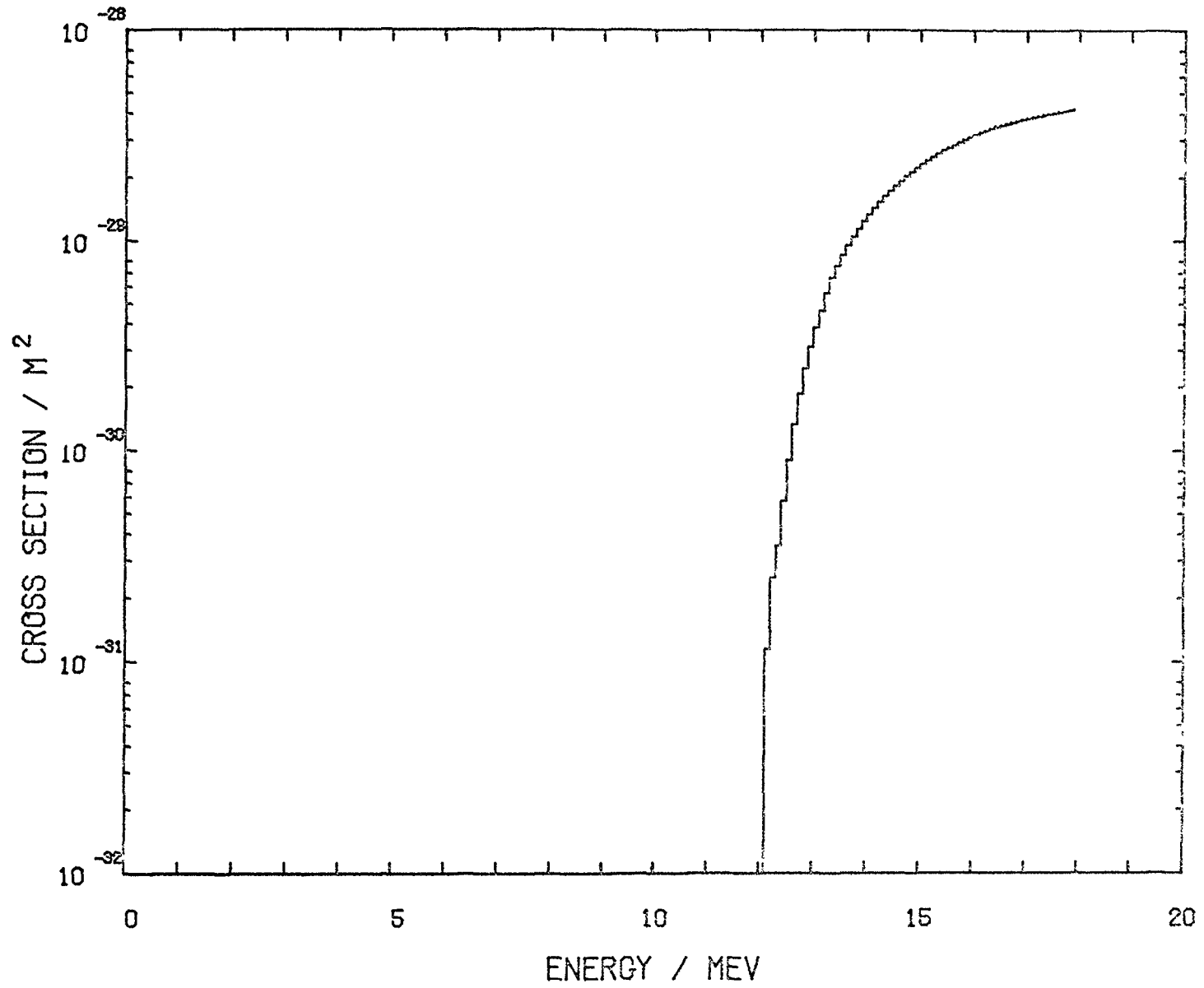


Fig. 30 Cross section curve for the reaction  $Zn\ 64 (N,2N) Zn\ 63$ .

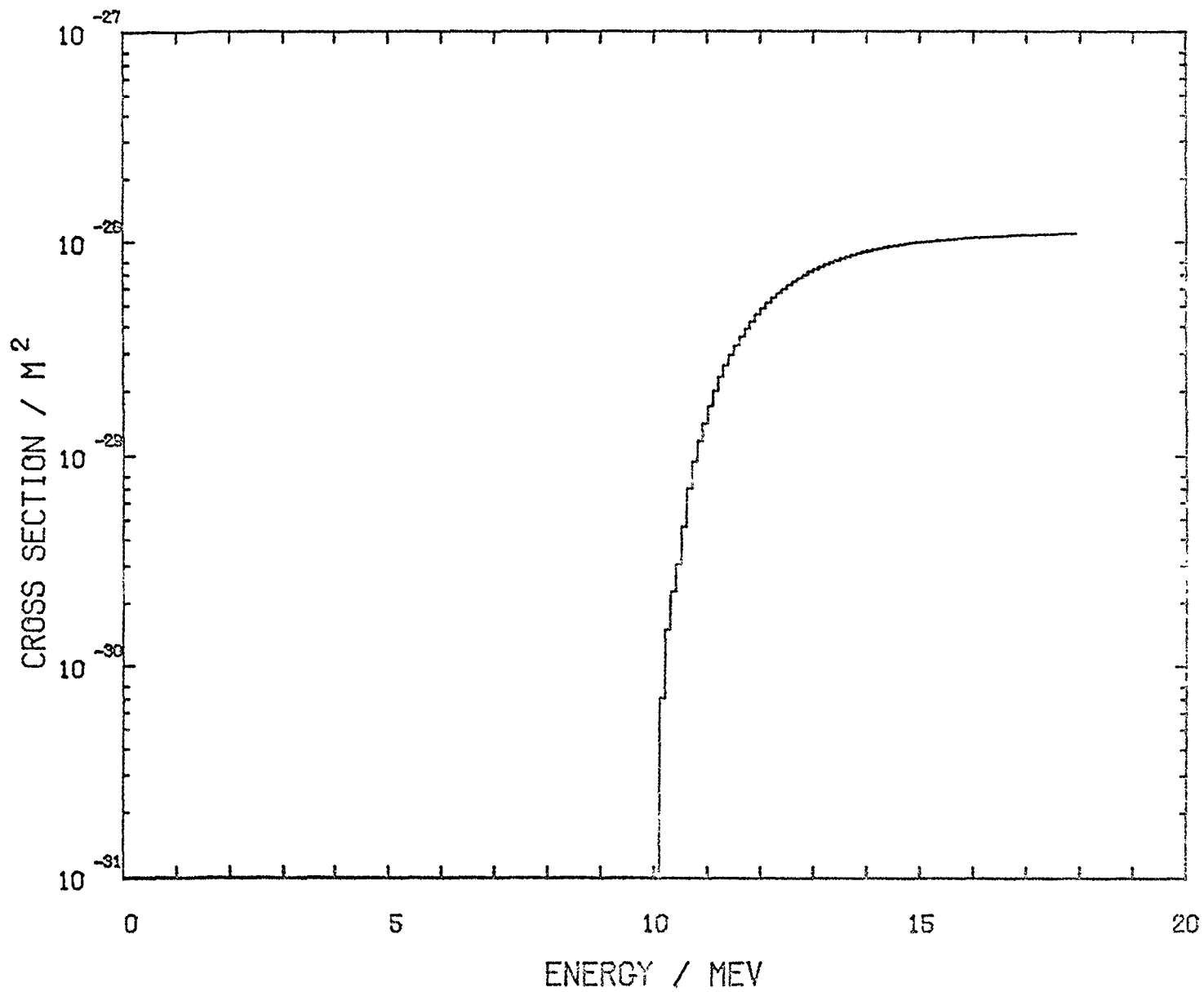


Fig. 31 Cross section curve for the reaction CU 65 (N,2N) CU 64.

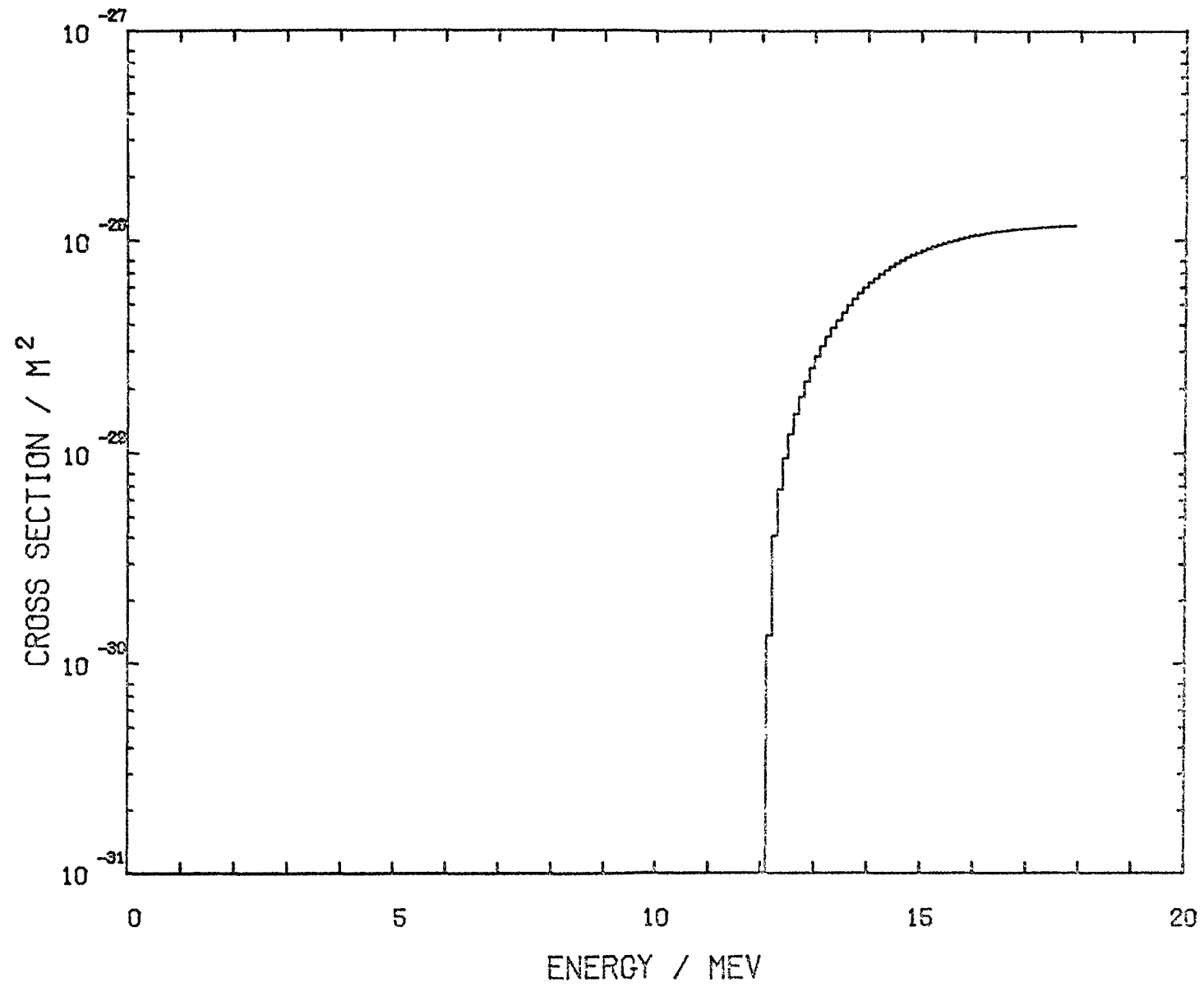


Fig. 32 Cross section curve for the reaction ZR 90 (N,2N) ZR 89,



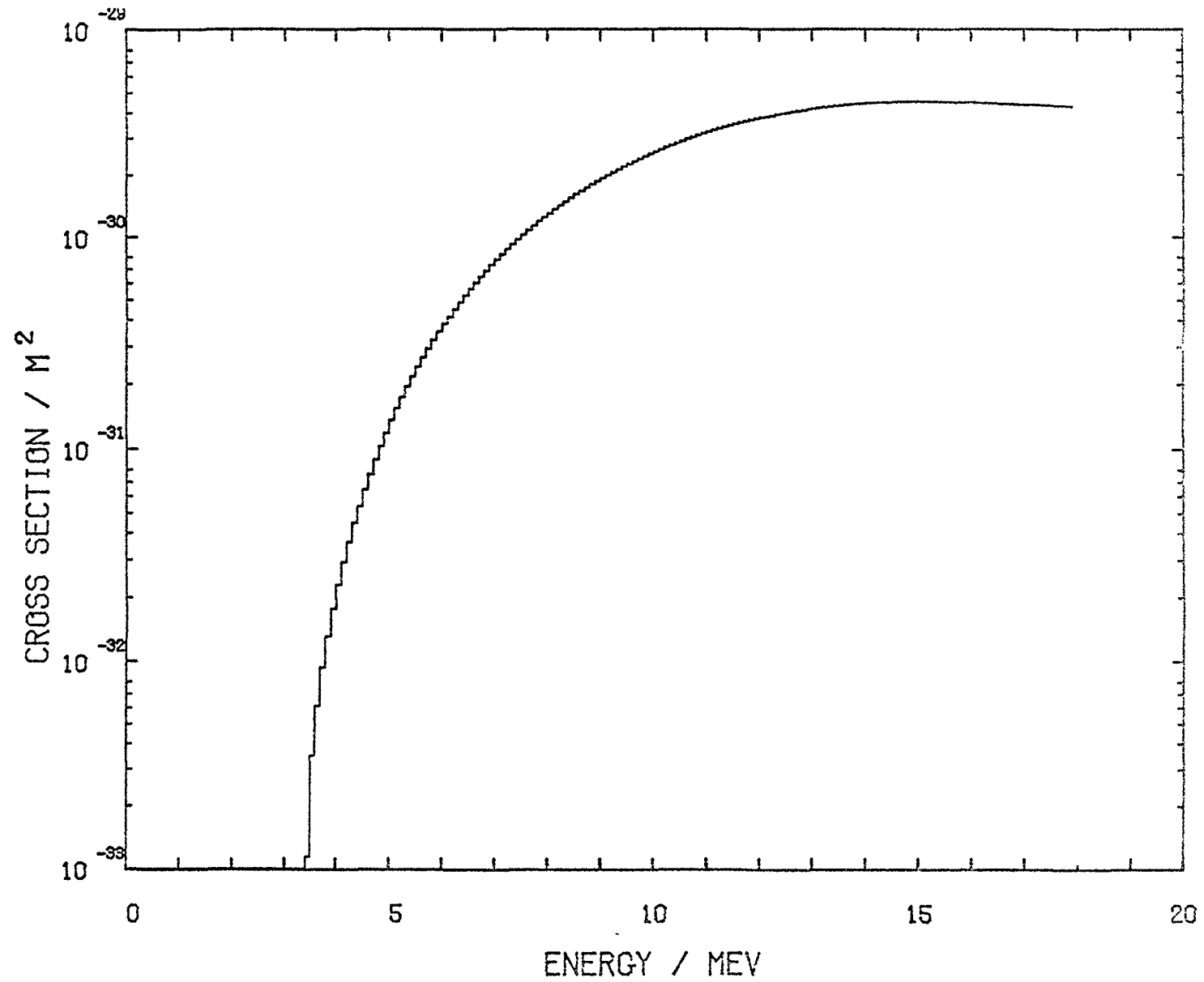


Fig. 33 Cross section curve for the reaction ZR 90 (N,P)Y 90.

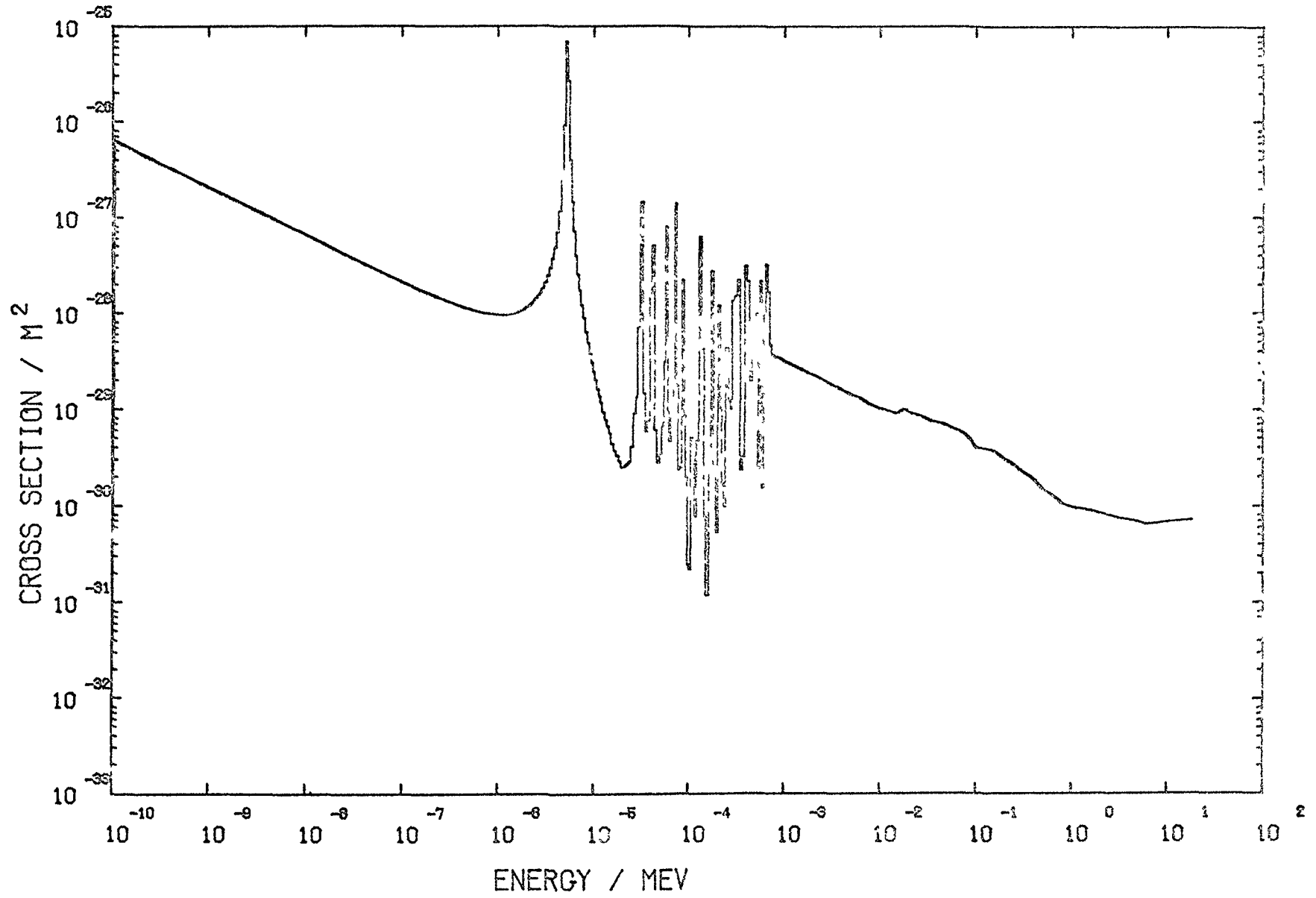


Fig. 34 Cross section curve for the reaction AG 109 (N,G) AG 110 M

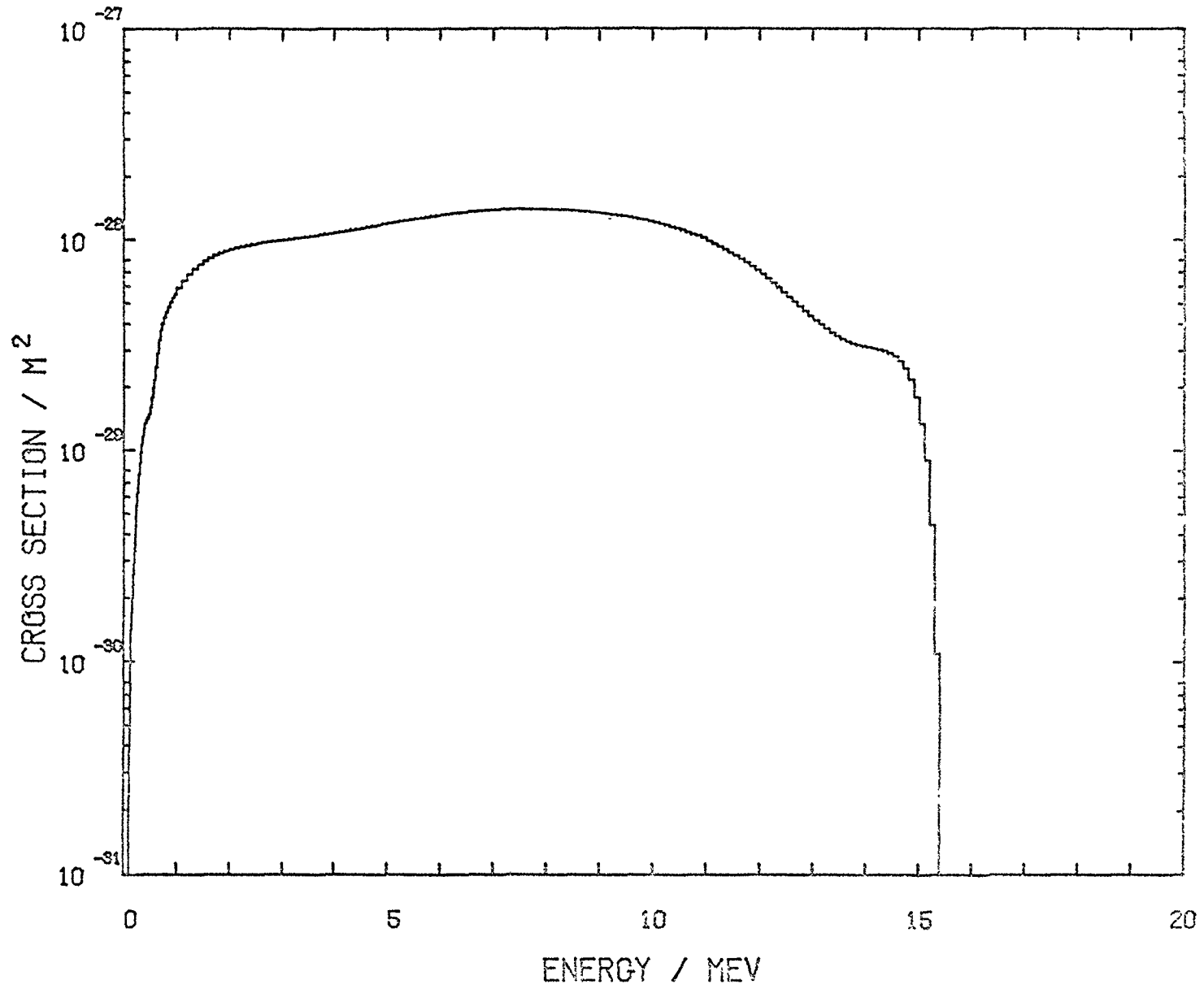


Fig. 35 Cross section curve for the reaction RH 103 (N,N') RH 103 M.

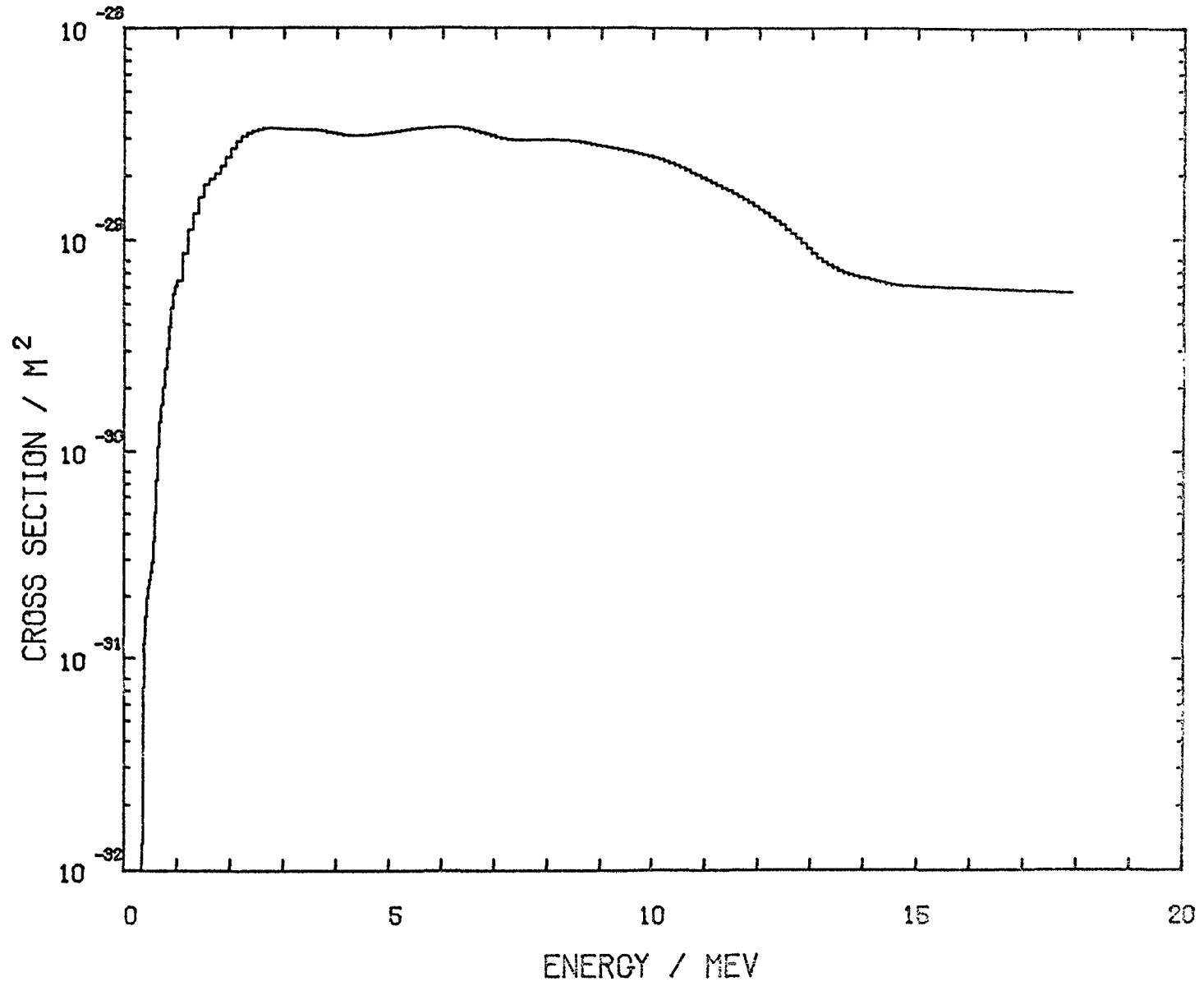


Fig. 36 Cross section curve for the reaction IN 115 (N,N') IN 115 M.

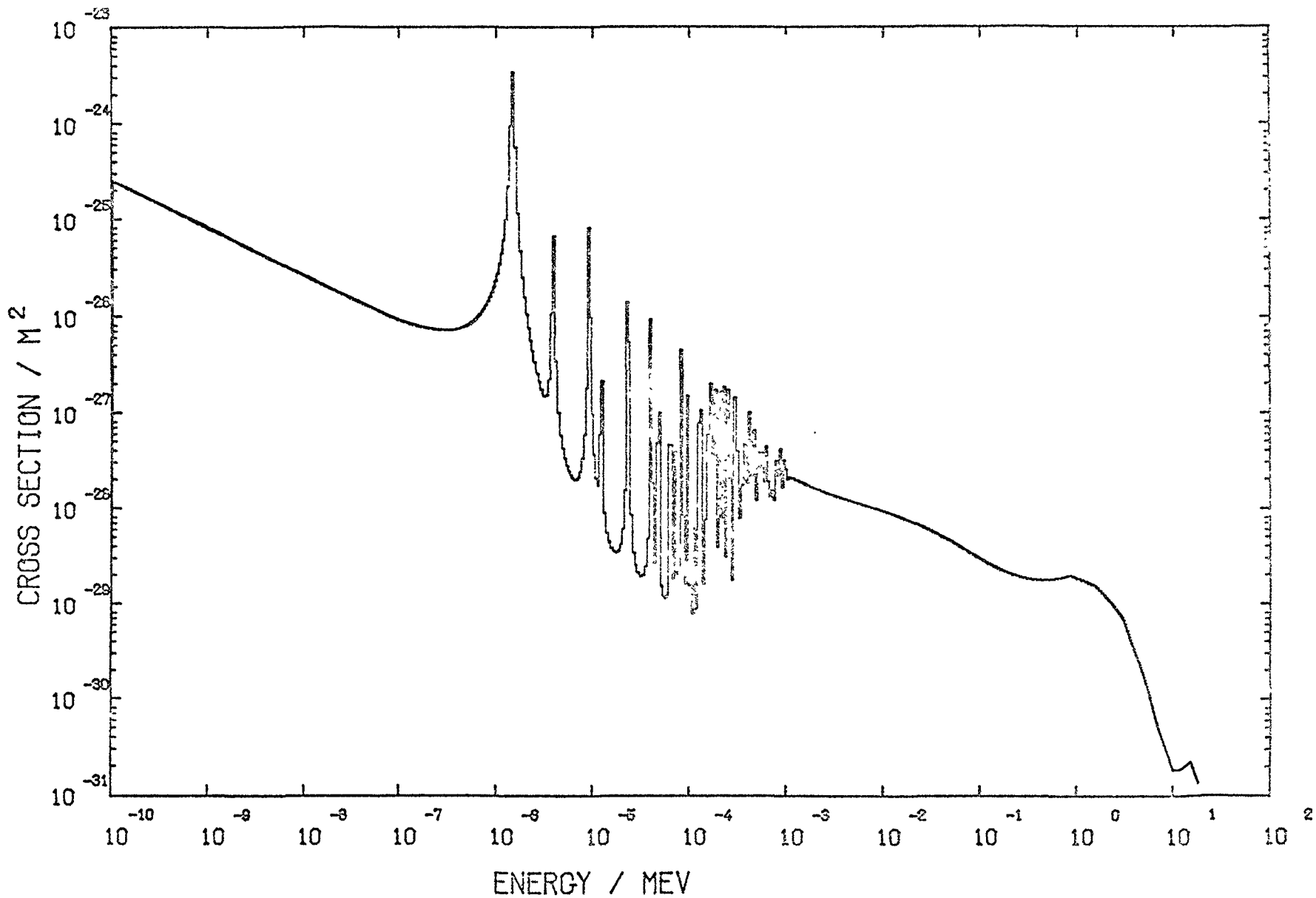


Fig. 37 Cross section curve for the reaction IN 115 (N,G) IN 116 M.

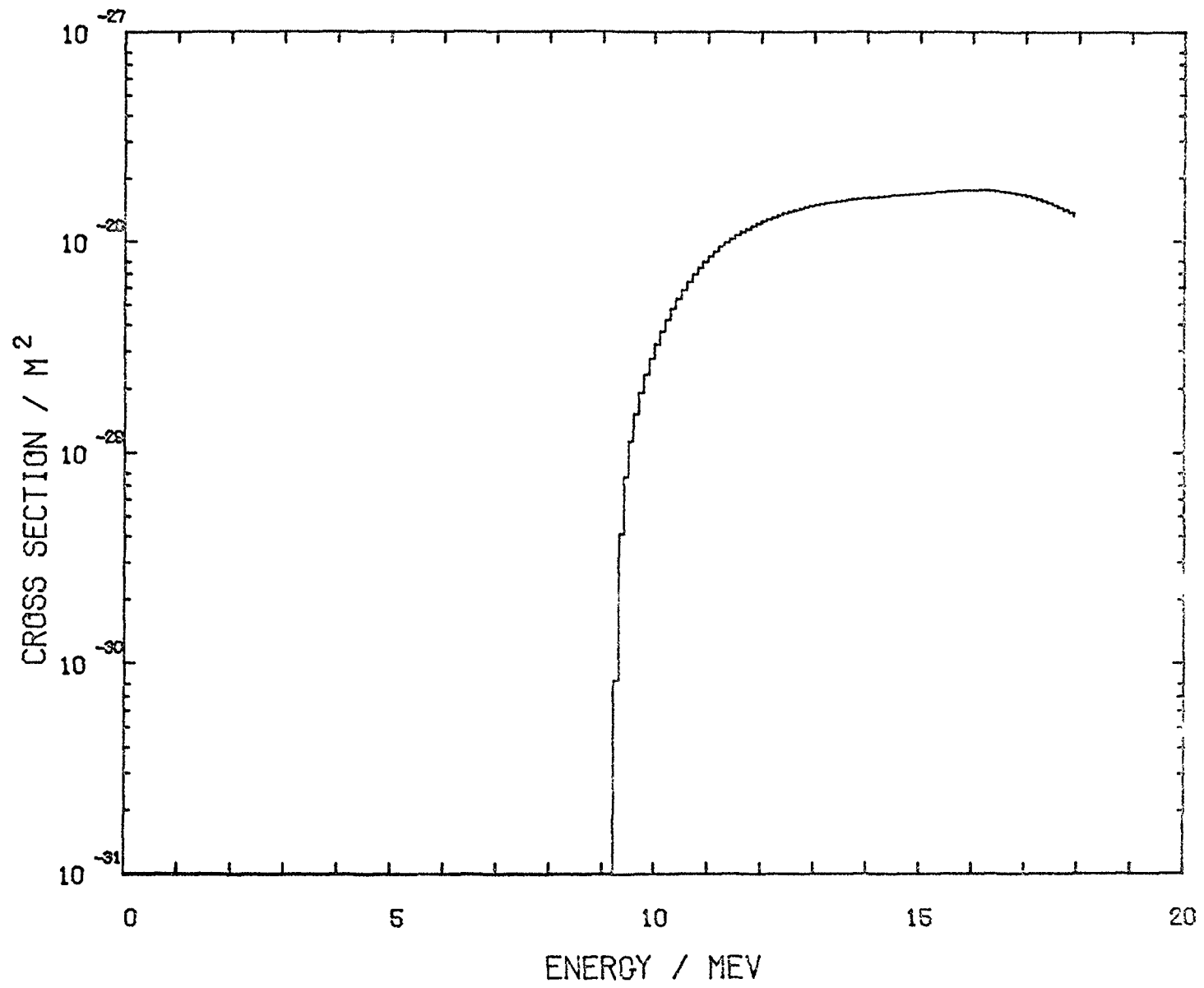


Fig. 38 Cross section curve for the Reaction  $I\ 127\ (N,2N)\ I\ 126$ .

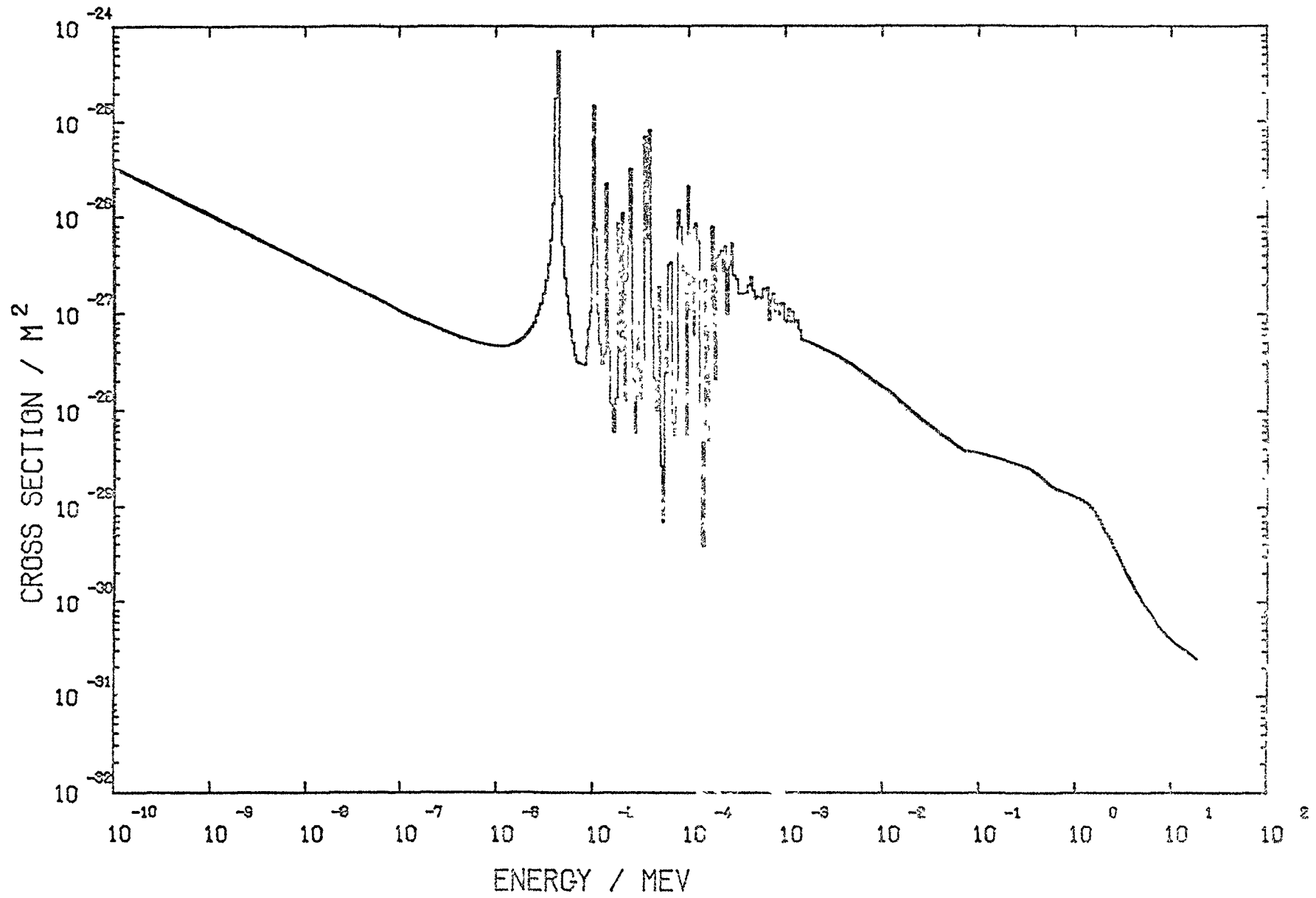


Fig. 39 Cross section curve for the reaction TA 181 (N,G) TA 182.

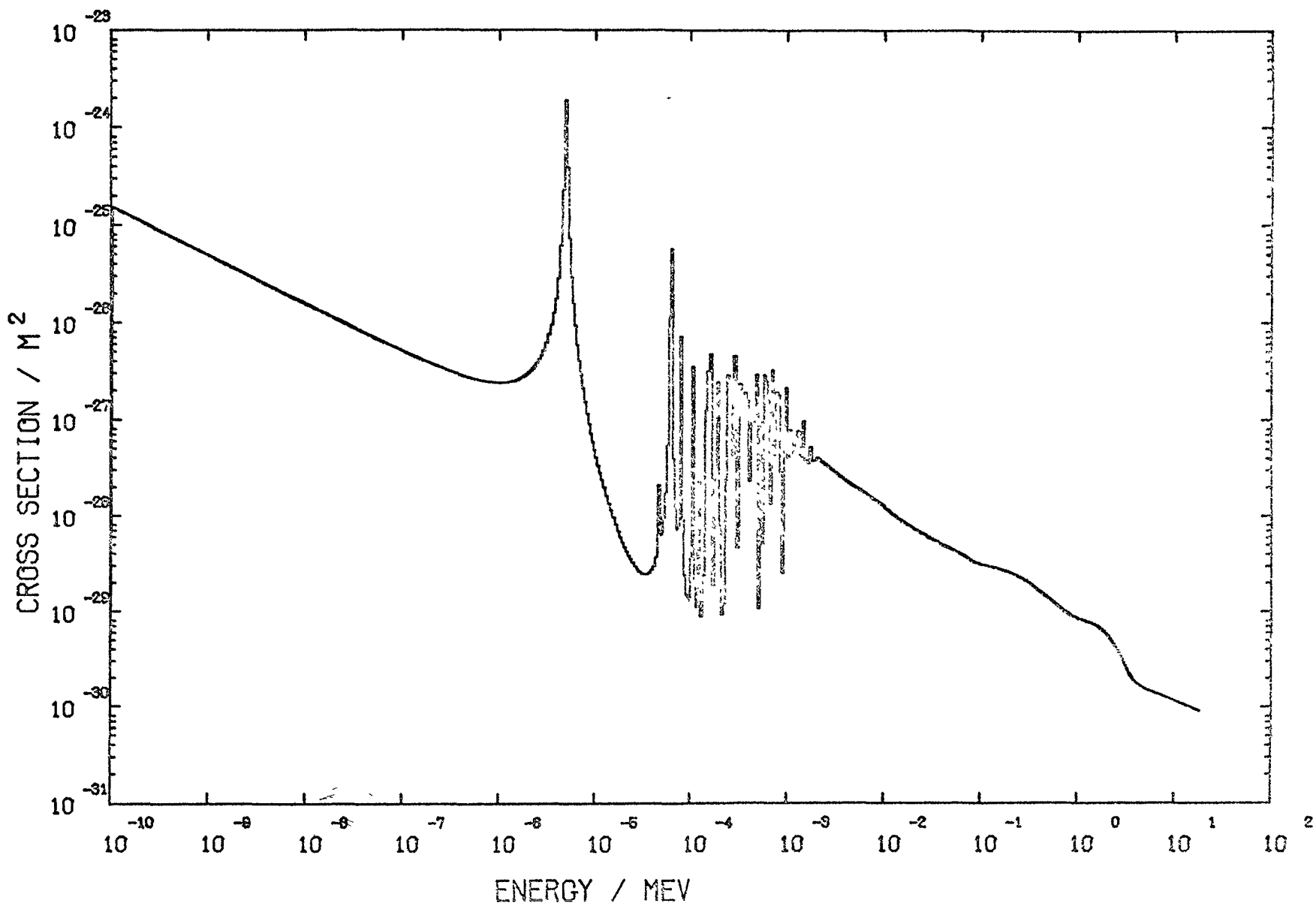


Fig. 40 Cross section curve for the reaction Au 197 (N,G) Au 198.



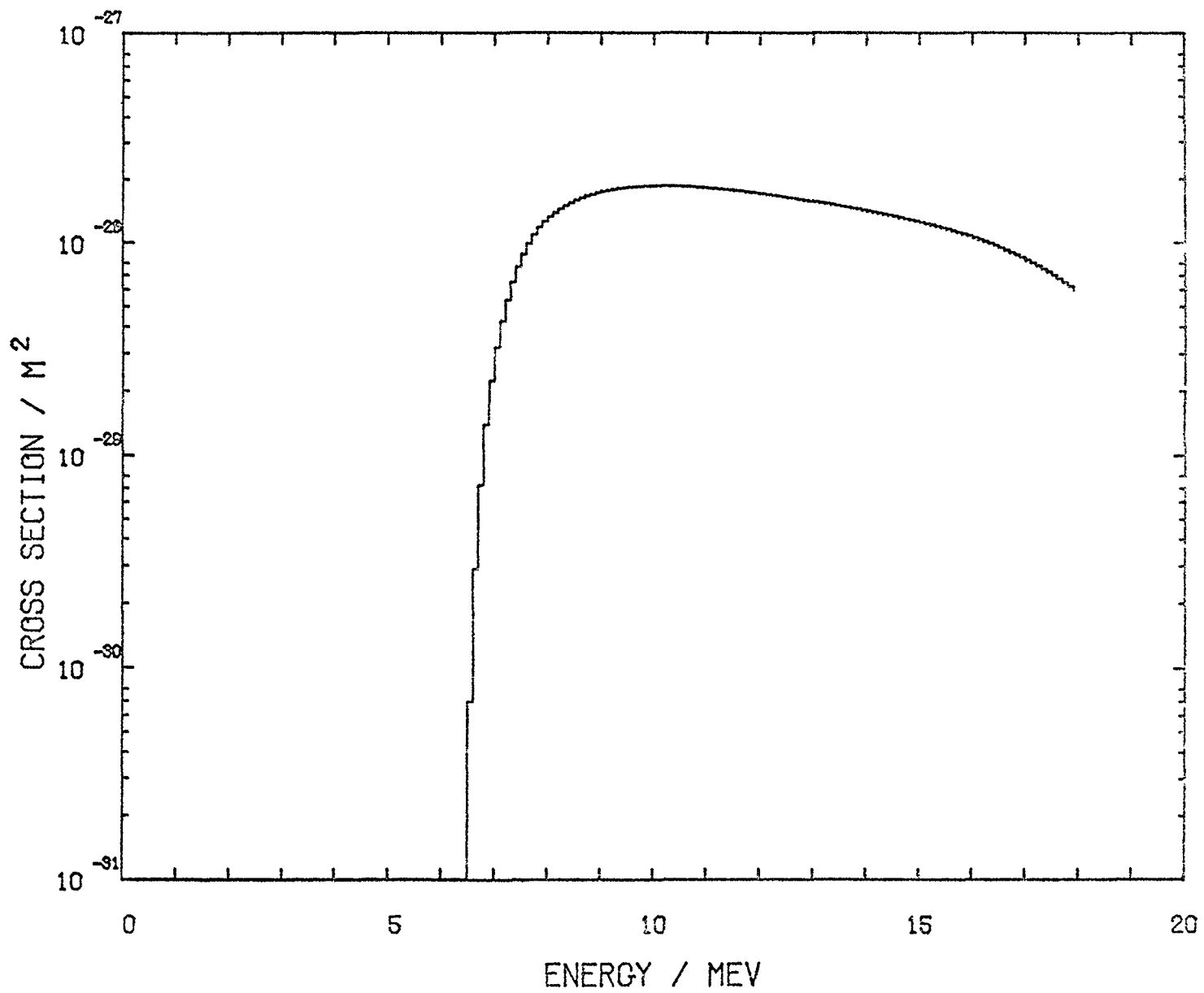


Fig. 41 Cross section curve for the reaction TH 232 (N,2N) TH 231.

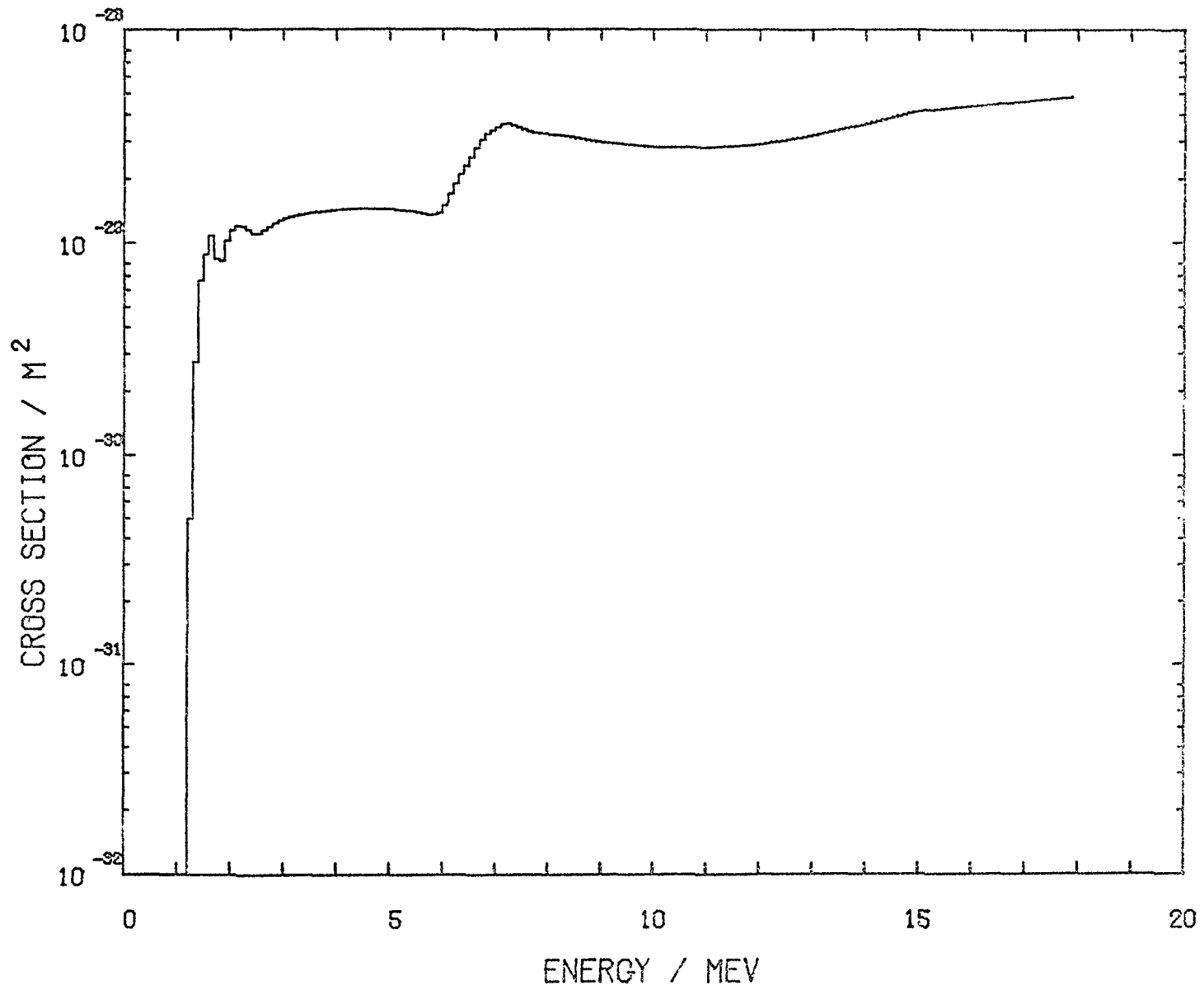


Fig. 42 Cross section curve for the reaction TH 232 (N,F) F.P.

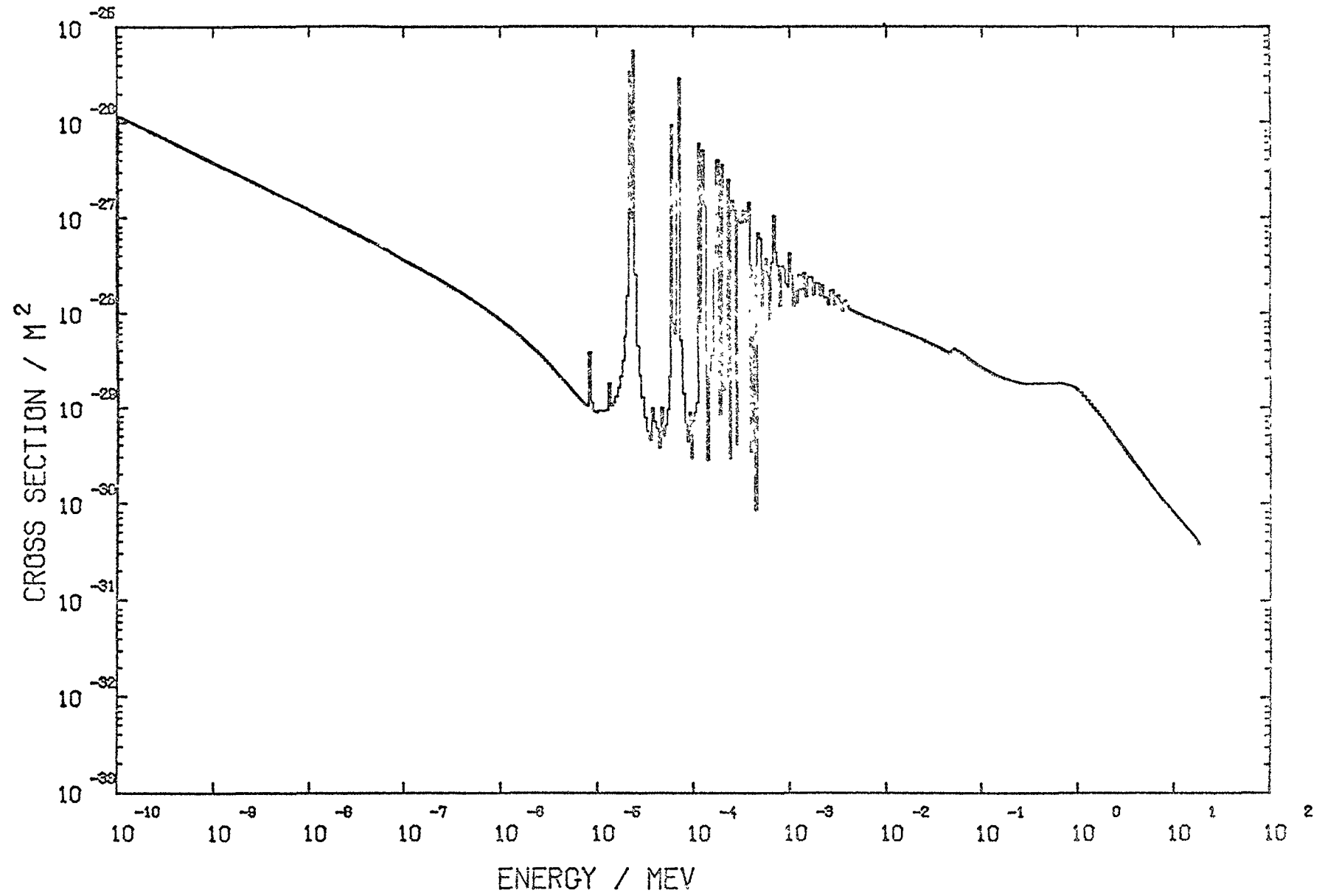


Fig. 43 Cross section curve for the reaction TH 232 (N,G) TH 233.

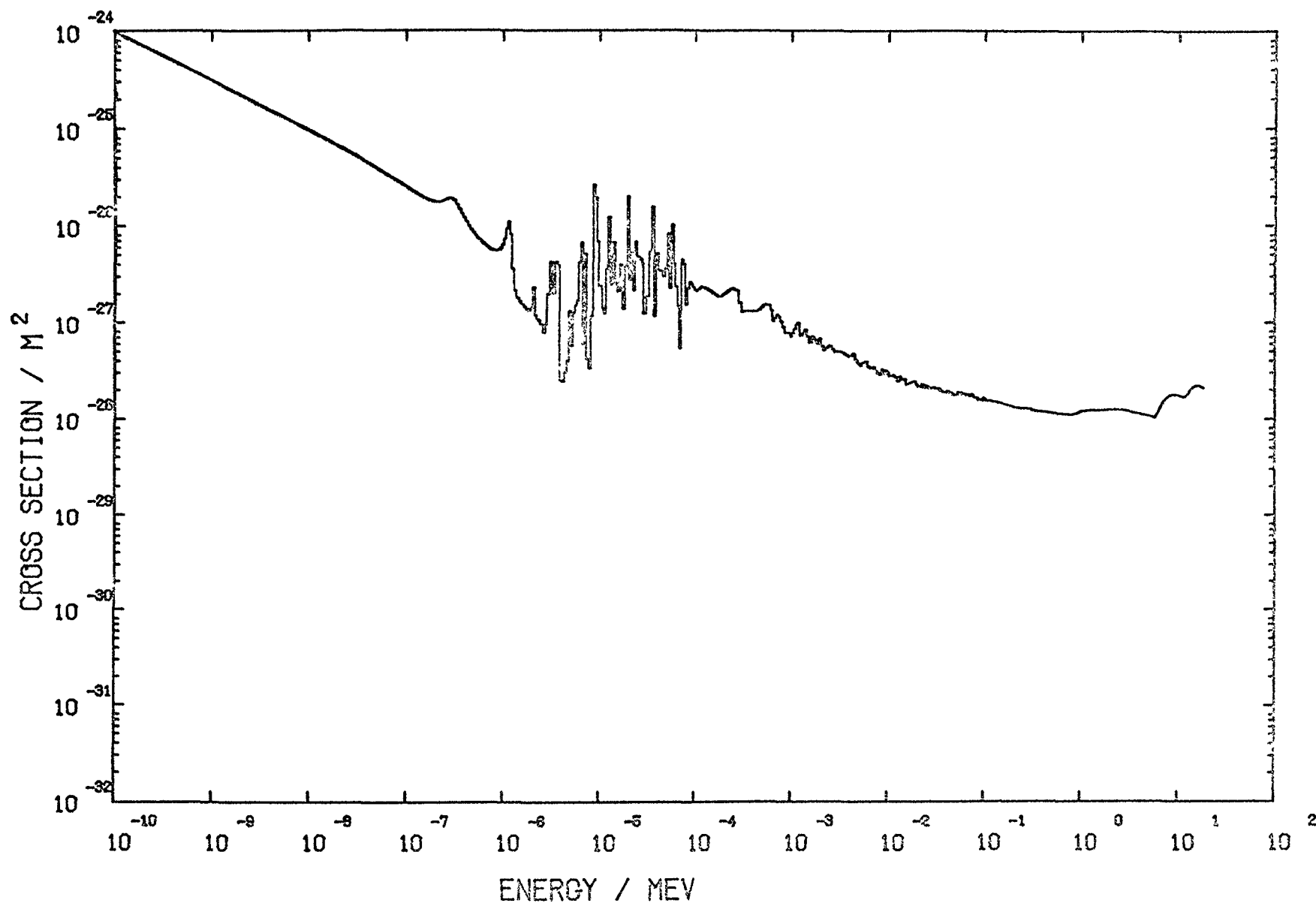


Fig. 44 Cross section curve for the reaction U 235 (N,F) F.P.

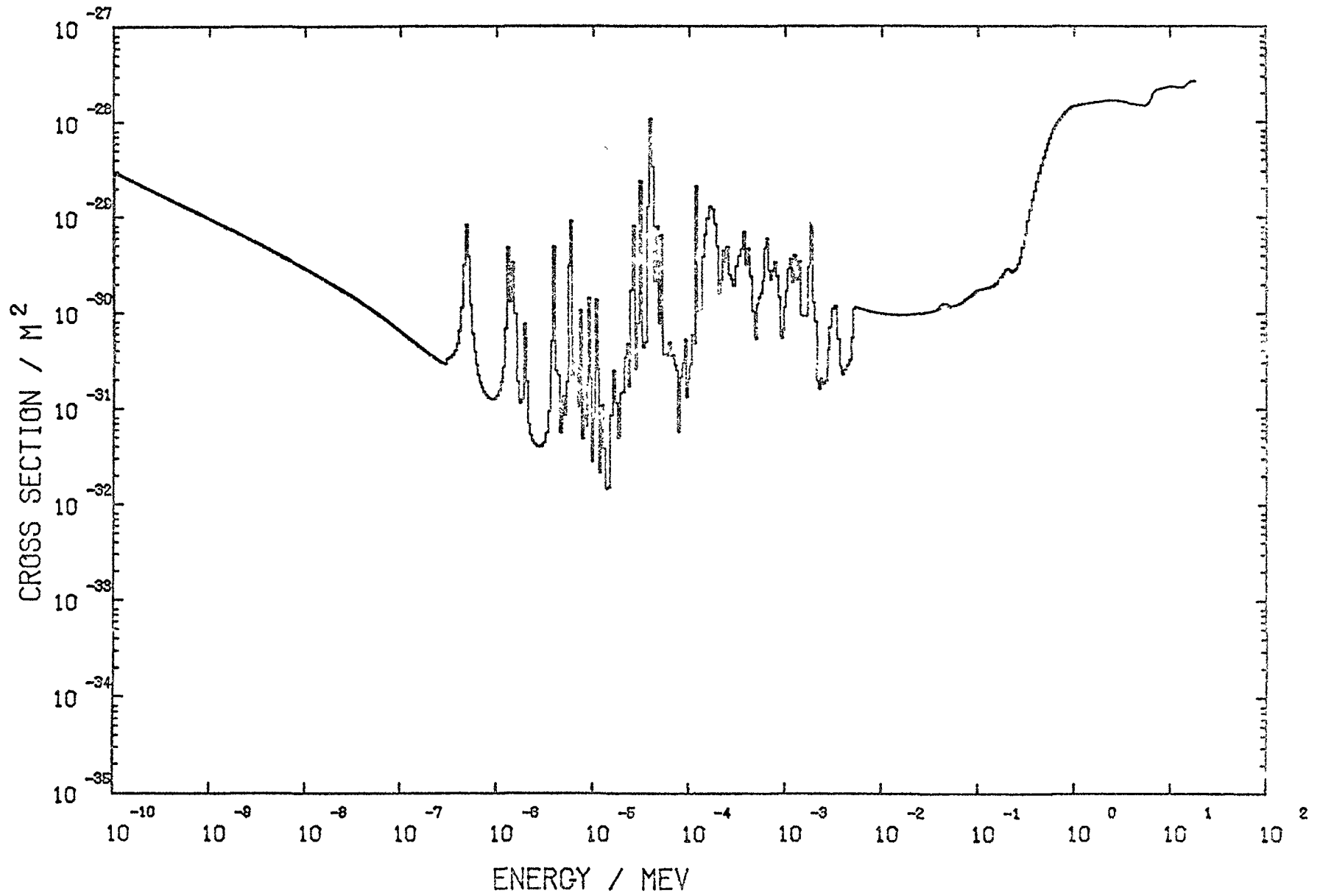


Fig. 45 Cross section curve for the reaction  $^{237}\text{Np}(n,f)$  F.P.

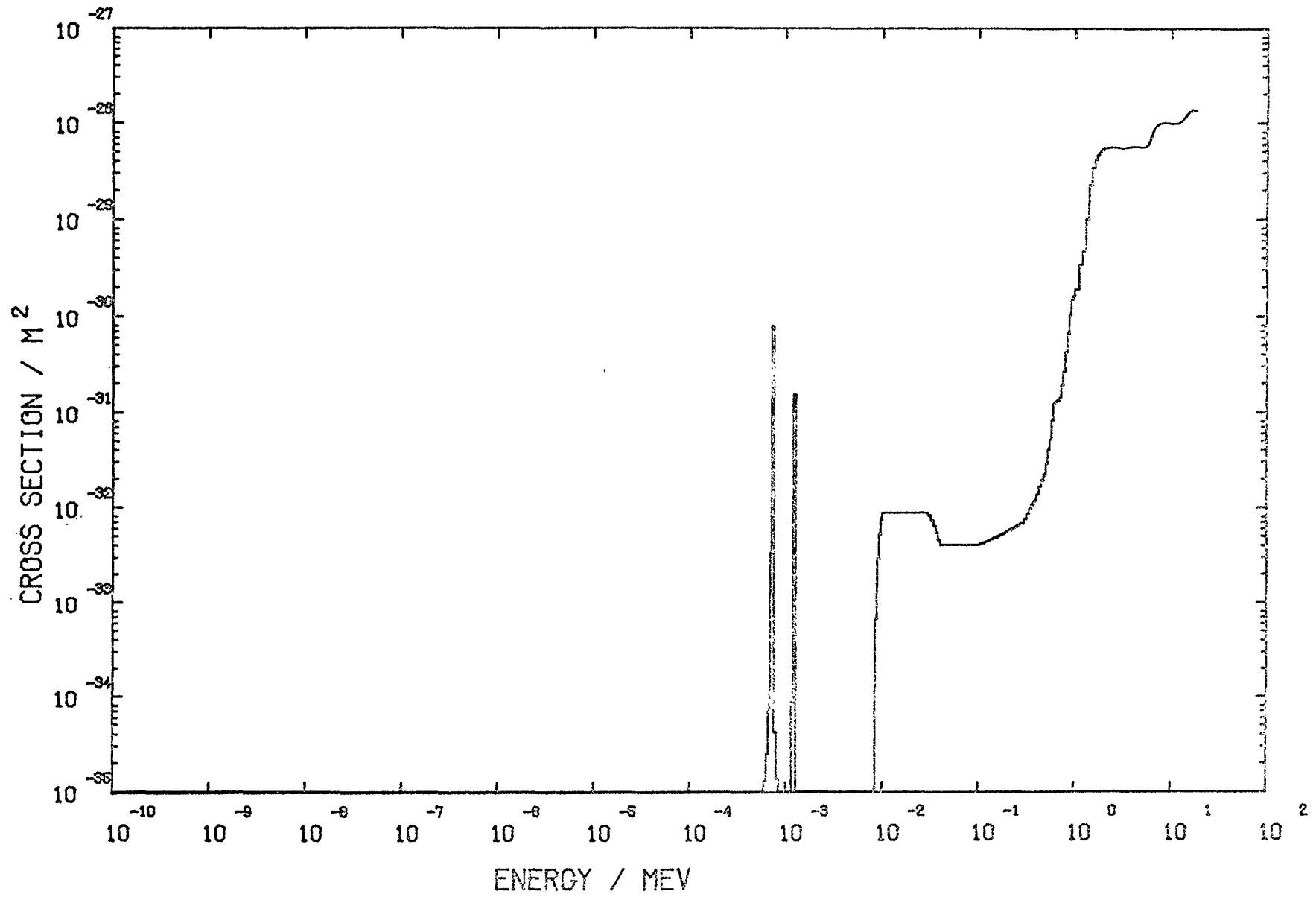


Fig. 46 Cross section curve for the reaction U 238 (N,F) F.P.

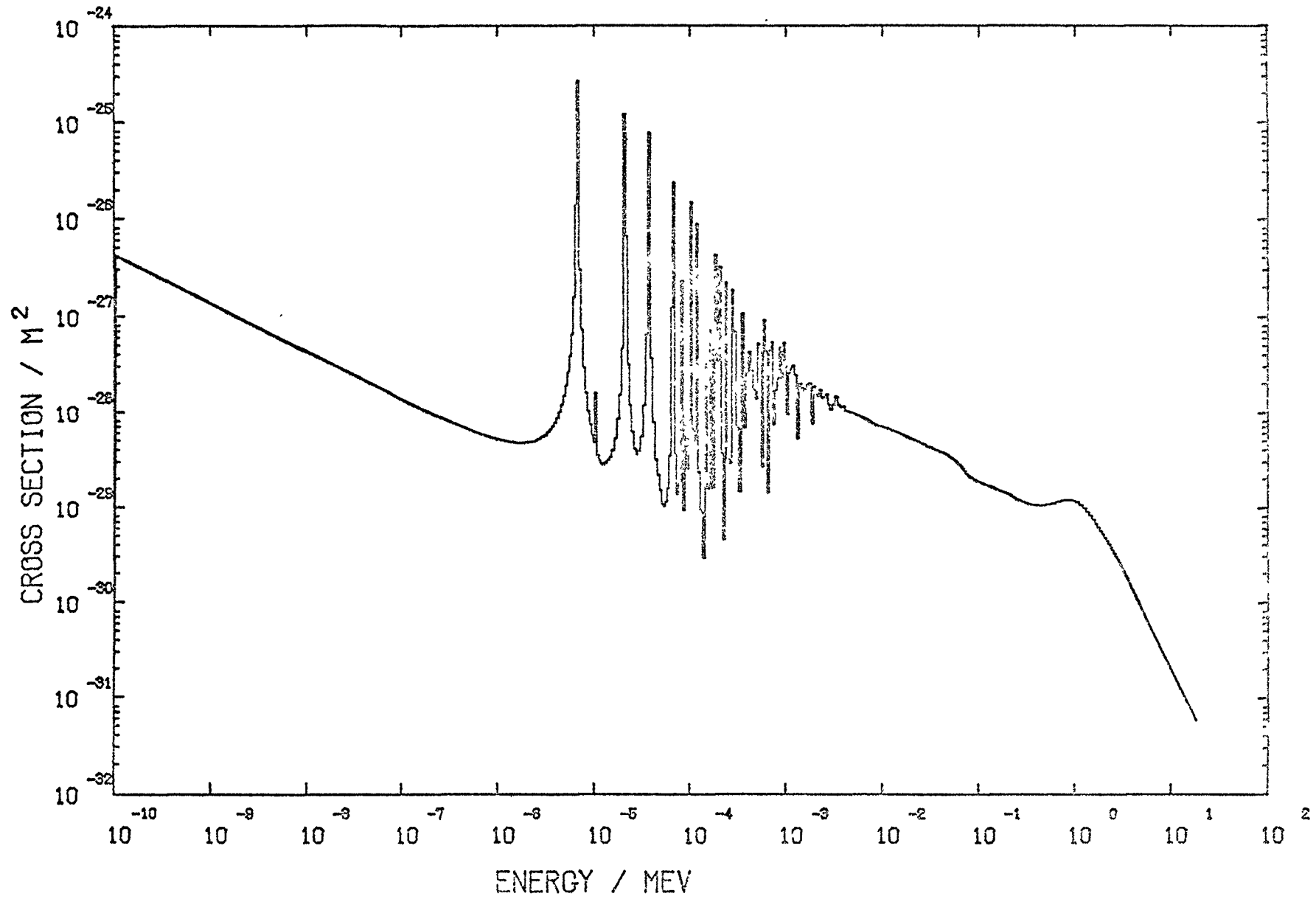


Fig. 47 Cross section curve for the reaction  $U^{238}(n, \gamma)U^{239}$ .

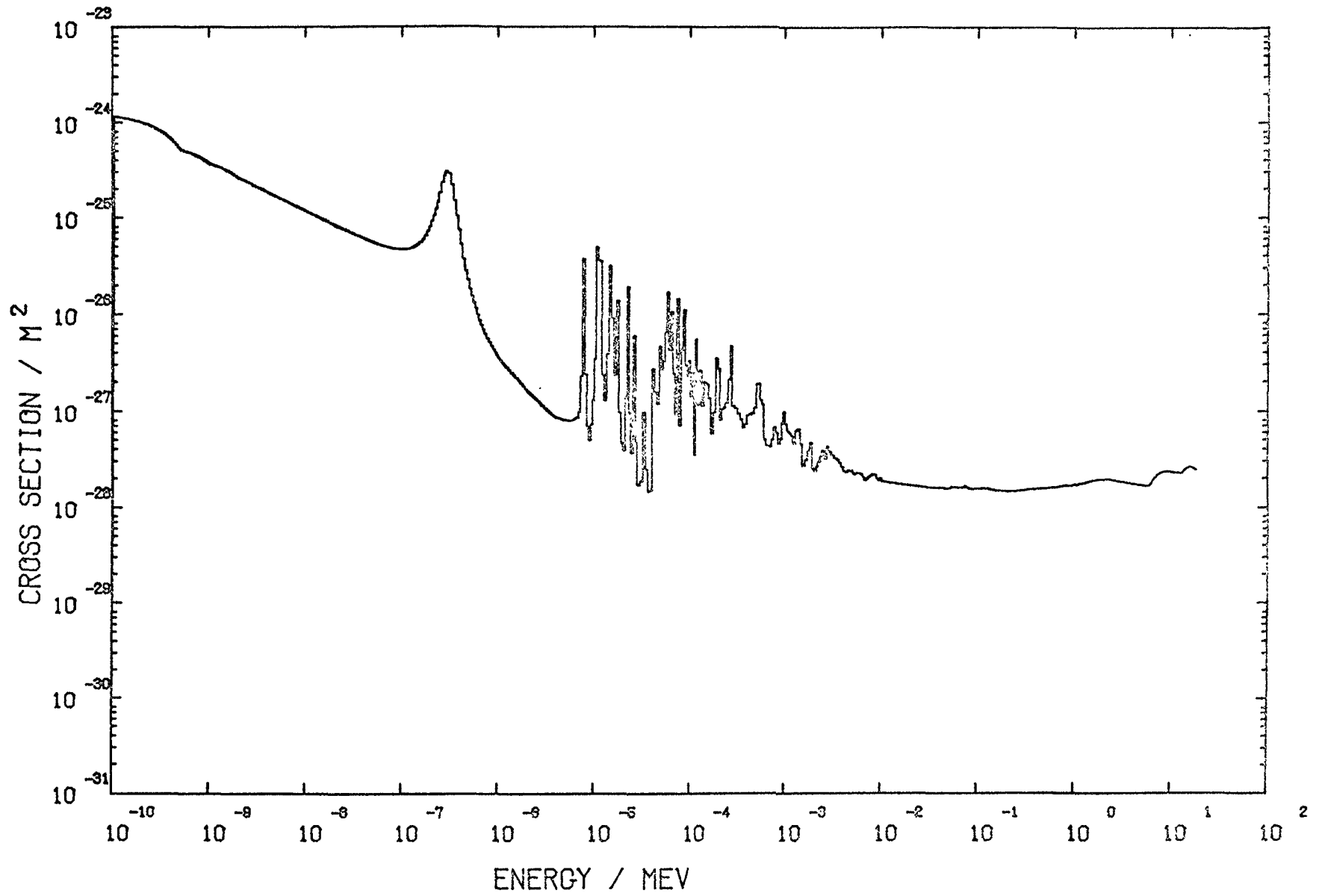


Fig. 48 Cross section curve for the reaction PU 239 (N,F) F.P.



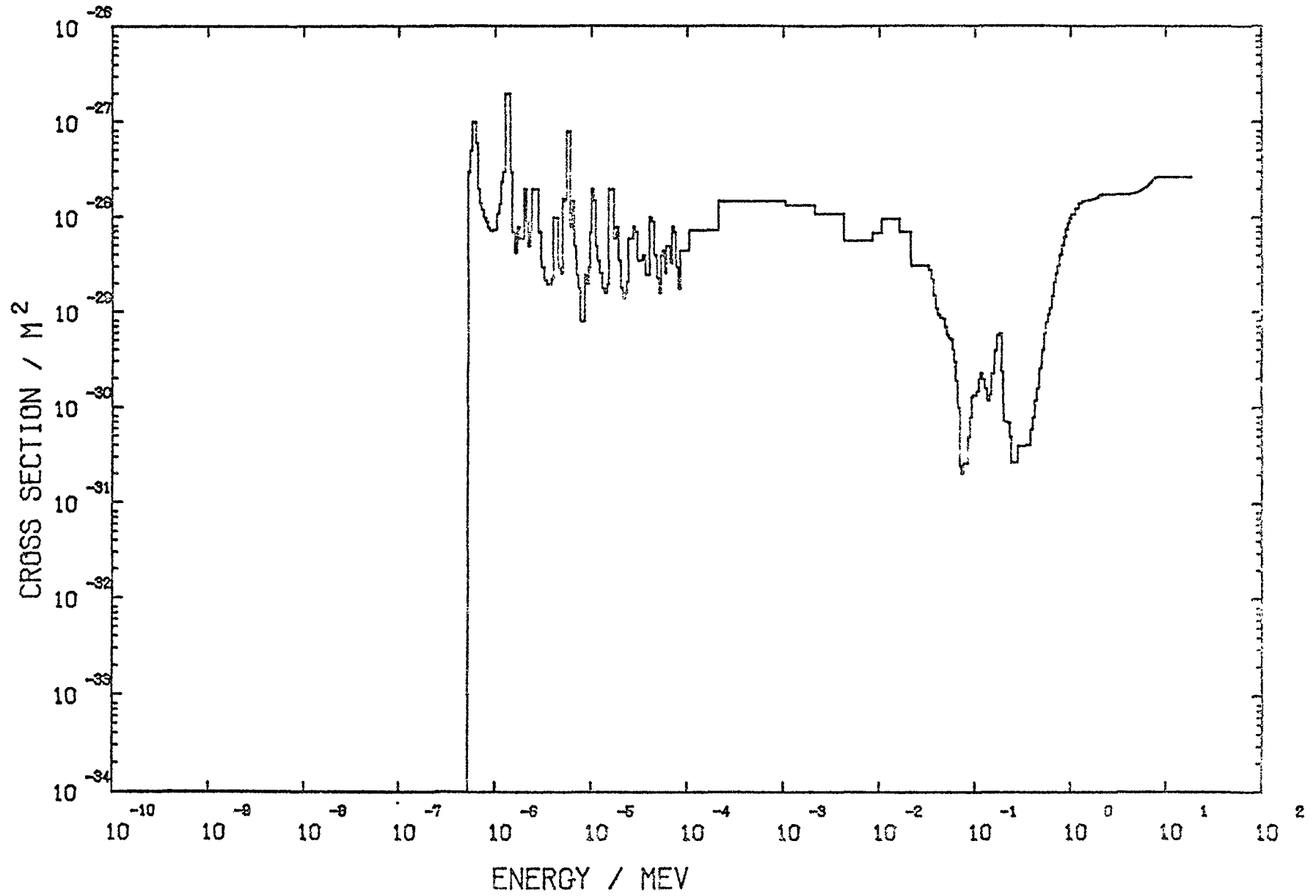


Fig. 49 Cross section curve for the reaction AM 241 (N,P) F.P.

## SHIELDING EFFECT OF FOIL COVERS

W.L. Zijp, H.J. Nolthenius, N.J.C.M. van der Borg  
Stichting Energieonderzoek Centrum Nederland  
Petten, Netherlands

### Abstract:

For neutron spectrum determinations one often irradiates activation detectors in boxes of cadmium, or of another material. Several models for the neutron attenuation in such foil covers are being studied. Preliminary experience is presented.

In the SAND-II computer program for neutron spectrum unfolding there is an option to take into account the neutron flux density attenuation in covers of gold, cadmium and boron.

It assumes a very simple model to describe this shielding effect (see model 1 described below). In some preliminary calculations we investigated whether other models would give different results.

In these calculations we modified the computer program SELFS |1|, which modifies the 620 group cross section values for the detection reaction, to take into account the selfshielding of the neutrons in the field.

In a similar way the cross sections were now modified to take also into account the effect of attenuation of the incident neutron flux density in the foil cover.

We now will consider several models for the calculation of the neutron attenuation in the foil covers. First we will consider slab-type covers, and after that box-type covers.

All models assume exponential attenuation along the direction of the path of the incident neutrons.

### Slab-type covers:

Model 1. This model assumes infinite slabs for the foil and the two covers on either side of the foil. This model assumes also a beam flux density perpendicularly incident on the cover slab. It is the model used in the SAND-II program package for covers of gold, cadmium and boron.

$$G_s(E) = e^{-\tau(E)}$$

where:

$$\tau(E) = N_V \cdot \sigma(E) \cdot d$$

This factor has then to be multiplied with the selfshielding factor (based now on isotropic incidence).

Model 2. This model takes into account simultaneously the attenuation in the cover and the selfshielding in the foil. It assumes isotropic incidence on the infinite slabs of cover material and foil material.

$$G(E) = \frac{1}{\tau(E)} = \{E_3(\tau_s) - E_3(\tau_s + \tau)\}$$

where:

$$\tau_s = \tau_s(E) = \{N_V \cdot \sigma_\tau(E) \cdot d\}_{\text{shield}}$$

$$\tau = \tau(E) = \{N_V \cdot \sigma_{\text{act}}(E) \cdot d\}_{\text{foil}}$$

Model 3. The mathematical formulae from model 2 can also be applied when the thickness of the cover does not denote the thickness of a plane slab, but half of the mean chord length, determined by the geometry (cylindrical box) of the actual cover. In general one has the following expression for the mean chord length:

$$\langle l \rangle = \frac{4 \times \text{volume}}{\text{surface}}$$

In this way model 3 gives a finite size correction to model 2.

#### Box type covers:

The next models separate the effects of attenuation in the cover and the of selfshielding in the foil. They assume a cover in the form of a cylindrical box (outer height H, outer radius R, wall thickness d).

Model 4. At the centre of the box a point detector is assumed. Foil activation can only be induced by neutrons whose original direction is towards the box centre.

There is of course azimuthal symmetry. Integration has to be performed over the angle  $\theta$  between line of incidence and positive X-axis.

Model 5. At the centre of the box a detector with line geometry along the cylinder axis is assumed.

All incident neutrons have directions towards this axis, and show full isotropy in each vertical plane through this axis.

There is again azimuthal symmetry. Integration has to be performed over the angle  $\theta$  and over the intercept with the cylinder axis.

Model 6. At the centre midplane of the box a detector with disc geometry is assumed, just fitting inside the box.

There is isotropic incidence. Integration has to be performed over the angle  $\theta$ , the radius parameter  $\rho$  and the angle  $\nu$ , between the projection of the line of incidence and the positive X-axis.

- Some preliminary data on shielding factors based on these models have been obtained. Calculations have been made for the following conditions:
- two covers: a) 1 mm cadmium with an atomic density of  $0.004634 \times 10^{28} \text{m}^{-2}$ ;  
                   b) 3.5 mm boron carbide;  $\rho = 2320 \text{ kg/m}^3$ ; 90%  $^{10}\text{B}$ ; atomic density of  $^{10}\text{B} = 0.0336 \times 10^{28} \text{m}^{-2}$ .
  - four spectra: CFRMF,  $\Sigma\Sigma$ , HFR and LFR.
  - two fictitious cross sections: a constant unit cross section and a  $1/\nu$  cross section

These preliminary results are listed in tables 1 and 2.

The cylindrical box used in the calculations had the following dimensions inner height 10 mm; inner radius 1.5 mm.

Half of the mean chord length is then 0.981 mm for the cadmium box, and 3.16 mm for the boron carbide box.

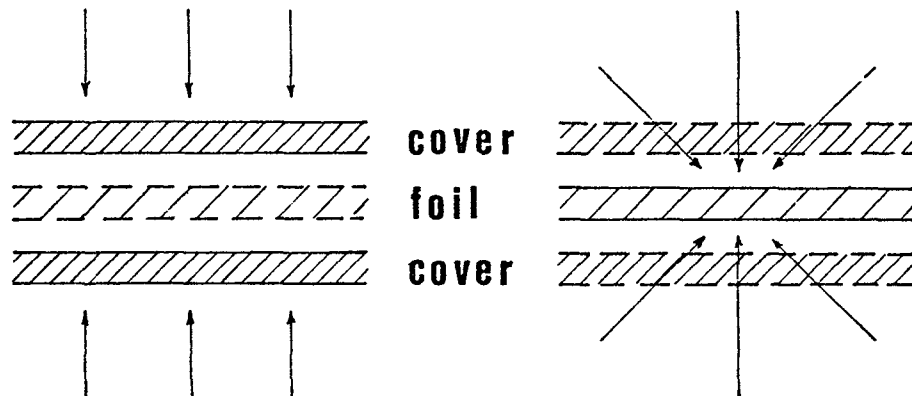
Table 1: Shielding factors according to several models (unit cross section)

	cadmium shield				boron carbide shield			
	CFRMF	$\Sigma\Sigma$	HFR	LFR	CFRMF	$\Sigma\Sigma$	HFR	LFR
<u>slab covers:</u>								
1) perpendicular beam	0.969	0.969	0.841	0.351	0.950	0.955	0.607	0.177
2) isotropic incidence	0.876	0.877	0.756	0.312	0.854	0.863	0.522	0.135
3) same, but with finite size correction	0.880	0.879	0.757	0.313	0.864	0.872	0.531	0.139
<u>box type cover:</u>								
4) point detector	0.960	0.960	0.831	0.346	0.942	0.948	0.595	0.169
5) line detector	0.938	0.939	0.811	0.336	0.928	0.934	0.578	0.160
6) disc detector	0.950	0.950	0.821	0.341	0.937	0.944	0.589	0.166

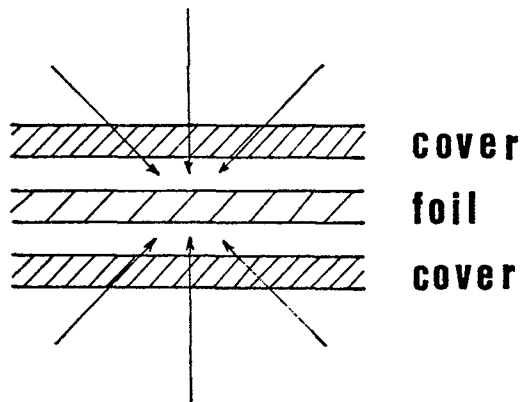
Table 2: Shielding factors according to several models (1/v cross section)

	cadmium shield				CFRMF	$\Sigma\Sigma$	HFR	LFR
	CFRMF	$\Sigma\Sigma$	HFR	LFR				
<b>slab covers:</b>								
1) perpendicular beam	0.967	0.967	0.125	0.0178	0.789	0.816	0.00512	0.000582
2) isotropic incidence	0.871	0.872	0.102	0.0144	0.630	0.667	0.00283	0.000284
3) same, but with finite size correction	0.873	0.874	0.102	0.0145	0.646	0.683	0.00307	0.000316
<b>box type covers:</b>								
4) point detector	0.960	0.960	0.120	0.0171	0.767	0.798	0.00448	0.000495
5) line detector	0.937	0.938	0.113	0.0161	0.734	0.769	0.00388	0.000416
6) disc detector	0.949	0.950	0.116	0.0165	0.756	0.789	0.00428	0.000468

### SLAB GEOMETRY

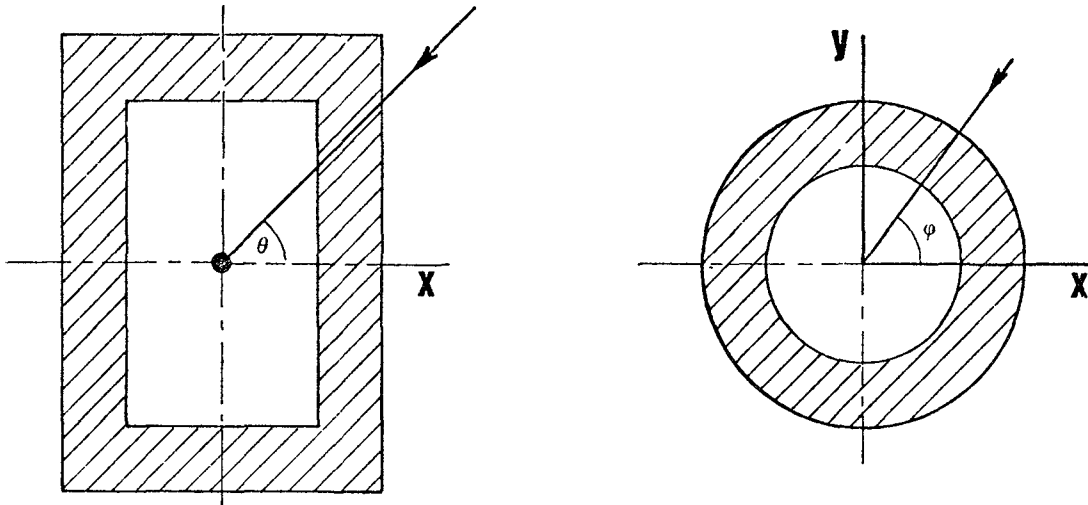


separate approaches  $G_{tot} = G_s * G_{ss}$

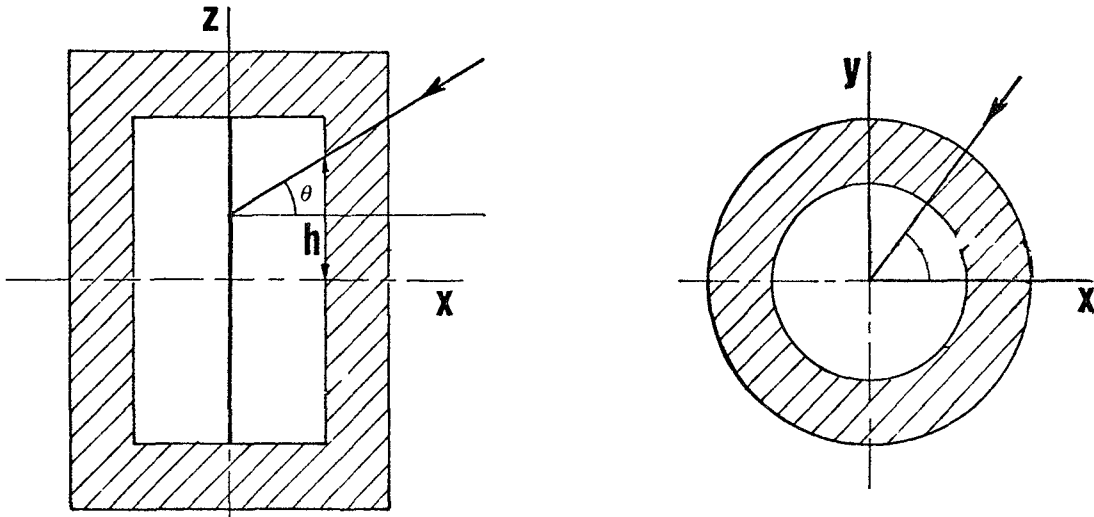


combined approach  $G_{tot} = G_{s,ss}$

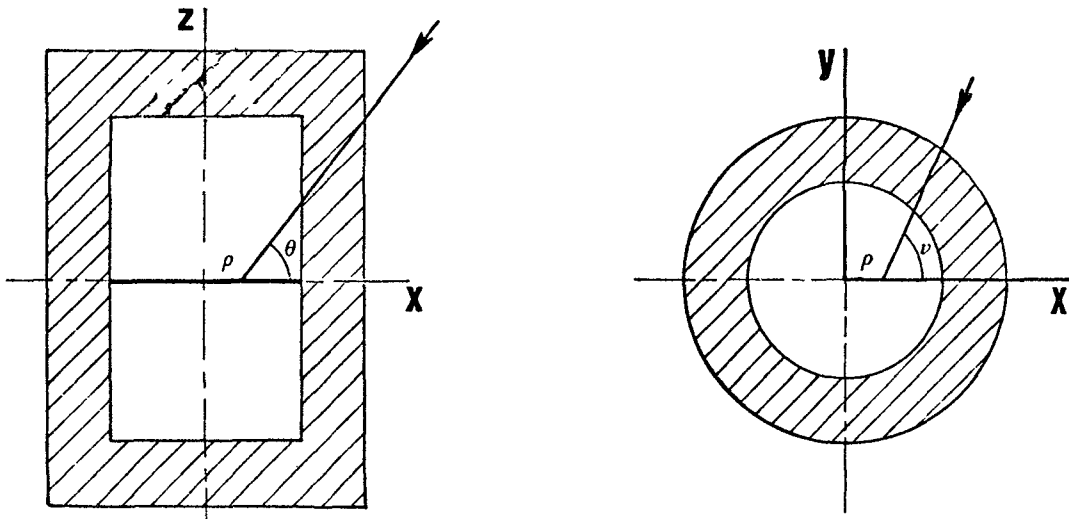
**z** **CYLINDRICAL BOX**



**centered foil with point geometry**



**centered foil with line geometry**



**centered foil with disc geometry**

SPECTRUM UNFOLDING IN THE HIGH NEUTRON ENERGY RANGE;  
COMPARISON OF DETECTOR SETS AND UNFOLDING PROCEDURES

L.J.M. Kuijpers<sup>x</sup>

ASSOCIATION EURATOM-KFA  
Inst. für Reaktorentwicklung  
Kernforschungsanlage Jülich  
Federal Republic of Germany

ABSTRACT

Operating speeds of modified SAND-II like codes were reviewed. The modifications, tested on High Energy Neutron Spectrum unfolding problems, did not materially decrease the operating time as compared to the standard version of SAND-II. Experiments with detector sets were aimed at checking calculated designs for a fusion reactor.

1. Introduction

Neutron spectrometry in the high energy range has to be applied in controlled thermonuclear reactor experiments<sup>1</sup>. At the moment these experiments are aimed at checking calculated designs for a fusion reactor. In the near future this fusion reactor will be based on the deuterium-tritium fusion reaction. Tritium has to be regenerated via neutron induced reactions -the neutrons for which are produced by the fusion reactions- since it cannot be found in large quantities in nature. Since the thermal  ${}^6\text{Li}(n,\alpha)t$  and the threshold  ${}^7\text{Li}(n,\alpha n)t$  reaction are the only neutron induced reactions which offer any promise for tritium breeding, the fusion plasma volume has to be surrounded with a blanket consisting of lithium material. The interaction of the neutrons with the blanket structure is described by the energy- and space-dependent neutron flux density distribution. Via this distribution investigation can be made into the tritium breeding, induced radioactivity and radiation damage of various blanket materials.

At the KFA Jülich a research program on blanket designs has been set up with the construction of a stainless steel cylinder (1.2m outer diameter), filled with lithium metal<sup>2</sup>. Results from calculations and measurements on this model blanket are compared and in this way research can be made into the accuracy of the present nuclear data and the validity of computational models.

(<sup>x</sup> Present adress: PHILIPS Research Laboratories, Eindhoven, Netherlands)

## 2. Experimental procedure<sup>3</sup>

In order to simulate the fusion neutron source in this model blanket, a neutron generator, based on the D-T reaction, is used, the target of which is placed in the centre of the model. In the 90° direction with respect to the deuteron beam the neutrons produced have an energy of about 14.1 MeV.

The most promising method for measurements proved to be the irradiation of activation detectors. From the reaction rates measured neutron spectra can be unfolded with a suitable program, which, however, will need some input information on the neutron spectrum. From several tests for this unfolding the SAND II<sup>4</sup> program was selected, because with this program acceptable output spectra could be calculated, even in the case no extra information in the input spectrum was provided. Due to experimental circumstances spectra will be considered only in the energy range above 2 MeV, after all being the range of importance in fusion reactor experiments.

For the most accurate calculation of the neutron spectra at various positions in the 90° direction the three dimensional Monte Carlo code MORSE is used<sup>5</sup>; in these calculations the ENDF/B-III cross sections for the blanket materials are used.

The measured reaction rates of the activation detectors are compared to those, calculated with the aid of the Monte Carlo neutron spectra, using the most recent cross section data for the activation materials. From the measured values neutron spectra are unfolded with the SAND II program and compared to the calculated spectra.

As for the first aim of the model experiment, checking the present nuclear data and the computational model, it can be stated that in general small differences between measurements and calculations are observed; this may indicate nuclear data of adequate accuracy for the lithium material and a computational model, valid for this study<sup>3,6</sup>.

## 3. Unfolding neutron spectra

The Monte Carlo calculated spectra can thus be considered as reference spectra for the lithium model blanket. The result of the unfolding process -for the 2.0-14.1 MeV energy region- depends on a number of variables:

- the input spectrum;

The best results will be obtained with the use of the most detailed input information. Since the information available is based on calculations with one program, the average of a number of spectra calculated for different positions in the lithium model blanket is used as input spectrum, the so



called "reference blanket spectrum". This might not be the best method to pursue <sup>7</sup>.

- the convergence criterion;

In the studies described here after each iteration step the quantity  $R_i$  is calculated for each activation reaction, denoting the ratio of measured to calculated activity for reaction  $i$ ; the standard deviation of the  $(R_i - 1)$ 's is determined, too. The iteration process is stopped if the change in the standard deviation between two successive steps is less than 1%.

- the number of reaction rates applied and the origin of the cross section data used;
- modifications in the principles of the unfolding procedure or the use of different principles, however, based on the method of iterative adjustment.

Tests in which the latter two points are studied, are the main subject described in this paper.

### 3.1 Testing detector set compositions

For three different positions in the lithium blanket unfolding runs were made with different numbers of measured reaction rates (with a minimum of 6, a maximum of 11 in threshold reaction rates applied); three cross section libraries were tested, viz. the CCC 112B <sup>4</sup>, the LAPENAS <sup>8</sup> and the ENDF/B-IV <sup>9</sup> library. Results of three runs for the position 0.308m (distance from the target) in the lithium model blanket are given in fig. 1.

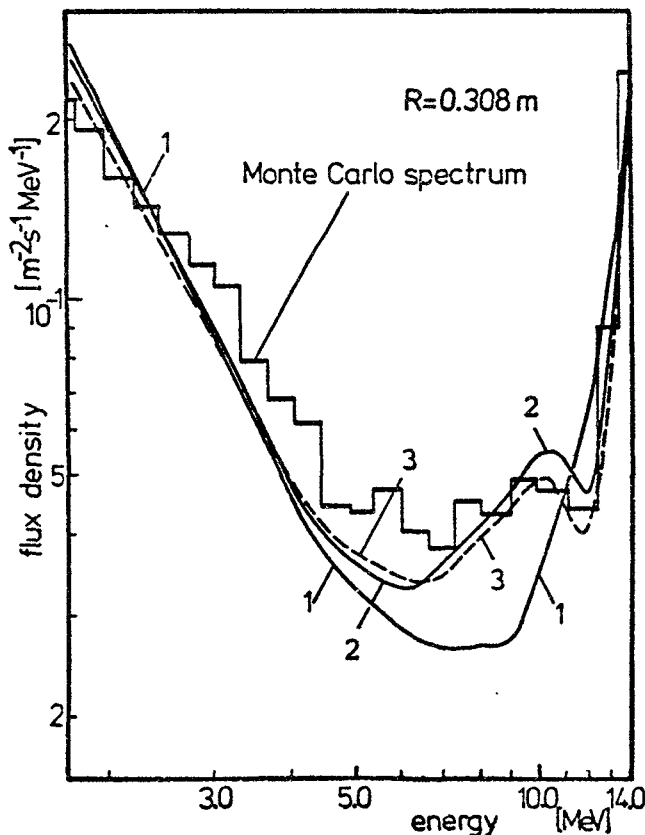


Fig.1 Results of three different unfolding runs for the position 0.308m in the lithium blanket. It concerns an application of the CCC 112B (1) and the ENDF/B-IV and CCC 112B (2 and 3) with the maximum and minimum number of reactions; the Monte Carlo spectrum is also shown

If equal numbers of reaction data out of each library are applied, however, without the  $^{127}\text{I}(n,2n)^{126}\text{I}$  reaction, the numbers of iteration steps for each run have almost equal values. The standard deviations of the output data are smallest when the ENDF/B-IV library is applied, slightly larger values are obtained with the CCC 112B and the LAPENAS file. The deletion of the  $^{127}\text{I}(n,2n)^{126}\text{I}$  reaction does not only improve the value of the standard deviation but also the shape of the unfolded spectrum if compared to the Monte Carlo calculations. When the iodine reaction is used, the characteristic pattern of the reference blanket spectrum at 10-11 MeV is lost during the iteration process, especially when the CCC 112B library is applied (see fig. 1, curve 1).

The results obtained from an application of the CCC 112B, the LAPENAS or the ENDF/B-IV library with 6 measured reaction rates are almost equal in shape (see fig. 1, curves 2 and 3).

As shown in fig. 1, it is obvious that with the application of 6 reaction rates the unfolding yields the best result, compared to the Monte Carlo spectrum. However, it is questionable if the result of the unfolding process with this small number of reactions can be considered as a reliable one. This can be made more clear if the uncertainty in the output spectrum is calculated. A suitable method for calculating this uncertainty is the use of an extended version of the SAND II program, in which version Oster's error analysis<sup>10,7</sup>, based on a Monte Carlo procedure, is applied. In fig. 2 and 3 uncertainties

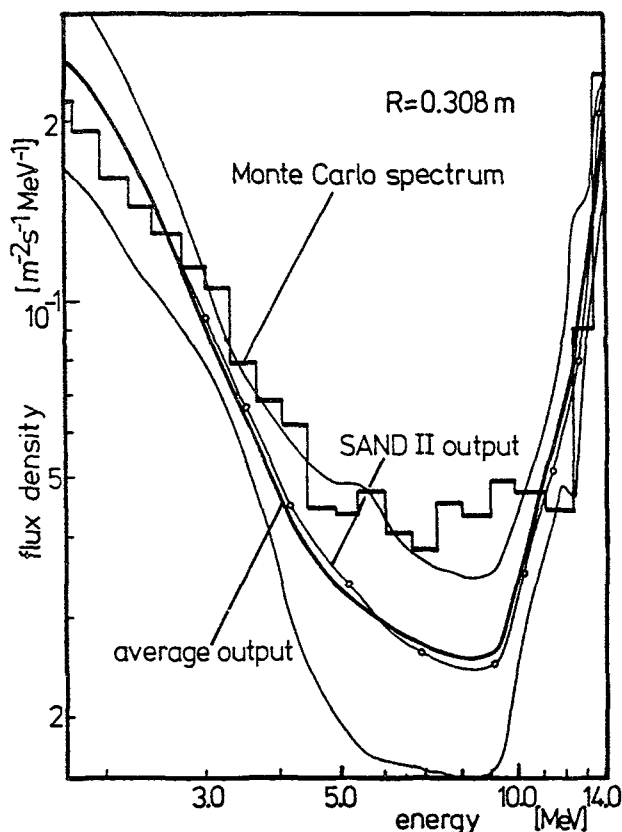


Fig.2 Uncertainties in unfolded spectra; curves are plotted at a distance of two standard deviations from the average output. For this position 0.308m a maximum number of reactions (with  $^{127}\text{I}(n,2n)^{126}\text{I}$ ) is applied (compare fig.1, curve nr.1)

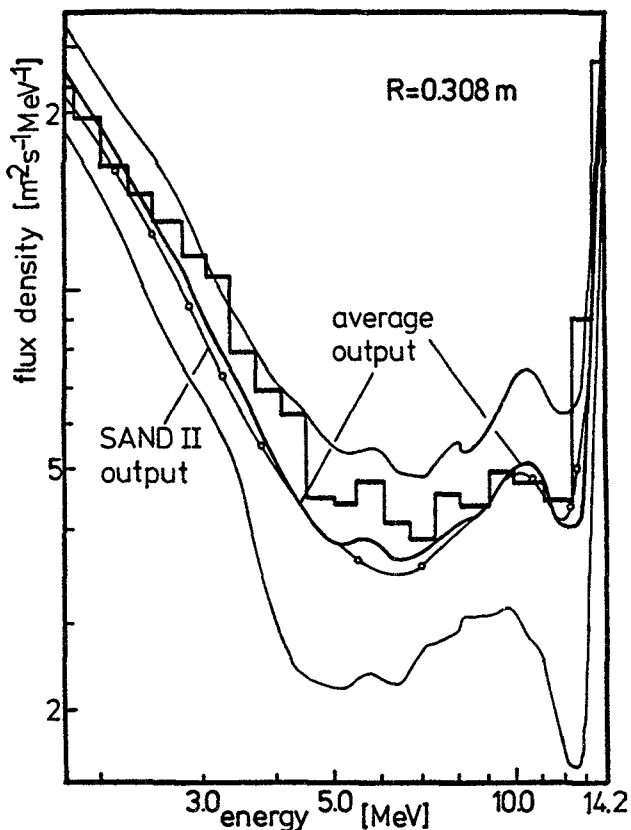


Fig.3 Uncertainties in unfolded spectra; curves are plotted at a distance of two standard deviations from the average output. For this position 0.308m only six reactions are applied (compare fig.1 curve nrs.2 and 3)

for the output spectra are plotted for the cases a maximum number of reactions (with the  $^{127}\text{I}(n,2n)^{126}\text{I}$  reaction) or only six reactions are applied. In the case six reactions are used, the uncertainty in the 7-12 MeV energy region is much larger, which will be due to this smaller number of reactions used and the shape of the neutron spectrum in general. To diminish this uncertainty thus the maximum number of reactions has to be applied.

From the investigation described, it can be concluded that the ENDF/B-IV library, supplemented with data for  $^{24}\text{Mg}(n,p)^{24}\text{Na}$  and  $^{64}\text{Zn}(n,p)^{64}\text{Cu}$  from the LAPENAS and for  $^{63}\text{Cu}(n,2n)^{62}\text{Cu}$  from the CCC 112B library, will deliver the best results for this kind of spectra.

This sort of analysis cannot give detailed information for errors in cross section data or measurements; it can only be a preliminary indication where these might be present. Especially for the iodine reaction cross section data in the CCC 112B library, it can be concluded that errors are probably present there.

### 3.2 Comparison of different unfolding procedures

The SAND II program is one of the most frequently applied unfolding methods and is based on the iterative adjustment principle. After each iteration step a ratio of measured to calculated activity for each reaction applied is determined and weighting factors, denoting the relative contribution of each

reaction in each energy group, are calculated. The flux density in each energy group is modified by a factor, which is the sum of the different ratios of measured to calculated activity, weighted with the factors mentioned above. In the frame of this work it should be studied if the SAND II program is the best one available if the convergence speed or the shape of the output spectrum is taken into consideration. In literature various unfolding codes are described <sup>11,12</sup> in which many iteration steps (100-1000) are required before an acceptable output spectrum is reached. Since in the tests described above the SAND II program proved to be a suitable one for spectrum unfolding in the high energy range, this study is restricted to an investigation of methods by which output spectra, equal or better in shape, are obtained with iteration step numbers of equal magnitudes.

### Aitken extrapolation

By applying the Aitken extrapolation in combination with the SAND II iteration procedure, the iteration process will be speeded up. The Aitken extrapolation is based on the results of three iteration steps from which flux density values for each energy group are calculated <sup>13,15</sup>. The investigation has been carried through by some modifications in the original SAND II program, so that after three iteration steps one extrapolation is performed. All results calculated for the output spectrum with and without extrapolation are thus comparable.

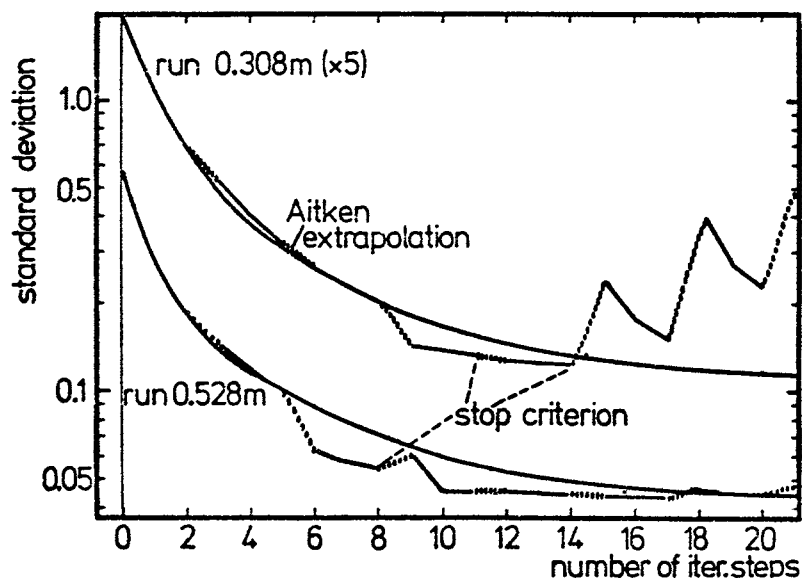


Fig.4 Standard deviations, dependent on the number of iteration steps, in the ratios of measured to calculated activity for two SAND II runs, applying the Aitken extrapolation after every three iteration steps. It concerns one run for the position 0.308m and one for the position 0.528m, with respectively 13 (Monte Carlo) calculated reaction rates and 11 measured ones

This program version has been applied to an iteration run for the position 0.528m in the model blanket with 11 measured reaction rates, using the reference blanket spectrum as input spectrum.

It has also been tested for the position 0.308m with 13 reaction rates, determined via the Monte Carlo calculated spectrum and the ENDF/B-IV / CCC 112B library. As input spectra the reference blanket spectrum and a constant spectrum were used here. In this way differences between SAND II output spectra with and without Aitken extrapolation cannot be caused by inconsistencies in cross sections or measured reaction rates.

The results for the standard deviation of the factors  $(R_i - 1)$  as a function of the iteration step number are shown in fig. 4. In order to compare output spectra a stop criterion has to be used here, so those results are considered as being valid, for which the standard deviation value is decreased. It would namely be possible that the value for the standard deviation remains constant while the shape of the output spectrum is changed in an unrealistic way.

For the run with measured reaction rates comparable results are obtained with and without Aitken extrapolation as long as the standard deviation value is decreased. In the third extrapolation the standard deviation is influenced by the peak character of the spectrum (14 MeV peak is made slightly too high, thus influencing the results for all calculated reaction rates); with the number of extrapolations the shape grows worse and more oscillations occur.

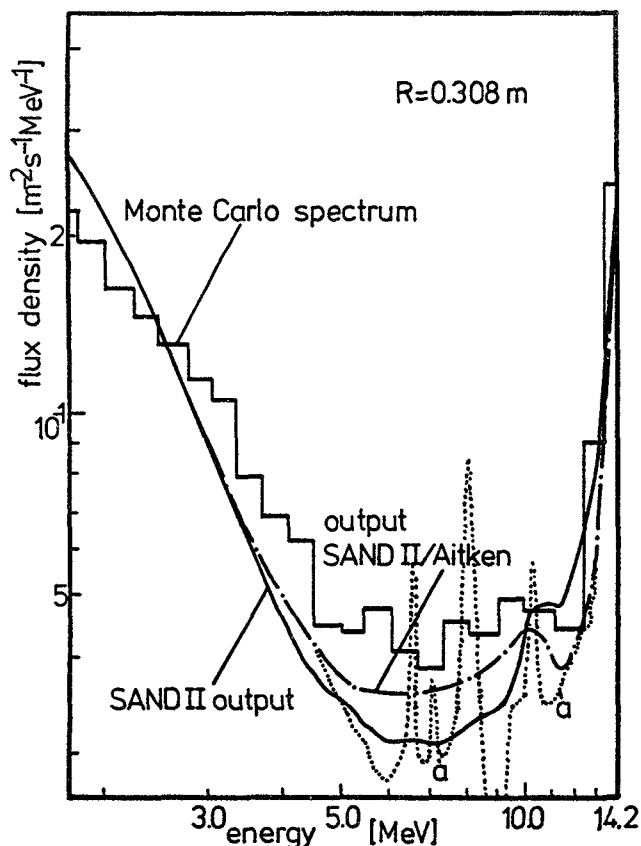


Fig.5 Results of the unfolding process when the Aitken extrapolation is applied. The result shown is for stopping in the first case (given in fig.4). Line a shows the result for increasing standard deviation. The SAND II and the Monte Carlo spectrum are also shown

For the run with calculated reaction rates (input reference blanket spectrum) two output spectra can be considered (see fig.4, stop criterion). The shape of the spectrum first calculated is slightly better, compared to the Monte Carlo spectrum; the second one has a shape, comparable to the SAND II output spectrum. With a further growing number of extrapolations the standard deviation increases strongly and oscillations occur. Results on the shape of the output spectra are given in fig.5. With the constant input spectrum no oscillations occur, however, the shape of the output spectrum is worse compared to the SAND II output.

In general, it can be stated that the iteration process cannot be accelerated appreciably; it is also questionable which spectra should be considered as valid output spectra.

#### Other iterative procedures

A presumably more rapid iterative procedure was proposed by Schmotzer and Levine <sup>14</sup>, who base themselves on a method proposed by Fortney and Levine <sup>12</sup>. For each activation detector a factor for each energy group is calculated. The flux density in each energy group is modified by a number calculated from the sum of these factors, each of them multiplied by an "acceleration" factor. This "acceleration" factor is based on the deviations from unity of the ratios of measured to calculated activity.

This method has been tested with reaction rates measured at the position 0.528m in the model blanket, using the reference blanket spectrum as input

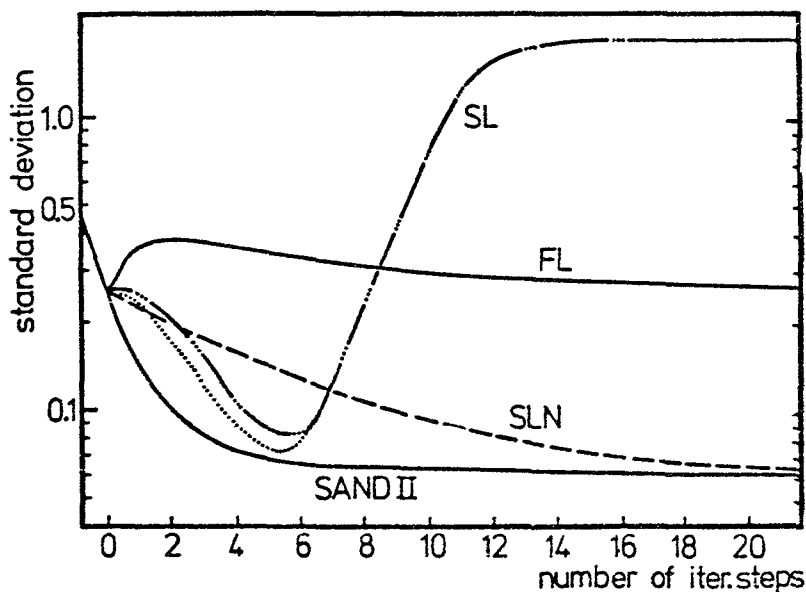


Fig.6 Standard deviations, dependent on the number of iteration steps, for unfolding runs based on the SAND II method (SAND II), the Fortney Levine (FL) and Schmotzer Levine principle (SL, two different acceleration factors) and also the weighted Schmotzer Levine (SLN) iteration process

spectrum and the ENDF/B-IV and CCC 112B cross section libraries. For this run the ITER subroutine of the SAND II program was reprogrammed; results obtained are directly comparable to those calculated with the original SAND II program.

Results for the standard deviations as a function of the iteration step number are given in fig.6.

The original Fortney/Levine method proved to be a very slow one. The application of the Schmotzer/Levine principle resulted in equal output spectra with about the same standard deviation for the factors ( $R_i-1$ ) after a comparable number of iteration steps as can be obtained with the SAND II program. However, after reaching this value the standard deviation increases again, as is shown in fig. 6. A change in the "acceleration" factor slightly modifies the standard deviation in the first iteration steps, however, the overall pattern remains the same. Results for the ratios of measured to calculated activity as a function of the iteration step number for some reactions are shown in fig. 7.

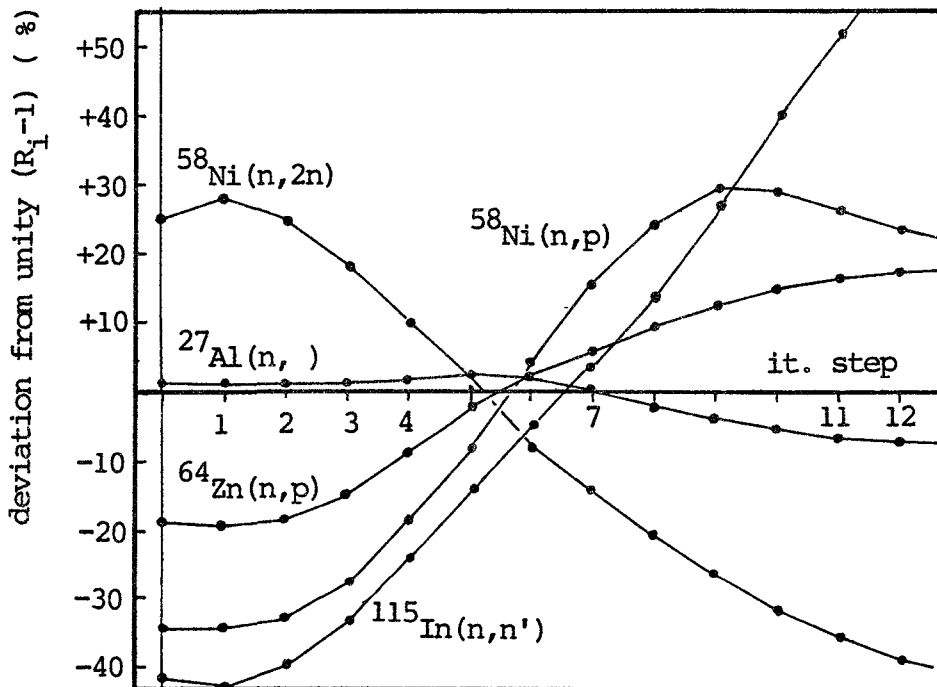


Fig.7 Results for the deviations from unity (%) of the factors  $R_i$  for five threshold detectors as a function of the iteration step number for the Schmotzer Levine unfolding process

In order to avoid a possible influence of the reference blanket spectrum, these runs were repeated with a constant input spectrum. However, no differences in the character of standard deviation values could be observed. The reason for this effect is the fact that the 14 MeV peak is made too high, which is probably due to the non weighted character of the modification factor in the Schmotzer/Levine procedure. This effect was investigated by a reprogram-

ming so that the flux density is modified in the same way as mentioned above, however weighted with the expression for the detector contribution used in this procedure. <sup>7</sup>

Results are also shown in fig. 6. It can be observed that the standard deviation is decreased in a slower way than with the SAND II procedure. However, after 20-25 iteration steps standard deviations of equal magnitude and the output spectra of the same shape are obtained, compared to the case that the iteration process is stopped in the SAND II program (change in standard deviation in two successive steps less than 1%).

Deviation from unity for the factors  $R_i$ , applying the SAND II program or the weighted Schmotzer/Levine method with acceleration factors, based on different numbers, are shown in table I. Only small differences can be observed.

Table I Output characteristics for 11 threshold reactions, when applying the SAND II procedure or the Schmotzer Levine iteration process (with three different acceleration factors) in its weighted version

reaction	SAND II	S/Levine with acc. factor		
		2.2	1.5	—
$^{24}\text{Mg}(n,p)^{24}\text{Na}$	-9.99%	-10.28%	-10.12%	-9.80%
$^{27}\text{Al}(n,\alpha)^{24}\text{Na}$	0.59	0.26	0.45	0.75
$^{27}\text{Al}(n,p)^{27}\text{Mg}$	3.51	3.09	3.07	3.21
$^{56}\text{Fe}(n,p)^{56}\text{Mn}$	-12.00	-12.19	-12.08	-11.88
$^{58}\text{Ni}(n,2n)^{57}\text{Ni}$	-1.71	-0.67	-0.80	-1.26
$^{58}\text{Ni}(n,p)^{58}\text{Co}$	-0.57	-0.66	-0.94	-1.14
$^{59}\text{Co}(n,\alpha)^{56}\text{Mn}$	7.20	7.04	7.21	7.46
$^{63}\text{Cu}(n,2n)^{62}\text{Cu}$	2.60	3.56	3.57	3.36
$^{64}\text{Zn}(n,p)^{64}\text{Cu}$	0.54	-0.65	-0.86	-0.98
$^{115}\text{In}(n,n')^{115}\text{In}$	0.78	-0.09	-0.08	-0.43
$^{127}\text{I}(n,2n)^{126}\text{I}$	10.14	10.41	10.60	10.76
St. deviation	6.50	6.60	6.61	6.60
number of it.steps	8	25	25	25

Not taking into account the acceleration factor, it can be stated that the weighted Schmotzer/Levine procedure has a somewhat more complicated character than the SAND II method, without yielding better results. SAND II should be considered as a more suitable program for all kinds of purposes.



# THE MODIFYING FACTOR IN UNFOLDING

W.L.Zijp, H. C. Rieffle

Stichting Energieonderzoek Centrum Nederland  
Petten, Netherlands

## Abstract:

The algorithm of the SAND-II unfolding program allows the study of the influence of a single detection reaction in adjusting for each energy group the flux density, when the input data for the unfolding process are available.

The components of the modifying factor are considered. Some preliminary experience is presented.

In neutron spectrum unfolding procedures one has a set of equations of the following type:

$$\alpha_i = \int_0^{\infty} \sigma_i(E) \cdot \phi_E(E) \cdot dE \quad (\text{for } i = 1, 2, \dots, n)$$

where  $\alpha_i$  denotes the measured saturation activity per target nucleus;  $\sigma_i(E)$  the energy dependent activation cross section;  $\phi_E(E)$  the flux density per unit energy interval, and  $n$  the number of detectors.

The unfolding calculations were performed in 620 energy groups.

Let  $i$  denote the activation reaction,  $j$  the energy group and  $k$  the iteration step. For each activation foil the SAND-II program calculates a quantity  $R_i$ , the ratio of the measured and the calculated activity for detector  $i$ .

$$\alpha_i^c = \sum_{j=1}^m \sigma_{ij} \cdot \phi_j^{(k)}$$
$$R_i^{(k)} = \alpha_i^m / \alpha_i^c$$

The modification of the spectrum proceeds as follows:

$$\phi_j^{(k+1)} = M_j^{(k)} \cdot \phi_j^{(k)}$$

where the modification factor  $M_j^{(k)}$  is defined by the relation:

$$\ln M_j^k = \frac{\sum_{i=1}^n W_{ij}^{(k)} \cdot \ln R_i^k}{\sum_{i=1}^n W_{ij}^{(k)}}$$

where the weighting  $W_{ij}^k$  is defined by the expression:

$$W_{ij}^{(k)} = \sigma_{ij} \cdot \phi_j^{(k)} / \sum_{j=1}^m \sigma_{ij} \cdot \phi_j^{(k)}$$

The modifying factor can be written as:

$$M_j^{(k)} = \exp \left\{ \sum_{i=1}^n W_{ij}^{(k)} \cdot \ln R_i^{(k)} / \sum_{i=1}^n W_{ij}^{(k)} \right\}$$

or:

$$M_j^{(k)} = \prod_{i=1}^n \{R_i^{(k)}\}^{W_{ij} / \sum_{i=1}^n W_{ij}} = \prod_{i=1}^n M_{ij}^{(k)}$$

One therefore may say, that the modifying factor for the j-th energy group and the k-th iteration step can be considered as the weighted harmonic mean of the ratios of measured and calculated activities, where the average is taken over all detection reactions.

The change for group j is mainly determined by that reaction, which has the largest influence on  $M_j^{(k)}$ .

Consider now the modifying factor for a separate detector i:

$$M_{ij}^{(k)} = \{R_i^{(k)}\}^{W_{ij} / \sum_{i=1}^n W_{ij}} = \left( \frac{\alpha_i^m}{\alpha_i^c} \right)^{W_{ij} / \sum_{i=1}^n W_{ij}}$$

This factor will differ much from 1 in two circumstances:

- $\alpha_i^c$  deviates strongly from  $\alpha_i^m$ ;
- the response  $W_{ij}$  is relatively large.

Note that by definition of  $W_{ij}$  one has:

$$\sum_{j=1}^m W_{ij}^{(k)} = 1$$

One can now make a rough scheme of the conditions where the response  $W_{ij}$  may become important.

spectrum	reaction type	eV region	keV region	MeV region
thermal reactor spectrum	capture	+ +	+ / o	-
	threshold	-	-	+ +
fast reactor spectrum	capture	o	+ +	+
	threshold	-	-	+ +

where:

- ++ denotes appreciable response;
- + denotes good response;
- o denotes moderate response;
- no or little response.

We have made an extension to our version of the SAND-II program, by which it is possible to plot for all reactions the modifying factor as function of the energy, by calculating the group values for  $M_{ij}^{(k)}$ .

We have plotted the modifying factors for the first iteration step, since in that case one was interested in the tendencies for changing the input spectrum.

The plots for the spectra of STEK-4000, CFRMF,  $\Sigma\Sigma$  and LFR show that the threshold reactions have, as expected, only influence in the MeV region. All non-threshold reactions have large influence on the intermediate energy region (say between 1 eV and 100 keV).

Looking at the pictures for cases with and without the  $\text{In}(n,n')$  reaction (i.e. the reaction with the lowest threshold in the detector set used) one can observe that the influence of non-threshold reactions extends to the lowest threshold energy for all threshold reactions which indicate modifications.

Remark: This lowest threshold is often that of the  $\text{In}(n,n')$  reaction, except for the  $\Sigma\Sigma$  case, where the reaction  $^{232}\text{Th}(n,f)$  has the lowest threshold (1.1 MeV).

#### The STEK-4000 spectrum (figure 1):

Here we observe for  $k=1$  that all non-threshold reactions systematically indicate, that the input spectrum has to be lowered in the intermediate energy region, in order to arrive at a better consistency between measured and calculated reaction rates.

Furthermore all threshold reactions tend to increase the input spectrum in the MeV region. These tendencies indicate clearly that the input spectrum for STEK-4000 requires modification towards larger contributions in the higher energy region.

#### The CFRMF spectrum (figure 2):

In the resonance region one can observe two rather strong opposite tendencies:  $^{59}\text{Co}(n,\gamma)$  tries to increase the spectrum, while  $^{238}\text{U}(n,\gamma)$  tries to decrease the spectrum.

The modifying factor for the  $^{59}\text{Co}(n,\gamma)$  reaction is roughly 1.4. In the next iteration ( $k=2$ ) this value is much lower: 1.10, while the  $^{238}\text{U}(n,\gamma)$  indication remained the same. This effect is not yet fully understood.

The  $\Sigma\Sigma$  spectrum (figure 3):

Remarkable is here the pattern for  $^{115}\text{In}(n,\gamma)$  which shows for lower energies a negative tendency. Only  $^{197}\text{Au}(n,\gamma)$  tries to modify in a positive way. After the first iteration these two reactions still show opposite tendencies.

The LFR spectrum (figure 4):

In this case several reactions have been applied with and without cadmium cover. By application of a cadmium cover one decreases the total response, but obtains from a smaller response more pronounced information at somewhat higher energies. This is most clearly demonstrated by the  $^{55}\text{Mn}(n,\gamma)$  and the  $^{239}\text{Pu}(n,\gamma)$  reactions.

The reactions  $^{115}\text{In}(n,\gamma)$  and  $^{239}\text{Pu}(n,\gamma)$  should not be applied inside a cadmium cover, because the lowest resonance peaks are too close to the cadmium cut-off, and the model for the calculation of the cadmium cover correction can not take this into account accurately enough.

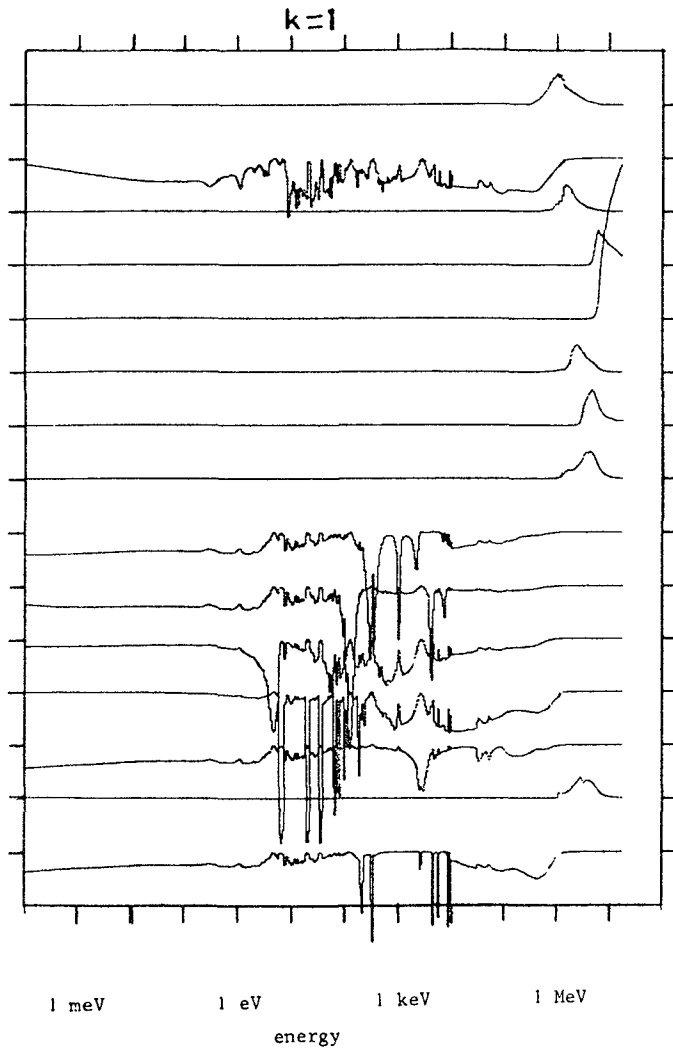
Figure 5 shows the responses of all bare detectors, deleting at the input all reaction rates obtained under a cadmium cover. Remarkable is the fact that above the cadmium cut-off such relatively large modification factors are obtained for the  $(n,\gamma)$  reactions. There seems to be a rather small tendency for decreasing the spectrum in the energy range from 10 eV to 10 keV. The threshold reactions tend to increase the spectrum above 0.7 MeV.

Coming back to the figure 4, which shows also results for some threshold reactions irradiated under cadmium cover, one observes that high threshold reactions give indication for lowering the spectrum.

This holds for  $^{27}\text{Al}(n,p)$  with  $E_{\text{eff}} = 4.7$  MeV;  $^{56}\text{Fe}(n,p)$   $^{56}\text{Mn}$  with  $E_{\text{eff}} = 6.0$  MeV;  $^{27}\text{Al}(n,\alpha)^{24}\text{Na}$  with  $E_{\text{eff}} = 7.2$  MeV; and  $^{48}\text{Ti}(n,p)$   $^{48}\text{Sc}$  with  $E_{\text{eff}} = 7.6$  MeV.

# STEK

155



- 115 In (n,n') 115 In m
- 235 U (n,f) FP
- 238 U (n,f) FP
- 56 Fe (n,p) 56 Mn
- 48 Ti (n,p) 48 Sc
- 47 Ti (n,p) 47 Sc
- Ti (n,x) 46 Sc
- 54 Fe (n,p) 54 Mn
- 55 Mn (n, $\gamma$ ) 56 Mn
- 59 Co (n, $\gamma$ ) 60 Co
- 197 Au (n, $\gamma$ ) 198 Au
- 238 U (n, $\gamma$ ) 239 U
- 23 Na (n, $\gamma$ ) 24 Na
- 58 Ni (n,p) 58 Co
- 58 Fe (n, $\gamma$ ) 59 Fe

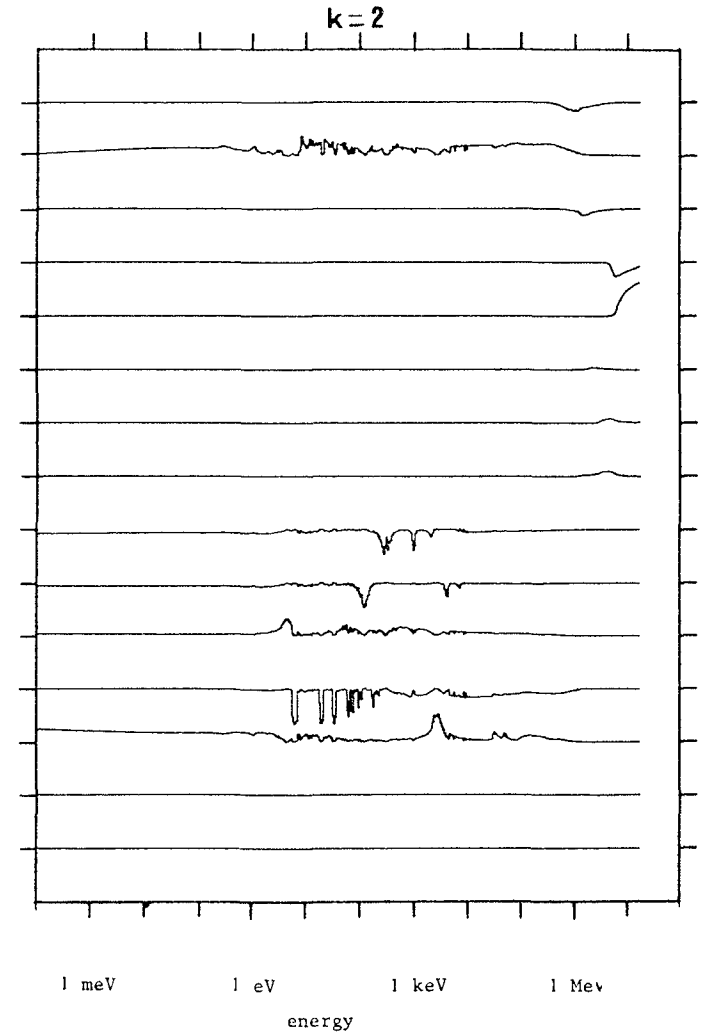
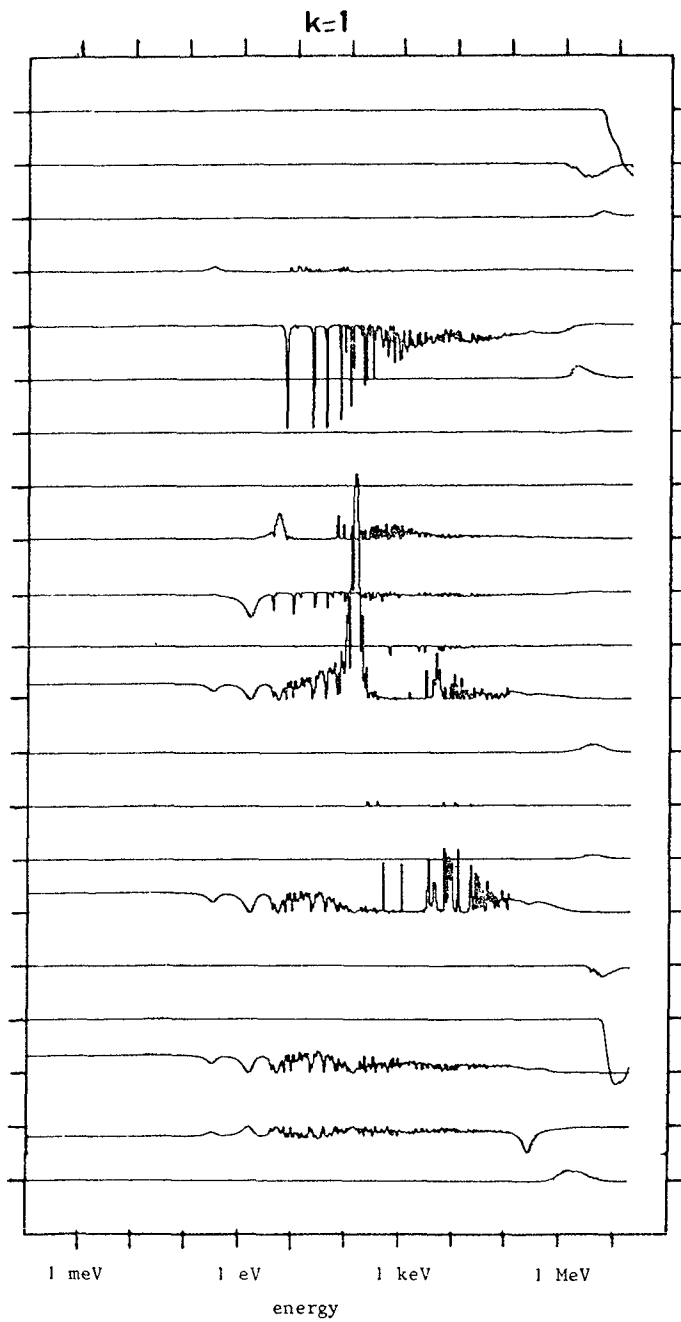
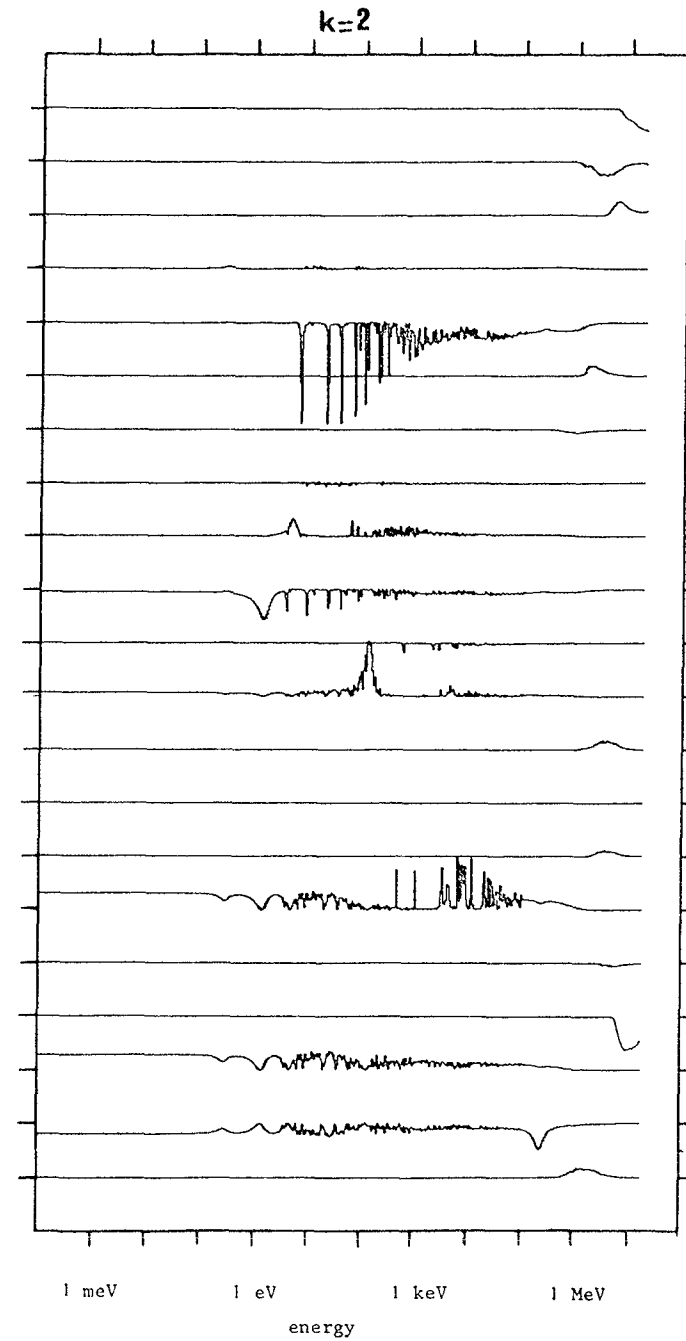


fig.1



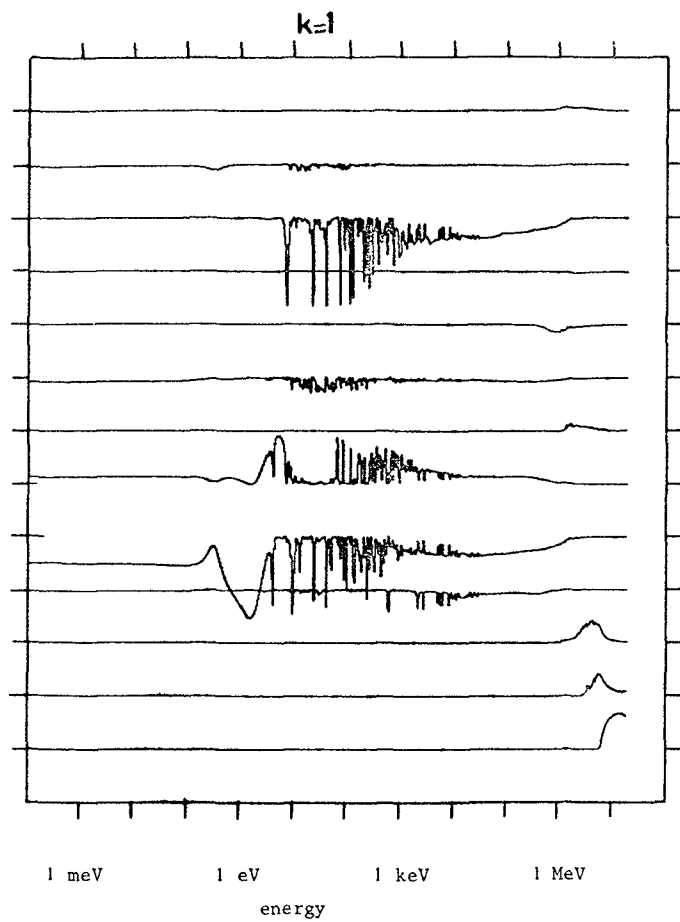
- CFRNF**
- 48 Ti (n,p) 48 Sc
  - 47 Ti (n,p) 47 Sc
  - Ti (n,x) 46 Sc
  - 239 Pu (n,f) FP
  - 238 U (n,γ) 239 U
  - 238 U (n,f) FP
  - 237 Np (n,f) FP
  - 235 U (n,f) FP
  - 197 Au (n,γ) 198 Au
  - 115 In (n,γ) 116 In m
  - 63 Cu (n,γ) 64 Cu
  - 59 Co (n,γ) 60 Co
  - 58 Ni (n,p) 58 Co
  - 58 Fe (n,γ) 59 Fe
  - 54 Fe (n,p) 54 Mn
  - 45 Sc (n,γ) 46 Sc
  - 27 Al (n,p) 27 Mg
  - 27 Al (n,α) 24 Na
  - 10B (n,α) total He
  - 6Li (n,α) total He
  - 115 In (n,n') 115 In m

fig.2



$\Sigma \Sigma$

157



- 115 In (n,n') 115 In m
- 239 Pu (n,f) FP
- 238 U (n, $\gamma$ ) 239 U
- 238 U (n,f) FP
- 237 Np (n,f) FP
- 235 U (n,f) FP
- 232Th (n,f) FP**
- 197 Au (n, $\gamma$ ) 198 Au
- 115 In (n, $\gamma$ ) 116 In m
- 63 Cu (n, $\gamma$ ) 64 Cu
- 58 Ni (n,p) 58 Co
- 27 Al (n,p) 27 Mg
- 27 Al (n, $\alpha$ ) 24 Na

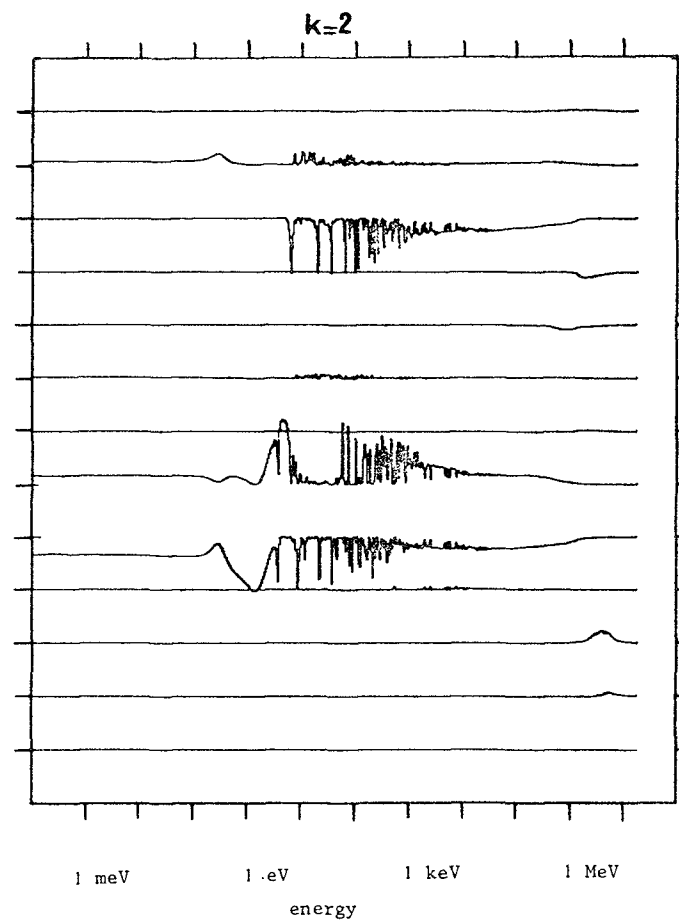
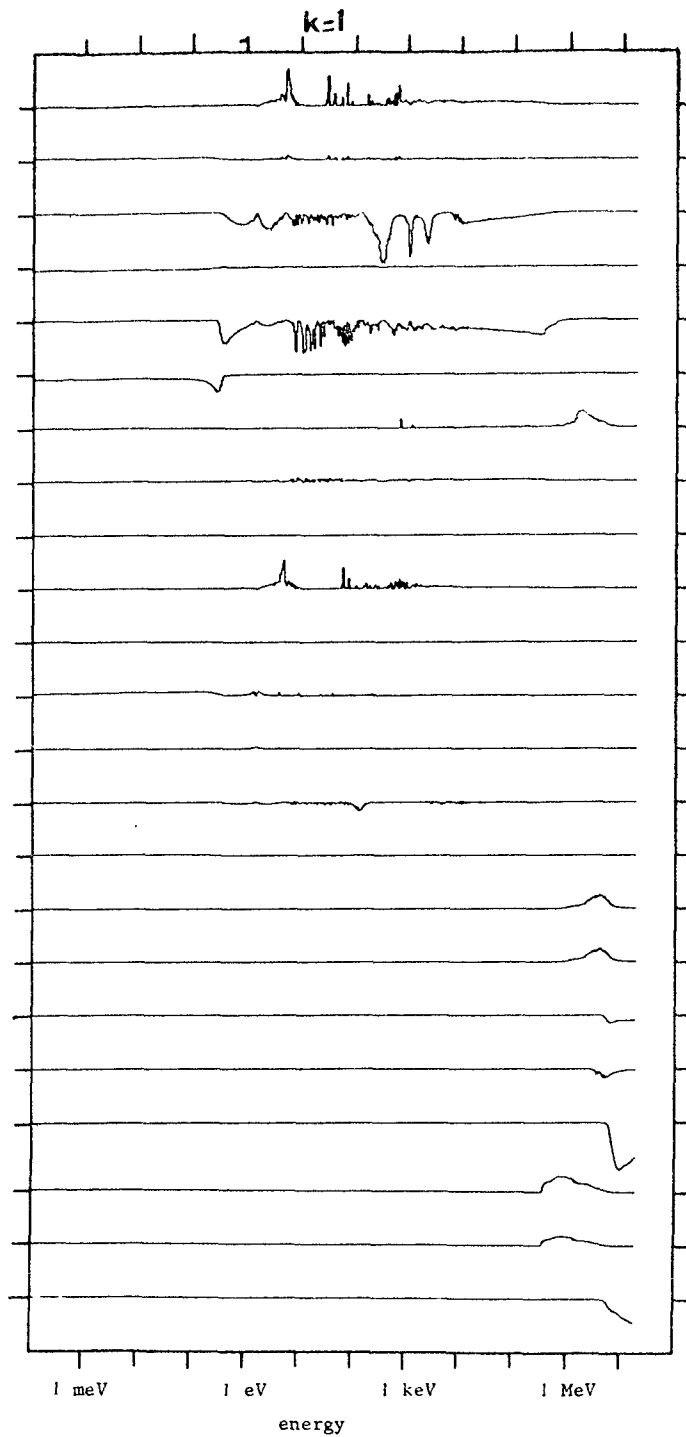


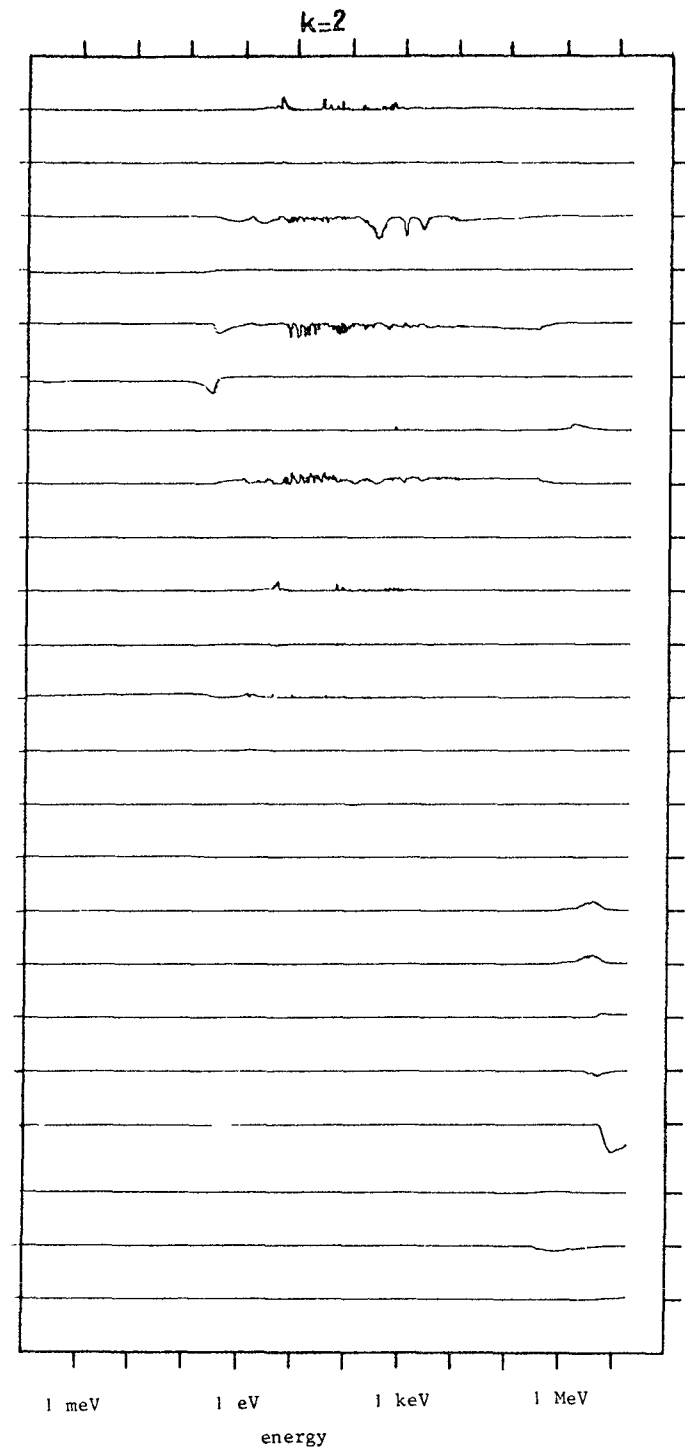
fig.3



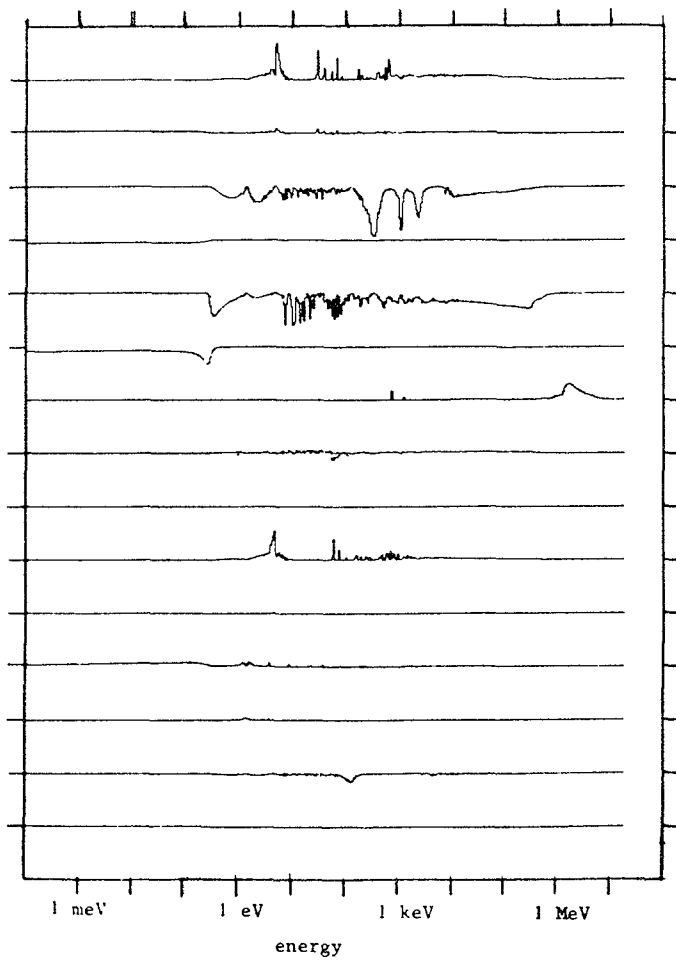
**LFB**

- 109 Ag (n, $\gamma$ ) 110 Ag m
- 109 Ag (n, $\gamma$ ) 110 Ag m
- 55 Mn (n, $\gamma$ ) 56 Mn
- 55 Mn (n, $\gamma$ ) 56 Mn
- 239 Pu (n,f) FP
- 239 Pu (n,f) FP
- 238 U (n,f) FP
- 235 U (n,f) FP
- 235 U (n,f) FP
- 197 Au (n, $\gamma$ ) 198 Au
- 197 Au (n, $\gamma$ ) 198 Au
- 115 In (n, $\gamma$ ) 116 In m
- 115 In (n, $\gamma$ ) 116 In m
- 59 Co (n, $\gamma$ ) 60 Co
- 59 Co (n, $\gamma$ ) 60 Co
- 58 Ni (n,p) 58 Co
- 58 Ni (n,p) 58 Co
- 56 Fe (n,p) 56 Mn
- 27 Al (n,p) 27 Mg
- 27 Al (n, $\alpha$ ) 24 Na
- 115 In (n,n') 115 In m
- 115 In (n,n') 115 In m
- 48 Ti (n,p) 48 Sc

fig.4







**LFR**

- 115 In (n,n') 115 In m
- 109 Ag (n,γ) 110 Ag m in Cd
- 109 Ag (n,γ) 110 Ag m
- 55 Mn (n,γ) 56 Mn in Cd
- 55 Mn (n,γ) 56 Mn
- 239 Pu (n,f) FP in Cd
- 239 Pu (n,f) FP
- 238 U (n,f) FP
- 235 U (n,f) FP in Cd
- 235 U (n,f) FP
- 197 Au (n,γ) 198 Au in Cd
- 197 Au (n,γ) 198 Au
- 115 In (n,γ) 116 In m in Cd
- 115 In (n,γ) 116 In m
- 59 Co (n,γ) 60 Co in Cd
- 59 Co (n,γ) 60 Co

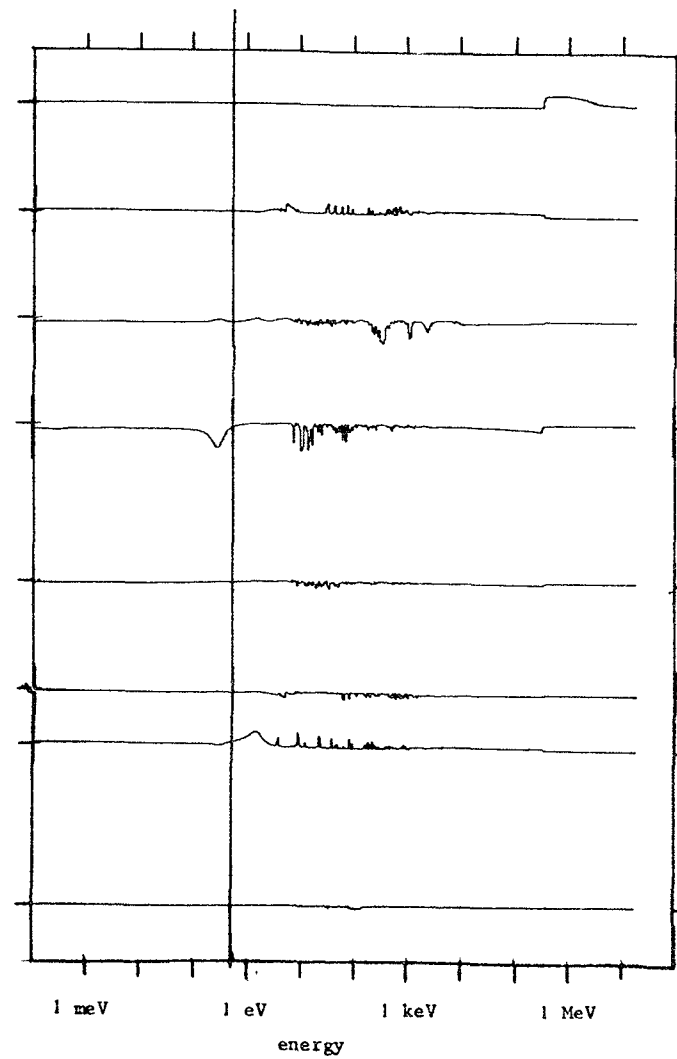


fig.5

## THE CERTAINTY PARAMETER IN UNFOLDING

W.L. Zijp, H.C. Rieffle

Stichting Energieonderzoek Centrum Nederland  
Petten, Netherlands.

### Abstract:

A new parameter is studied which gives the relative change in the sum of squares of deviation for a relative change in the group flux density. Large values for this certainty parameter indicate close bounds for the solution spectrum. Small or zero values indicate that for those regions large variations in the solution have little or no effect on the sum of squares, so that wide margins in the solutions are allowed. The parameter can in principle be applied to all unfolding programs.

In neutron spectrum unfolding procedures one has a set of equations of the following type:

$$\alpha_i = \int_0^{\infty} \sigma_i(E) \cdot \phi_E(E) \cdot dE \quad (\text{for } i = 1, 2, \dots, n)$$

where  $\alpha_i$  denotes the measured saturation activity per target nucleus;  $\sigma_i(E)$  the energy dependent activation cross sections, and  $\phi_E(E)$  the flux density per unit energy interval, and  $n$  the number of detectors.

When applying this unfolding process computer programs like SAND-II, RFSP-JÜL and CRYSTAL BALL one has to provide the following input information:

1. experimental reaction rates;
2. differential cross section data;
3. an input spectrum representing the best available knowledge on the spectrum.

The quality of the output spectrum can be considered from different points of view:

- the variations in the output spectrum, corresponding to the experimental errors in the input activities;
- the variations in the output spectrum, corresponding to the uncertainties in the cross section data;
- the variations in the output spectrum, resulting from different choices for the input spectrum;

- the improvement ratio  $|I|$ , defined as the ratio of the coefficient of variation of the input spectra, and the coefficient of variation of the corresponding output spectra.

At present we are considering the merits of a new parameter defined by the expression:

$$\gamma_j = - \frac{dS}{d\phi_j} / \frac{S}{\phi_j}$$

where  $S$  is the sum of the squares of the deviations in the reaction rates.

$$S = \sum_{i=1}^n g_i \{ (\alpha_i^m - \alpha_i^c) / \alpha_i^m \}^2$$

where the weights  $g_i$  should preferably be taken inversely proportional to the variance in the measured activities.

In these expressions the following subscripts are used:

- j to indicate the energy group;
- m to indicate the measured value;
- c to indicate the calculated value.

The sign of  $\gamma_j$  is the same as the sign for infinitesimal changes in  $\phi_j$ , which tend to decrease the value of  $S$ .

The size for  $\gamma_j$  indicates how strong the effect on  $S$  is of a small change in  $\phi_j$ . Large values of  $\gamma_j$  indicate a small variability (i.e. a strong certainty) of the value for  $\phi_j$ , while small values of  $\gamma_j$  indicate a large variability (i.e. a small certainty) for  $\gamma_j$ .

Note that  $S$  not necessarily is equal to the minimum value for the sum of squares of deviations, since the various unfolding programs have different algorithms.

The certainty parameter  $\gamma_j$  can in principle be defined for all available unfolding programs. However, the program SAND-II does not require values for the errors in the measured activities. In such cases one has to take the weights equal to 1.

The position of the extremes in the plot of this certainty parameter as function of energy seems often to correspond with the peaks in the curve of the improvement ratio. This is shown in figure

There are indications that the  $\gamma(E)$  curve should have roughly the same pattern as the curve for the modifying factor  $\phi_{out}(E)/\phi_{in}(E)$ .

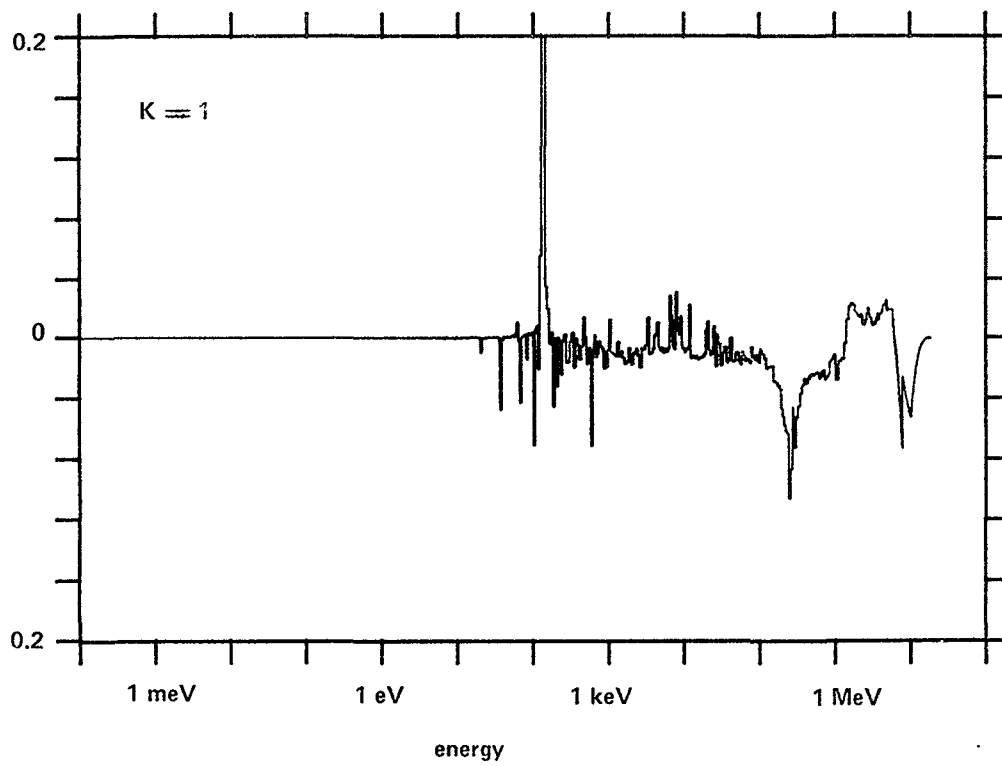
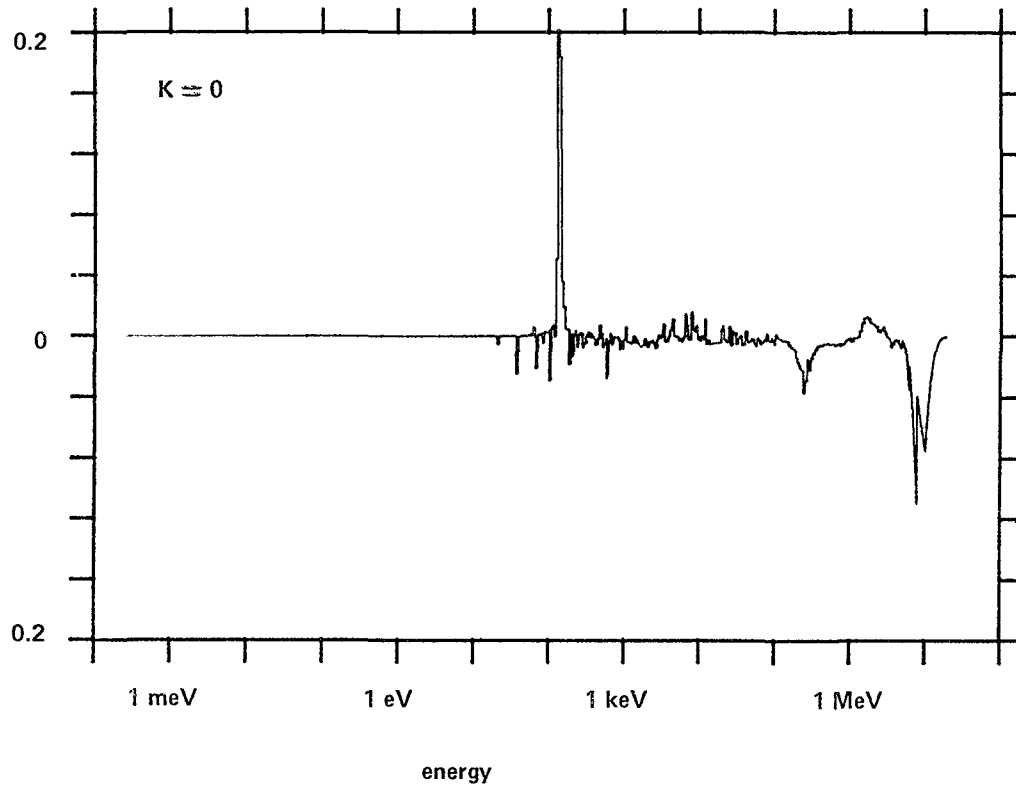


Fig. 1. CERTAINTY PARAMETER FOR CFRMF SPECTRUM.

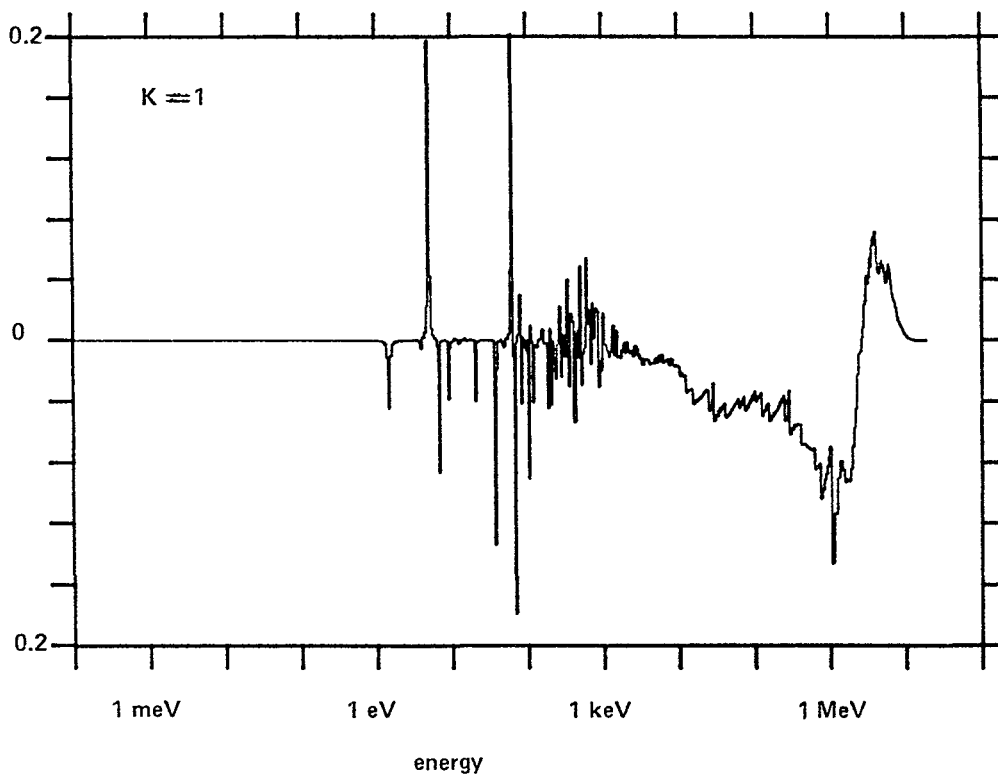
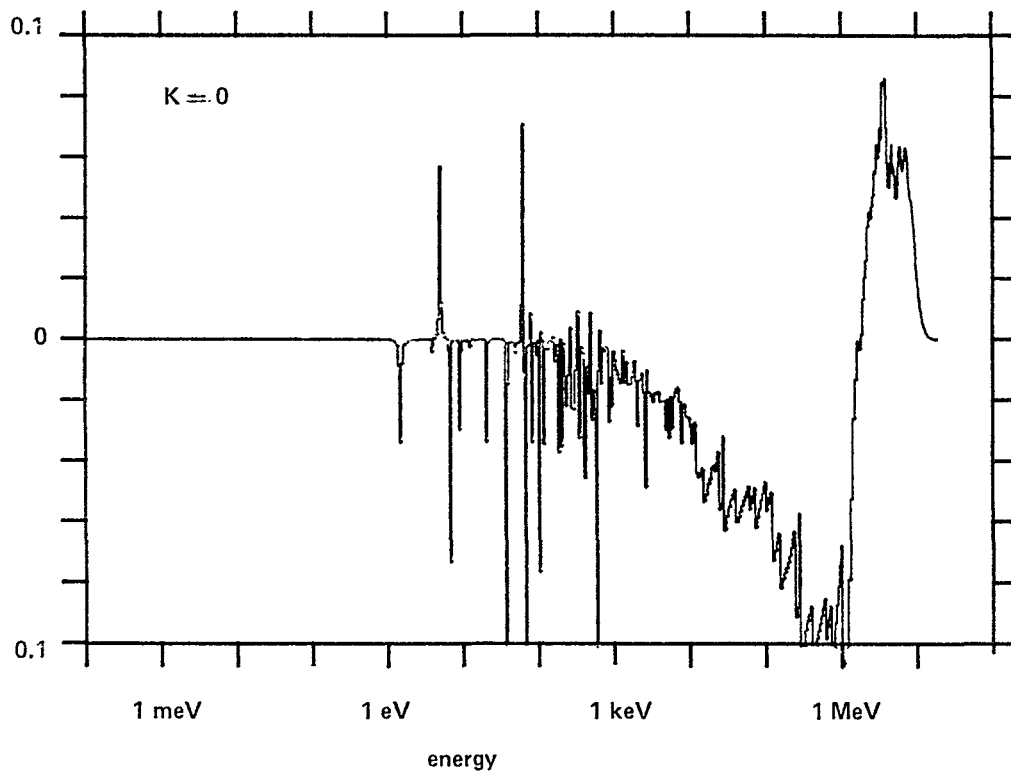


Fig. 2. CERTAINTY PARAMETER FOR SIGMA-SIGMA SPECTRUM.

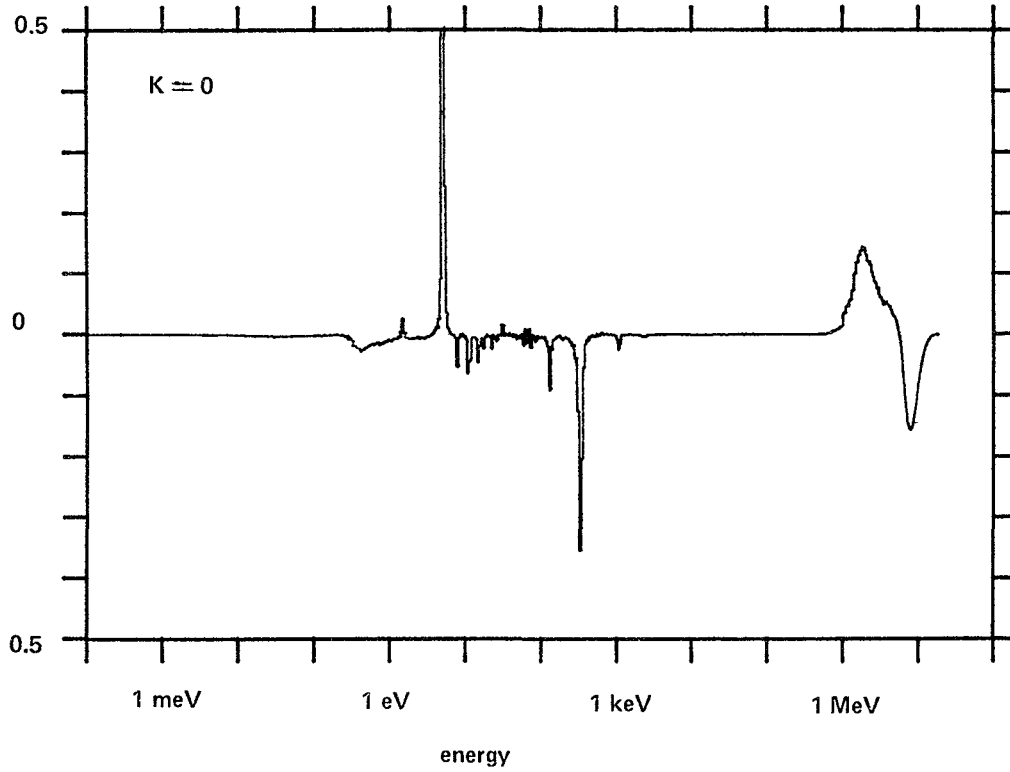


Fig. 3. CERTAINTY PARAMETER FOR LFR-VC SPECTRUM.

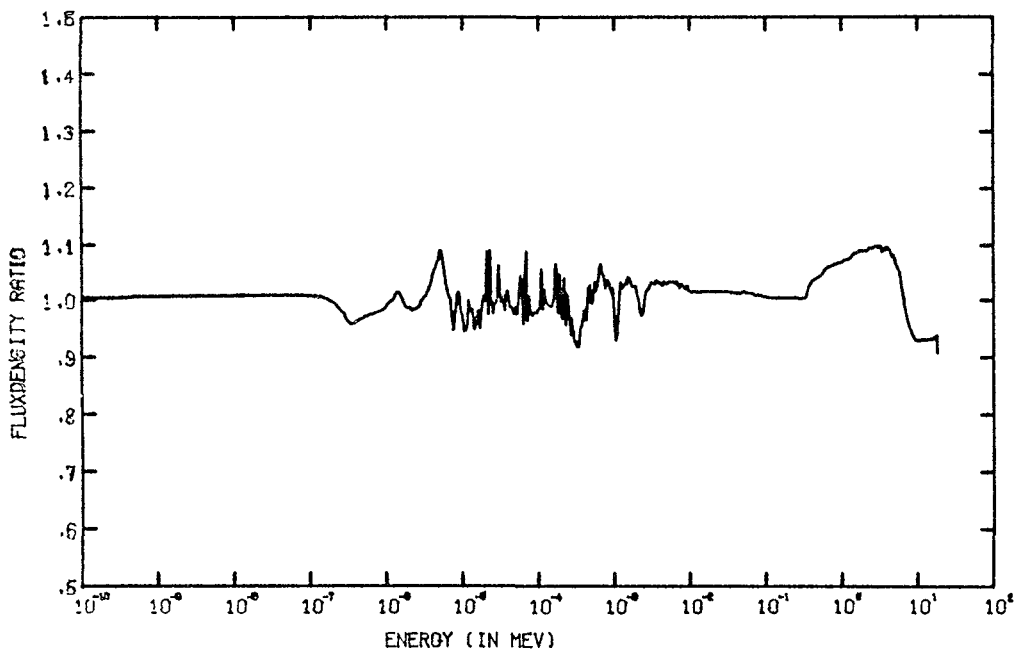


Fig. 4. RATIO  $\phi_{out} / \phi_{in}$  FOR LFR-VC SPECTRUM.

Reference:

- [1] Zijp, W.L.: "Review of activation methods for the determination of neutron flux density spectra"  
Report RCN-241 (Reactor Centrum Nederland, Petten, 1976).  
Also published in Proc. 1st ASTM-Euratom Symposium on Reactor Dosimetry, held in Petten, September 22-26, 1975.  
Report EUR 5667 e/f, Part I, p. 233 (CEC, Luxembourg, 1977).

## ERRORS IN DAMAGE FUNCTION ANALYSIS

W.R. Burrus

Tennecomp Systems  
Oak Ridge, Tenn. 37830, U.S.A.

### Short communication

A central problem in understanding propagation of errors in radiation change experimentation is in dealing with underdetermined linear relations of the form  $Ax = b$ , where  $A$  is a known matrix (possibly singular),  $x$  is an unknown vector, and  $b$  is vector of observation (with, say, an estimated variance matrix  $V(b)$ ).

If one has a good estimate  $x^0$  of  $x$  and an estimate of the variance matrix  $V(x^0)$  which describes the uncertainty of  $x^0$ , then it is easy to show that the standard least squares solution of

$$\begin{pmatrix} A \\ I \end{pmatrix} x = \begin{pmatrix} b \\ x^0 \end{pmatrix} \quad V \begin{pmatrix} b \\ x^0 \end{pmatrix} = \begin{pmatrix} V(b) & 0 \\ 0 & V(x^0) \end{pmatrix} \quad (1)$$

gives a solution consisting of  $\tilde{x}$  and  $V(\tilde{x})$ .

It is easy to extend the standard least squares solution to include correlated errors in the matrix  $A$ . One simply adds  $E(\tilde{x}_t^0 \tilde{A}_t \tilde{x}_t^0)$  to  $V(b)$  (2) above. Note that (1) can always be easily solved numerically if determinate  $[V(x^0)] \neq 0$  where  $E$  is the "expectation" or mean of its operand. If  $x^0$  is a "good" estimate, then it is valid to use "small error approximation" and drop higher order terms.

The problem with this approach is that the determinants of the required  $x^0$  and  $V(x^0)$  is subjective. It is shown by means of several simple examples that no subjective input is really necessary to get valid limits to fluence for radiation damage; (for example, the non-negativity of both the neutron spectrum and the damage sensitivity function is all that is needed).

The so-called "mild perturbation" methods (SAND being an example) take a more liberal view toward characterizing a priori information by expressing the solution  $x$  as

$$x = \alpha x^0 + z$$

where  $\alpha$  is a normalization constant to be determined as part of the problem, and  $z$  is the "small perturbation" which is "small" compared to  $x$ . It is easy



to generalize ordinary least squares to take into account the constant normalization, but it is a vital difference in viewpoint which is important.

The constant  $\alpha$  is a "critical" difference between the classical "least squares" method and the "mild perturbation" method, in that it represents a distinctly different viewpoint as to a priori information. Actually, the mathematical techniques of both approaches (although often applied inconsistently) are essentially equivalent and reasonably well understood by the more informed proponents of both viewpoints.

Another approach to a priori information is the use of convex combination of "catalog members" and is an extension to the very conservative technique of applying "non-negativity" constraints on window functions.

## THE QUADRUPLE TECHNIQUE

W.L. Zijp, H.J. Nolthenius, N.J.C.M. van der Borg

Stichting Energieonderzoek Centrum Nederland  
Petten, Netherlands.

### Abstract:

The quadruplet technique, comprising the irradiation of a triple foil (or "sandwich") in combination with a single foil with the same thickness, can yield a better response than the triple foil technique. In principle the quadruplet method can improve the sensitivity in neutron spectrum unfolding by means of activation detector responses. The computer program SELFS which can determine group cross section values, modified for selfshielding in the SAND-II 620 group structure, has been extended to allow application of the quadruple foil technique.

### 1. INTRODUCTION

The quadruple foil technique comprises the irradiation of a set of three foils (the triple foil) of the same material, radius and thickness, and a fourth foil of the same material and dimensions.

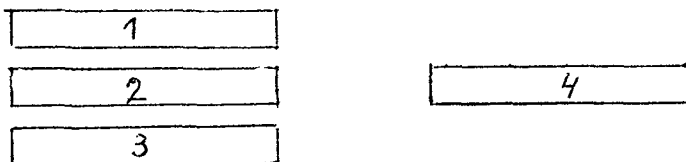
The irradiation of the triple foil and the single foil can occur simultaneously, but then they cannot be irradiated at exactly the same spot and the single foil should be positioned in such a way that its activation is not influenced by the flux density depression around the triple foil and the other way around.

Any gradient in the flux density should be corrected for, while a spectrum gradient is not allowed. An alternative approach is to irradiate the triple foil and the single foil at the same location, but in different irradiations at well-known reactor power.

With the triple foil technique one measures the ratio of the average activity of the outer foils over that of the activity of the inner foil. With the quadruple foil technique one can obtain much larger differences between the activity of the single foil and the inner foil of the triplet.

Some experience has been obtained with the quadruplet technique applied to neutron spectrum determinations, using spectrum unfolding programs with the SAND-II 620 groups structure. The cover effect and the selfshielding effect in the foil were taken into account using an extension of the selfshielding program SELFS |1|.

## 2. NOTATION



$k$  = index for foil ( $k=1, \dots, 4$ );

$\alpha_k$  = saturation activity of product nuclide in foil  $k$  per target atom;

$\sigma_j$  = activation cross section for group  $j$ ;

$\sigma_j^{\text{tot}}$  = total cross section for group  $j$ ;

$t$  = thickness of foil;

$N_v$  = number of target atoms per unit volume;

$\tau_j = N_v \cdot \sigma_j^{\text{tot}} \cdot t$  = dimensionless thickness parameter, important for self-shielding calculations;

$G_k(\tau_j)$  = selfshielding factor for foil  $k$ , for neutrons in energy group  $j$ .

Since only one detector material will be considered here, it is not necessary to use a subscript to indicate the type of detector material.

## 3. ACTIVATION OF FOILS

### 3.1. Single foil

The activity of a single foil can be written as:

$$\alpha = \sum_{j=1}^{620} \sigma_j \cdot \phi_j \cdot G(\tau_j)$$

### 3.2. Triple foil technique

In thermal neutron environments the triple foil is enclosed in a cadmium cover. In a fast neutron reactor spectrum the cadmium cover can be deleted. The triple foil technique is based on the determination of the difference between the average activity of the outer foils and the activity of the inner foil.

When the foils constituting the triplet have the same thickness one can derive the relations:

$$\alpha_1 = \sum_{j=1}^{620} \sigma_j \cdot \phi_j \left\{ \frac{1}{2}G(\tau_j) - G(2\tau_j) + \frac{3}{2}G(3\tau_j) \right\}$$

$$\alpha_2 = \sum_{j=1}^{620} \sigma_j \cdot \phi_j \left\{ \frac{3}{2}G(3\tau_j) - 3G(2\tau_j) + \frac{3}{2}G(\tau_j) \right\}$$

Therefore the selfshielding factor to be applied for the difference between foil (1) and foil (2) in the triple foil technique, when the foils are equally thick, is:

$$G_{\text{triplet}} = G_{1-2}(\tau_j) = \frac{3}{2} G(3\tau_j) - 3G(2\tau_j) + \frac{3}{2} G(\tau_j)$$

### 3.3. Quadruple foil technique

In the quadruple foil technique one irradiates one cadmium covered foil and one cadmium covered triple foil of the same material for the (n,γ) detection reaction of interest. In fast neutron spectra one may delete the cadmium cover.

The principle is that one subtracts the activity of the inner foil (2) of the triplet from the activity of the separate foil (4), taking due account of the foil thicknesses.

When all four foil thicknesses are equal, one obtains the relations:

$$\alpha_4 - \alpha_2 = \sum_{j=1}^{620} \sigma_j \cdot \phi_j \{2G(\tau_j) - 2G(2\tau_j)\}$$

Therefore the selfshielding factor to be applied in the quadruple foil technique, for the activation difference between foil (4) and foil (2) with equal thickness, is given by:

$$G_{\text{quadruplet}} = G_{4-2}(\tau_j) = 2G(\tau_j) - 2G(2\tau_j)$$

## 4. CALCULATION OF SELFSHIELDING FACTORS

The values  $G(\tau)$  are supplied by the computer program SELFS, which can be used in combination with the SAND-II program.

The equation used in the original program SELFS is based on the following assumptions:

- the neutron flux density can be considered as monoenergetic in each energy group;
- the cross section can be taken constant in these energy groups;
- the neutron flux density incident on the foil is isotropic;
- there are no multiple interactions;
- the foil may be considered as a plane slab (i.e. there are no edge effects);
- the flux density depression outside the foil is not taken into account;
- the effect of Doppler broadening is negligible;
- there is no foil cover which attenuates the incident neutron flux density.

Under these conditions one has:

$$G(\tau) = \{1 - 2E_3(\tau)\}/2\tau$$

where  $E_3$  is the third exponential integral defined by the expression:

$$E_3 = \int_1^{\infty} (e^{-\tau x}/x^3).dx$$

This approach enables us to introduce effective cross sections (i.e. cross sections modified for selfshielding) in the form:

$$(\sigma_i)_{\text{mod}} = \sigma_i \cdot G(\tau_i)$$

#### Numerical example

Using  $\tau=0.10$  one obtains  $G_{\text{triplet}} = 0.036$  and  $G_{\text{quadruplet}} = 0.194$ .

Using  $\tau=0.20$  one obtains  $G_{\text{triplet}} = 0.060$  and  $G_{\text{quadruplet}} = 0.266$ .

#### 5. INFLUENCE OF FOIL COVER

The original program SELFS has been modified in order to take into account the neutron flux density attenuation in a foil cover. In practice we use foil covers of aluminium, cadmium and boron carbide.

Let the subscript  $s$  indicate the shield or foil cover. Let  $\tau_s = (N_V \cdot \sigma \cdot t)_s$  denote the dimensionless thickness parameter for the foil shield.

One can derive that for a single foil covered by a shield, when infinite slab geometry is applicable, one has the relation:

$$G_4^s = \frac{1}{\tau} \{E_3(\tau_s) - E_3(\tau_s + \tau)\}$$

Remark: When  $\tau_s=0$ , one has  $E_3(0) = \frac{1}{2}$ , so that then the previous relation is obtained.

Similarly, one has for the total triple foil:

$$G_{1+2+3}^s = \frac{1}{3\tau} \{E_3(\tau_s) - E_3(\tau_s + 3\tau)\}$$

and for the mid foil:

$$G_2^s = \frac{1}{\tau} \{E_3(\tau_s + \tau) - E_3(\tau_s + 2\tau)\}$$

From the relation

$$A_1 + A_2 + A_3 = A_{1+2+3}$$

or

$$G_1 t_1 + G_2 t_2 + G_3 t_3 = G_{1+2+3} t_{1+2+3}$$

one obtains since  $t_1=t_2=t_3=t$  and  $t_{1+2+3}=3t$ :

$$G_1 = G_3 = (3G_{1+2+3} - G_2)/2$$

And thus:

$$G_{1-2}^S = (3G_{1+2+3}^S - 3G_2^S)/2$$

or:

$$G_{\text{triplet}}^S = G_{1-2}^S = \frac{1}{2\tau} \{E_3(\tau_S) - 3E_3(\tau_S + \tau) + 3E_3(\tau_S + 2\tau) - E_3(\tau_S + 3\tau)\}$$

Furthermore:

$$G_{\text{quadruplet}}^S = G_{4-2}^S = \frac{1}{\tau} \{E_3(\tau_S) - 2E_3(\tau_S + \tau) + E_3(\tau_S + 2\tau)\}$$

Fig. 1 shows the modified (effective) cross sections for activation of the gold foils of 0.1 mm thickness, when the quadruplet technique is applied without cadmium cover. When a 1 mm thick cadmium cover is applied, the plots shown in figure 2 are obtained.

Plot a: refers to activation of foil 2;

Plot c: refers to activation of foil 4;

Plot b: refers to difference in activation of foils 1 and 2;

Plot d: refers to difference in activation of foils 4 and 2.

One can observe several interesting effects:

- The mid foil (2) is not activated by neutrons with energies of the first and dominant resonance. The effective cross section shows a deep and narrow valley;
- The attenuation is rather strong for the lowest energies. For foil 2 it is stronger than for foil 4;
- The activation difference  $\alpha_1 - \alpha_2$  is generally smaller than the activation difference  $\alpha_4 - \alpha_2$ . This means that the response (in terms of counting rate) is better for the quadruplet method than for the triplet method;
- The curves for the effective cross sections for  $\alpha_1 - \alpha_2$  and  $\alpha_4 - \alpha_2$  are rather similar. This means that the triple foil technique and the quadruple foil technique have roughly the same energy resolutions.

## 6. CONCLUSIONS

To determine the neutron flux density in the energy region of cross section resonances of activation detectors the quadruplet technique has some

advantages over the triple foil technique. The main advantage is that a larger difference in activation of the two foils is obtained.

When furthermore a suitable cover (e.g. cadmium) is used to decrease the activation by thermal neutrons, one obtains in principle a much larger difference in activation.

For application of this method it is necessary to calculate the shielding and selfshielding factors in a fine group structure.

Preliminary experience has been obtained using the SAND-II group structure and a simple attenuation model (isotropy: plane slab geometry).

The accuracy of this technique might be increased by the following steps:

- Application of smaller group width in the resonance region;
- Introduction of a better geometry model for the selfshielding correction;
- Incorporation of a better scattering model;
- Use of more accurate cross section data, when these become available.

## 7. REFERENCES

[1] Zijp, W.L.; Nolthenius, H.J.: "Neutron selfshielding of activation detectors used in spectrum unfolding"

Report RCN-231 (Reactor Centrum Nederland, Petten, 1975).

Table 1: Results for gold foils (r=10 mm; t=0.1 mm), irradiated in the LFR VC plug with a 1/E spectrum

	measurements	calculations
<u>foils inside Al cover</u>		
$\alpha_1/\alpha_2$	1.049	1.059
$\alpha_1/\alpha_3$	1.002	0.999
$\alpha_4/\alpha_2$	1.226	1.260
<u>foils inside Cd box</u>		
$\alpha_1/\alpha_2$	1.409	1.379
$\alpha_1/\alpha_3$	1.01	1.000
$\alpha_4/\alpha_2$	1.973	1.948

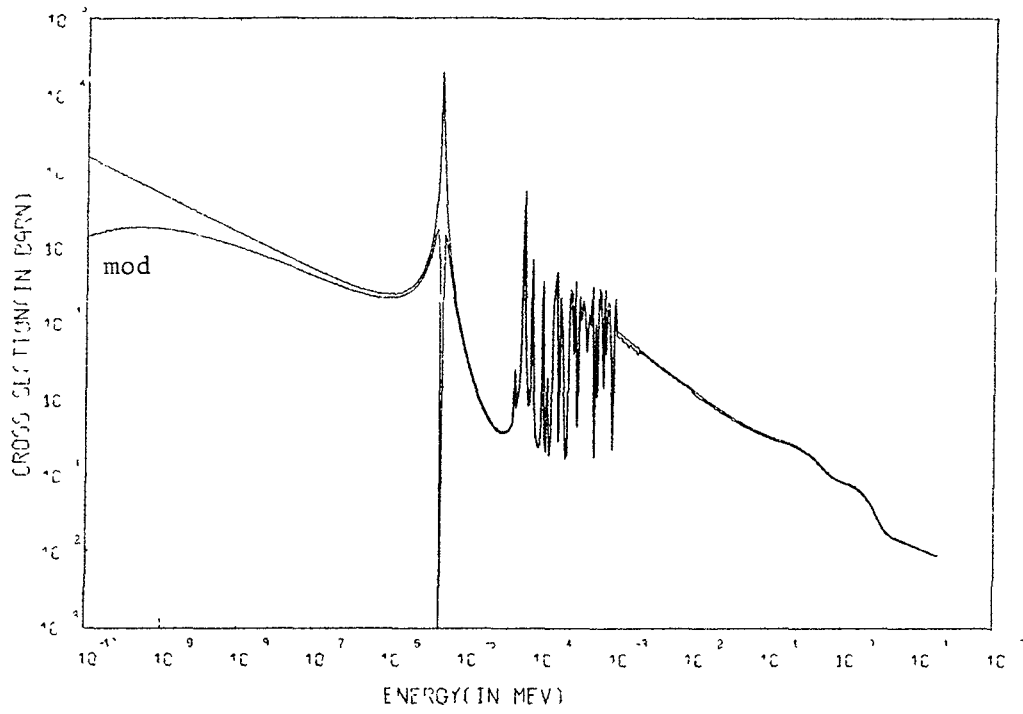


FIG 1a CROSS SECTION CURVE FOR THE REACTION Au197G A2

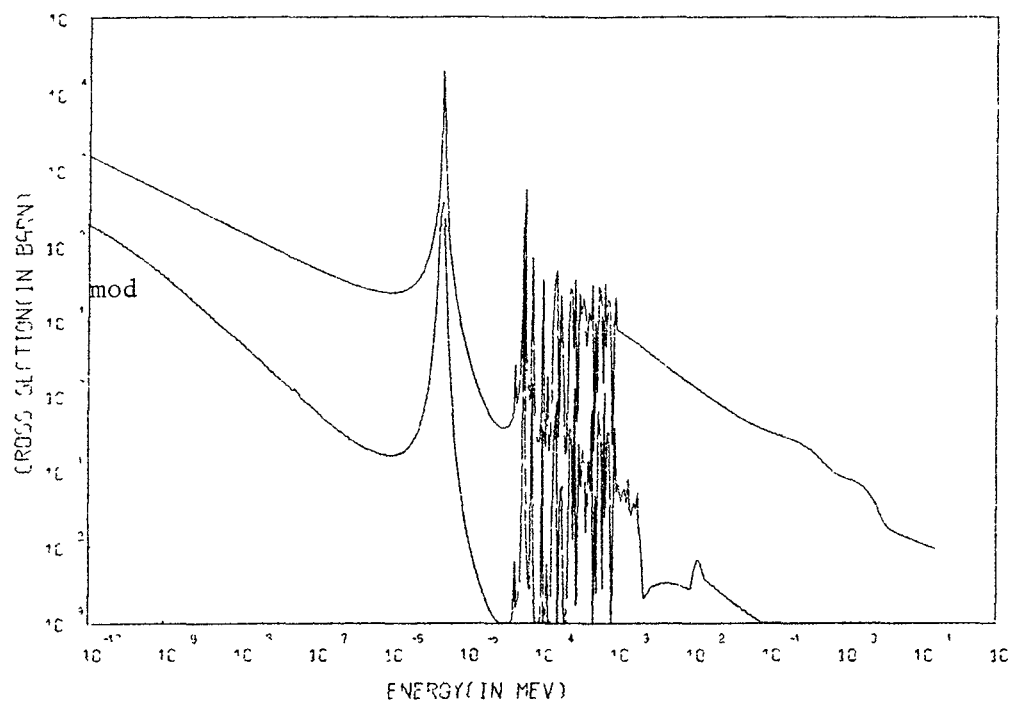
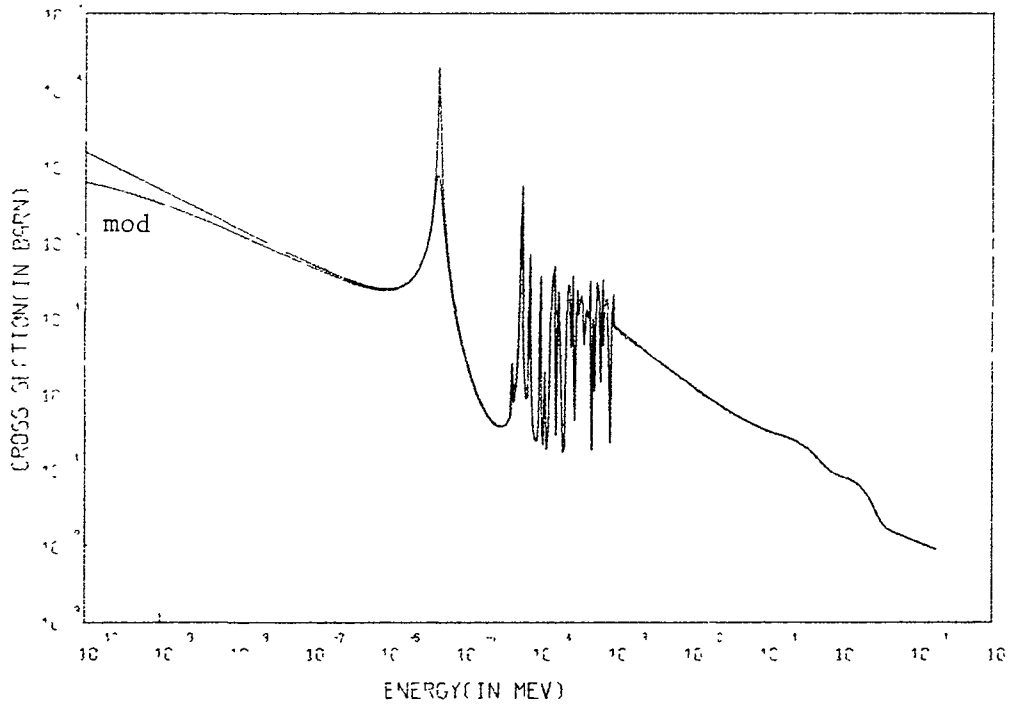


FIG 1b CROSS SECTION CURVE FOR THE REACTION Au197G A1-A2





MG 4788 FIG 1c CROSS SECTION CURVE FOR THE REACTION Au197G 64

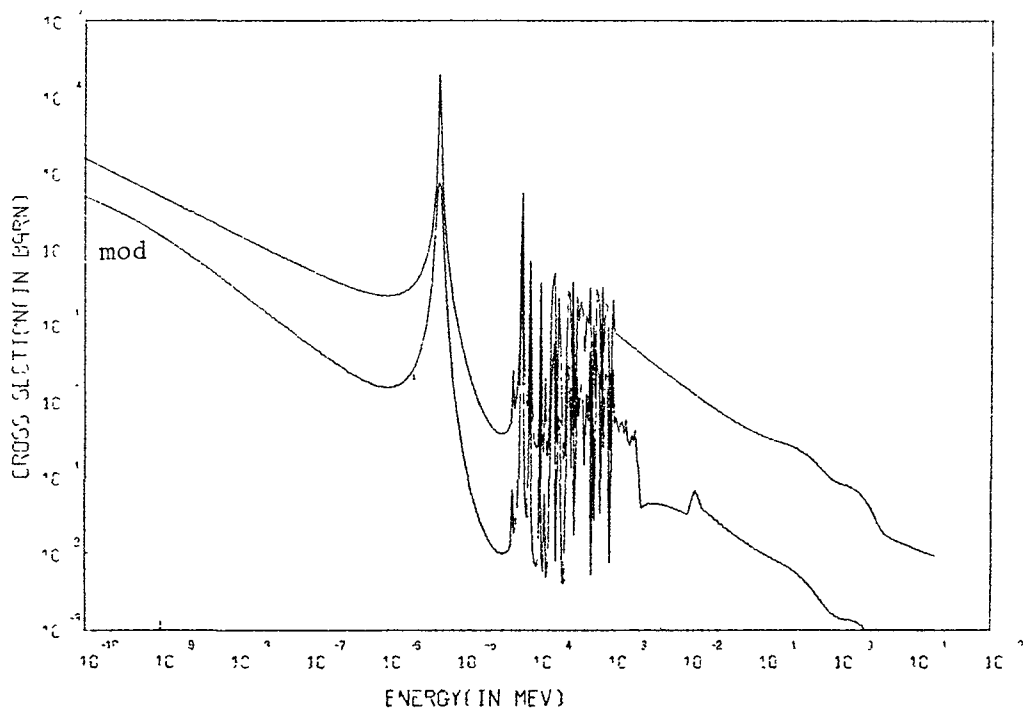


FIG 1d CROSS SECTION CURVE FOR THE REACTION Au197G. 64-62

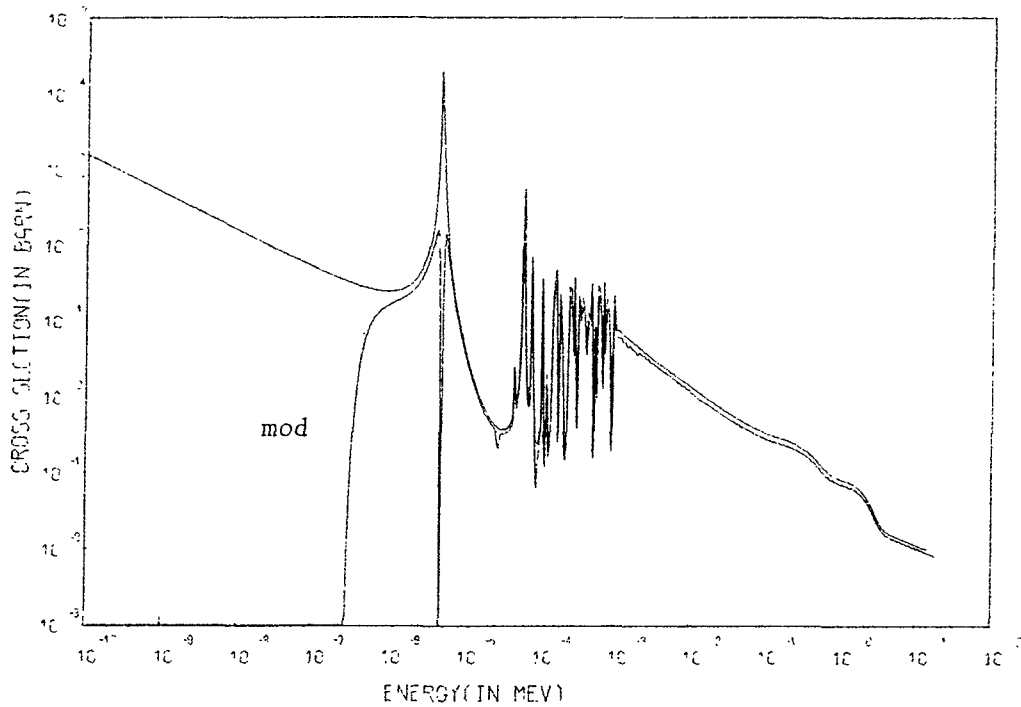


FIG 2a CROSS SECTION CURVE FOR THE REACTION Au197G 62 WITH CL-COVER

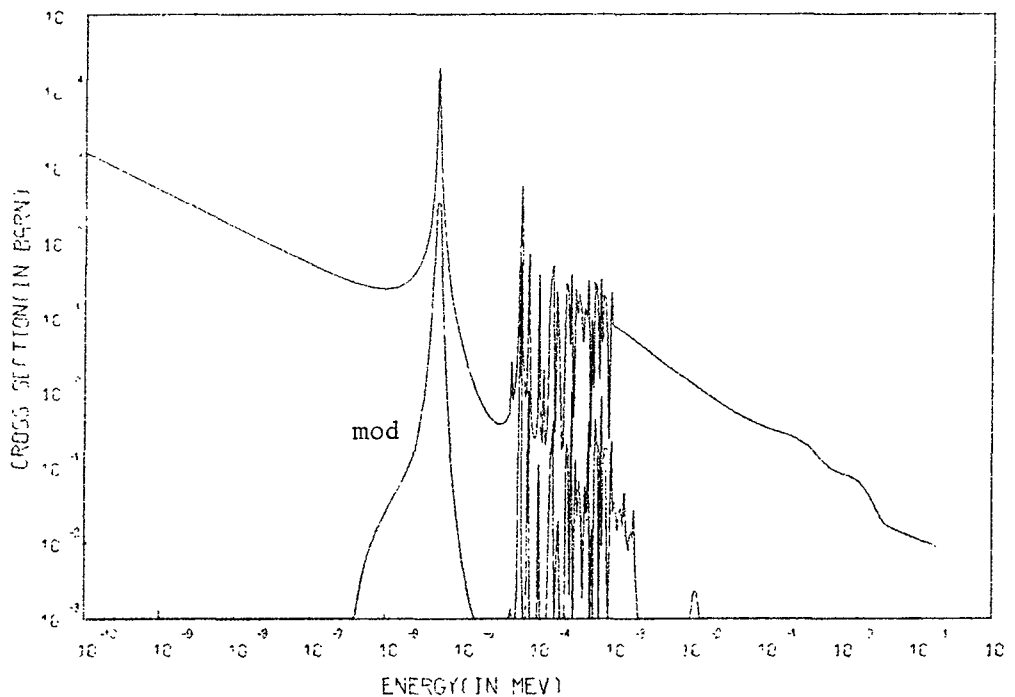


FIG 2b CROSS SECTION CURVE FOR THE REACTION Au197G 61-62 WITH CD-COVER

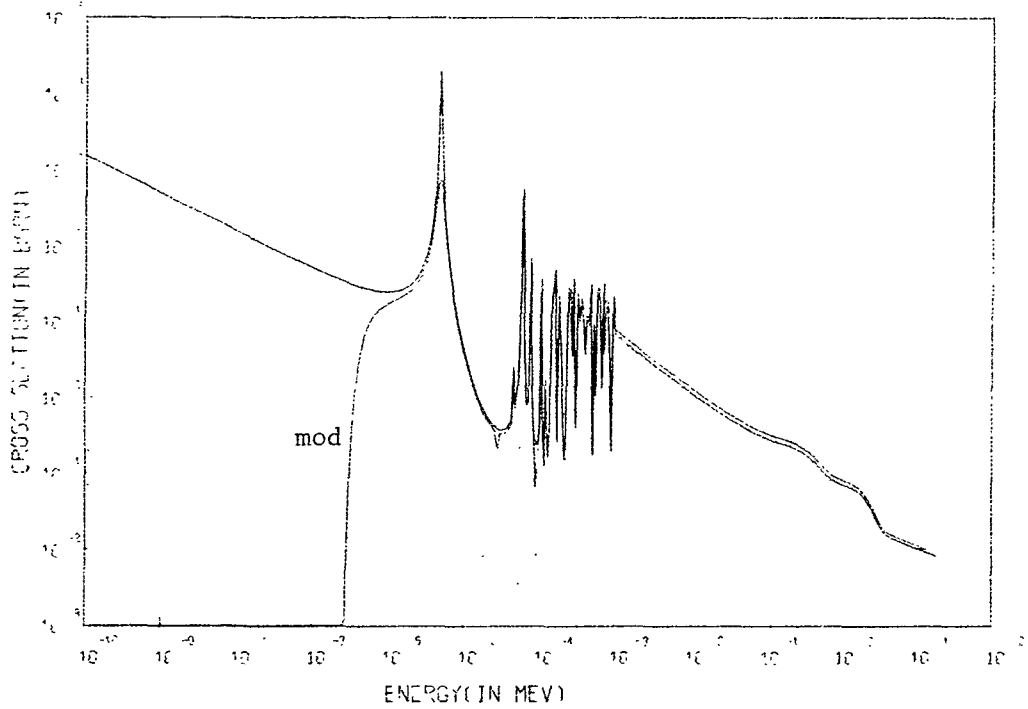


FIG 4789- FIG 2c CROSS SECTION CURVE FOR THE REACTION AU197G 64 WITH CD-COVER

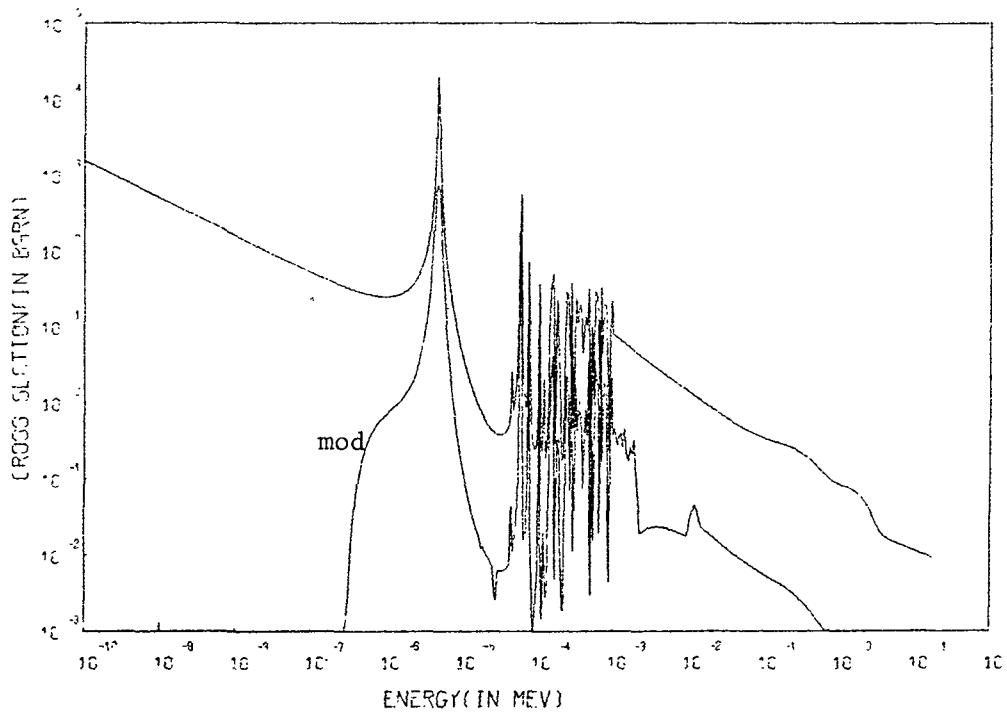


FIG 2d CROSS SECTION CURVE FOR THE REACTION AU197G 64-62 WITH CD-COVE

## WINDOW FUNCTIONS AND BOUNDS IN MULTIPLE FOIL DOSIMETRY

F. W. Stallmann  
University of Tennessee  
Knoxville, Tennessee 37916  
and

F. B. K. Kam  
Oak Ridge National Laboratory\*  
Oak Ridge, Tennessee 37830

### ABSTRACT

The useful application of window function concepts in multiple foil dosimetry was shown. It was possible to correlate foil activations directly to property degradations or other internal properties whose magnitude was desired. This technique can in some cases bypass some of the unfolding problems and reduce the resulting errors.

### WINDOW FUNCTIONS AND BOUNDS IN MULTIPLE FOIL DOSIMETRY

The multiple foil dosimetry is based on the integral relation

$$\alpha_i = \int_0^{\infty} \sigma_i(E) \phi(E) dE \quad , \quad (1)$$

where  $\alpha_i$  is the measured activity of the  $i$ -th foil,  $\sigma_i(E)$  its activation cross section, and  $\phi(E)$  the unknown neutron flux, both considered as functions of the neutron energy  $E$ . Unfolding procedures are used to obtain from the measured activities estimates of the spectrum or, more realistically, estimates of certain integral responses of the spectrum with given response functions  $R(E)$ , namely

$$I_R = \int_0^{\infty} R(E) \phi(E) dE \quad . \quad (2)$$

These integrals will be called "spectral parameters". Most unfolding methods are based on linear estimation; that is the estimate for the spectral parameter is expressed as a linear combination of the activities with suitable coefficients  $c_i$ . Thus, if  $\hat{I}_R$  represents the estimate for  $I_R$  we have

$$\hat{I}_R = \sum_{i=1}^n c_i \alpha_i \quad . \quad (3)$$

---

\*Operated by Union Carbide Corporation for the Department of Energy.

By combining formula (1) with formula (3) we find that  $\hat{I}_R$  is like  $I_R$  a spectral parameter as in formula (2), namely

$$I_R = \int_0^{\infty} W(E)\phi(E)dE \quad , \quad (4)$$

where the response function  $R(E)$  has been replaced by the "window function"  $W(E)$  which is a linear combination of the activation cross sections

$$W(E) = \sum_{i=1}^n c_i \sigma_i(E) \quad . \quad (5)$$

The term window function is based on the notion that  $\hat{I}_R$  is obtained by looking at the spectrum through a window provided by the foil combinations.

The concept of window functions is very useful for a quick, qualitative assessment of any estimate as well as the potential and limitations of multiple foil dosimetry in general. The goodness of the estimate  $\hat{I}_R$  depends on how well the window function  $W(E)$  is able to approximate the response function  $R(E)$  and this can be gathered by just glancing at both functions. The goodness of the approximation is expressed quantitatively through

$$\epsilon(E) = W(E) - R(E) \quad (6)$$

and thus the goodness of the estimate through

$$\hat{I}_R - I_R = \int_0^{\infty} \epsilon(E)\phi(E)dE \quad . \quad (7)$$

The uncertainties in formula (7) can, of course, only be determined if some a priori estimate of the range of  $\phi(E)$  is available. However, the smaller  $\epsilon(E)$  is the less dependent in the goodness of the estimate  $\hat{I}_R$  on the a priori knowledge of the spectrum. Measuring uncertainties in the activity and cross section measurements must be added to the uncertainties in formula (7). The uncertainties in the activities are propagated straightforwardly to those of  $\hat{I}_R$  based on formula (3). Cross section uncertainties will be included in formula (6) and formula (7) via formula (5). They may also be included in the activity uncertainties via formula (1), which is mathematically equivalent.

Bounds instead of estimates for  $I_R$  can be determined if window functions are chosen which are consistently larger or consistently smaller than the response function  $R(E)$ . Such bounds are completely independent of any a priori assumption about the spectrum except that it is always non-negative. Linear

programming methods are used to determine the smallest upper bound and the largest lower bound for a given set of activity measurements. If Gaussian distribution of the measuring errors is assumed, a quadratic programming problem arises; however, linear approximation is not expected to worsen the computed bounds substantially.

It should be pointed out that the actual computations of either estimates or bounds do not use the window function concept explicitly. It is, however, extremely useful for the interpretation of the results. As much as a picture says more than a thousand words, so does a single display of the window function and the related coefficients  $c_i$  provide more useful information than a thousand lines of computer output. The window function concept has been proven especially useful to investigate the following three questions:

1. What a priori information about the spectrum is needed to obtain a reliable estimate of  $I_R$ ? Or conversely which spectral parameters can be estimated with sufficient accuracy without detailed a priori knowledge of the spectrum?
2. What foils are needed to obtain a good estimate or bound? Part of the answer can be inferred from the size of the coefficients  $c_i$  in formula (3). If  $c_i$  is relatively small the corresponding foil may be eliminated without changing substantially the final result. Even small contributions may, however, be needed to keep  $W(E)$  larger or smaller than  $R(E)$ ; so additional checks are necessary. One should also be aware of the fact that there may be several different foil combinations which are equally well suited. Thus, a very large coefficient  $c_i$  does not necessarily indicate that the corresponding foil is irreplaceable.
3. The interpretation of estimates and bounds through window functions makes it also easy to assess the uncertainties due to measuring errors. It will be obvious whether a result can be substantially improved by improving the accuracy of the measurements, whether additional foils are needed, or whether estimates and bounds must primarily rely on neutron transport calculations.

These questions are especially important for the design of experiments. Since no actual measurements are involved in the approximation of a given response function  $R(E)$  by a suitable window function  $W(E)$ , answers can be obtained before the experiment is carried out.

An added uncertainty is encountered for damage integrals

$$I_D = \int_0^{\infty} D(E)\phi(E)dE \quad (8)$$

which are used to estimate material change due to neutron irradiation. The response function  $D(E)$  is here largely unknown and must be determined experimentally. If it can be assumed that  $D(E)$  is sufficiently close to some window function, whatever its shape may be in detail, then it is only necessary to estimate the coefficients  $c_i$  of that window function through experiments. In other words a direct correlation between foil activation and measured damage may be established. This assumption is likely to be true for energies above 0.5 MeV. Additional experiments are needed to determine the exact fraction of the damage attributable to slower neutrons.

One problem which has never been sufficiently investigated is that of the influence of energy grouping in relation to unfolding procedures. Activation cross sections show numerous resonance peaks which can be realistically represented only in a very fine energy grid. It is usually assumed that the neutron spectrum is sufficiently smooth to permit averaging over larger energy intervals without introducing substantial uncertainties. These uncertainties are usually disregarded, but they are by no means unimportant. A very crude grid of, say, 30 or less energy intervals has many advantages for the unfolding procedures. Not only is the amount of computation drastically reduced but bounds and estimates may also be more realistic if credible bounds for spectrum averaged cross sections could be obtained. This requires a detailed analysis of cross section and spectrum uncertainties which may be quite involved but should be worth the effort.

APPLICATION DES METHODES DE LA PROGRAMMATION  
LINEAIRE AU DEPOUILLEMENT DES RESULTATS DE MESURES PAR ACTIVATION

J. Dorlet  
C.E.A., DE/RDE, B.P.561  
F-92542 Montrouge(Cedex)  
France

ABSTRACT

Using only the data (cross sections library and measured reaction rates), the well known methods of linear programming furnishes :

- consistency of the data
- if the data are consistent, bracketting for any damage function.

On the other hand some unfolding computer code exists. We use a SAND II procedure.

In this paper, we use both methods to obtain a maximal set of consistent data.

We show that some of a priori inconsistent detectors are, in fact, those for which the consistent data set furnishes a narrow, thus interesting bracketting.

INTRODUCTION

Si on se donne une bibliothèque multigroupe des sections efficaces et des taux de réaction mesurés, on a un système d'équations linéaires de la forme

$$\sum_{J=1}^{NG} \sigma(I, J) \times \phi(J) = A(I) \quad (I = 1, ND) \quad (1)$$

où ND est le nombre de détecteurs utilisés et NG le nombre de groupes de la bibliothèque.



Si les mesures ont été effectuées dans un but de dosimétrie, les inconnues  $\phi(J)$  du système (1) ne sont pas recherchées pour elles-mêmes mais pour évaluer un dommage

$$D = \sum_{J=1}^{NG} FD(J) \phi(J) \quad (2)$$

connaissant la fonction FD.

Le problème est donc le suivant :

Connaissant : -  $\sigma(I, J)$              $I = 1, ND ; J = 1, NG$   
 -  $A(I)$                              $I = 1, ND$   
 -  $FD(J)$                              $J = 1, NG$

Trouver l'encadrement de D défini par les contraintes :

$$\phi(J) \geq 0 \quad J = 1, NG$$

La solution complète de ce problème mathématiquement bien posé a été publiée en 1949 par G.B. DANTZIG .

Il s'agit de la méthode du simplexe , base de ce qui constitue aujourd'hui la programmation linéaire (1).

Par solution complète nous voulons dire le moyen de réaliser effectivement un code de calcul admettant en entrées les sections efficaces, la fonction de dommage et les taux de réactions, et prévoyant en sortie tous les cas possibles, à savoir :

- 1) les données sont incompatibles
- 2) on donne l'encadrement  $D_{MIN} < D < D_{MAX}$ , même dans les cas  $D_{MIN} = 0$  et/ou  $D_{MAX} = + \infty$ , avec une solution  $\phi$  pour chacune des bornes finies.

Ce papier présente un exemple réel d'utilisation d'un tel programme. Les entrées utilisées (sections efficaces, taux de réaction) ont été intégralement publiées dans (2). La "fonction de dommage" FD choisie est arbitrairement la fonction  $FD(J) = 1$  ( $J = 1, NG$ ), c'est à dire que l'on cherche l'encadrement de la fluence totale compatible avec les entrées.

Le code est optimisé pour répondre à l'objection suivante : "si on espère que l'encadrement obtenu sur les fonctions de dommage sera assez étroit pour être intéressant, c'est parce que les sections efficaces réelles sont étroitement corréllées. Alors les entrées seront souvent incompatibles et le programme linéaire ne fournira aucun résultat exploitable".

## I - DESCRIPTION DU TRAITEMENT COMPLET D'UN CAS (principe).

On dispose de deux outils de base

1) Un code de type itératif permettant de trouver un spectre approprié et fournissant une solution approchée même lorsque les données sont incompatibles. Dans la suite on désignera ce code par C.ITER.

2) Un code de type linéaire permettant de savoir si les données sont compatibles et fournissant, dans les cas de compatibilité, l'encadrement de la dose pour une fonction arbitraire FD. Dans la suite on désignera ce code par C.LIN.

### I-1 - Organigramme de la partie automatique du traitement.

Nous proposons la procédure décrite dans l'organigramme présenté Fig.I et que nous allons commenter

a) On utilise C.LIN pour savoir si l'ensemble des données est compatible. Si oui le problème est résolu. On gardera l'ensemble des données et C.LIN pour des besoins de dosimétrie, C.ITER (éventuellement assorti de conditions particulières) pour des besoins de spectrométrie.

b) Si non on utilise C.ITER qui fournit une solution approchée  $\phi_0$

c) parvenus à ce point nous savons que l'ensemble n'est pas compatible et nous allons chercher à extraire des données un ensemble compatible maximal. Pour celà on part de l'idée suivante : en dehors d'un éventuel résultat aberrant qui apparaîtra assez vite quelle que soit la procédure employée, l'incompatibilité ne peut provenir que de détecteurs dont les réponses sont fortement corréllées. Mais il s'agit de corrélation sur le spectre réel et c'est pourquoi il est certainement préférable d'utiliser  $\phi_0$ . La procédure utilisée est la suivante :

On calcule toutes les distances angulaires

$$D(I, J) = \alpha \quad (I, J = 1, ND)$$

où

$$\cos \alpha = \frac{\sum_{K=1}^{NG} \text{sig}(I,K) \times \text{sig}(J,K) \times (E(K+1) - E(K)) \times \phi_0(K)}{\sqrt{\sum_{K=1}^{NG} (\text{sig}(I,K))^2 \times (E(K+1) - E(K)) \times \phi_0(K)} \quad \sqrt{\sum_{K=1}^{NG} (\text{sig}(J,K))^2 \times (E(K+1) - E(K)) \times \phi_0(K)}}$$

On met en ordre les détecteurs de façon à couvrir le maximum d'espace (pour la distance choisie) avec le minimum de détecteurs. On appelle PERO (I) la permutation obtenue. On la construit par :

$$D(\text{PERO}(1), \text{PERO}(2)) = \text{MAX}(D(I, J)) \\ I, J = 1, ND$$

Puis pour  $K \geq 3$  :

$$\sum_{N=1}^{K-1} D(\text{PERO}(K), \text{PERO}(N)) = \text{MAX}_{I=1, ND} \sum_{N=1}^{K-1} D(I, \text{PERO}(N))$$

L'ordre ainsi défini est tel que la boucle D qui va suivre a des chances d'aboutir à un nombre de détecteurs compatibles suffisamment élevé. Pour alléger les notations, nous désignons maintenant par la suite naturelle  $A_1, A_2 \dots A_{ND}$  l'ordre choisi dans la boucle D et par PER(I) la permutation permettant de retrouver l'ordre initial des détecteurs (à la première entrée dans la boucle on a donc  $\text{PER} = (\text{PERO})^{-1}$ ). On garde en mémoire  $(\text{PERO})^{-1}(ND)$ .

d) On utilise le code C.LIN pour savoir si les premiers détecteurs sont compatibles et on calcule l'encadrement de  $A_{P+1}$ . S'il y a incompatibilité on rejette le détecteur P en ND après avoir vérifié que l'on n'a pas  $\text{PER}(P) = (\text{PERO})^{-1}(ND)$  : en effet si  $\text{PER}(P) = (\text{PERO})^{-1}(ND)$ , cela signifie que tous les détecteurs suivants ont déjà été rejetés.

S'il y a compatibilité on conserve l'ordre et on retourne en début de boucle avec P + 1 détecteurs.

## Résultat de cette procédure

On obtient donc à la fin de ce programme automatique un sous ensemble de P détecteurs ayant les propriétés suivantes :

- L'ensemble de données  $\sigma_i, A_i (i = 1, P)$  est compatible
- Cet ensemble est incompatible avec tout détecteur supplémentaire.

REMARQUE : Le programme n'est pas optimisé en ce sens qu'il peut exister un ensemble de détecteurs compatibles plus grand. En fait, grâce à la procédure c), le nombre P sera suffisant pour le traitement ultérieur. Il nous semblerait au moins imprudent d'automatiser ce traitement.

### I-2 - Traitement ultérieur.

Les résultats de la phase automatique décrite en I-1-sont résumés par :

- la liste des détecteurs compatibles retenus (base)
- un tableau comparant, pour chaque détecteur rejeté (hors base), l'encadrement fourni par la base et le taux de réaction mesuré.

REMARQUE : Dans les 2 codes, il est recommandé pour des raisons de stabilité numérique ou de vitesse de convergence de se ramener au cas où tous les taux de réaction mesurés sont égaux à 1. Dans ce cas le tableau final ne comporte que 2 colonnes et son emploi est très facile.

On essaie alors de classer chaque détecteur hors base dans l'une des catégories suivantes :

1) mesure aberrante : la précision à priori de la mesure ne permet pas de faire entrer la valeur dans l'encadrement calculé.

2) Détecteur inutile : l'encadrement calculé n'est pas beaucoup plus grand que l'erreur expérimentale (on trouve par exemple  $0,87 < A_i < 0,94$  alors que la mesure de  $A_i$  est faite à 10% près) on

doit alors considérer que cette mesure confirme les résultats de la base et ne pas l'introduire dans des calculs de dosimétrie.

3) Détecteur mal utilisé : l'encadrement calculé est beaucoup plus grand que l'erreur expérimentale (on trouve par exemple  $1,05 < A_i < 3$ ). Dans ce cas l'introduction de ce détecteur dans la base n'introduit pas de contraintes très fortes et il est tout à fait probable que l'on peut retrouver un ensemble compatible en remplaçant par ce détecteur l'un des détecteurs de la base. Ceci n'est intéressant que si le détecteur supprimé contenait moins d'information que  $A_i$ . On réutilise donc C.LIN sur l'ensemble  $\{Base + D_i\}$  en supprimant successivement chaque détecteur et en calculant l'encadrement du détecteur écarté lorsque l'ensemble restant est compatible. On détermine ainsi le détecteur le moins utile que l'on place dans la catégorie définie ci-dessus en 2). L'ensemble de P éléments compatibles ainsi construit permet de donner des encadrements pour tous les détecteurs précédemment hors base. Il se peut que certains soient alors compatibles et puissent servir à construire une base plus grande dans laquelle on évitera maintenant d'introduire des détecteurs inutiles.

Résultat final . Le traitement est terminé lorsque les détecteurs ont été classés en 3 catégories seulement :

- 1) base (maximale)
- 2) détecteurs inutiles incompatibles avec la base
- 3) détecteurs aberrants

On peut alors utiliser ces résultats,

- soit en dosimétrie : encadrement de D, pour FD donnée, en utilisant seulement la base maximale.

- soit en spectrométrie. La question est alors de savoir s'il convient dans ce cas de conserver ou non les détecteurs inutiles contenus ou non dans cette base maximale avant d'utiliser le code itératif pour obtenir un spectre nominal . Aucune des idées exposées ici ne contient d'éléments de réponse à cette question.

## II - APPLICATION AUX RESULTATS OBTENUS AUPRES DU REACTEUR CALIBAN(ref.2)

Dans cette partie nous allons donner les résultats obtenus à l'aide du programme linéaire à partir des données considérées du point de vue de la dosimétrie. Il s'agit de l'étude de 4 points du réacteur CALIBAN, en lesquels un soin particulier avait été apporté au recalage des mesures de 10 taux de réaction. Ces résultats sont rappelés planche II, la bibliothèque multigroupe utilisée étant rappelée planche III.

Les calculs effectués référence 2 à l'aide du code itératif seul ayant montré une compatibilité excellente, la procédure (c) était ici inutile. Au prix d'un temps d'ordinateur relativement élevé (> 10 mn IRIS 80 par spectre) on disposait pour chaque point d'un spectre nominal et d'une base comportant suivant les cas 9 ou 10 détecteurs. Par contre la méthode de calcul d'encadrement de dose que nous avons proposée dans la référence 3 et souvent utilisée depuis se révélait impraticable dans ce cas, résultat qui est à l'origine de la présente étude.

Nous allons donc présenter ici les traitements postérieurs à l'obtention d'une base.

### II-1 - Choix de la base par élimination du détecteur le moins utile (point B) .

On utilise le code linéaire avec 9 détecteurs en entrée et on calcule l'encadrement du 10e détecteur lorsqu'il y a compatibilité.

On obtient le tableau I :

Det supprimé	Rh	In	Ni	Fe	Al	Mg	U <sub>5</sub>	U <sub>8</sub>	N <sub>p</sub>	Pu
Autres det compatibles	oui	non	oui	non	non	non	non	non	oui	non
Taux mini	0,748	X	1,82	X	X	X	X	X	1,11	X
Taux maxi	0,929	X	2,19	X	X	X	X	X	1,35	X

Au vu de ces résultats, on choisit la base obtenue en supprimant Rh pour les calculs ultérieurs de dosimétrie.

Pour les 3 autres points (cavité, F, C) on conserve la base formée des 10 détecteurs.

II-2 - Utilisation des bases choisies en dosimétrie : encadrements de fonctions de dommage.

On a choisi d'encadrer les "taux de réaction" particuliers suivants :

- Fluence totale  $\phi$  :  $FD(E) = 1$
- Energie moyenne multipliée par  $\phi$  :  $FD(E) = E$

Les résultats constituent le tableau II :

Taux de réaction	CAVITE		POINT F		POINT B		POINT C	
	MIN	MAX	MIN	MAX	MIN	MAX	MIN	MAX
$\int \phi(E) dE$ ( $nxcm^{-2}xs^{-1}$ )	$5,81.10^{10}$	$7,23.10^{10}$	$9,80.10^9$	$1,39.10^{10}$	$5,20.10^9$	$9,91.10^9$	$3,69.10^9$	$7,34.10^9$
$\int \phi(E) \times E dE$ ( $MeV \times nxcm^{-2}xs^{-1}$ )	$1,02.10^{11}$	$1,11.10^{11}$	$1,76.10^{10}$	$1,99.10^{10}$	$9,87.10^9$	$1,20.10^{10}$	$6,23.10^9$	$7,73.10^9$

On constate que le second taux de réaction est beaucoup mieux prévu que le premier. Si pour chaque encadrement on représente le résultat par la valeur moyenne et l'erreur relative, le tableau de ces erreurs (en %) est le suivant :

	CAVITE	POINT F	POINT B	POINT C
Erreur sur $\int \phi(E) dE$	11	17	31	33
Erreur sur $\int \phi(E) E dE$	4,5	6	9,7	10,7

Ceci tient au fait que la fonction  $FD(E) = E$  ressemble beaucoup plus aux sections efficaces utilisées que la fonction  $FD(E)=1$ . Il est donc raisonnable, pour des fonctions de dommages réelles, de s'attendre à des résultats encore plus précis (cf tableau I)

## CONCLUSION

Sur un ensemble de mesures particulièrement précises, on a vérifié la prévision faite dans la référence (3) par voie théorique : lorsque des mesures de taux de réaction sont compatibles, il est possible de fournir 2 spectres appropriés orthogonaux entre eux. Cependant de tels résultats sont utilisables pour prévoir des taux de dommage avec une précision très suffisante.

## REFERENCES

- (1) Applications et prolongements de la programmation linéaire.  
DUNOD 1966 -  
Traduction par E.VENTURA, de l'ouvrage antérieur de G.B.DANTZIG :  
Linear programming and extensions  
P.V.P. PRINCETON (NEW JERSEY)
- (2) Réacteur pulsé CALIBAN. Détermination des spectres appropriés de neutrons. Méthode itérative appliquée aux détecteurs à activation et de fission  
- J. MORIN - J. DORLET -  
(Communication au 2e Symposium A.S.T.M. - EURATOM sur la dosimétrie en réacteur - PALO ALTO 3-7 octobre 1977)
- (3) Type of information contained in the results of activation measurements. Application to the final development of results of the neutron Benchmark program. - J. DORLET -  
(à publier)



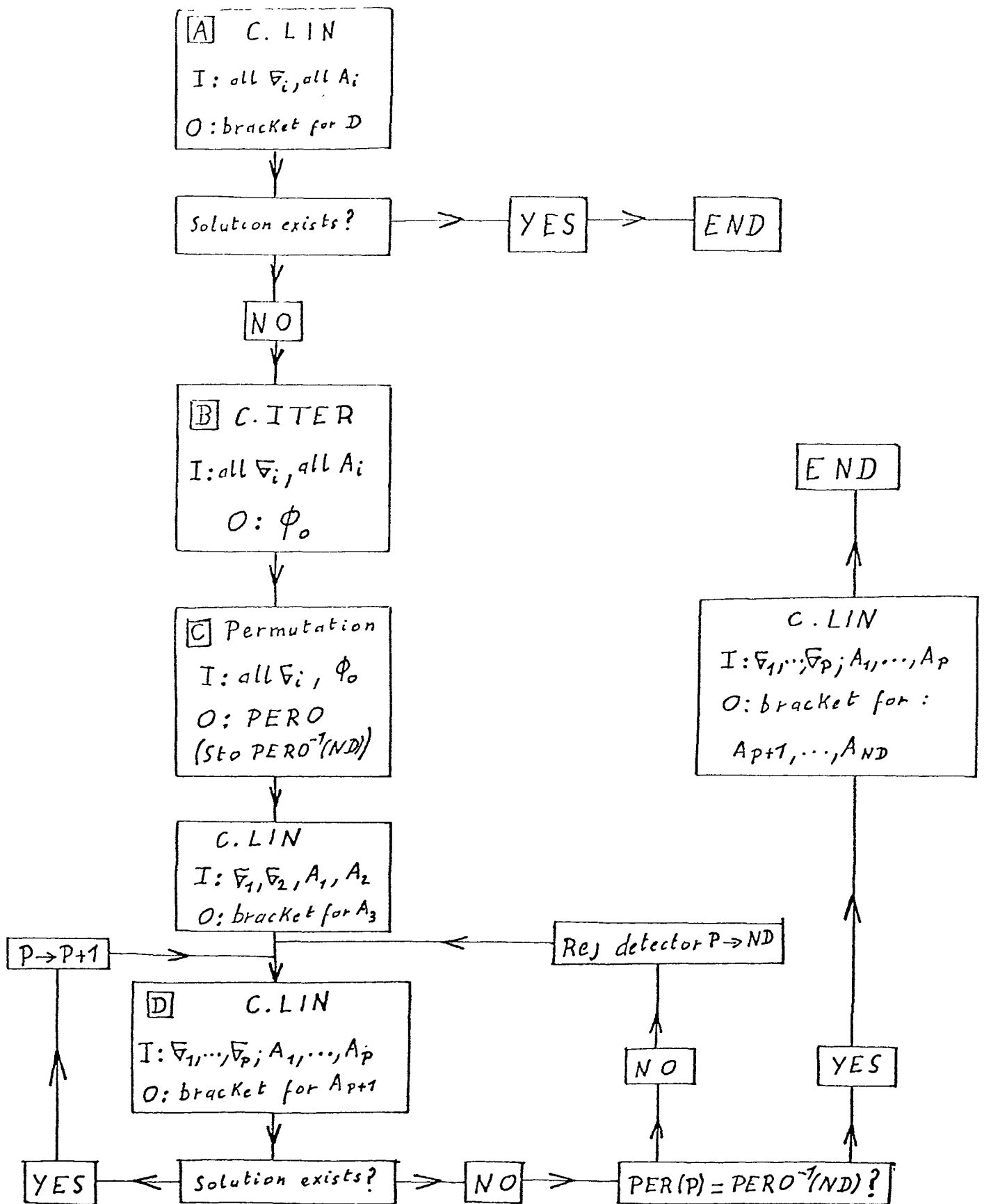


Fig I : Research of a first basis

- P L A N C H E   I I -

-----

Détecteurs	Points de mesure	Cavité centre	F extérieur	B extérieur	C extérieur
$^{103}\text{Rh}$		$4,16 \cdot 10^{10}$	$7,25 \cdot 10^9$	$4,81 \cdot 10^9$	$2,49 \cdot 10^9$
$^{115}\text{In}$		$7,95 \cdot 10^9$	$1,35 \cdot 10^9$	$7,80 \cdot 10^8$	$4,48 \cdot 10^8$
$^{58}\text{Ni}$		$5,25 \cdot 10^9$	$9,10 \cdot 10^8$	$5,10 \cdot 10^8$	$3,02 \cdot 10^8$
$^{56}\text{Fe}$		$5,50 \cdot 10^7$	$9,35 \cdot 10^6$	$5,10 \cdot 10^6$	$2,93 \cdot 10^6$
$^{27}\text{Al}$		$2,75 \cdot 10^7$	$4,88 \cdot 10^6$	$2,75 \cdot 10^6$	$1,63 \cdot 10^6$
$^{24}\text{Mg}$		$5,50 \cdot 10^7$	$10^7$	$5,50 \cdot 10^6$	$2,85 \cdot 10^6$
$^{235}\text{U}$		$9,15 \cdot 10^{10}$	$1,71 \cdot 10^{10}$	$1,22 \cdot 10^{10}$	$9,55 \cdot 10^9$
$^{238}\text{U}$		$1,22 \cdot 10^{10}$	$2,14 \cdot 10^9$	$1,26 \cdot 10^9$	$7,45 \cdot 10^8$
$^{237}\text{Np}$		$7,90 \cdot 10^{10}$	$1,43 \cdot 10^{10}$	$7,95 \cdot 10^9$	$5,15 \cdot 10^9$
$^{239}\text{Pu}$		$1,43 \cdot 10^{11}$	$2,50 \cdot 10^{10}$	$1,78 \cdot 10^{10}$	$1,52 \cdot 10^{10}$

- P L A N C H E . . . I I I . -

ENERGIES MeV	N	27Al	24Mg	56Fe	58Ni	54Fe	115In	103Rh	238U	237Np	239Pu	235U
0 - 10 <sup>-6</sup>	1							0		19	53350	122500
0,01 - 0,01	2							0,6		20	10000	30000
0,1 - 0,1	3							18		15	1850	1700
0,2 - 0,2	4							70		30	1750	1500
0,3 - 0,3	5							110		50	1600	1350
0,4 - 0,4	6						0	135		85	1600	1250
0,5 - 0,5	7						0,17	180	0	200	1600	1200
0,6 - 0,6	8						0,5	550	0,14	550	1600	1200
1 - 1	9				0		7,5	620	1,4	1200	1620	1180
1,1 - 1,1	10				0,13		65	650	25	1500	1680	1200
1,2 - 1,2	11				0,3		90	750	40	1550	1720	1220
1,7 - 1,7	12				5		170	830	120	1650	1900	1240
2,2 - 2,2	13				46		245	900	560	1700	2000	1300
2,3 - 2,3	14				70	0,5	290	910	580	1720	2020	1320
2,4 - 2,4	15				85	3	300	950	570	1750	2020	1320
2,4 - 2,9	16				140	70	325	1020	560	1760	2000	1350
2,9 - 3,4	17				215	135	350	1050	540	1720	1950	1260
3,4 - 3,9	18				315	220	360	1080	540	1700	1900	1220
3,9 - 4,5	19				400	310	360	1110	550	1650	1850	1210
4,5 - 4,6	20				450	350	360	1120	550	1600	1800	1180
4,6 - 4,7	21				480	370	360	1150	560	1600	1800	1180
4,7 - 5	22				500	400	360	1190	560	1550	1800	1150
5 - 5,1	23				520	420	360	1200	565	1550	1800	1120
5,1 - 5,2	24				530	430	360	1210	570	1550	1800	1120
5,2 - 5,6	25				560	450	350	1250	600	1580	1800	1140
5,6 - 6	26				600	490	350	1300	650	1600	1820	1200
6 - 6,1	27				620	510	342	1300	710	1700	1850	1260
6,1 - 6,2	28				625	520	340	1300	730	1720	1900	1300
6,2 - 6,7	29				650	540	340	1320	820	1850	2020	1400
6,7 - 7,2	30				650	560	330	1380	910	2100	2200	1600
7,2 - 7,7	31				660	560	320	1380	960	2300	2300	1700
7,7 - 8,2	32				660	570	310	1380	1000	2320	2400	1750
8,2 - 8,7	33				650	570	300	1400	1000	2330	2450	1800
8,7 - 9,2	34				640	560	285	1400	1010	2400	2400	1850
9,2 - 9,7	35				610	555	270	1350	1010	2400	2400	1850
9,7 - 10,2	36				600	550	255	1280	1010	2400	2400	1850
10,2 - 11	37				580	540	220	1100	1000	2400	2450	1800

# SPECTRUM UNFOLDING BY THE LEAST-SQUARES METHOD<sup>\*</sup>

F. G. Perey  
Neutron Physics Division  
Oak Ridge National Laboratory  
Oak Ridge, Tennessee 37830

## ABSTRACT

The method of least squares is briefly reviewed, and the conditions under which it may be used are stated. From this analysis, a least-squares approach to the solution of the dosimetry neutron spectrum unfolding problem is introduced. The mathematical solution to this least-squares problem is derived from the general solution. The existence of this solution is analyzed in some detail. A  $\chi^2$ -test is derived for the consistency of the input data, which does not require the solution to be first obtained. The fact that the problem is technically nonlinear, but should be treated in general as a linear one, is argued. Therefore, the solution should not be obtained by iteration. Two interpretations are made for the solution of the code STAY'SL, which solves this least-squares problem. The relationship of the solution to this least-squares problem to those obtained currently by other methods of solving the dosimetry neutron spectrum unfolding problem is extensively discussed. It is shown that the least-squares method does not require more input information than would be needed by our current methods in order to estimate the uncertainties in their solutions. From this discussion it is concluded that the proposed least-squares method does provide the best complete solution, with uncertainties, to the problem as it is understood now. Finally, some implications of this method are mentioned regarding future work required in order to exploit fully its potential.

---

<sup>\*</sup>Research sponsored by the Department of Energy under contract with Union Carbide Corporation.

## Introduction

The usual solution to the dosimetry neutron spectrum unfolding problem is an attempt at providing a detailed spectrum based upon activation measurements obtained in this spectrum given *a priori* knowledge of the corresponding dosimetry cross sections. As is well known, a very detailed, exact (i.e., unique) spectrum cannot be obtained for this problem. Most popular dosimetry unfolding codes such as SAND-II,<sup>1</sup> SPECTRA,<sup>2</sup> and CRYSTAL BALL,<sup>3</sup> or those based on their algorithms, obtain their solution by introducing some additional information in the form of a "trial spectrum." This trial spectrum is clearly some form of *a priori* information about the solution. In a recent paper<sup>4</sup> we analyzed the propagation of the uncertainties in the input data to the solution of these codes. While it is clear what the meaning of the uncertainties is for the activation data and the cross sections, some discussion of the "uncertainties in the input trial spectrum" and their effects upon the solution is desirable. In many favorable cases of activation data analysis, if the trial spectrum is selected "close to a physical one," the solution of these codes exhibits a weak dependence upon the trial spectrum.<sup>5</sup> This aspect of the uncertainties in the solution is usually handled by means of several calculations performed using "several different physical trial spectra," and a subjective evaluation of the reliability of the solution due to "trial spectrum sensitivity" is made.<sup>5</sup> If we wanted to be quantitative about these uncertainties, we could explore in some fashion the whole space of "physically valid trial spectra" by say numerical methods and extract some measure for these uncertainties. Certainly, if we did this, we would somewhat improve the credibility of the solution since in essence we would convert the somewhat arbitrary trial spectrum used to obtain the solution to a rather complete statement of the *a priori* knowledge about the solution, including its uncertainties. We believe, therefore, that part of the difficulties associ-

ated with the credibility of our usual solutions are related to the lack of precision in the statements which we either directly or indirectly make about the *a priori* information used and in some sense lower that information to the rank of "intuitive information,"<sup>6</sup> which calls for subjective evaluation. The second problem with our current methods is the fact that we in general cannot prove *a priori* what desirable or undesirable features our algorithms have in addition to those purposely put in. Such knowledge must be obtained through numerical experiments, inter-comparison of codes in special cases, etc.;<sup>7</sup> and such knowledge obtained *a posteriori* in specific examples may not necessarily be valid for somewhat new situations. It is for this reason that we proposed a new approach to the problem<sup>4</sup> which we think goes a long way toward eliminating these difficulties. In this paper we discuss at greater length this least-squares approach and some of the features and advantages of the solution.

### The Least-Squares Approach

We review first briefly the general method of linear least-squares in order to establish a notation and state clearly the assumptions upon which the solution is obtained. We shall use as much as possible a description based on the physics of the situation rather than the more precise statistical language.<sup>8</sup>

Given some "observations"  $y_i^o$  of  $n$  "quantities,"  $\bar{y}_i$ , forming the abstract vector  $Y^o$ ,  $Y^o \equiv \{y_i^o\}$ . Let these observations,  $y_i^o$ , have "errors,"  $e_i$ , associated with them. We consider the quantities  $\bar{y}_i$  to be random variables and the abstract vector  $\bar{Y} \equiv \{\bar{y}_i\}$  to be therefore a multivariate. If the experimental results are unbiased, we can say that they provide us with an estimate of the joint density function of  $\bar{Y}$  if we identify  $Y^o$  with its expectation value,  $Y^o = E[\bar{Y}]$ , and from the  $e_i$ 's we obtain its covariance matrix  $M \equiv \{m_{ij}\}$ , with  $m_{ij} = E[e_i, e_j]$ . No assumptions need be made about the form of the joint density function of  $\bar{Y}$ , and we emphasize that

only its second moments, the  $m_{ij}$ 's, are specified. We introduce a "model" whereby  $\bar{Y}$  is defined in terms of  $m$  "parameters,"  $\bar{p}_j$ , which form the abstract parameter vector  $\bar{P}$ . Therefore,  $\bar{P}$  is also considered to be a multivariate. Let us first take a model for  $\bar{Y}$  which is linear in  $\bar{P}$ ; we may write:

$$\bar{Y} = D \cdot \bar{P} \quad , \quad (1a)$$

where the dot we place between vectors and matrices denotes ordinary matrix multiplication and the  $n \times m$  "design matrix"  $D$  is not a function of  $\bar{P}$ . When  $n = m$ , the equation (1a) can be solved exactly, to obtain the estimated joint density function of  $\bar{P}$  from the estimated joint density function of  $\bar{Y}$ , if the design matrix  $D$  is not singular. For the case of  $n > m$ , our system of equations (1a) is overdetermined and what we seek is a "best average solution" in some sense. The method of least-squares obtains this solution by minimizing the " $\chi^2$ -function":

$$\chi^2 = (Y^\circ - \hat{Y})^\dagger \cdot M^{-1} \cdot (Y^\circ - \hat{Y}) \quad , \quad (2a)$$

where the symbol  $\dagger$  denotes the transpose of vectors and matrices and  $\hat{Y}$  denotes some estimate of the expectation value of  $\bar{Y}$  based upon some estimate  $\hat{P}$  of the expectation value of  $\bar{P}$ ,  $\hat{Y} = D \cdot \hat{P}$ . The vector  $Y^\circ - \hat{Y}$  is the "residual vector" and in this case is just  $Y^\circ - D \cdot \hat{P}$ . The minimum value of the  $\chi^2$ -function is obtained by adjusting  $\hat{P}$  and provides us with an "unbiased" estimate<sup>8</sup> for the joint density function of  $\bar{P}$  characterized also only by its expectation value  $P'$  and its covariance matrix  $N'_p$ . This least-squares solution for the joint density function of  $\bar{P}$  is often said to be "best" or "most likely" by virtue of the "minimum variance theorem"<sup>8</sup> which guarantees that it minimizes the variance of any linear combination of the parameters  $\bar{p}_j$ . We shall not prove here these very important properties of the least-squares solution, nor derive the solution, which is:<sup>8</sup>

$$P' = (D^\dagger \cdot M^{-1} \cdot D)^{-1} \cdot D^\dagger \cdot M^{-1} \cdot Y^\circ \quad , \quad (3a)$$

$$N'_p = (D^\dagger \cdot M^{-1} \cdot D)^{-1} \quad . \quad (4a)$$

When we refer to the solution of the problem, we mean both  $P'$  and  $N'_p$  since they are required for a somewhat meaningful specification of the joint density function of  $\bar{P}$ . We are indeed extremely limited in the kinds of useful statements we can make if we only obtain  $P'$ . The solution, (3a) and (4a), will always exist since the covariance matrices  $M$  and  $D^\dagger \cdot M^{-1} \cdot D$  are in principle nonsingular. This is the case because the covariance matrix  $M$  is symmetric, as well as positive definite, and at least one "independent piece of information" is required to be associated with each observation  $y_i^\circ$ . The "error" associated with this "independent piece of information" will contribute only to the diagonal of  $M$  and this is sufficient to make the matrix  $M$  nonsingular. Therefore, if in practice a singular covariance matrix  $M$  is found, it is due to an oversight or mistake. The same arguments can be made about the covariance matrix  $D^\dagger \cdot M^{-1} \cdot D$ , although here it is relatively easier to overlook the fact that although two different "labels" were used for two parameters they are the same quantity, since they enter in the model in exactly the same way. Such singularities can therefore be removed easily.

The above statement of the problem is known as a linear least-squares one, for obvious reasons. In many situations the model for  $\bar{Y}$  is nonlinear in the parameter  $\bar{P}$ ,  $\bar{Y} = F(\bar{P})$ , and the solution cannot be obtained as indicated above. In such cases an approximate solution can still be found using the least-squares method by linearizing the model. To do so we expand the model in a Taylor series in the parameters, which is truncated after the second term:

$$\bar{Y} \approx Y + D \cdot (\bar{P} - P) \quad , \quad (1b)$$

where the design matrix  $D$  is made up of the partial derivatives of the



model,  $F(\bar{P})$ , with respect to the parameter  $\bar{P}$  and evaluated at  $\bar{P} = P$ . The linearization of the model by (1b) is good only for  $\bar{P}$  close to  $P$ . Since  $\bar{P}$  is a multivariate which can assume a large range of values, the approximation (1b) can be said to be always bad in some domain of  $\bar{P}$ . However, if we choose  $P$  in the neighborhood of the solution,  $P'$ , assuming that it exists, and if the standard deviations of the joint density function of  $\bar{P}$  are small compared to the expectation values and/or if the model is not very nonlinear in the sense that the elements of  $D$  are not very sensitive to  $P$ , the approximation (1b) may be a relatively good one. A general discussion of the consequences of the linearization of the model is not our purpose since we will return to it later in connection with the dosimetry problem. Therefore, assuming the linear approximation (1b) can be made, we can proceed as for the linear case and write down explicitly the  $\chi^2$ -function:

$$\chi^2 = (Y^\circ - Y - D \cdot (\hat{P}-P))^\dagger \cdot M^{-1} \cdot (Y^\circ - Y - D \cdot (\hat{P}-P)) \quad (2b)$$

The comparison of (2b) with (2a) allows us to write immediately the solution for the minimum value of  $\chi^2$  which is obtained from (3a) and (4a) by substituting  $Y^\circ - Y$  for  $Y^\circ$  and  $P' - P$  for  $P'$  to get:

$$P' - P = (D^\dagger \cdot M^{-1} \cdot D)^{-1} \cdot D^\dagger \cdot M^{-1} \cdot (Y^\circ - Y) \quad , \quad (3b)$$

$$N'_p = (D^\dagger \cdot M^{-1} \cdot D)^{-1} \quad . \quad (4b)$$

Since frequently the initial choice of  $P$  is a poor one for the expansion (1b), the solution is then obtained by iteration in the hope that the solution will converge. It is important to note that the need to iterate is not an essential aspect of the method if the initial expansion "point"  $P$  yields a solution  $P'$  which is close to it. Iterating is, however, necessary if the model is highly nonlinear and  $P'$  is far from  $P$ . In this case the convergence of the process may or may not occur and when it does occur it may be at a "local minimum" which is a function of the starting value  $P$ .

If we can formulate our dosimetry data analysis problem as a least-squares one, the solution will be the most likely one and therefore better, or at least no worse, than any other one not based upon minimizing the  $\chi^2$ -function. In addition, the properties of this solution will be well known and fully understood.

It is evident that our activation measurements in the spectrum, the  $a_i^o$ 's and their uncertainties, meet the requirements to be some observations of the type  $y_i^o$  needed for a least-squares problem. The activations  $\bar{a}_i$  can be defined in terms of the fluxes  $\bar{\phi}_j$  and cross sections  $\bar{\sigma}_j^i$ ; our model for these quantities is clearly:

$$\bar{a}_i = \sum_j \bar{\sigma}_j^i \bar{\phi}_j \quad . \quad (5)$$

Since we can approximate our integral statement by expression (5) to any degree of accuracy, the "model" is exact by virtue of the definition of the quantities called the  $\bar{\sigma}_j^i$ 's. We may rewrite (5) in a more compact notation if we introduce the vector  $\bar{\Phi}$  for the  $\bar{\phi}_j$ 's,  $\bar{\Phi} \equiv \{\bar{\phi}_j\}$ , and the vectors  $\bar{\Sigma}^i$  for the  $\bar{\sigma}_j^i$ 's,  $\bar{\Sigma}^i \equiv \{\bar{\sigma}_j^i\}$ . Equation (5) then becomes:

$$\bar{a}_i = \bar{\Sigma}^{i+} \cdot \bar{\Phi} \quad . \quad (6)$$

It is clearly implicit in our use of the name "dosimetry neutron spectrum unfolding" for dosimetry data analysis, that the "flux quantities" are usually considered as "parameters" in the problem and we have indicated this in Eq. (5) by treating them as variates by our notation  $\bar{\phi}_j$ . The code DANTE,<sup>9</sup> which to our knowledge is the only current code which approaches dosimetry data analysis as a general least-squares problem as we do, treats the  $\bar{\phi}_j$ 's as the only parameters entering the model for the  $\bar{a}_i$ 's. DANTE does so by treating the cross sections as constants and solves the corresponding linear least-squares problem. Since at this stage of our knowledge of the dosimetry cross sections their estimated accuracies are often poorer than the estimated accuracies of the measured activations, ignoring the

cross section uncertainties by treating the cross sections as constants will significantly affect the estimated uncertainties in the spectrum. This point does not appear to have been generally appreciated for the "dosimetry unfolding problem" or even for the "many channel unfolding problem" where the "response matrix," which plays the role of the dosimetry cross sections in the dosimetry problem, is not considered as a variate on the same footing as the spectrum and consequently the uncertainties in the response matrix are not handled adequately.

In a dosimetry analysis problem we always have fewer activation measurements  $a_i^o$  than we have quantities  $\bar{\sigma}_j^i$  and  $\bar{\phi}_j$ , or even  $\bar{\phi}_j$ 's. There is, therefore, no unique solution for the  $\bar{\phi}_j$ 's, even if the  $a_i^o$ 's were known perfectly, unless we are willing to add more information than just the activation measurements. Of course we could solve the problem of activation data analysis by representing the  $\bar{\phi}_j$ 's by a few parameters and this has been done in the past, but such ways of handling the difficulties are generally considered inadequate. In the least-squares method information is in the form of "observations" and therefore what we seek in solving the problem by this method is to supplement the  $a_i^o$ 's with "other observations" which will produce an overdetermined set of equations for the  $\bar{\sigma}_j^i$ 's and  $\bar{\phi}_j$ 's. Two requirements must be met by the "quantities" used as "other observations": they must have "errors" associated with them and must be related to the parameters  $\bar{\sigma}_j^i$  and  $\bar{\phi}_j$  by means of a "model." Preferably this model must be exact, or considered so, since otherwise we need to introduce still more "observations" to overdetermine the approximate quantities in the model. It is evident that from a formal point of view the choice of "other quantities" to obtain an overdetermined set of equations is arbitrary and a solution can be found for each set of "other quantities" which meet the two basic requirements stated above. This arbitrariness in the choice of "other observations" can be largely removed if we consider the intended use of the solution sought. From

the concept that we want the "best solution" for a specific use, it often becomes very clear what "best set of other observations" is needed, in addition to the measured  $a_j^o$ 's of the problem. In the remainder of this paper we shall assume that what we are after is in some sense the "very best solution" consistent with our current knowledge. It is not evident that this particular solution is always the one desired, but we believe that it is the one which will be most useful for many uses and will serve to indicate the methodology. The idea of "very best solution" has implicit in it the fact that we have used to obtain it all observations which were ever made, for whatever purpose, related to the  $\bar{\sigma}_j^i$ 's and  $\bar{\phi}_j$ 's of this problem and that these observations are exploited to the fullest extent of our current knowledge.

We will first consider the  $\bar{\sigma}_j^i$ 's and show how this can be accomplished. The direct use of every experimental result related to the  $\bar{\sigma}_j^i$ 's is not practical even if in principle feasible. However, we can come close to achieving our goal if we consider that our "evaluations" of the  $\bar{\Sigma}^i$ 's attempt to represent all previous measurements and can be used directly as observations if they have "errors," or covariance matrices, associated with them. If we treat such evaluations of the  $\bar{\Sigma}^i$ 's as observations, their "model" becomes exact since it is the identity matrix. It is unfortunate that most of our evaluations of the  $\bar{\Sigma}^i$ 's do not have data covariance information associated with them since they cannot be used for our purpose until such information has been added to them. A formalism has been developed within the context of ENDF/B to represent such data covariance information,<sup>10</sup> and hopefully all the dosimetry cross sections of ENDF/B-V will have "data covariance files" and could be used directly. We shall therefore assume that it is practical to use evaluated  $\bar{\Sigma}^i$ 's to generate our "best solution" even if now the needed covariance matrices,  $N_{\Sigma}^{ij}$ , must be added to them. By doing so we have added to the  $a_j^o$ 's one "observation" per  $\bar{\sigma}_j^i$  and the required overdetermination of the  $\bar{\sigma}_j^i$ 's is achieved.

Let us now turn our attention to the  $\bar{\phi}_j$ 's. It is evident that we have a very efficient method in overdetermining the  $\bar{\sigma}_j^i$ 's since only one "observation" is used for each  $\bar{\sigma}_j^i$  and the same technique can be utilized for the  $\bar{\phi}_j$ 's. A method which can always be used is to estimate the  $\bar{\phi}_j$ 's by means of calculations based upon a "model" of the system which produced the spectrum in which the foils were irradiated. Because our model for these calculations is bound to be approximate and we must use imperfectly known nuclear data as input, these estimates for the  $\bar{\phi}_j$ 's will only be approximate and have "errors" associated with them. If we do estimate the uncertainties in these calculations, then the result is that we may use the calculated fluxes directly as observations. Of course, we should supplement these calculations of the  $\bar{\phi}_j$ 's with direct measurements of the  $\bar{\phi}_j$ 's if these are available and obtain effectively an evaluation for  $\bar{\Phi}$ , complete with covariance matrix  $N_{\Phi}$ . The approach we advocate in the treatment of the spectrum is related to what is done in the code RADAK.<sup>11</sup> RADAK is a general purpose "spectrum analysis code" which does a "simultaneous unfolding" from several detectors. It is primarily intended to be used with "many channel" detectors, but some activation foils may be included. As such, it is not a dosimetry unfolding code, but since no correlations are allowed between the "many channel" detectors output and the activation data, it is effectively equivalent to one where the  $\bar{\phi}_j$ 's are first obtained from the many channel detectors and then used to analyze the dosimetry data. In the cases where RADAK can be used, i.e., there are many channel detector data available for the complete spectrum, the solution we seek, the "best possible one," can be obtained by combining the output of RADAK with the results of model calculations. It is, therefore, merely a question of strategy about how to proceed in this case, and the result should be independent of the approach. However, when the dosimetry cross sections extend below the energy range of the many channel detectors, we must make use of model calculations to provide

the necessary overdetermination of the spectrum, in that energy range at least, before we can exploit the activation data.

If we proceed as outlined above, by supplementing our measured activations  $a_j^o$ , and their covariance matrix  $N_{A^o}$ , with a synthesis of all our previous observations concerning the  $\bar{\sigma}_j^i$ 's in the form of fully "evaluated cross sections," with expectation values  $\bar{\Sigma}^i$  and covariance matrices  $N_{\Sigma^i}$ , and a synthesis of all our previous knowledge of the  $\bar{\phi}_j$ 's in the form of a fully "evaluated spectrum," with expectation value  $\bar{\Phi}$  and covariance matrix  $N_{\bar{\Phi}}$ , we will have in a direct sense the "best input data" and our solution can be called the "best possible solution." It should be clear that whatever is our intended use of the solution spectrum it can never be called "best" if we do not use fully all the information concerning the dosimetry cross sections in the form of "best evaluations" for the  $\bar{\Sigma}^i$ 's. Therefore, our different "best solutions" can only come from what we use as "best evaluations of  $\bar{\Phi}$ ." It is conceivable that different intended use of the solution will dictate different "best assumptions" to be made in the evaluation of  $\bar{\Phi}$  and therefore we will have different "best evaluations" of  $\bar{\Phi}$ . It should be clear, however, that in order to be used in our problem the evaluations of  $\bar{\Phi}$  must be complete in the sense of having a covariance matrix  $N_{\bar{\Phi}}$  which corresponds to the assumptions made in the evaluation.

In this lengthy introduction we have attempted to justify in detail and in a logical manner the use of what is often called "*a priori* information about the solution." It is often perceived that only some class of *a priori* information such as non-negativity of the spectrum is "non-controversial."<sup>6</sup> We hope to have shown that this need not be the case and that the often perceived failure<sup>6</sup> of having found a satisfactory solution to the "few-channel unfolding problem" does not lie in the need for "detailed" *a priori* information, but rather in the fact that the detailed *a priori* information used in the past was poorly quantified.

We contend that any amount of detailed *a priori* information about the solution, if it succeeds in overdetermining the parameters of the problem, can provide a satisfactory solution if it is complete, i.e., has "uncertainties" associated with it, and the assumptions under which the complete *a priori* information is generated are justified and understood. From a purely mathematical point of view, the statement of the "input values of  $\Sigma^i$ ,  $N_{\Sigma ij}$ ,  $\Phi$  and  $N_{\Phi}$ " constitute the assumptions under which the solution is obtained and there is therefore nothing "controversial" about the solution since the assumptions are clearly stated.

### The Mathematical Formulation

In this section we merely transcribe in mathematical language the ideas discussed in the previous section. To simplify the notation we introduce the abstract cross section vector  $\bar{\Sigma}$ ,

$$\bar{\Sigma} \equiv \begin{pmatrix} \bar{\Sigma}^1 \\ \bar{\Sigma}^2 \\ \bar{\Sigma}^3 \\ \vdots \end{pmatrix}, \quad (7)$$

and the abstract parameter vector  $\bar{P}$ ,

$$\bar{P} \equiv \begin{pmatrix} \bar{\Phi} \\ \bar{\Sigma} \end{pmatrix}. \quad (8)$$

We shall refer to the evaluations of  $\bar{\Phi}$  and  $\bar{\Sigma}$ , treated as "observations," by the abstract vector  $P$  and its covariance matrix  $N_P$ :

$$P \equiv \begin{pmatrix} \Phi \\ \Sigma \end{pmatrix}, \quad N_P \equiv \begin{pmatrix} N_{\Phi} & 0 \\ 0 & N_{\Sigma} \end{pmatrix}. \quad (9)$$

We have shown in Eq. (9) by the symbol 0 for the off-diagonal matrices of  $N_P$  that we assume, as will be generally the case, that the evaluations of  $\bar{\Phi}$  and  $\bar{\Sigma}$  are uncorrelated. This is not necessarily always the case, since it is possible that some of the dosimetry cross sections of the

problem, some  $\bar{\Sigma}^i$ , enters also in the evaluation of  $\bar{\Phi}$  as could be for instance the case of the  $^{235}\text{U}$  fission cross section. In such cases the off-diagonal matrices of  $N_p$  will not be zero. It is not essential for the problem that  $N_p$  be diagonal in the space of  $\Phi$  and  $\Sigma$  which should therefore represent the true situation. However, it is convenient later to consider  $N_p$  to be diagonal in the space of  $\Phi$  and  $\Sigma$  purely from a presentation point of view. We shall therefore state that without loss of generality we consider  $N_p$  to be diagonal in the space of  $\Phi$  and  $\Sigma$ , which does not mean that we consider  $N_\Phi$  and  $N_\Sigma$  to be diagonal.

As previously discussed, we consider our evaluations of  $\bar{\Phi}$  and  $\bar{\Sigma}$  as "observations" as well as the abstract vector  $A^\circ$  made up of the measured activations  $a_i^\circ$ ,  $A^\circ \equiv \{a_i^\circ\}$ . In the notation of the previous section we have therefore:

$$Y^\circ \equiv \begin{pmatrix} P \\ A^\circ \end{pmatrix}, \quad M \equiv \begin{pmatrix} N_p & 0 \\ 0 & N_{A^\circ} \end{pmatrix}. \quad (10)$$

In Eq. (10) we indicate, by our notation 0 for the off-diagonal matrices of  $M$ , that the "observations"  $A^\circ$  and  $P$  are uncorrelated. It is strictly not necessary to make this assumption, in order to use the least-squares method, if we are willing to invert the full matrix  $M$ , as shown by (3) and (4). However, as we will show in the next section, if  $M$  is diagonal in the space of  $P$  and  $A^\circ$ , it is only necessary for us to "formally" invert the matrix  $N_p$  without actually doing so explicitly. When  $M$  is not diagonal in the space of  $P$  and  $A^\circ$ , we have to invert it explicitly to get the solution and this may not be practical since the rank of  $M$  may well be of the order of a few hundred or even a few thousand. We shall therefore assume that in order to be practical our method requires that  $P$  and  $A^\circ$  be uncorrelated. The meaning of this requirement is that in our evaluations of  $\bar{\Phi}$  and  $\bar{\Sigma}$  we must not use any data which are correlated to  $A^\circ$ . This restriction appears at first sight to



be a strong limitation of the method since it might force us to exclude from the evaluations some types of data obtained in standard and benchmark fields. We have already discussed a procedure for by-passing such difficulties<sup>4</sup> and we shall not return to it in this paper. (Mathematically speaking, it is the fact that M is diagonal in the space of P and A° which justifies our use of the term prior information to describe the evaluations of  $\bar{\Phi}$  and  $\bar{\Sigma}$ , i.e., they can be made without using our knowledge of A°.)

Having identified the "observations," Y° and M, for our least-squares problem we must now establish a "model" for the quantities  $\bar{Y}$ , i.e., obtain the complete design matrix. It is clear that P stands for the quantity  $\bar{P}$  and therefore our model for these observations is the identity matrix!! It is therefore linear and exact. Our "observations" A° stand for the quantity  $\bar{A}$ , with  $\bar{A} \equiv \{\bar{a}_j\}$  and  $\bar{a}_j$  is defined by Eq. (6). Since  $\bar{a}_j$  is a bilinear product of some of the elements of  $\bar{P}$ , our model for  $\bar{A}$  is non-linear. In order to obtain our design matrix we must linearize the model. We shall do so by performing an expansion about the estimated expectation values of  $\bar{\Phi}$  and  $\bar{\Sigma}$ , i.e.,  $\Phi$  and  $\Sigma$ , we get:

$$\bar{a}_j = \Sigma^{i\dagger} \cdot \Phi + \Phi^\dagger \cdot (\bar{\Sigma}^i - \Sigma^i) + \Sigma^{i\dagger} \cdot (\bar{\Phi} - \Phi) + (\bar{\Sigma}^i - \Sigma^i)^\dagger \cdot (\bar{\Phi} - \Phi) \quad , \quad (11)$$

since the expansion terminates the expression (11) is therefore exact regardless of the values of  $\Phi$  and  $\Sigma^i$ , as can be verified by performing the operations indicated. The linearization of (11) is accomplished by dropping the last term only. It is clear that "very little approximation" is made by dropping the last term since if our evaluations are "reasonably close" to the solution the contributions of this term will be small. This is so because to contribute significantly both  $\Sigma^i$  and  $\Phi$  must be significantly wrong in the same energy region; the signs of the differences must be such that no appreciable cancellations occur in the summations over energy and this sum is to be compared with the total activation. These three requirements to make the approximation poor must be met simultaneously

and therefore we can already conjecture that the model being "quasi-linear" most of the time we expect the linearization to be a good approximation and consequently our need to iterate to find the solution will be infrequent. We shall return later to a discussion of this point. In order to find the design matrix, we must rewrite (11) in a form similar to (1b):

$$\bar{A} \approx A + G \cdot (\bar{P} - P) \quad , \quad (12)$$

where  $A \equiv \{a_j\}$  and  $a_j = \Sigma^{j\top} \cdot \Phi$ . The "sensitivity" matrix  $G$  is therefore given by:

$$G = \begin{pmatrix} \Sigma^{1\top} & \Phi^\top & 0 & 0 & \dots \\ \Sigma^{2\top} & 0 & \Phi^\top & 0 & \dots \\ \Sigma^{3\top} & 0 & 0 & \Phi^\top & \dots \\ \vdots & \vdots & \vdots & \vdots & \vdots \end{pmatrix} . \quad (13)$$

Because the quantities  $\bar{A}$ , for which we have observations  $A^\circ$ , have a non-linear model, it is convenient to write  $\bar{P}$ , for which we have observations  $P$ , as if it also had a non-linear model. This can be accomplished exactly as follows:

$$\bar{P} = P + I \cdot (\bar{P} - P) \quad , \quad (14)$$

where  $I$  is the identity matrix. Using (12) and (14) and (1b) we find by inspection that for our non-linear least-squares problem we have:

$$Y = \begin{pmatrix} P \\ A \end{pmatrix} \quad , \quad D = \begin{pmatrix} I \\ G \end{pmatrix} . \quad (15)$$

This completes the mathematical formulation of our non-linear dosimetry least-squares problem since we have defined or derived appropriately the quantities:  $Y^\circ$ ,  $M$ ,  $Y$ ,  $D$  and  $\bar{P}$ , which were introduced in the previous section as needed to state such a problem.

It is clear from the above mathematical formulation of the problem that what we are solving for in our least-squares approach is:

Given,

1. activation measurements in a spectrum,  $A^\circ$  and  $N_{A^\circ}$ ,
2. *a priori* information about the dosimetry cross sections,  $\Sigma$  and  $N_\Sigma$ ,
3. *a priori* information about this spectrum,  $\Phi$  and  $N_\Phi$ .

what is the most likely value of the spectrum and its uncertainty,  $\Phi'$  and  $N_\Phi'$ ?

Because we have also used the dosimetry cross sections as parameters, we could also answer the question, "What is the most likely value of the dosimetry cross sections and their uncertainties,  $\Sigma'$  and  $N_\Sigma'$ ?" if we so desired.

### The Mathematical Solution

In the preceding sections we have stated the general least-squares method, given its solution, and formulated a least-squares problem for dosimetry data analysis. In this section we obtain the solution explicitly in terms of the input data and emphasize that it is extremely easy to compute and always exists. We could rewrite (2b) using the previous section as:

$$\chi^2 = \begin{pmatrix} P - \hat{P} \\ A^\circ - A - G \cdot (\hat{P} - P) \end{pmatrix}^\dagger \cdot \begin{pmatrix} N_p & 0 \\ 0 & N_{A^\circ} \end{pmatrix}^{-1} \cdot \begin{pmatrix} P - \hat{P} \\ A^\circ - A - G \cdot (\hat{P} - P) \end{pmatrix}, \quad (16)$$

and proceed, using standard techniques,<sup>8</sup> with the direct minimization of  $\chi^2$  by varying  $\hat{P}$ . In doing so we would not make use of the previously stated results (3b) and (4b). After some suitable manipulation we would obtain the solution:

$$P' - P = N_p \cdot G^\dagger \cdot (N_A + N_{A^\circ})^{-1} \cdot (A^\circ - A), \quad (17)$$

$$N_p - N'_p = N_p \cdot G^\dagger \cdot (N_A + N_{A^o})^{-1} \cdot G \cdot N_p \quad , \quad (18)$$

where the symbol not previously defined is  $N_A$  which is defined as:

$$N_A \equiv G^\dagger \cdot N_p \cdot G \quad . \quad (19)$$

$N_A$  is the covariance matrix of the vector  $A$ . We recall that the vector  $A$  is calculated from the input vector  $P$ , more specifically if  $A \equiv \{a_j\}$ ,  $a_j$  is given by:

$$a_j = \Sigma^{j\dagger} \cdot \Phi \quad . \quad (20)$$

Therefore,  $A$  and  $N_A$  are the predictions, based upon our *a priori* evaluations of  $\bar{\Phi}$  and  $\bar{\Sigma}$ , for the observed activities  $A^o$  and  $N_{A^o}$ .  $A$  and  $N_A$  play a crucial role in obtaining the solution  $P'$  and  $N'_p$ , as is evident from (17) and (18), since it is through them that we can make use of the dosimetry data of the problem:  $A^o$  and  $N_{A^o}$ .

We shall now indicate how we can obtain the results (17) and (18) from (3b) and (4b) using the definitions for the quantities  $Y^o$ ,  $M$ ,  $Y$ ,  $D$  and  $\bar{P}$  presented in the previous section. We shall consider this a proof of the results (17) and (18) since the derivation of (3b) and (4b) is well known.

Since  $N_p$  and  $N_{A^o}$  are square matrices, the inverse of  $M$  is:

$$M^{-1} = \begin{pmatrix} N_p^{-1} & 0 \\ 0 & N_{A^o}^{-1} \end{pmatrix} \quad . \quad (21)$$

Similarly, the inverse of  $N_p$  in (21) is obtained from the inverse of  $N_\Phi$  and  $N_\Sigma$  under the assumption that  $N_p$  is diagonal in the space of  $\Phi$  and  $\Sigma$ , as we shall take it to be for purposes of the following discussion. We have already discussed the reasons why if  $M$  is a "correct" covariance matrix of some observations it must be non-singular and therefore its inverse exists. The arguments apply directly to  $N_{A^o}$  since in our problem  $A^o$  corresponds to actual measurements. They should also

apply to  $N_{\phi}$  and  $N_{\Sigma}$  since these are taken as observations and if our evaluations are done correctly they can be traced to direct observations. In practice, however,  $N_{\phi}$  and  $N_{\Sigma}$  are likely to be singular for several reasons. We shall return later to a discussion of the covariance matrices  $N_{\phi}$  and  $N_{\Sigma}$  since they play an important role in our problem. We will therefore now proceed with the proof, as if  $N_{\phi}$  and  $N_{\Sigma}$  were non-singular, postponing until later our justification for doing so.

If we rewrite (3b) as:

$$(D^{\dagger} \cdot M^{-1} \cdot D) \cdot (P' - P) = D^{\dagger} \cdot M^{-1} \cdot (Y^{\circ} - Y) \quad , \quad (22)$$

and substitute the appropriate expressions for  $D$ ,  $M^{-1}$ ,  $Y^{\circ}$  and  $Y$ , we get:

$$(N_p^{-1} + G^{\dagger} \cdot N_{A^{\circ}}^{-1} \cdot G) \cdot (P' - P) = G^{\dagger} \cdot N_{A^{\circ}}^{-1} \cdot (A^{\circ} - A) \quad . \quad (23)$$

From (4b) we also get:

$$N_p' = (N_p^{-1} + G^{\dagger} \cdot N_{A^{\circ}}^{-1} \cdot G)^{-1} \quad . \quad (24)$$

We can readily rearrange the terms in (23) to obtain:

$$N_p^{-1} \cdot (P' - P) = G^{\dagger} \cdot N_{A^{\circ}}^{-1} \cdot (A^{\circ} - A - G \cdot (P' - P)) \quad . \quad (25)$$

A very elegant way to proceed from (25) is to introduce after Dragt *et al.*<sup>12</sup> the auxiliary quantity:

$$X \equiv N_{A^{\circ}}^{-1} \cdot (A^{\circ} - A - G \cdot (P' - P)) \quad , \quad (26)$$

and write (25) as:

$$P' - P = N_p \cdot G^{\dagger} \cdot X \quad . \quad (27)$$

If we then multiply (27) from the left by  $G$ , use the definition (19), after substitution of  $G \cdot (P' - P)$  in (26), we get:

$$X = (N_A + N_{A^{\circ}})^{-1} \cdot (A^{\circ} - A) \quad . \quad (28)$$

We need not worry about the existence of the inverse of  $N_A + N_{A^0}$  since it will always exist because the covariance matrix  $N_{A^0}$  is non-singular and  $N_A$  is symmetric. Substitution of (28) back into (27) yields our solution. In a similar fashion we can derive (18) from (24).

This basically concludes our proof and we can see that the expressions to obtain the solution  $P'$  and  $N_p'$  are very simple to calculate. This is clearly so when we show the simple form that  $N_A$  takes. From the definition (19) and using for  $N_p$  we have:

$$N_A = G \cdot \begin{pmatrix} N_\Phi & 0 \\ 0 & N_\Sigma \end{pmatrix} \cdot G^\dagger, \quad (29)$$

$N_A$  can therefore be written as the sum of two contributions:

$$N_A = N_A^\Phi + N_A^\Sigma, \quad (30)$$

where:

$$N_A^\Phi \equiv \{n_{ij}^\Phi\} = \{\Sigma^{i\dagger} \cdot N_\Phi \cdot \Sigma^j\}, \quad (31)$$

and:

$$N_A^\Sigma \equiv \{n_{ij}^\Sigma\} = \{\Phi^\dagger \cdot N_{\Sigma ij} \cdot \Phi\}. \quad (32)$$

When  $N_p$  is not diagonal in the space of  $\Phi$  and  $\Sigma$ , an additional "cross term" is required in  $N_A$ .

### Covariance Matrices of Evaluations

The primary purpose of this section is to justify some statements made in the previous section and clearly indicate some of the consequences for our solutions of certain approximations we are likely to make in the handling of covariances of evaluations. We claimed that the solution to the least-squares problem always existed because the covariance matrix  $M$  was always non-singular. However, during the course

of our proof when we came to invert the covariance matrices  $N_\phi$  and  $N_\Sigma$  we pointed out that in practice they were likely to be singular, but that we should proceed as if they were not. It is clear that since the matrix  $M$  cannot be in principle singular, we can say that its singularity resulted from a "mistake." We argue that this is possibly true, but wish to consider that the "mistake" was intentional in the sense that it corresponds to some approximation we intend to make and we are interested in obtaining a solution under such conditions. We shall show that we need not explicitly change our formulation to recognize this fact and can proceed as if these approximations had not resulted in a singular matrix for  $N_\phi$  or  $N_\Sigma$ . This property of our least-squares problem has very important practical consequences. On the one hand, if we have written a computer code to solve it, we can use it for obtaining solutions under various approximations which result in singular covariance matrices without having to change the code or otherwise communicate this fact to the code. On the other hand, it may be a disadvantage since we may not recognize that we have made some approximations we did not intend to make. Since this discussion will shed light upon the role which the covariance matrices of our evaluations play in general, and in the least-squares problem in particular, we shall carry it in some details. However, because a complete discussion of this interesting and possibly not well appreciated aspect of "uncertainties" in evaluations would carry us too far from our subject, we will not approach it in its greatest generality, but rather from a practical point of view.

We first emphasize that the covariance matrices  $N_\phi$  and  $N_\Sigma$  need not be singular. However, we conjecture that they may be singular under the assumptions we are likely to make at this stage in the handling of uncertainty information in evaluations and if we follow in the use of the least-squares method the same practices used with our current codes. We shall not argue against these assumptions and practices since they may be justi-

fied if only on grounds of convenience. Since at this stage rather little experience exists in the treatment of uncertainties in evaluations we are likely to concentrate on the description of the major or gross features of the problem and therefore the statement of the uncertainties is bound to be crude in the sense of having not too much detail. We may also, as is done in ENDF/B,<sup>10</sup> make some rather crude approximations which have great convenience as far as representing and processing the information to generate covariance matrices of processed data. These approximations being fully consistent with the perceived accuracies of the estimated uncertainties. Also, as a matter of convenience we may select a standard group structure to do our analyses with the result that it is not tailored to each problem, and in any problem this group structure is likely more detailed than is really needed or justified on the basis of information available, at least in some energy regions. The combination of the above two practices, which are likely to occur, will almost surely result in covariance matrices  $N_{\phi}$  and  $N_{\Sigma}$  which are singular. This is so because the dimension of our covariance matrices, the number of groups we use, will almost surely exceed their rank, which in a very direct sense corresponds to the "amount of information" we have included in our evaluations regarding their "uncertainties."

In order to facilitate the discussion let us consider some specific examples which we think embody the essence of the problem and may easily be generalized. For example, we take the spectrum in an energy region where there are several group fluxes  $\phi_j$ . We suppose that in our evaluation of the spectrum the statements concerning the uncertainties are such that the several group fluxes  $\phi_j$  should be considered as fully correlated. The covariance matrix of these group fluxes will have a dimension equal to the number of groups, but its rank will be one; it will therefore be singular and consequently the full covariance matrix  $N_{\phi}$  will also be singular and cannot be inverted. It is important to



note that since our covariance matrices are symmetric and positive definite the above mechanism is the only one which can be responsible for their singularity, a statement we shall not prove here. It is clear that since the several  $\phi_j$ 's are fully correlated they can be replaced by a single auxiliary variable and an exact linear transformation which relates it to the  $\phi_j$ 's. If these  $\phi_j$ 's were from "real independent measurements," this would be an inconsistency of sorts, but since we are dealing with "evaluations taken as measurements" this may not be a mistake and we can easily handle the problem. We could do so by formally replacing these  $\phi_j$ 's by the single auxiliary variable and the exact linear transformation, which could be obtained by inspection. The singularity of our covariance matrix of the parameters would then be removed and we could solve for the auxiliary parameter directly instead of these  $\phi_j$ 's. However, having obtained the solution for this auxiliary parameter, we could use our exact transformation to obtain the solution for the  $\phi_j$ 's and the resulting spectrum would be identical to the one obtained by the direct application of (17) and (18). We shall not formally introduce the transformation and prove this point by mathematical manipulations because it should be clear that what we have done is merely change the definition of the "parameter vector" and the transformation is already embedded in our sensitivity matrix G. In conclusion we see that we can always ignore the fact that the covariance matrices of our evaluations are singular and proceed formally as if they were not!

This discussion should make it clear that in a dosimetry problem the number of groups we use to analyze the problem does not at all correspond to the number of parameters we have. The number of parameters is determined by the rank of the covariance matrices from our evaluations. In practice we do not need to know how many parameters we really have to solve the problem, but it can easily be determined by inspection of the correlation matrix of  $\Phi$  and  $\Sigma$ . It should also be clear now that any

structure we have in our input spectrum in energy regions where the evaluations state that the spectrum is fully correlated is reproduced in our solution exactly. An extreme example of this is when our covariance matrix is fully correlated over the whole energy range. The auxiliary parameter is the normalization of the spectrum and the transformation is the shape of the spectrum. In this case, no matter how many activation measurements we have, the shape of the spectrum will remain unchanged and only its normalization will be determined. On the other hand, even with a single activation measurement, if the input covariance matrix  $N_{\phi}$  does not correspond to a fully correlated spectrum, both the shape and normalization of the spectrum are adjusted. It is important to keep in mind that what is being adjusted in the spectrum is entirely determined from the structure of the input covariance matrix based upon the uncertainties in the evaluation and is unrelated to the number of groups used or the number of activations available.

#### A Test for Consistency of the Data

We have already stressed the fact that the least-squares solution does not require that the joint density functions of the input data be normal. The only requirement is that the covariance matrices represent the second moment of the density functions. If the form of the density functions were known, or assumed to be known, we could go further than just obtain the solution (17) and (18); we could extract some additional information from the numerical value of the minimum of the  $\chi^2$ -function in the sense of being able to test the "likelihood" of the input data. Since such tests are often very useful in detecting mistakes, we believe that at least for purposes of such investigations we should assume that the density functions are known and argue on the basis of the "central limit theorem"<sup>8</sup> that we should take them to be normal. It is then

possible to perform two tests on the distribution of the input data. The well-known  $\chi^2$ -test may be used to estimate the likelihood of the input data set on the basis of the minimum value of  $\chi^2$ . In order to do so one needs to establish the number of degrees of freedom in the problem. If we have  $m$  cross sections and fluxes and  $n$  activation measurements, the total number of input quantities is  $m + n$ , but since we solve for  $m$  parameters we have only  $n$  degrees of freedom. Therefore, the  $\chi^2$  minimum corresponds to  $n$  degrees of freedom. We shall now show that the minimum value of  $\chi^2$  is entirely determined from the values of the input data. The minimum value of  $\chi^2$ ,  $\chi_m^2$ , is obtained by substituting the value of  $P'$  given by (17) for  $\hat{P}$  in (16). We therefore have,

$$\chi_m^2 = (P-P')^\dagger \cdot N_p^{-1} \cdot (P-P') + (A^\circ-A')^\dagger \cdot N_{A^\circ}^{-1} \cdot (A^\circ-A') \quad . \quad (33)$$

We may rewrite (33) as:

$$\chi_m^2 = \chi_p^2 + \chi_A^2 \quad . \quad (34)$$

Using (27) we may evaluate  $\chi_p^2$  as:

$$\chi_p^2 = (A' - A)^\dagger \cdot X \quad , \quad (35)$$

and also from (27), operating upon it with  $G$ , we get:

$$A' - A = N_A \cdot X \quad . \quad (36)$$

Substituting (36) into (35), we have:

$$\chi_p^2 = X^\dagger \cdot N_A \cdot X \quad . \quad (37)$$

To evaluate  $\chi_A^2$  we rewrite (26) as:

$$A^\circ - A' = N_{A^\circ} \cdot X \quad , \quad (38)$$

substituting (38) into the expression for  $\chi^2$  in (33), we have:

$$\chi_A^2 = X^\dagger \cdot N_{A^\circ} \cdot X \quad . \quad (39)$$

Using now (37) and (39), we obtain the desired result, if we use the expression (28) for X:

$$\chi_m^2 = (A^\circ - A)^\dagger \cdot (N_A + N_{A^\circ})^{-1} \cdot (A^\circ - A) \quad . \quad (40)$$

It is therefore clear from (40) that the minimum value of  $\chi^2$  can be evaluated easily from the input data. We can then test the likelihood of the input data, prior to obtaining the solution, by means of a  $\chi^2$ -test on  $\chi_m^2$  using as the number of degrees of freedom the number of activation measurements.

The second test on the input data can also be made from (40) by looking at the "randomness" of the terms which make up  $\chi_m^2$ . There are n terms which we must sum in the final stage of the computation of  $\chi_m^2$  in (40), and to each term we can associate a particular activation. The "fit" may not be good if one or a few activations contribute mostly to  $\chi_m^2$  and should be taken as a possible indication of a mistake to be investigated.

Finally, we should indicate that the predictions for the activations one will obtain from the solution P' can be obtained without solving for P'. If we operate on (17) with G from the left, we immediately get:

$$A' = A + N_A \cdot (N_A + N_{A^\circ})^{-1} \cdot (A^\circ - A) \quad . \quad (41)$$

If we now multiply (18) on the left by G and on the right by  $G^\dagger$ , we obtain:

$$N_A' = N_A - N_A \cdot (N_A + N_{A^\circ})^{-1} \cdot N_A \quad , \quad (42)$$

which gives us the covariance matrix of the activations calculated from the solution without having to explicitly calculate  $N_p'$  either.

### The Non-Linearity of the Problem

Our problem is a non-linear least-squares one. Since such problems are usually solved by iteration, as well as all of our current methods,

we must now discuss when we may gain from an iterative scheme to get our solution. We shall show that, although an iterative procedure will always somewhat improve the solution, in many practical situations such improvements may not be very significant and therefore some doubt always exists about its usefulness.

When solving a non-linear least-squares problem we must always linearize the model and in so doing make an approximation; in our case this was done in (12). Such linearization procedure involves an expansion, and the best expansion to make is about the solution. Since we usually do not know the solution, such expansion must be made about some "trial value" from which a trial solution is obtained. This "trial solution" is then used as a new "point" about which the model is expanded again. Therefore an iterative procedure is developed and progress toward a "converged solution" is usually monitored by observing the successive improvements in the  $\chi^2$  minimum at each step. In our case we chose as an expansion point the *a priori* evaluations  $P$  in order to generate  $P'$  and  $N'_p$ . It would appear that if we now go back and expand again our model using  $P'$  in (12) instead of  $P$ , we would get a better solution. We will now develop such an iterated solution. In order to develop a notation which incorporates iteration numbers in it, let us expand the model about  $P_n$ , instead of  $P$  in (12), and call the solution  $P_{n+1}$  instead of  $P'$ . If we proceed exactly as we did to obtain (17) and (18), we get:

$$P_{n+1} - P = N_p \cdot G_n \cdot (N_{A_n} + N_{A^0})^{-1} \cdot (A^0 - A_n - G_n \cdot (P - P_n)) \quad , \quad (17a)$$

$$N_p - N_p^{n+1} = N_p \cdot G_n^+ \cdot (N_{A_n} + N_{A^0})^{-1} \cdot G_n \cdot N_p \quad , \quad (18a)$$

where  $A_n$  is the activation vector calculated using  $P_n$ ,  $G_n$  is the sensitivity matrix (13) calculated using  $P_n$  and the quantity  $N_{A_n}$  is defined analogously to  $N_A$  in (19) and is:

$$N_{A_n} = G_n^+ \cdot N_p \cdot G_n \quad . \quad (19a)$$

If we now calculate the  $\chi^2$ -minimum for our iterated solution (17a),  $\chi^2_{m,n+1}$ , by proceeding exactly as we did to derive (40) from (17), we get:

$$\chi^2_{m,n+1} = (A^\circ - A_n - G_n \cdot (P - P_n))^\dagger \cdot (N_{A_n} + N_{A^\circ})^{-1} \cdot (A^\circ - A_n - G_n \cdot (P - P_n)) \quad . \quad (40a)$$

If we compare the above results to those obtained from the expansion about the *a priori* evaluations, we see two differences. The first one is the replacement of  $G$  and  $N_A$  by  $G_n$  and  $N_{A_n}$ , and the second one the replacement of  $A$  by  $A_n + G_n \cdot (P - P_n)$ . It is clear that if our input data  $A^\circ, N_{A^\circ}$  and  $P, N_p$  are "fairly consistent" to the extent that our *a priori* evaluations predict "well" the measurements  $A^\circ$ , that is we may compute  $A$  such that it agrees with  $A^\circ$  within the combined uncertainties  $N_A$  and  $N_{A^\circ}$ , then the  $\chi^2_m$  calculated using (40) will correspond to approximately one per degrees of freedom. In such cases within the uncertainties we will have  $A \approx A_n$ . Even if our data are somewhat "inconsistent" but not very improbable, say with a  $\chi^2_m$  less than 2 per degrees of freedom, then the approximation  $A \approx A_n$  may not be very good, but it is likely that within the uncertainties we will have  $A \approx A_n + G_n \cdot (P - P_n)$ . What we are arguing is that as long as our data are not too inconsistent then a linear model is very good; the non-linearity of the model is not important. As is well known,<sup>8</sup> if the model is exactly linear, it is not necessary to iterate to find the solution. In our case this should be reflected in our results (17a), (18a) and (40a) which will be close to (17), (18) and (40) if the data are not too inconsistent. We can see that directly if we substitute in (17a), (18a) and (40a)  $A = A_n + G_n \cdot (P - P_n)$  to get:

$$P_{n+1} - P = N_p \cdot G_n \cdot (N_{A_n} + N_{A^\circ})^{-1} \cdot (A^\circ - A) \quad , \quad (17b)$$

$$N_p - N_p^{n+1} = N_p \cdot G_n^\dagger \cdot (N_{A_n} + N_{A^\circ})^{-1} \cdot G_n \cdot N_p \quad , \quad (18b)$$

$$\chi^2_{m,n+1} = (A^\circ - A) \cdot (N_{A_n} + N_{A^\circ})^{-1} \cdot (A^\circ - A) \quad . \quad (40b)$$

Our solution (17b) and (18b) still does not quite look like the original one (17) and (18) since we have  $G_n$  and  $N_{A_n}$  instead of  $G$  and  $N_A$ . However, since  $N_{A_n} \approx N_A$  within the uncertainties of these quantities which are controlled by  $N_p$ , the  $\chi^2$ -minimum (40b) is not very different from the  $\chi^2_m$  given by (40) and therefore the results (17b) and (18b) are equivalent to (17) and (18) or more exactly the differences are not measurable from the  $\chi^2$ -minimum. We conclude then that if our data are not too unlikely, in the sense that  $\chi^2_m$  given by (40) is less than about 2 per degrees of freedom, we have little to gain by iterating in order to find the solution, the improved precision in the solution being not justified by its accuracy.

We see from the above analysis that the value of  $\chi^2_m$ , the "consistency" of our input data, indicates to us when we may gain significantly by an iteration scheme to get the solution. Such potential gains exist only when  $\chi^2_m$  per degrees of freedom is large. Unfortunately, in such cases we may not exploit fully the benefit of iterating to improve our results since the data are then so unlikely that the credibility of the solution is low. We must assume that very likely a mistake has been made somewhere and should be corrected to restore some credibility in the answer. We will not discuss the various methods which may be used in such situations; these different strategies, however, have all the same result, which is to reduce effectively  $\chi^2_m$  to be about one per degrees of freedom. There is then very little need to iterate in order to find the solution which would not become much more credible.

The above result which may appear surprising – very little use of the non-linearity of the model can be taken advantage of by iterations which would improve the solution – is not unique to our dosimetry problem. This feature is common to all non-linear least-squares problems where a "few integral results" are available and *a priori* knowledge about the solution is introduced in the form of "fully evaluated differential data" to exploit

these "integral results." In this strategy we merely want our "*a posteriori* evaluations" to reflect the "new information" present in the integral data. It is clear that through the "integral data" we cannot learn much about the "differential quantities" unless we have "strong inconsistencies." When the integral data are relatively consistent with our differential data, the integral results will not cause our knowledge of the individual differential quantities to be modified. Their values and their variances will not be changed significantly, i.e.  $P' \approx P$  and the diagonal elements of the covariance matrices  $N_p'$  and  $N_p$  will also be about the same. What the least-squares method does is change as little as possible each parameter, but modifies as many as possible in such a highly correlated fashion to reproduce as best it can the integral results. In such conditions the only significant information we get deals with the correlations of the differential quantities and these are expressed by the off-diagonal elements of  $N_p'$  the output or *a posteriori* covariance matrix. The potential for improvements in our knowledge of the individual differential quantities exists, and therefore the need for an iterated solution, only when there are very significant differences between, or inconsistencies in, our two types of input data. Their usefulness in improving our knowledge of the individual differential quantities is, however, limited by our inability to claim with confidence that the "inconsistencies" are "real" and not the results of "mistakes."

The above discussion is very general and does not make use of the explicit form of the "model" of the integral quantities in our dosimetry problem. There are two situations where the dosimetry method is often used, and the model becomes "effectively linear" even though  $\chi_m^2$  may be large. These situations occur when either  $\bar{\Phi}$  or  $\bar{\Sigma}$  is known *a priori* to a much higher relative accuracy than the other. In such cases the model is "quasi-linear" because the non-linear terms  $(\bar{\Sigma}^i - \Sigma^i)^\dagger \cdot (\bar{\Phi} - \Phi)$  become effectively small in an absolute sense whether we choose our *a priori* or *a posteriori* estimates



to expand the model. In these cases again iterations are not needed, even though  $\chi_m^2$  may be large, because the model is "effectively linear" and the "differential quantities" which are not as well known relatively will be the only ones changed significantly. These situations may occur in "standard fields applications" when  $N_\phi$  is relatively much better known and in "practical applications" where it is  $N_\Sigma$  which is relatively much better known.

### The Least-Squares Analysis Code STAY'SL

The above method of analysis of dosimetry data has been incorporated into a computer code STAY'SL which has been documented<sup>13</sup> and is available from the Radiation Shielding Information Center (RSIC) at Oak Ridge National Laboratory.

In STAY'SL we calculate explicitly only the values of  $\Phi'$  and  $N_\phi'$ ; therefore, two possible interpretations of the code output can be made. The first one is that the full solution for  $P'$  is not obtained, although both  $\Phi$  and  $\Sigma$  are "adjusted." A code for generating the full solution (i.e., including  $\Sigma'$  and  $N_\Sigma'$ ) will soon be released. The other interpretation is that in STAY'SL the cross sections (i.e.,  $\Sigma$ ) are assumed to be only "formally adjustable" during the analysis in order to propagate their uncertainties to the solution. The covariance matrix  $N_{A_0}$  of the measured activations was modified by adding to it the matrix  $N_A^\Sigma$ , given by (31), and obtained from an estimate of  $N_\Sigma$ , in order to take into account the fact that our "model" [i.e., expression (5)] is inexact. In doing so we claim to have properly taken into account the "approximations" in our model (i.e., the cross sections). This second interpretation of the solution of STAY'SL has, we believe, some interesting implications concerning the general use of the method of least-squares when the "model" is known to be deficient and suitable "methods" or "approximation" parameters may be introduced, with assigned uncertainties, such that within these uncertainties the "model" can be claimed to be exact.

## Comparison with Other Methods

It is evident from the above discussion that the least-squares method has the potential for providing a solution which incorporates in principle all of the available information concerning the problem in a straightforward manner and at the same time giving us the "best" such solution in the sense of the minimum variance theorem. In practice this potential can only be realized at some costs. We will first discuss briefly each type of information used as input and analyze how close in practice, and at what costs, we can come to utilize "all of the information" available.

Concerning the activation measurements, it should be relatively easy to use all of the information available. In particular, the correlations of the different activations, which are not used at all presently or are used in an unknown manner through the use of so-called "calibrated methods," should be easily handled. In order to do so, however, the experimentalist must provide the covariance matrix of the measurements or preferably report the analysis of the uncertainties in the data in such a way that these estimates may be evaluated and the covariance matrix easily generated from the information. In the past such types of information were not used very explicitly; therefore, there was little incentive to provide it in a clear fashion and only the standard deviations of the activations were usually reported.

Concerning the dosimetry cross sections, it should also be possible to come close to utilizing most of the information available. The starting point is always a detailed evaluation of the differential data. In the past very few evaluations were made with enough details available concerning the uncertainties in the evaluated data to allow the covariance matrices to be generated. In the ENDF/B files it is now possible to communicate this information<sup>10</sup> and hopefully in ENDF/B-V all dosimetry cross sections will have data such that the covariance matrices can be generated for any group structure. Our knowledge of the dosimetry cross

sections does not come only from differential measurements. However, if we have evaluated differential data files with correlations indicated, they can be exploited, using the same least-squares method discussed here, to generate new evaluations which incorporate the results of integral measurements obtained in benchmark and standard fields. We have already discussed<sup>4</sup> that some care must be exercised regarding how we accomplish this last step if we are not to run into large computational problems. We therefore believe that the methodology exists for generating dosimetry cross sections which will come close to reflecting adequately almost all of our information regarding how well we know them.

We believe then that the major obstacle which must be overcome to use "all of the information" available in our solution to the dosimetry analysis problem is the determination of appropriate  $\Phi$  and  $N_\Phi$ . Because this problem is specific to every spectrum being analyzed, we can only discuss it in general terms. The approach to this problem is, however, straightforward even if we will usually run into practical difficulties in finding its solution. The *a priori* spectrum  $\Phi$  can always be obtained as a combination of whatever data are available and the results of appropriate transport calculations. Since this is what is often done now in order to generate the "input spectrum" to our current methods, we shall not discuss this aspect further. Therefore, it may be perceived at this stage that the major obstacle will be the generation of an appropriate covariance matrix  $N_\Phi$ . The procedure for obtaining  $N_\Phi$  is in principle easy since it is merely a statement of how well we believe we know  $\Phi$ . Although some subjective elements will always exist in our estimation of  $N_\Phi$ , some degree of credibility can be achieved if we analyze with care the source of our uncertainties in  $\Phi$ . It is often perceived that the "uncertainties" in  $\Phi$  come from two major sources: uncertainties in the basic nuclear data used in the computations and

approximations made in the computations. Using sensitivity methods, it is in principle straightforward to propagate the uncertainties of the input data to the resulting spectrum. The question of the approximations made in the computations is more difficult, but the covariance matrix  $N_{\phi}$  must certainly reflect the uncertainties in  $\phi$  due to them.

In the near future, since much of our information is not codified in the appropriate form, some of the benefits of the method may not be realized. We have already discussed<sup>4</sup> the fact that in such cases all we can expect is more credible answers than we currently obtain merely by using more credible input data. In the past, various methods<sup>7</sup> have been devised to compare the various unfolding codes. A particularly useful one is to obtain the solution to a given problem using the same input data by different codes and compare the ratios of the output and input spectra. The comparison of these ratios for different codes such as SAND-II, SPECTRA and CRYSTAL BALL is very instructive since it shows rather large differences which are indicative of the various algorithms used. For these codes this ratio is not unique for a given problem, but also depends upon a number of input quantities having to do with the algorithms and not related to the problem being solved. In the case of the least-squares method, this ratio can easily be obtained from (17) and is simply:

$$\frac{\phi_j^i}{\phi_j} = 1 + \sum_{i,k,\ell,r} m_{\phi_{j\ell}} \sigma_{\ell}^i \phi_{\ell} w_{ik} (a_k^{\circ} - \sigma_r^k \phi_r) \quad , \quad (43)$$

where  $m_{\phi_{j\ell}}$  is the relative covariance of the flux  $\phi_j$  and  $\phi_{\ell}$  and the  $w_{ik}$ 's are the matrix elements of the matrix  $(N_A + N_{A^{\circ}})^{-1}$ , the weight matrix  $W$ , all other symbols in (43) having been defined previously.

It is evident that the purpose of any dosimetry spectrum unfolding code is to modify the "input spectrum" in order to obtain an output spectrum which is consistent with the measured activations. It is also

clear that we want these modifications of the input spectrum to occur in such a way that they are consistent with how well we know various features of the input spectrum. How well we know the various features of the input spectrum is, of course, problem-dependent and is communicated by means of the covariance matrix  $N_\phi$ . Even though the unfolding codes SAND-II, SPECTRA, and CRYSTAL BALL do not require that we directly input  $N_\phi$ , we may view them as strategies to obtain the solution (43) and therefore look upon the algorithms as having built into them an effective covariance matrix  $N_\phi$ . A difficulty with these codes is that this effective covariance matrix is unknown, fixed once and for all, and to be used in all unfolding situations regardless of how well we know the input spectrum  $\phi$ . It is also evident that this effective covariance matrix is different for each one of these codes. Consequently, it is difficult to compare the solutions of these codes with the output of STAY'SL since we cannot use exactly the same input data. In fact, it is difficult to compare the output of these codes among themselves because they all in a direct sense do not solve exactly the same problem due to their different effective  $N_\phi$ .

It is clear from the algorithms of SAND-II, SPECTRA, and CRYSTAL BALL that these codes can produce a solution which will reproduce as well as we care to state the measured activities. However, we know that often this is done by introducing in the solution what is referred to as "unphysical oscillations." In fact, we use that name to indicate that these features of the solution are thought inconsistent with our *a priori* knowledge of the spectrum. Therefore, we must conclude that it is possible to operate these codes in such a manner that their effective covariance matrices are unreasonable. This fact is well known and is often expressed by saying that these codes cannot be used as "black boxes" and require considerable expertise to be used to generate acceptable solutions.<sup>5</sup> It is therefore not possible to use as a figure of

merit for the solutions how well the input activities are numerically reproduced.

There exists a very straightforward way to compare the various methods. It is to ask, "How well do the different solutions predict the results of computations based upon them?" By "how well," we mean how small are the uncertainties in the results of computations using the solution. A measure of these uncertainties is the variance of the results in question. In order to be able to answer this very important question we need to know what are the uncertainties in the solution (i.e., its covariance matrix  $N'_{\phi}$ ). In the case of the least-squares method,  $N'_{\phi}$  is given simply using relation (18). In the case of the other methods, we do not know what the uncertainty in their solution is since it is usually not calculated in any well defined manner. We have discussed previously<sup>4</sup> how to generate the uncertainties in the solution of the usual unfolding codes on the basis of the input data uncertainties, but will repeat here some of the method since it will allow us to make a very strong argument as to why not only in theory but also in practice we should use the least-squares method.

The solution to the problem,  $\phi'$ , by whatever method it is calculated, is a function of the input quantities  $A^{\circ}$ ,  $\phi$  and  $\Sigma$ . A straightforward method to propagate to the solution the uncertainties in the input data is to calculate the sensitivity of the solution to the input parameters. Let us construct such a sensitivity matrix  $S$  given by:

$$d\phi' = S \cdot \begin{pmatrix} dA^{\circ} \\ d\phi \\ d\Sigma \end{pmatrix} . \quad (44)$$

The elements of the matrix  $S$  are the partial derivatives of the output fluxes with respect to all the input data. Since in our usual methods we do not have a simple expression which relates the solution to the input data, the matrix  $S$  must be obtained by numerical methods and

this may be a very large computational task which can be carried out at least in principle. (Some of the diagonal elements of the matrix S are related to the often used "improvement ratios."<sup>7</sup>) Once one has the matrix S, we can obtain the covariance matrix  $N_{\phi}^!$  by the relation:

$$N_{\phi^!} = S \cdot \begin{pmatrix} N_{A^{\circ}} & 0 & 0 \\ 0 & N_{\phi} & 0 \\ 0 & 0 & N_{\Sigma} \end{pmatrix} \cdot S^{\dagger} \quad , \quad (45)$$

where the matrices  $N_{A^{\circ}}$ ,  $N_{\phi}$  and  $N_{\Sigma}$  are the very same quantities which were discussed in connection with the least-squares method. Expression (45) indicates that if we are interested in obtaining the uncertainties in the solution of our usual methods we must generate and use the same covariance matrices required by the least-squares method. The problems which may be perceived in using the least-squares method due to the requirement of having such covariance matrices are therefore not unique to it but also present when we want to answer the question, "What are the uncertainties in the solution?", regardless of how we obtain the solution. If we obtained  $N_{\phi}^!$ , using (45) for our current methods, we then could answer the question: How good are the predictions which we can make using the solutions?. In order to pick a large class of possible applications in which we might use  $\phi^!$ , let us consider a "result" r which is obtained as a linear combination of the  $\phi_j^!$ 's. We define r in terms of the vector R whose elements are the coefficients of the linear combination of the  $\phi_j^!$ ; we therefore write

$$r = R^{\dagger} \cdot \phi^! \quad . \quad (46)$$

Then the variance of r, which we write as  $V_r$ , is just:

$$V_r = R^{\dagger} \cdot N_{\phi^!} \cdot R \quad . \quad (47)$$

The vector R is completely arbitrary and we might suggest that several such vectors R may be of particular importance in our dosimetry problem.

For instance, we might think of  $r$  as being one of the activations which were measured, in which case  $R$  is just  $\Sigma^i$ . Another pertinent example is one where  $r$  is some damage parameter, in which case  $R$  is the corresponding "damage function."

In some very real sense, if we carried out the above calculations, we could say that the better method is the one which produces the smaller value of  $V_r$ . The minimum variance theorem guarantees that whatever is the set of input data and the vector  $R$  the solution from the least-squares method is guaranteed to give the smallest variance  $V_r$ . We can now continue our discussion of the comparison of the different codes on the basis of how well their solutions reproduce the measured activations. As we discussed before, the codes SAND-II, SPECTRA, and CRYSTAL BALL could be run such that the numerical values of the "output activations" agree with the measured values better than the output of STAY'SL, but we would be wrong to conclude that their solution is therefore better. We have just proven that this "numerically better agreement" is purely fortuitous since the uncertainties in these numbers, whether we actually compute them or not, are likely to be bigger and can be no smaller than those obtained by the least-squares method. In addition, the running time by the least-squares method is not larger for the same size problem.

### Summary and Conclusions

The problem of dosimetry neutron spectrum unfolding has received considerable attention and much progress has been made in developing algorithms (SAND-II, SPECTRA and CRYSTAL BALL) which are perceived to give much promise even though their solutions to the same problem are sometimes quite different. Through extensive comparisons of the output of these codes for the same problem and the development of various quantities to allow some aspects of the solutions to be investigated, much insight has been gained into these algorithms and the nature of the few-



channel unfolding problem. Dosimetry spectrum unfolding, as practiced now with these codes, still remains difficult and requires much expertise to produce generally acceptable solutions. Until now very little attention has been given to the problem of analyzing in a credible manner the uncertainties in the solutions, with the exception of the SAND-II code where Monte Carlo is used to provide an estimate of some of the uncertainties. We have shown that the propagation to the solutions of these codes of the uncertainties in the input data was in principle straightforward. The uncertainty in the solution due to all of the input data uncertainties, as given by their covariance matrices, can be obtained by generating the sensitivity matrix of the solution with respect to the input data. This method of obtaining the uncertainties in the solution of these codes requires, however, a large computational effort which probably would be prohibitive for routine use. The approach to uncertainty estimate of SAND-II could also be improved to take into account important correlations which are currently neglected, but this method<sup>4</sup> also runs rapidly toward large computational problems. We believe that, if these calculations were made, a large part of the subjectivity currently needed to assess the "goodness" of these solutions would be eliminated. There would, however, still remain a problem related to the heuristic nature of these algorithms for the solution.

We have shown in this paper, and a previous one,<sup>4</sup> that given the input data required to obtain our current solutions and estimate the uncertainties due to the input data, a solution can be obtained using the least-squares method. We have reviewed in some detail the assumptions of the least-squares method and some of the properties of its solution in an effort to establish that this least-squares method did not require any more assumptions than we currently make. The solution by the least-squares method is extremely easy to obtain given the required input data, is unique and in a very real physical sense provides the

best possible solution under the circumstances (i.e., the assumptions made and the intended use of the solution), and also easily provides the uncertainties in the spectrum. We, therefore, believe that this least-squares method provides the solution which we have sought for the dosimetry spectrum unfolding. A computer code STAY'SL, which calculates this solution, is now available.

Although the method now exists for computing a satisfactory solution to the dosimetry unfolding problem, much work remains to be done in most cases in order to obtain the best answers. We believe that most of our efforts should be devoted to the codification of our uncertainties in the evaluations used as input data to be able to generate covariance matrices. Although this is likely to be a substantial amount of work, we also think that much of the methodology exists to carry out this task. In particular, with respect to dosimetry cross sections, where much thought has already gone into this problem and a formalism created in ENDF/B to handle the covariance matrix information, hopefully most of these data will soon become available with ENDF/B-V. Regarding the uncertainties in the input spectrum, much progress has already been made in the area of computing the sensitivity coefficients in transport applications in order to propagate nuclear data uncertainties. However, much work remains to be done regarding the estimation of uncertainties in transport problem solutions due to the various approximations made.

Finally, although the method of least-squares we propose is very likely satisfactory for most problems, in some situations it may not be entirely adequate to obtain only the second moment of the joint density function of the spectrum as the least-squares method does. We believe that as we gain experience with the least-squares method and improve considerably our perception of the uncertainties in nuclear data the need may arise to go beyond their representation in terms of only the second moment of the density functions. Then more powerful methods

capable of dealing with higher moments of the density functions will be needed. How urgently we need to explicitly develop such methods for the dosimetry problem is a matter of conjecture now and will depend, we believe, very much upon the progress we make in understanding the nature of the uncertainties in nuclear data and the problems we face when trying to handle only the second moments of their estimated joint density functions. To a large degree the nature of those more powerful methods will be dictated by the kinds of problems we encounter.

### Acknowledgments

I acknowledge with great pleasure the assistance of many colleagues in the dosimetry community for stimulating my interest in this field and acting as an invaluable source of information, in particular the members of the CSEWG Dosimetry Subcommittee, its chairman, Ben Magurno, and W. L. Zijp.

I wish to thank especially R. W. Peelle for his continued willingness to participate in long discussions held while the ideas presented in this paper were being explored and formulated. His thorough criticisms of the first draft of this paper were particularly helpful in pointing out the major weaknesses of the original presentation.

The seemingly endless iterative procedure developed to generate this paper would have been unbearable without J. C. Gentry's willingness to retype it *ad infinitum*, and I thank her for it.

### REFERENCES

1. C. A. Oster, W. M. McElroy, and J. M. Marr, "A Monte Carlo Program for SAND-II Error Analysis," HEDL-TME-73-20 (February 1973).
2. C. R. Greer, J. A. Halbleib, and J. V. Walker, "A Technique for Unfolding Neutron Spectra from Activation Measurements," ISC-RR-67-746 (December 1967).
3. F. B. K. Kam and F. W. Stallmann, "CRYSTAL BALL — A Computer Program for Determining Neutron Spectra from Activation Measurements," ORNL/TM-4601 (June 1974).

4. F. G. Perey, "Uncertainty Analysis of Dosimetry Spectrum Unfolding," Proceedings Second ASTM-EURATOM Symposium on Reactor Dosimetry, Palo Alto, California, October 3-7, 1977 (to be published).
5. R. Dierckx and V. Sangiust, "Unfolding Codes for Neutron Spectra Evaluation Possibilities and Limitations," ISPRA, June 1975, EUR/C/IS/365/75e.
6. W. R. Burrus, "FERD and FERDO Type of Unfolding Codes," in ORNL/RSIC-40 (October 1976).
7. W. L. Zijp and H. J. Nolthenius, "Progress Report: Intercomparison of Unfolding Procedures," in ORNL/RSIC-40 (October 1976).
8. B. R. Martin, Statistics for Physicists, Academic Press, London, 1971.
9. M. Petilli, "The Unfolding Code DANTE and its Application," in ORNL/RSIC-40 (October 1976).
10. F. G. Perey, "The Data Covariance Files for ENDF/B-V," ORNL/TM-5938, ENDF-249 (July 1977).
11. A. K. McCracken and M. J. Grimstone, "The Experimental Data Processing Program RADAK," Proceedings of the Specialists Meeting on Sensitivity Studies and Shielding Benchmarks, OECD and IAEA, Paris, October 1975.
12. J. B. Dragt, J. W. M. Dekker, H. Gruppelaar, and A. J. Janssen, Nucl. Sci. Eng. 62, 117 (1977).
13. F. G. Perey, "Least-Squares Dosimetry Unfolding: The Program STAY'SL," ORNL/TM-6062, ENDF-254 (October 1977).

PROGRESS REPORT ON THE IAEA ACTIVITY  
ON NEUTRON SPECTRA UNFOLDING BY  
ACTIVATION TECHNIQUE

International Atomic Energy Agency, Vienna

C. Ertek

B. Cross

M.F. Vlasov

Abstract

This paper reviews the current status and procedures associated with neutron spectrum unfolding by activation technique within the IAEA programme on standardization of reactor radiation measurements.

Experimental efforts and calculations related to unfolding are briefly reviewed, including additional activation foils, neutron self-shielding factors, impurities, gamma-ray absorption effects, interlaboratory co-operation, re-evaluation of some cross-sections, scattering effects, the methods of analysis of neutron flux spectra.

I. Introduction

The International Atomic Energy Agency has set up a programme on standardization of reactor radiation measurements (1). The programme was initiated by the Physics Section of the Seibersdorf Laboratory in co-operation with the Nuclear Data Section, the Reactor Physics Section of the Division of Nuclear Power and Reactors and with the support of the Computer Section.

Among several techniques used at present for neutron spectrometry (time-of-flight, semiconductor counters, scintillation counters, track counting, ionisation etc.), the foil activation technique has several advantages. These advantages, especially for in-pile measurements, were recognized by scientists and this technique is now commonly used in many laboratories.

The development of the multiple foil neutron activation technique in the last years has allowed one to obtain detailed spectrum information for the whole energy range of importance for reactor technology. Only a rough estimation of the thermal and fast neutron flux can be obtained when using less sophisticated techniques.

Specialists working in this field have realized (Meetings of IAEA Consultants in Vienna in 1973, 1974; and at Petten in 1975; ASTM-EURATOM Symposium, Petten, 1975) that due to insufficient standardization, this technique cannot be used in a consistent way on an international scale. It was suggested that the Agency should take some actions concerning the necessary standardization.

These actions should include:

1. Intercomparison of available computer programmes for spectrum unfolding in order to recommend the best ones for general use;
2. Preparation of a recommended energy-dependent neutron activation cross section file;

3. Recommendation of best values for the relevant disintegration parameters, such as half-lives, gamma yields etc.;
4. Preparation of suitable standard active foils to permit standardization of the foil activity measurements;
5. Preparation of suitable non-active foils having the same size as standard active ones.

In order to assess the opinion of the international scientific community regarding their abilities and needs concerning neutron dosimetry a questionnaire has been distributed.

Brief analysis (2) of the responses to the questionnaire:

About 200 copies of the questionnaire have been distributed to reactor centers in Member States (1). At this time 105 responses have been received. These may be divided into two categories:

1. Responses of high interest for this programme: 80 (including 16 from developing countries);
2. Responses of low interest: 25 (from centers where no research related to this programme is underway).

The main questions from the questionnaire and the answers received are summarized to illustrate in more detail the interest of institutes to different points related to our programme:

Question 13. Would you like to receive recommended cross section files for threshold detectors, prepared and maintained by the IAEA?

Answers: 71 yes, including 15 from developing countries.

Question 16. Would you like the IAEA to assist you in obtaining a computer code which would be recommended on the basis of the proposed international intercomparison?

Answers: 54 yes, including 14 from developing countries.

Question 17. Would you be interested in obtaining from the IAEA unirradiated standard foil material for use as threshold detectors?

Answers: 44 yes, including 15 from developing countries.

Question 18. Would you like to obtain from the IAEA standard radioactive sources for calibration, related to above-mentioned materials?

Answers: 44 yes, including 15 from developing countries.

33 of the responding institutes (including 4 from developing countries) show that they have enough experience and equipment to benefit from this programme immediately. These institutes have some unfolding computer programmes, partly written in these laboratories themselves and partly received from outside, as well as information on neutron cross sections of different qualities.

20 institutes (including 6 from developing countries) would like to introduce the multiple foil activation technique for spectra determination, provided they will get assistance from the IAEA.

The sophisticated codes, the SAND II (12) and the CRYSTAL BALL (48) are available for distribution by the Agency. At present, special permission must be required from ERDA for every individual request.

## II. Present Status and Activities

### 1. Saturation Activities

#### 1.1. Disintegration parameters of the radionuclides.

The corresponding half-lives and  $\gamma$ -ray yields of the produced radionuclides for the reactions indicated in TABLE 1 are under investigation by the IAEA Nuclear Data Section. Following the IWGRRM recommendations, a list of the 90% response intervals for these reactions in various neutron spectra have been obtained by IAEA's Seibersdorf Laboratory. Some saturation activities were obtained in SNIF, Standard Neutron Irradiation Facility, installed near the core of the ASTRA swimming pool type reactor at Seibersdorf Laboratory. The SNIF is a cylindrical irradiation container (diameter 43 cm, height 46 cm) with lead walls and a neutron filter of boron carbide to reduce the gamma dose rate and the thermal neutron flux. A detailed description of the SNIF is given elsewhere (3 - 5).

The results can be seen in TABLE 2. Ertek's results are preliminary and the work is still in progress. Nevertheless, the comparison of two sets of results show interesting systematical differences between the two experiments which were performed with an approximately two years' interval. The following factors may be responsible for these differences:

TABLE 1. Reactions indicating first (I) and second (II) foil sets.

$^{23}\text{Na}(n,\gamma)^{24}\text{Na}$	(I)	$^{63}\text{Cu}(n,\gamma)^{64}\text{Cu}$	(II)
$^{24}\text{Mg}(n,p)^{24}\text{Na}$	(II)	$^{63}\text{Cu}(n,\alpha)^{60}\text{Cu}$	(II)
$^{27}\text{Al}(n,p)^{27}\text{Mg}$	(I)	$^{63}\text{Cu}(n,2n)^{62}\text{Cu}$	(II)
$^{27}\text{Al}(n,\alpha)^{24}\text{Na}$	(II)	$^{90}\text{Zr}(n,2n)^{89}\text{Zr}$	(I)
$^{31}\text{P}(n,p)^{31}\text{Si}$	(II)	$^{103}\text{Rh}(n,n')^{103}\text{Rh}^m$	(I)
$^{32}\text{S}(n,p)^{32}\text{P}$	(I)	$^{109}\text{Ag}(n,\gamma)^{110}\text{Ag}^m$	(I)
$^{45}\text{Sc}(n,\gamma)^{46}\text{Sc}$	(I)	$^{115}\text{In}(n,\gamma)^{116}\text{In}^m$	(I)
$^{46}\text{Ti}(n,p)^{46}\text{Sc}$	(II)	$^{115}\text{In}(n,n')^{115}\text{In}^m$	(II)
$^{47}\text{Ti}(n,p)^{47}\text{Sc}$	(II)	$^{127}\text{I}(n,2n)^{126}\text{I}$	(I)
$^{48}\text{Ti}(n,p)^{48}\text{Sc}$	(II)	$^{197}\text{Au}(n,\gamma)^{198}\text{Au}$	(II)
$^{55}\text{Mn}(n,\gamma)^{56}\text{Mn}$	(I)	$^{232}\text{Th}(n,f)$	(II)
$^{54}\text{Fe}(n,p)^{54}\text{Mn}$	(I)	$^{232}\text{Th}(n,\gamma)^{233}\text{Th}$	(I)
$^{56}\text{Fe}(n,p)^{54}\text{Mn}$	(II)	$^{235}\text{U}(n,f)$	(I)
$^{58}\text{Fe}(n,\gamma)^{59}\text{Fe}$	(I)	$^{238}\text{U}(n,f)$	(I)
$^{59}\text{Co}(n,\gamma)^{60}\text{Co}$	(II)	$^{238}\text{U}(n,\gamma)^{239}\text{Pu}$	(II)
$^{58}\text{Ni}(n,p)^{58}\text{Co}$	(I)	$^{237}\text{Np}(n,f)$	(II)
$^{58}\text{Ni}(n,2n)^{57}\text{Ni}$	(I)	$^{239}\text{Pu}(n,f)$	(II)

TABLE 2. Reaction Rates.

Reaction	Isotopic Abundance %	Radiation (keV)	Half-life	CZOCK (3) Sat.Act. (dps)x10 <sup>-15</sup>	ERTEK, C. Sat.Act. (dps)x10 <sup>-15</sup> (without Cd)	With Cd Cover
<sup>24</sup> Mg(n,p) <sup>24</sup> Na	100	γ, 1368.55	15 h	0.015 <sub>±2.3%</sub>	0.0176 <sub>±2.7%</sub>	0.00842 <sub>±2.6%</sub>
<sup>27</sup> Al(n,α) <sup>24</sup> Na	100	γ, 1368.55	15 h	0.0074 <sub>±1.2%</sub>	0.00988 <sub>±1.6%</sub>	0.00842 <sub>±2.6%</sub>
<sup>27</sup> Al(n,p) <sup>27</sup> Mg	71.4	γ, 843.76	9.46 min	0.0283 <sub>±4 %</sub>	—	—
<sup>32</sup> S (n,p) <sup>32</sup> P	100	β	14.3 d	0.385 <sub>±1 %</sub>	—	—
<sup>46</sup> Ti(n,p) <sup>46</sup> Sc	100	γ, 889.3	83.85 d	0.0767 <sub>±2.4%</sub>	—	—
<sup>47</sup> Ti(n,p) <sup>47</sup> Sc	69	γ, 159.4	3.4 d	0.109 <sub>±1.1%</sub>	—	—
<sup>48</sup> Ti(n,p) <sup>48</sup> Sc	100	γ, 983.3	43.8 h	0.003 <sub>±2.8%</sub>	—	—
<sup>54</sup> Fe(n,p) <sup>54</sup> Mn	100	γ, 834.81	312.6 d	0.476 <sub>±1 %</sub>	—	—
<sup>56</sup> Fe(n,p) <sup>56</sup> Mn	99	γ, 846.6	2.576 h	0.0103 <sub>±3 %</sub>	0.0126 <sub>±3.4%</sub>	—
<sup>55</sup> Mn(n,γ) <sup>56</sup> Mn	99	γ, 846.6	2.576 h	21.8 <sub>±0.3%</sub>	34.028 <sub>±0.7%</sub>	11.625 <sub>±1.7%</sub>
<sup>58</sup> Ni(n,p) <sup>58</sup> Co	99.4	γ, 810.6	71.3 d	0.648 <sub>±1 %</sub>	0.677 <sub>±1.4%</sub>	—
<sup>103</sup> Rh(n,n') <sup>103</sup> Rh <sup>m</sup>	6.76	x, 20	56.116 min	6.47 <sub>±2.4%</sub>	—	—
<sup>115</sup> In(n,n') <sup>115</sup> In <sup>m</sup>	45.9	γ, 335	4.5 h	1.42 <sub>±1 %</sub>	1.895 <sub>±1 %</sub>	1.761 <sub>±2.1%</sub>
<sup>115</sup> In(n,γ) <sup>116</sup> In <sup>m</sup>	83.4	γ, 1293.4	54.03 min	267 <sub>±2 %</sub>	—	—
<sup>197</sup> Au(n,γ) <sup>198</sup> Au	95.5	γ, 410.8	2.69 h	390 <sub>±0.2%</sub>	604.06 <sub>±0.2%</sub>	364.54 <sub>±1 %</sub>



- a) There are some changes in the core configuration due to burn-up, inclusion of new fuel elements, control rod movements etc.
- b) Reproducibility in the positioning of the assembly is not always satisfactory. This factor is an important one and it is unfortunately very common in reactor irradiations. It makes irradiation after long intervals unpredictable.
- c) Encapsulation of foil packages needs special attention. Different absorption and perturbation by containers may have some effect on the results.

Other effects and work on  $^{115}\text{In}(n,\gamma)^{116}\text{In}^m$ ,  $^{46}\text{Ti}(n,p)$ ,  $^{47}\text{Ti}(n,p)$ ,  $^{48}\text{Ti}(n,p)$ ,  $^{54}\text{Fe}(n,p)$  and  $^{103}\text{Rh}(n,n')^{103}\text{Rh}^m$  is in progress. Burn-up and slightly different core configuration effects will be investigated further.

### 1.2. Reactions $^{103}\text{Rh}(n,n')^{103}\text{Rh}^m$ and $^{199}\text{Hg}(n,n')^{199}\text{Hg}^m$ .

The absolute  $^{103}\text{Rh}^m$  disintegration rate produced by the reaction  $^{103}\text{Rh}(n,n')^{103}\text{Rh}^m$  in Rh-foils has been determined by K.H. Czock (6) at the IAEA's Seibersdorf Laboratory and introduced as a new detector for neutron flux density spectrum measurements.

Lately, some experiments with the reaction  $^{199}\text{Hg}(n,n')^{199}\text{Hg}^m$  have been performed after a suggestion from the IAEA Nuclear Data Section (7). This reaction is used in the USSR as a reactor dosimetry standard for integral measurements although insufficient cross section information is available (8 - 11). Mercury could be useful as detector for thermal and fast neutrons.

Mercuric acetate powder was irradiated in the ASTRA swimming pool type reactor and the SNIF container described above. When the pure powder was used, some evaporation took place during the irradiation. Therefore, different amounts of mercuric acetate, from 40 mg to 260 mg, were mixed with graphite, and the pellets were pressed. The irradiations were performed with and without Cd-cover. The activities of the pellets were assayed by Ge(Li)- $\gamma$ -spectrometry. Peaks at 158.37 and 374.0 keV are due to  $^{199}\text{Hg}^m$  (see Fig. 1).

Fig. 1 shows the ASTRA core and the SNIF results. It indicates the possibility to use the 134 keV peak from the reaction  $^{196}\text{Hg}(n,\gamma)^{197}\text{Hg}$  for thermal neutron detection together with the reaction  $^{199}\text{Hg}(n,n')^{199}\text{Hg}^m$  for the fast neutrons. The attenuation of the thermal neutrons in the SNIF facility can easily be seen by comparing the ratios of the peaks at 134 and 158 keV. This work will be continued.

### 1.3. Gamma ray absorption effects.

There are strong indications that the self-shielding and  $\gamma$ -self-absorption effects inside high Z materials such as Hg are not taken into account correctly. The absorption coefficient for 158 keV adopted by Vasil'ev (8) turned out to be about a factor of 0.57 smaller than given by Storm and Israel (50). Corrections up to 28 % had to be applied in our case when the latter's values are adopted. Although proper  $\gamma$ -self-absorption corrections were made, discrepancies up to 16% have been found between the activities as determined from the 158 keV and 374 keV peak areas, when the efficiency curve of the Ge-detector for point sources was used.

Part of such discrepancies might be explained by the application of point source calibration curves to extended sources measured at small distances from the detector.

#### 1.4. Neutron self-shielding factor.

##### 1.4.1. Energy dependent self-shielding factors.

In the self-shielding factor determination there are many discrepancies between calculations and experimental results (13). For the flux depression factor, the theory of Skyrme (14) as modified by Ritchie and Eldridge (15) yields still higher values than the measured ones. Unexplained discrepancies between the results of experiment and theory remain (16). A.M. Barsky and H.J. Nolthenius have published a series of self-shielding G factors for a few activation detectors (13). The  $\sigma$ -values, modified with G should be used in the computer codes. The cross section values for neutron self-shielding are used (13) by SAND-II in the activity mode to calculate the activity of the foil. This activity is divided by the activity calculated with the original uncorrected cross section to obtain the integral self-shielding correction G factor from literature (17 - 23). The justification of using the total cross section to find the G factor and applying this factor to the activation cross section needs further careful investigations. One of the main conclusions of Barsky's (13) was that the self-shielding factors at individual resonance peaks are much lower at low energies than "expected". The "expected" results are the experimental results of G factors found by McElroy (18), Fabry (24) and Selander (25). Also (13) the self-shielding factors which are calculated for foils with a strong scattering contribution to the total cross section seem to be incorrect. An overestimation of the self-shielding is found for these reactions.

These results showed that unfortunately the prediction of self-shielding and other related factors like edge factor and flux depression are far from being satisfactory. Especially, if one takes the case of self-shielding of  $^{59}\text{Co}$  in the CFRMF neutron spectrum (26, 27) and  $1/E$  neutron spectrum, the discrepancies are high (Table 8 and Fig. 7 of Ref. 13). With the CFRMF spectra and  $1/E$  neutron spectrum, the use of total cross sections from the ENDF/B-IV file yield much too low G values, especially at the resonance peak region. However, Barsky and Nolthenius (13) do not give the results obtained by the ENDF/B-IV absorption cross section values. Calculations with ENDF/B-III without scattering cross sections underestimate the G values (Table 9 of Ref. 13).

For  $^{55}\text{Mn}$ , both the ENDF/B-III without scattering and the ENDF/B-IV with total cross sections give G values much lower than "expected" for the resonance peaks at energies of a few hundred eV (Table 10 and Fig. 9 of Ref. 13).

##### 1.4.2. $^{115}\text{In}(n,\gamma)^{116}\text{In}^m$ resonance parameters.

These results show clearly that more calculations and experiments are needed to find the effective and accurate ways of estimating (if possible) the self-shielding and related factors, especially in low energy resonance peaks.

Bearing in mind this need, an abstract (PHI/I 13) under the title "An investigation on the thickness dependence of the total and capture cross section determination" has been prepared by C. Ertek (28). In this work a detailed investigation of the capture and total cross-section measurements for the  $^{115}\text{In}(n,\gamma)^{116}\text{In}^m$  capture reaction around the 1.456 eV first

resonance is discussed. Sample thickness determination criteria are reviewed from statistical and systematic points of view. It has been established (29) that most of the results from old activation measurements on radiative-capture cross-sections for 14 - 15 MeV neutrons are in error due to the fact that corrections for secondary neutron capture in the sample have been ignored. The present work (to be issued as an IAEA publication of Seibersdorf Laboratory) shows clearly the systematic error involved in the radiative-capture cross section and possibly in the total cross section determination in the electron volt range for the above capture reaction. These results are applicable to any other detector material for the unfolding foil activation technique.

That work investigates in detail the specific activation rates (activity per nucleus per second) for a variety of target foil thicknesses ranging from  $1.10^{-4}$  cm to  $23.10^{-4}$  cm in the 1.456 eV resonance region. Special attention is paid to the energy distribution of neutrons in thin targets. The dependence of thickness in the competition between absorption and scattering events is investigated in detail. The report describes the results (using the model of S. Pearlstein and E.V. Weinstock (30)) of the  $^{115}\text{In}(n,\gamma)^{116}\text{In}^m$  capture reaction, when a beam of mono-energetic neutrons of 1.456 eV resonance energy impinges perpendicular to indium targets of different thicknesses.

#### 1.4.3. Sample thickness selection criteria.

The present work brings a new criterium instead of the imprecise  $N\sigma d \ll 1$  or  $N\sigma d < 1$  criteria: i.e. the thickness of the foil must be chosen before the transmission measurement, such that by using the best available cross-section data, activity per nucleus per second is calculated as a function of target thickness starting from  $10^{-2}$  cm up to  $10^{-6}$  cm range. The thickness for which the curve shows a saturation behaviour must be chosen for a resonance parameter  $\sigma_0$  determination. Probably, this thickness will be extremely thin. In this case, some alloy of the material similar to Fleck's must be used (31).

The  $N\sigma d \ll 1$  criteria is not satisfied in most of the early transmission measurements, e.g. in the resonance parameters measurement of  $^{113}\text{Cd}$ , the thinnest sample used was 0.002809 cm thick and it gave in  $N\sigma d$  value of 1.00 which does not satisfy this condition (32).

The experimental results of this work showed clearly that the penetration of neutrons into the sample was deeper than predicted (33). This result is in agreement with the recent results of L. Kuijpers (34).

Even for a one micron cover thickness, considerable influence on the detector activity could be seen around 1.456 eV. In the target preparation a difference of 0.1 micron thickness has a very considerable influence on the experimental determination of the peak cross-section point,  $\sigma_0$ . Recent results (35) clearly indicate that the evaporated foils tested were more uniform (thickness variations  $\leq 1\%$ ) than those foils of a similar thickness produced by rolling. The great majority of foils are rolled for transmission measurements.

#### 1.4.4. Scattering Effects.

The experimental results and the calculations are in agreement with S. Pearlstein's (30) conclusions that the scattering effects on foil activation are significant. The effects are largest for thin resonance

detectors,  $1/v$  detectors of almost any practical thickness in a beam flux, and thick resonance detectors in an isotropic flux. The development has been restricted, in the isotropic case, to foils irradiated in a void (30) or in water (36, 37) whereas often the foil or its cadmium cover is embedded in a scattering and absorbing medium. In the latter case the incoming flux may no longer be isotropic, thereby violating one of the basic assumptions of the calculation given in Ref. (30). The magnitude of the scattering effect found by Parlstein (30) does not agree with Tsuchihashi and Iizumi (38). Walker (36) concludes that contrary to earlier predictions (37), the flux perturbation theories based upon isotropic models cannot be used to predict the perturbations induced in all non-isotropic fluxes. These results show that in a region near an absorber or boundary, the flux depression actually decreases due to the increased importance of second and third flight scatterings back into the region of the foil. This "boundary" effect is extremely important in "relative" flux measurements for neutron spectrum dosimetry with perturbing foils in the vicinity of reactor fuel plates and control rods since the flux perturbations will be functions of position from the absorber. This is very important for the preparation of foil packages in the vicinity of power reactors. Because of this effect, the perturbation, for example, due to a 2 cm diameter foil of thickness 0.1 cm, may differ as much as 20% from its isotropic value. The maximum change occurs within one mean free path of the boundary. Unfortunately, the water gap between reactor fuel plates is usually of this order of magnitude. Thus, it is concluded that very thin foils should be used for accurate neutron flux measurements.

If the foil packages are irradiated in air, near, for example, the pressure vessel, extensive streaming calculations (e.g. 39,40) should be considered for each experimental set-up. Thus it is highly desirable to have a special study group working only on these effects in specific irradiation arrangements for neutron dosimetry and damage determinations especially in reactor materials. Synthesis of the available results on specific foil arrangements are lacking.

On the other hand, the synthesis of the scattering and/or double differential cross-section measurements with total and partial cross-section measurements is required for nuclei for which these cross-sections are relatively well known.

Parametrization of R-Matrix multi-level formula (41, 42) including resolution and Doppler broadening for heavy nuclei needs further refinements in this application.

Resonance self-shielding calculations using the probability table method (known as PTM) are extremely promising for the resolution of the problems stated (43).

### 1.5. Impurities.

The material used as neutron dosimeters must be accurately defined and contain a minimum amount of impurities. Enriched isotopes are sometimes required. A pool of such materials including fissionable materials should be established, possibly by the IAEA at its Seibersdorf Laboratory (44). The Agency should promote the establishment of a close working relationship between different centers which fabricate and provide such detector materials (44). Some further steps toward that action have been taken at the Seibersdorf Laboratory. Investigation of the purity of some foils obtained is proceeding.

## 1.6. Reaction Rate Ratios.

There are some preparations for the double reaction rate ratio measurements, which are extremely sensitive to neutron spectral shape differences as described by Doroshenko et al. (45).

## 1.7. Interlaboratory Efforts.

Discrepancies of about 10% exist between absolute average cross-section measurements in the  $^{235}\text{U}$  fission neutron spectrum. An interlaboratory experiment is being organized under the sponsorship of the IAEA, in order to investigate these discrepancies and it involves the transfer of irradiated detectors (mainly Ni-58, U-238 and U-235 foils) between Mol (Belgium), Osaka (Japan), Seibersdorf Laboratory (IAEA), and laboratories participating in the US Interlaboratory LMFBR Reaction Rate (ILRR) Programme.

It was recommended by the "IAEA Consultants' Meeting on Integral Cross Section Measurements in Standard Neutron Fields" (Vienna, 15-19 Nov. 1976) that the scope of this intercomparison be enlarged so as to encompass as many contributions as possible from other interested laboratories (44). This action is awaiting the supply of these special foils from the National Bureau of Standards (NBS, USA) to Mol for irradiation as promised (46).

## 1.8. New activation foils.

The introduction of new suitable materials such as  $^{186}\text{W}$ ,  $^{231}\text{Pa}$ ,  $^{236}\text{U}$  etc. is under consideration and some preliminary encouraging results were obtained using  $^{186}\text{W}$  foils in ASTRA and SNIF facilities.

## 2. Evaluation of the Saturation Activity Results

### 2.1. SAND-II.

The SAND-II unfolding code has been obtained and converted to IBM-370/145; the documentation of the improved version has been prepared.

### 2.2. DETAN 74.

DETAN 74 (an auxiliary programme which computes integral detector responses and transforms detector cross-sections from any fine group structure into a coarse one and vice versa) has been rewritten into DETAN 75.

### 2.3. ENDF/B IV.

The ENDF/B IV cross-section library for dosimetry applications was rewritten by programme ENDFSAND-A into 621 group cross-sections as used by SAND II.

### 2.4. Re-evaluation of some cross-sections.

A new evaluation of some cross sections is in progress to improve the quality of the data.  $^{46}\text{Ti}$ ,  $^{47}\text{Ti}$ ,  $^{48}\text{Ti}$  cross-sections are re-evaluated by using new results (47).

### 2.5. CRYSTAL BALL.

We have received the computer code package CCC-233 (18) CRYSTAL BALL (48) for unfolding. It will take approximately 30 hours of machine time

before it is ready for preliminary calculations with the IAEA's computer IBM 370/158. Laboratories are kindly requested to send some (up to 250 digital values) of their best known flux spectra points together with some reaction rate results of activation foils to the first author of this report. Then we can perform the unfolding with SAND-II and eventually CRYSTAL BALL and send back the results.

## 2.6. Critical evaluation of codes.

The following procedure was suggested by McCracken (UK) in order to find the effect of the number of foils on the resulting spectrum:

- a) Take a suitable neutron spectrum
- b) Calculate the saturation activities using ENDF/B IV cross-section library (49)
- c) Divide the saturation activities into two subgroups
- d) Reestimate the flux densities using these two subgroups
- e) Taking one of the subgroup spectra, calculate the other groups' saturation activities or vice versa and compare the results.

We have already performed such calculations (TABLES 3 and 4) and have sent the results to McCracken. The results are encouraging since by the SAND-II analysis we were able to predict with few exceptions the reaction rates within 3 or 4%. Work is in progress as to the optimum number of foils and the ratio of thermal to threshold foils is concerned. Some activities will be deleted next.

## 2.7. Cf-252 Spectrum.

We plan to find the neutron flux density spectrum and compare the results by taking the measured saturation activities in the vicinity of Cf-252 and applying SAND-II. Some portion of this work has been performed but there were many difficulties in the low energy part of the spectrum. Further work is needed.

## 2.8. Other Spectra.

Procedure 2.7. will be systematically applied for LWR core spectrum, LWR pressure vessel spectrum, LMFBR core spectrum and CTR first wall spectrum.

## 2.9. Compilation Work.

Compilation work for spectra obtained by calculation and/or by direct spectrometry and for corresponding measured reaction rates is in progress as recommended by IWGRRM. The following environments were considered:

- 1) 1/E
- 2) Sodium
- 3) Iron block
- 4) LWR core and pressure vessel
- 5) HTGCR moderator
- 6) LMFBR core and blanket
- 7) CTR first wall and blanket
- 8) Fission spectrum.

TABLE 3. Comparison of reaction rates before and after procedure by SAND II. First set of foils ((I) in Table 1).

Reaction	Reaction rates (DPS/nucleus)		Difference (Col.3-Col.2) %
	before procedure	after procedure	
$^{23}\text{Na}(n,\gamma)^{24}\text{Na}$	3.997 E - 26	4.112 E - 26	+ 2.88
$^{27}\text{Al}(n,p)^{27}\text{Mg}$	8.853 E - 28	8.673 E - 28	- 2.03
$^{235}\text{U}(n,f)\text{FP}$	4.084 E - 23	4.193 E - 23	+ 2.67
$^{238}\text{U}(n,f)\text{FP}$	6.976 E - 26	6.984 E - 26	+ 0.11
$^{232}\text{Th}(n,\gamma)^{233}\text{Th}$	3.432 E - 24	3.502 E - 24	+ 2.04
$^{32}\text{S}(n,p)^{32}\text{P}$	1.474 E - 26	1.386 E - 26	- 5.97
$^{127}\text{I}(n,2n)^{126}\text{I}$	1.439 E - 28	1.331 E - 28	- 7.50
$^{45}\text{Sc}(n,\gamma)^{46}\text{Sc}$	1.713 E - 24	1.778 E - 24	+ 3.79
$^{115}\text{In}(n,\gamma)^{116}\text{In}^m$	8.984 E - 23	9.561 E - 23	+ 6.42
$^{54}\text{Fe}(n,p)^{54}\text{Mn}$	1.825 E - 26	1.754 E - 26	- 3.89
$^{58}\text{Fe}(n,\gamma)^{59}\text{Fe}$	1.251 E - 25	1.277 E - 25	+ 2.08
$^{58}\text{Ni}(n,2n)^{57}\text{Ni}$	6.104 E - 31	6.022 E - 31	- 1.34
$^{58}\text{Ni}(n,p)^{58}\text{Co}$	2.433 E - 26	2.360 E - 26	- 3.00
$^{90}\text{Zr}(n,2n)^{89}\text{Zr}$	1.955 E - 29	1.919 E - 29	- 1.84
$^{55}\text{Mn}(n,\gamma)^{56}\text{Mn}$	1.373 E - 24	1.406 E - 24	+ 2.40
$^{109}\text{Ag}(n,\gamma)^{110}\text{Ag}^m$	2.801 E - 24	2.688 E - 24	- 4.03
$^{103}\text{Rh}(n,n')^{103}\text{Rh}^m$	2.252 E - 25	2.180 E - 25	- 3.20

TABLE 4. Comparison of reaction rates before and after procedure by SAND II. Second set of foils((II) in Table 1).

Reaction	Reaction rates (DPS/nucleus)		Difference (Col.3-Col.2) %
	before procedure	after procedure	
$^{63}\text{Cu}(n,\alpha)^{60}\text{Co}$	9.927 E - 29	1.026 E - 28	+ 3.35
$^{239}\text{Pu}(n,f)\text{FP}$	8.453 E - 23	8.665 E - 23	+ 2.5
$^{238}\text{U}(n,\gamma)^{239}\text{U}$	1.117 E - 23	9.345 E - 24	-16.34
$^{197}\text{Au}(n,\gamma)^{198}\text{Au}$	6.836 E - 23	6.823 E - 23	- 0.19
$^{59}\text{Co}(n,\gamma)^{60}\text{Co}$	4.936 E - 24	4.810 E - 24	- 2.55
$^{63}\text{Cu}(n,\gamma)^{64}\text{Cu}$	4.404 E - 25	4.356 E - 25	- 1.09
$^{232}\text{Th}(n,f)\text{FP}$	1.727 E - 26	1.786 E - 26	+ 3.42
$^{24}\text{Mg}(n,p)^{24}\text{Na}$	2.966 E - 28	3.112 E - 28	+ 4.92
$^{46}\text{Ti}(n,p)^{46}\text{Sc}$	2.652 E - 27	2.654 E - 27	+ 0.075
$^{47}\text{Ti}(n,p)^{47}\text{Sc}$	4.061 E - 27	4.206 E - 27	+ 3.57
$^{48}\text{Ti}(n,p)^{48}\text{Sc}^*$	4.446 E - 29	4.828 E - 29	+ 8.59
$^{63}\text{Cu}(n,2n)^{62}\text{Cu}^*$	2.009 E - 29	2.031 E - 29	+ 1.095
$^{31}\text{P}(n,p)^{31}\text{Si}^*$	7.836 E - 27	8.045 E - 27	+ 2.67
$^{56}\text{Fe}(n,p)^{56}\text{Mn}^*$	2.366 E - 28	2.403 E - 28	+ 1.56
$^{237}\text{Np}(n,f)\text{FP}^*$	4.330 E - 25	4.279 E - 25	- 1.18
$^{27}\text{Al}(n,\alpha)^{24}\text{Na}^*$	1.281 E - 28	1.366 E - 28	+ 6.64
$^{115}\text{In}(n,n')^{115}\text{In}^m^*$	4.824 E - 26	4.949 E - 26	+ 2.59

\*) the curves "7 foils" in Figures 3 - 5 are obtained using the reactions indicated by asterisk in this Table.



## 2.10. Analytical Calculations.

The IAEA is promoting a systematic study of the merits and shortcomings of the most promising unfolding codes in comparison with analytical calculations and measurements other than activation foils.

## 2.11. Analysis protocol of fluxes.

In order to define a method of testing and analysis, the quantity called F is introduced in the following way:

$$F = \sqrt{\frac{\sum_i \Delta E_i \times \left( \frac{\phi_{\text{true}} - \phi_{\text{solution}}}{\phi_{\text{true}}} \right)^2}{\sum_i \Delta E_i}}$$

for each of the following energy ranges (10 ranges):  
 $10^{-10} - 10^{-7}/10^{-7} - 10^{-6}/\dots/10^0 - 10/10 - 18 \text{ MeV}.$

Differences in flux spectra will be measured by this quantity (examples Figure 2). Flux shape anomalies can be seen in Figures 3-5.

## 2.12. Self iteration.

B. Cross' (IAEA) idea to observe how closely the results of unfolding agreed with a synthetic spectrum used for calculating a self-consistent set of foil activities was completed recently by C. Ertek (IAEA) and B. Cross. The results proved very satisfactory.

## 2.13. High energy anomalies.

High energy anomalies have been observed in the Betatron neutron spectrum unfolding using SAND-II (Fig. 6).

### Final Remark

The success of the programme depends on the continuous and active interest of the laboratories of the Member States.

### Acknowledgements

The authors are grateful to W.N. McElroy (HEDL), C.Z. Serpan, Jr. (NRC), U. Farinelli (CNEN, CSN), A. Fabry (CEN-SCK), J.A. Grundl (NBS), S. Pearlstein (BNL), W.L. Zijp (ECN), A.K. McCracken (AEEW), S.B. Wright (UKAEA), P. Mas (CEA), I. Kimura (Osaka), V. Benzi (Centro di Calcolo, Bologna) and J.T. Routti (Helsinki University of Technology) for their guidance, interest in, and valuable and continued support of this programme.

The authors also thank A.J. Polliart, J.J. Schmidt, H. Houtermans, J.A. Larrimore, R.M. Lessler, J.A. Phillips and V. Chernyshev for support and valuable comments on this programme.

We are indebted to F.B.K. Kam and B.F. Maskewitz (Oak Ridge National Laboratory, USA) for sending us the computer code package CCC-233/CRYSTAL BALL for unfolding.

A final note of appreciation goes to T. Casta (ASTRA), K. Schürf, N. Haselberger and F. Reichel from Seibersdorf Laboratory for their many technical contributions.

#### REFERENCES

1. K.H. CZOCK, M. VLASOV, V. CHERNYSHEV, and B. CROSS, Interoffice Memoranda to the Director General, "The IAEA Programme on Standardization of Reactor Radiation Measurements", IAEA, (16 March 1976).
2. C. ERTEK, and B. CROSS, "Review of the Status of Intercomparison of Neutron Flux Spectrum Determination using Activation Detectors", Annual Meeting of the International Working Group on Reactor Radiation Measurements, IAEA, Vienna (10 - 12 Jan. 1977).
3. K.H. CZOCK, A.M.V. VAN DER VLOEDT, B. MALEKGHASSEMI, M. TAHER, N. HASELBERGER, "Dose Rate Determination by the Application of the Multiple Foil Activation Technique and Computer Programmes", IAEA, (Oct. 1976).
4. A. BURTSCHER, "Neutron Irradiation of Seeds, Tech.Rep.Ser. IAEA, No. 92, p. 97 (1968).
5. J. CASTA, "Radiobiological Application of Neutron Irradiation, Proceedings of a Panel, IAEA, p. 9 (1971).
6. K.H. CZOCK, N. HASELBERGER, and F. REICHEL, "The Disintegration of  $^{103}\text{Rh}^m$ ", International Journal of Applied Radiation and Isotopes, Vol. 26, pp. 417 - 421 (1975).
7. M. VLASOV, Private communication, Nuclear Data Section, IAEA (1977).
8. R.D. VASIL'EV, "Metrology of Neutron Radiation in Reactors and Accelerators", Publishing House for Standards, 76-0750, Moscow (1972).
9. BORNEMIZA, et al., "Atomki Kozlemeryek 10, 112 (1968).
10. HANKLA, et al., Nucl. Phys. 180 A, 157 (1972).
11. PETO, et al., Acta Phys. Ac.Sec.Hung. 33, 363 (1973).
12. W.N. MCELROY et al., "SAND-II, Neutron Flux Spectra Determinations by Multiple Foil Activation Iterative Method", TSIC Computer Code Collection. CCC112 (Oak Ridge National Laboratory, Radiation Shielding Information Center (May, 1969).
13. A.M. BARSKY, H.J. NOLTHENIUS, "Neutron Self-Shielding of Activation Detectors using Total Cross Section Values from the ENDF/B-IV Library, RCN-75-156 (Nov. 1976).
14. T.H.R. SKYRME, "Reduction in Neutron Density caused by an Absorbing Disc., UKAEA-MS 91 (1961).
15. R.H. RITCHIE, H.B. ELDRIDGE, "Thermal Neutron Flux Depression by Absorbing Foils, Nuc. Sci. Eng. 8, 300 (1960).

16. F. BENCH, "Flux Depression and the Absolute Measurement of the Thermal Neutron Flux Density", Atomkernenergie Vol. 25, No. 4 (1975).
17. N.P. BAUMANN, "Resonance Integrals and Selfshielding Factors for Detector Foils, DP-817 (E.I. du Pont de Nemours and Co., Savannah River Lab., Aiken, South Carolina, January 1963).
18. W.N. McELROY, "LMFBR Reaction Rate and Dosimetry 8th Progress Report for Period March-Sept. 1973", HEDL-TME-73-54, Hanford Engineering Dev. Lab., Richland, Washington, USA, Feb. 1974.
19. G.C. HANNA, "The Neutron Flux Perturbation due to an Absorbing Foil, a comparison of Theories and Experiments", Nuc. Sci. Eng. 15, 325(1963).
20. G.R. DALTON, R.K. OSBORN, "Flux Perturbations by Thermal Neutron Detectors", Nuc. Sci. Eng. 9, 198 (1961).
21. R.K. OSBORN, "A Discussion of Theoretical Analyses of Probe-Induced Thermal Flux Perturbations", Nuc. Sci. Eng. 15, 245 (1963).
22. M. BROSE, "Zur Messung und Berechnung der Resonanz Absorption vor Neutronen in Goldfolien", Nukleonik 6, 134 (1964).
23. T. NODA, H.J. NOLTHENIUS, "Neutron Selfshielding of Activation Detectors calculated with the Programs SELFS and SAND-II, RCN-75-092 (Reactor Centrum Nederland, Petten, July 1975).
24. A. FABRY, G. DE LEEUW, S. DE LEEUW, "The Secondary Intermediate Energy Standard Neutron Field at the Mol- Facility", Nuclear Technology, Vol. 25 (349-375), Feb. 1975.
25. W.N. SELANDER, "Theoretical Evaluation of Selfshielding Factors due to Scattering Resonances in Foils" AECL No. 1077 (Atomic Energy of Canada Limited, Chalk River, Ontario, June 1960).
26. G. DE LEEUW-GIERTS, S. DE LEEUW, H.H. HELMICK, J.W. ROGERS, "Neutron Spectrometry Data in LMFBR Benchmark and Standard Neutron Fields. ASTM-EURATOM Symposium on Reactor Dosimetry (Sep. 1975).
27. J.W. ROGERS, Y.D. HARKER, D.A. MILLSOP, "Fast Neutron Spectrum and Dosimetry Studies in the Coupled Fast Reactivity Measurements Facility. ASTM-EURATOM Symposium on Reactor Dosimetry (Sep. 1975).
28. C. ERTEK, Cont. Paper (PHI/I/13), "An Investigation on the Thickness Dependence of the Total and Capture Cross-Section Determination", International Conf. on the Interactions of Neutrons with Nuclei, Lowell, Mass., USA, 1976.
29. NEANDC Topical Conference on Capture Cross-Section Measurements, Harwell, 9 April 1975. Report AERE-R 8082, P. 19.
30. S. PEARLSTEIN, E.V. WEINSTOCK, "Scattering and Self-Shielding corrections in Cadmium-Filtered Gold, Indium and  $1/v$  Foil Activation Measurements", Nucl. Sci. and Eng. 29, 28-42 (1967).
31. C.M. FLECK, "Resonance Parameter Determination of the Main Resonance of Indium by Activation Foils", Nucleonik, Band 12, Heft 6.

32. R.O. AKYUZ, C. CANSOY, F. DOMANIC, "Parameters for the First Neutron Resonance of  $^{113}\text{Cd}$ , CNAEM Report No. 45 (1967).
33. C. ERTEK, B. CROSS, II. "Review of the Status of Intercomparison of Neutron Flux Spectrum Determination using Activation Detectors. Cont. Paper at the annual Meeting of the International Working Group on Reactor Radiation Measurements, IAEA Vienna, 10 - 12 Jan. 1977.
34. L. KULJPERS, "Experimental Model Studies for Fusion Reactor Blanket, PhD Thesis, Kernforschungsanlage Jülich GmbH, FRG.
35. C.J. SOFIELD et al., "Uniformity of Aluminium Foils", Nucl. Inst. and Methods, 138, 411-413 (1976).
36. J.V. WALKER, "The Effects of Flux Anisotropy on Thermal Neutron Flux Perturbations", Nuc.Sci. Eng. 22, 94-101 (1965).
37. G.R. DALTON, R.K. OSBORN, "The Effect of Flux Anisotropy on Neutron-Detector Foils", Nuc. Sci. Eng. 20, 481-492 (1964).
38. K. TSUCHIHASHI, M. IIZUMI, "Calculation of Effective Cut-Off Energies Taking into Account Scattering and Higher Resonances of Filters", Nuc. Sci. Tech. 2, 506 (1965).
39. G.P. BEER, "Differential Neutron Albedos for Cylindrical Water Surfaces", Nuc. Eng. and Design 33, 422-434 (1975).
40. G.P. BEER, "Neutron Streaming through Conical Ducts in a Water Shield", Nuc. Eng. and Design 33, 435-442 (1975).
41. A.M. LANE, R.G. THOMAS, "Rev. Mod. Physics 30, 257 (1958).
42. F. H. FRUHNER, "A Multi-Level Shape Analysis Program for Resonance Parameter Determination by Least-Squares Fitting of Several Sets of Neutron Transmission Data Simultaneously", KFK 2129, (Jan. 1976).
43. E.F. PLECHATY, D.E. CULLEN, "Resonance Self-Shielding Calculations using the Probability Table Method", UCID-17230 (Aug. 1976).
44. M. VLASOV, Editor, "IAEA Consultants' Meeting on Integral Cross-Section Measurements in Standard Neutron Fields", Vienna, 15-19 Nov. 1976, Summary Report, INDC(NDS)-81/L+M, March 1977.
45. J.J. DOROSHENKO, et al., "New Methods for Measuring Neutron Spectra with Energy from 0.4 eV to 10 MeV by Track and Activation Detectors", Nuclear Technology Vol. 33, May 1977.
46. Communication among McELROY, A. FABRY, H. HOUTERMANS, I. KIMURA and C. ERTEK, Vienna, Jan. 1977.
47. C. PHILIS, O. BERSILLON, D. SMITH, A. SMITH, ANL/NDM-27, January 77.
48. F.B.K. KAM, F.W. STALLMANN, CRYSTAL BALL Report ORNL-TM-4601 (Oak Ridge National Laboratory, Tennessee, June 1974).
49. B.A. MAGURNO, ENDF/B-IV Dosimetry File BN1-NCS-50446 (Brookhaven National Laboratory, April 1975).
50. E. STORM and H.I. ISRAEL, Nuclear Data Tables A-7, 565 (1970).

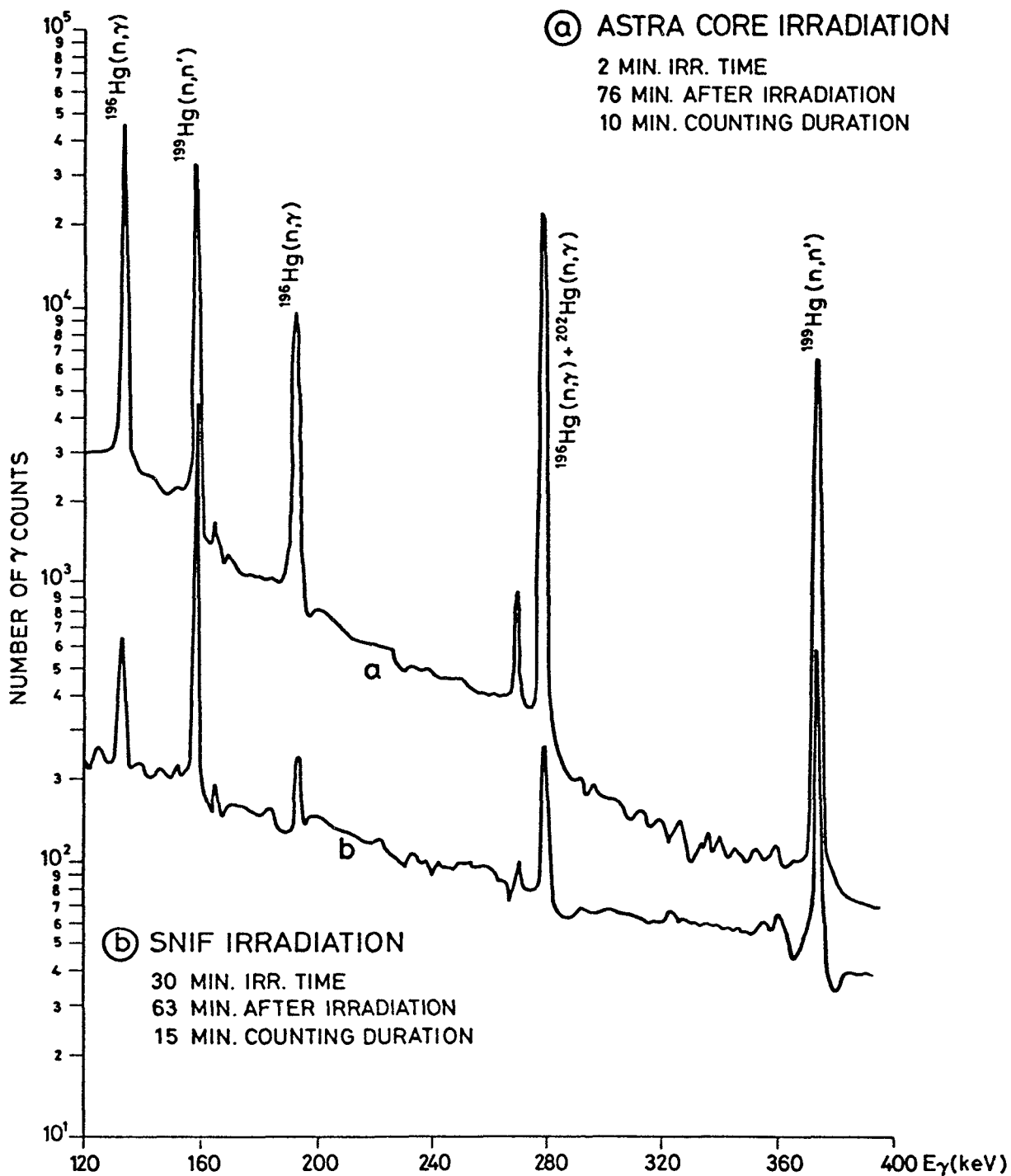


FIG. 1. GAMMA SPECTRA FROM Hg SAMPLES

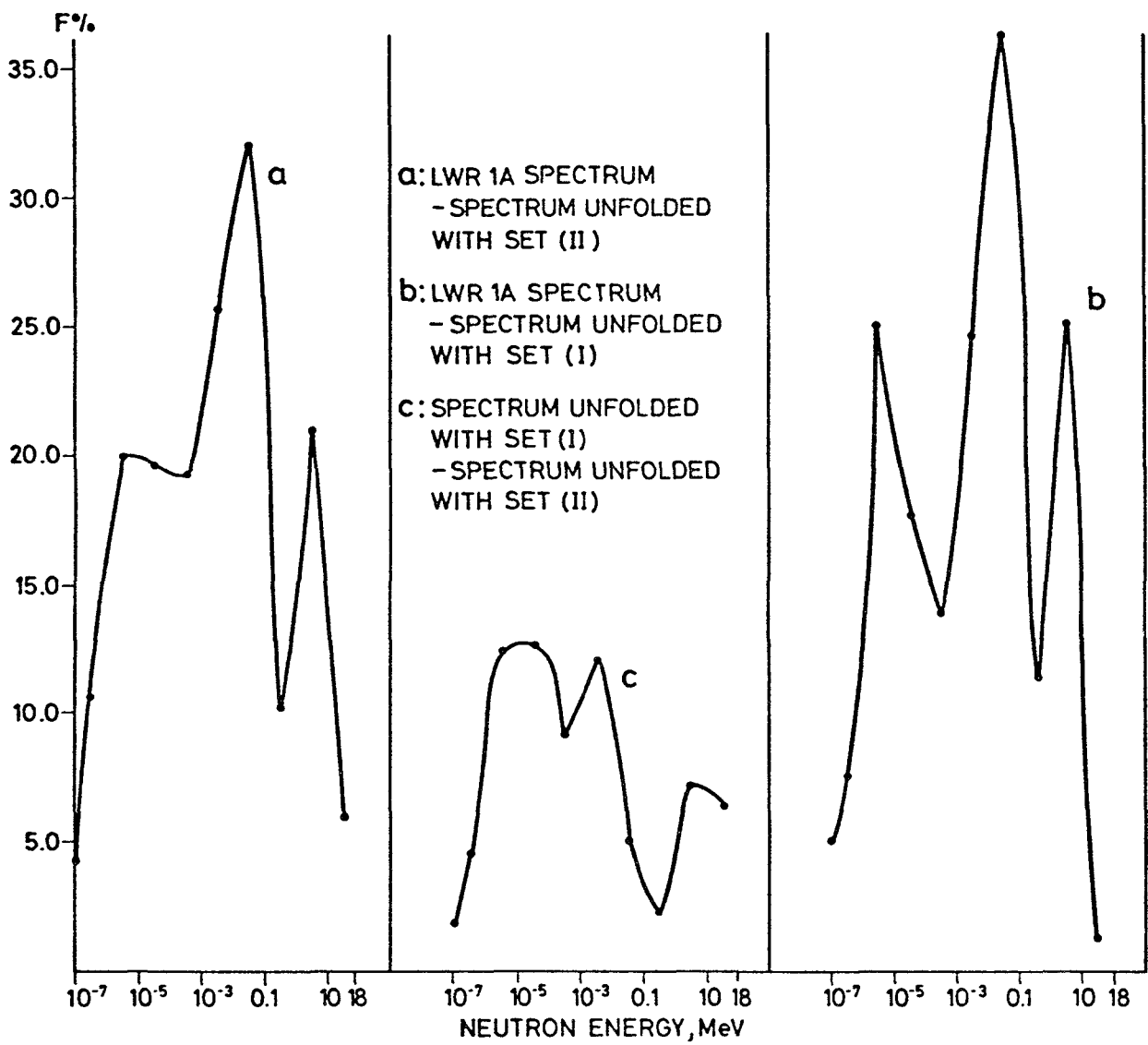


FIG.2. DIFFERENCES IN SPECTRA (F factors)

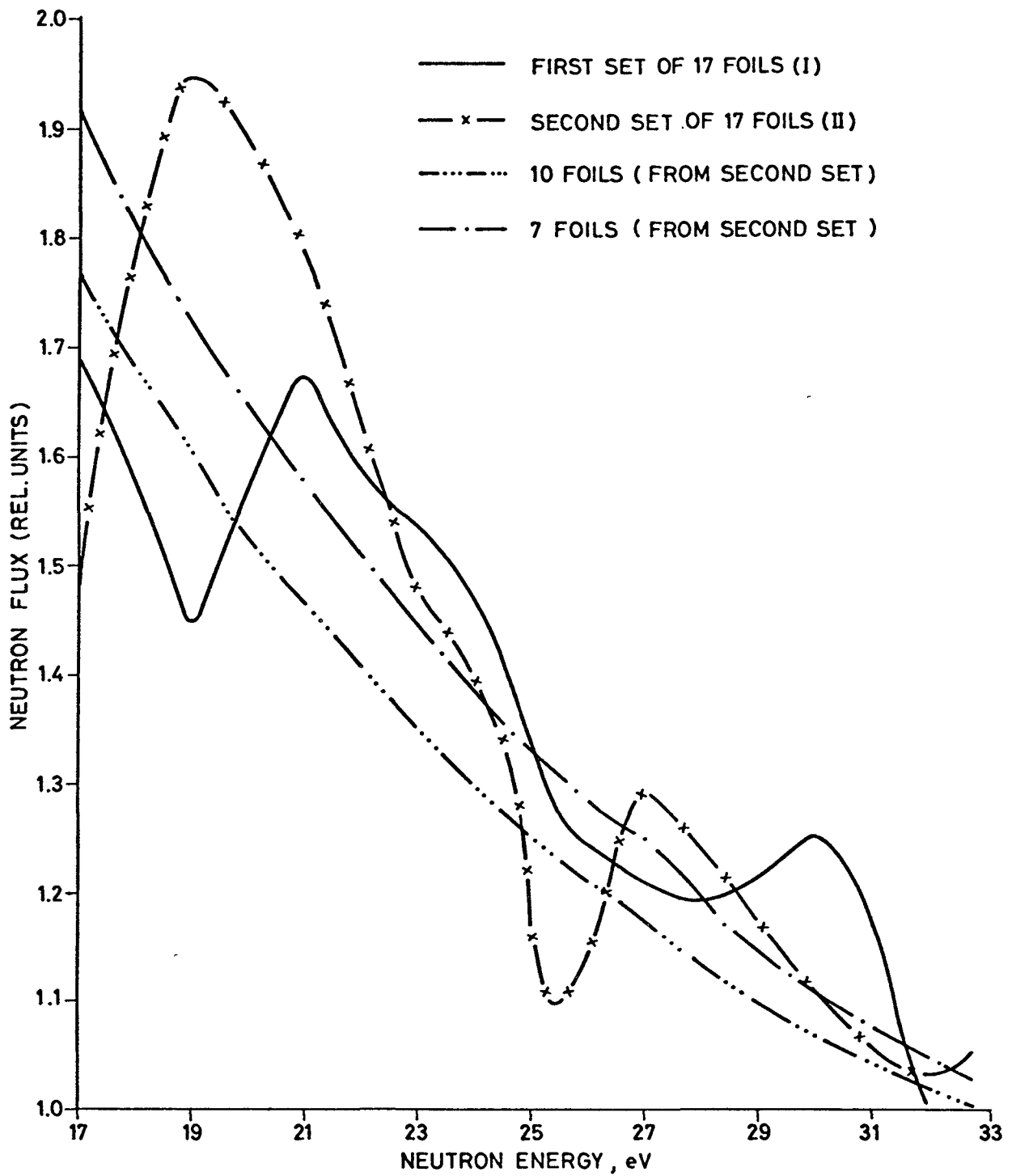


FIG. 3. PWR, UNFOLDED NEUTRON FLUXES

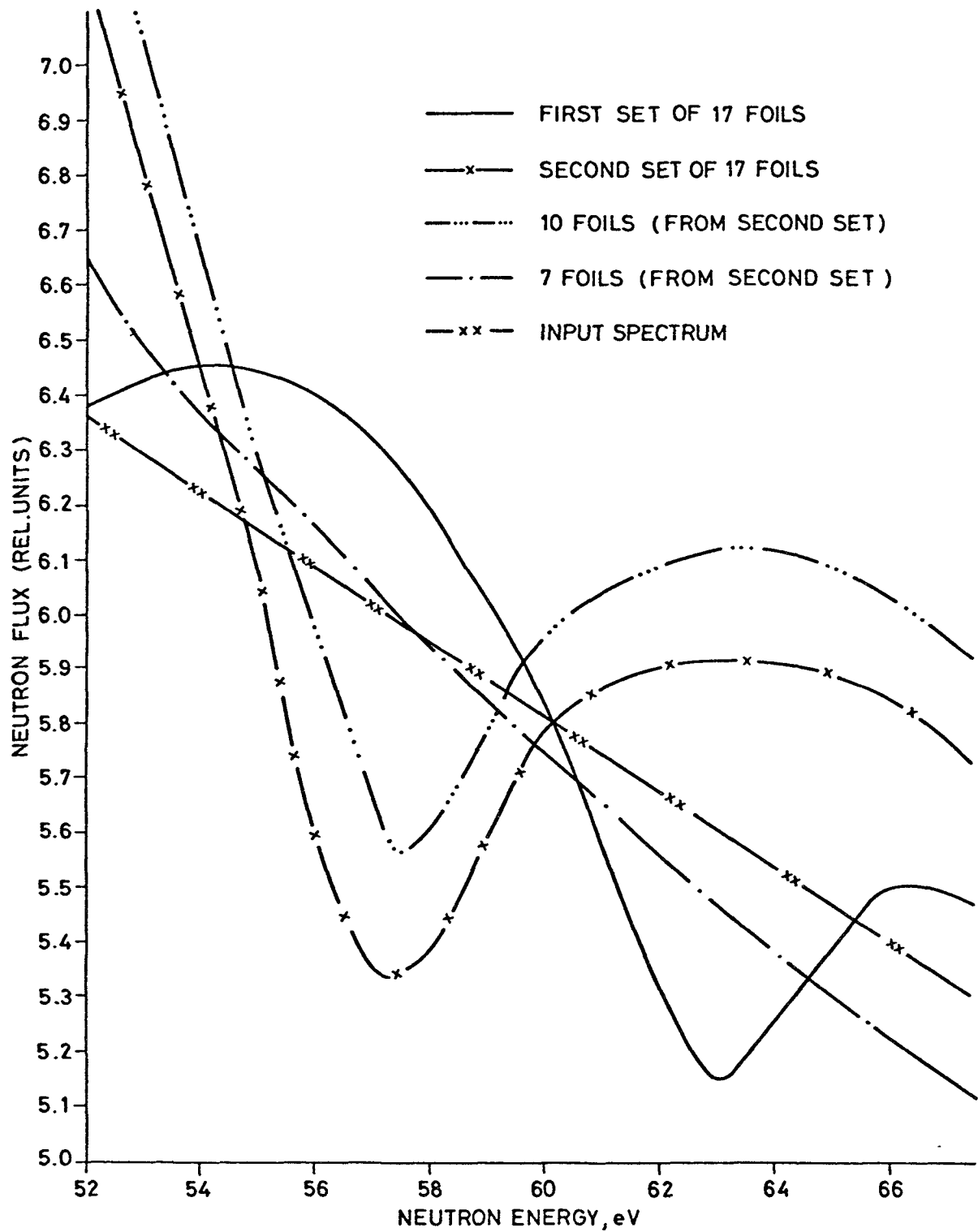


FIG. 4. PWR, UNFOLDED NEUTRON FLUXES



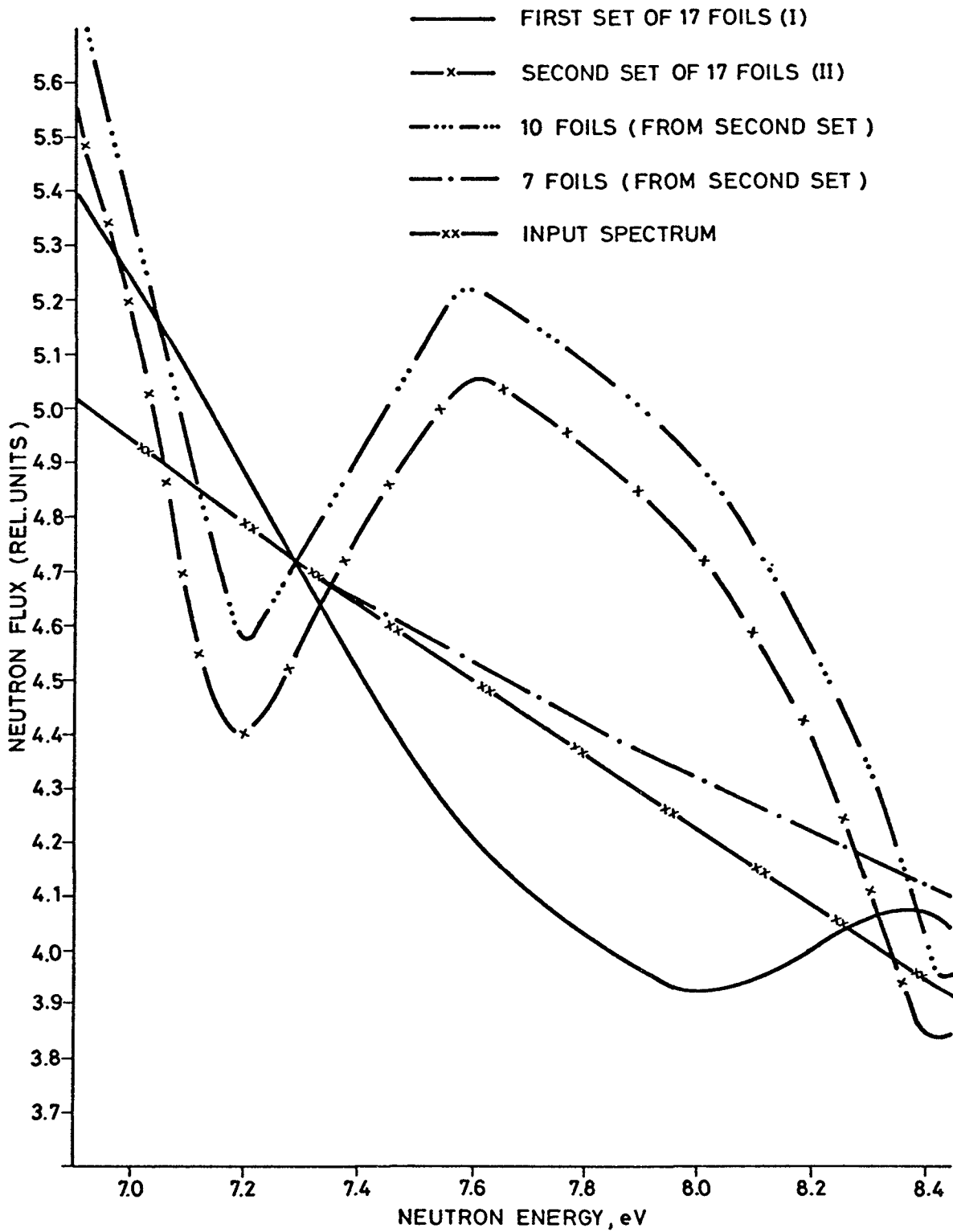


FIG. 5. PWR, UNFOLDED NEUTRON FLUXES

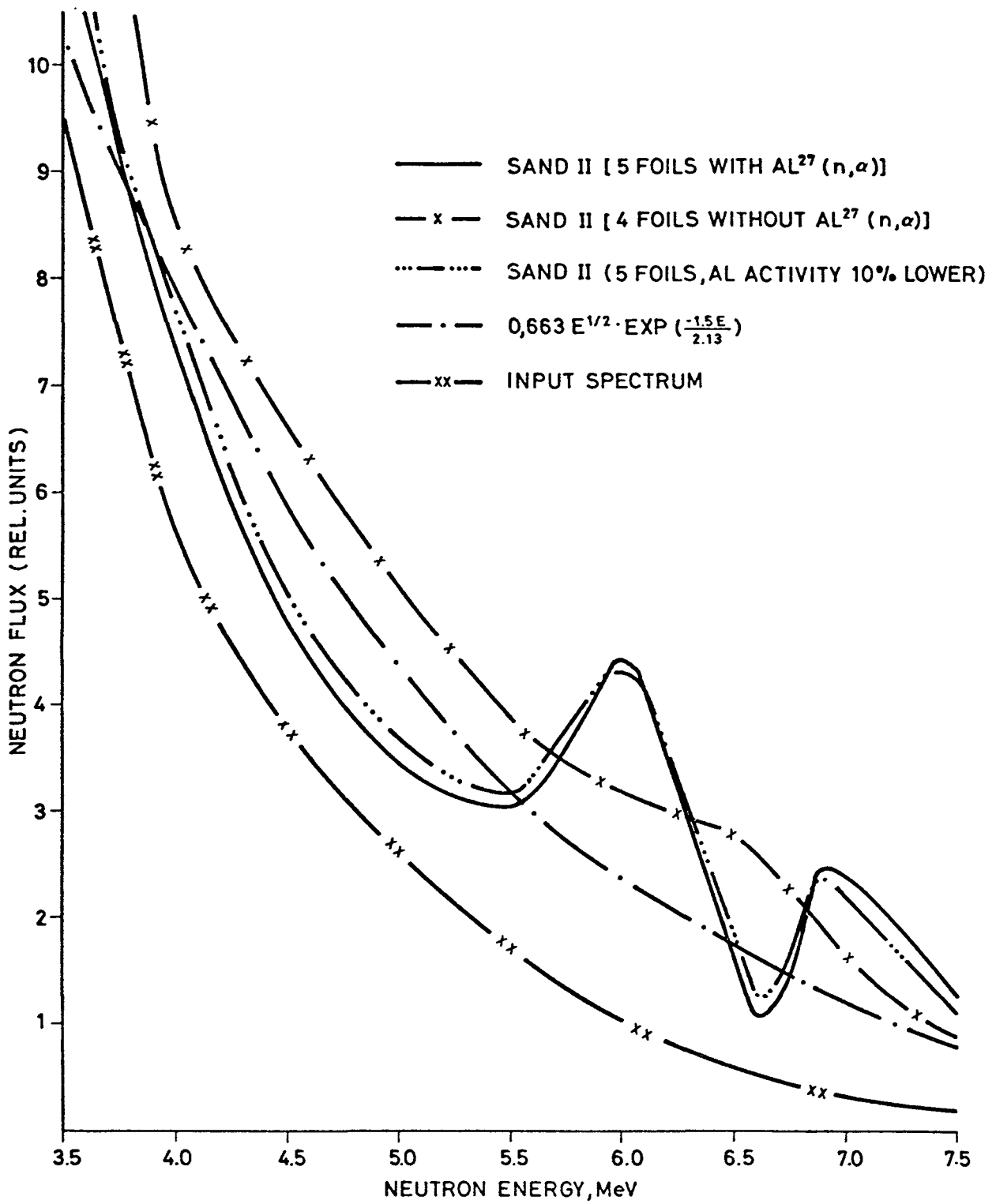


FIG.6. UNFOLDED NEUTRON FLUXES

PREPARATION OF CROSS SECTION FILES AND CORRECTIONS  
IN NEUTRON SPECTRUM UNFOLDING

M. Matzke

Physikalisch-Technische Bundesanstalt  
3300 Braunschweig, Germany

Abstract:

Using the reaction  $^{197}\text{Au}(n,\gamma)$  as a representative example, the influences of the energy group structure, material temperature and neutron selfshielding for foil activation methods are discussed. It is shown that the temperature effect has to be taken into account for the selfshielding correction but that it can be neglected together with the group structure effect in the evaluation of the dilute resonance integral, i.e. for an extremely thin foil. For the selfshielding correction, approximations are investigated using either the total or only the activation cross section for the shielding. A more detailed calculation including a first collision correction gives an impression of the range of uncertainties for the approximations.

## 1. Introduction

For the determination of neutron spectra by the multiple foil technique, one needs for each material the energy dependent cross section in an adequate group structure. Preparing these cross section files, various assumptions are generally made to reduce the elaboration (see e.g. [1]).

Three of these are:

- The group structure used has no influence on the results of unfolding;
- The Doppler broadening effect of resonances can be neglected;
- For the selfshielding correction, either the total or only the activation cross section may be used and a more detailed investigation of scattering is not necessary.

The first two assumptions have been discussed earlier (e.g. [1,2]), and they are repeated here only for reasons of completeness. For the selfshielding, only investigations of the resonance integral and not of the spectral dependence are known to the author

(e.g. [3]). To get an impression of the order of magnitude of the uncertainties one is working with, in this paper a few calculations are presented using the reaction  $^{197}\text{Au}(n,\gamma)^{198}\text{Au}$  as a representative example.

## 2. Group structure

Using the original ENDF/B-IV library [5] for the reaction  $^{197}\text{Au}(n,\gamma)$  together with the RESEND program by O. Ozer [4] one gets approximately 12000 cross section points as a function of energy for a stated evaluation uncertainty of 0.3 %. This function is given in Fig. 1 (compare also with [6]). For the SAND-II group structure [7] this mesh of cross section points is condensed into 620 groups in the energy range from  $10^{-10}$  MeV to 18 MeV (Fig.2). Looking at the lower keV region in Fig. 1 and Fig. 2, one finds that in all cases one group contains more than one resonance. Therefore, if in the calculation of integral quantities ( e.g. in the resonance integral) this group structure is used and the integral is replaced by a sum, systematic errors may arise due to the rather broad group structure. The resulting uncertainties may be larger in the case of a fast reactor spectrum than in a  $1/E$  spectrum, as the SAND-II group structure is more adequate to the lower eV region than to the keV region. But comparing resonance integrals for fine and coarse group structure, one can get an impression of the magnitude of systematic uncertainties.

The resonance integral of gold which one gets by dividing the cross section value at each point of Fig. 1 by  $E$ , where  $E$  is the energy and integrating from 0.5 eV to 18 MeV is  $I_R = 1563.8$  barn. This value agrees with that quoted by Magurno and Mughabghab (1564.7 barn) [6] and verifies the correct evaluation of the programs used here. The cross section given in Fig. 2 in SAND-II structure was calculated from the original cross section points by the CSTAPE program which is part of the SAND-II program package [7]. Using the SLACTS program [7] contained in the same package for the evaluation of the resonance integral, one gets  $I_R = 1569.5$  barn in agreement with a value of 1569.0 barn which can be evaluated from the Detan library [1] with the SLACTS program. For measurements in  $1/E$  spectra one may therefore use the SAND-II group structure leading to negligible uncertainties of the dilute resonance integral.

## 2. Selfshielding

Irradiating a foil of thickness  $d$ , the inner part is shielded by the outer. This leads to a decrease of the activation probability. This effect is taken into account by introducing a selfshielding factor defined as the ratio of the activation probability for a foil of thickness  $d$  to that of zero thickness.

If one assumes, for the irradiation of a foil, that the neutron flux density is isotropic, that the foil can be considered as an infinite plane slab and that there are no multiple interactions of the neutrons, the selfshielding factor for a neutron energy  $E_i$  can be calculated according to the relation [1] :

$$G_i(d) = \frac{1 - 2 E_3(\Sigma_t(i)d)}{2 \Sigma_t(i)d} \quad (1)$$

where  $\Sigma_t(i)$  is the total (activation plus scattering) cross section density for the energy  $E_i$ .  $E_3$  is the third exponential integral defined as:

$$E_3(t) = \int_1^{\infty} dx \frac{e^{-tx}}{x^3}$$

In equation (1) it is assumed that all the neutrons which are scattered in a first reaction leave the foil without any further activation probability. If, on the other hand, one supposes that the scattering does not influence the activation process at all, i.e. that the scattered neutrons can be regarded in the same way as the unscattered, one has to replace the total cross section in equation (1) by the activation cross section  $\Sigma_{act}$ . The more realistic case however can be estimated by a formula including a first collision correction [2]:

$$G_i(d) = \frac{1 - 2 E_3(\Sigma_t(E_i)d)}{2 \Sigma_t(E_i)d} + \frac{\Sigma_s(E_i)}{2 \Sigma_t(E_i)} \chi(\Sigma_t(E_i)d) \quad (2)$$

where  $\Sigma_s(E_i)$  is the scattering cross section density for the

energy  $E_i$  and  $\chi$  is a function given as

$$\chi(t) = \int_0^1 dx E_2(tx) \{ 2 - E_2(t(1-x)) - E_2(tx) \}$$

with

$$E_2(y) = \int_1^{\infty} dx \frac{e^{-tx}}{x^2}$$

In equation (2) it is assumed that the scattering is isotropic in the laboratory system and that there is no energy loss due to scattering. Equations (1) and (2) can also be used for group cross sections with a sufficiently fine group structure.

Using the total and the elastic scattering cross sections of the ENDF/B-IV library (MAT = 6283) for gold, together with the above mentioned RESEND and CSTAPE programs, a calculation of the different shielding approximations can be made. In Fig. 3, the results for a gold foil of 20  $\mu\text{m}$  thickness in the lower keV energy range are shown. The lowest curve is calculated by eq. (1) with  $\Sigma_t$ , i.e. in the case that all neutrons scattered once leave the foil without any further reaction. The middle curve corresponds to the same equation with  $\Sigma_{act}$  used instead of  $\Sigma_t$ . Here, all scattering processes are neglected i.e. one assumes that the scattered neutrons have the same activation probability as the unscattered. The upper curve including the first collision approximation (eq. (2)) always lies close to the middle curve.

This means that scattering may be neglected not only in the thermal energy region where the scattering cross section is negligible compared to the activation cross section, but even in the case of resonance scattering where scattering and activation cross section are approximately of the same magnitude. The reason for this is explained in [2] : The average path length in the foil is decreased due to the total cross section, but this decrease is partly cancelled after the scattering process. From these results, one might therefore conclude that the use of the activation cross section together with eq. (1) seems to be a sufficient approximation. On the other hand, if one considers the influence of the energy loss in the scattering process, one might get the opposite result, finding the total cross section more convenient for some cases.

In an elastic scattering process which is isotropic in the laboratory system the average relative energy loss is appr.  $2/(A+2)$  where A is the atomic number.

For gold this leads to an average relative energy loss of 1 % independent of the neutron energy, i.e. a loss of 10 eV for 1 keV neutrons and a loss of 10 meV for 1 eV neutrons. For neutron energies above the resonance region, the cross sections are nearly constant in the interval the neutrons can reach after scattering. The energy loss can therefore be neglected. In the eV energy region, the amount of energy loss is small compared to the width of the resonances and the energy loss will show no considerable change in the activation probability either [3]. But if one considers neutrons in the keV-resonance region, the average energy loss is approximately 10 eV. As the width of the resonances in this range is considerably smaller, one can conclude that neutrons scattered at a resonance energy lose so much energy that the activation after the scattering is unlikely. The discussion given here is based on rough assumptions. Further investigations are necessary. Nevertheless, one again gets an impression of the systematic uncertainties connected with the different approximations.

Summarizing the results: For energies above the resonance region, the approximation of the selfshielding effect by eq. (1) and the use of the activation cross section should be sufficient. The same holds for the eV energy region where the energy loss is smaller than the width of the resonances. In the keV energy region however, a use of the same approximation can lead to errors due to the energy loss in the scattering process. The systematic uncertainties connected with the example regarded here are always below 3-4 %.

### 3. Temperature dependence

The neutron cross sections in the ENDF library are usually given for a target temperature of OK. For higher temperatures there may be a change in the cross section behavior, especially a broadening in the resonances. For a single Breit-Wigner resonance this broadening can be estimated by a simple formula generally known from literature (e.g. [2]). As the width and the height of

a resonance are changed by the broadening, and the area below a resonance is unchanged, one expects no influence of the temperature on integral values (resonance integral, group cross sections) but an influence on the selfshielding factor, especially in the eV energy region.

This effect was tested by a few computer runs for the representative example of gold used here.

Using a relatively high temperature of 1000 K, the dilute resonance integral is changed from 1563.8 barn to 1564.2 barn, therefore giving no considerable effect. The selfshielding factor on the other hand changes by a larger amount. Using formula (1) for the point cross sections of Fig. 1 and using the activation cross section for the shielding, one gets a selfshielding factor for the resonance integral of a 40 mg/cm<sup>2</sup> gold foil of

$$G_{\text{act}} (T=0\text{K}) = 0.393$$

The use of the total cross section in the same formula yields:

$$G_{\text{tot}} (T=0\text{K}) = 0.373$$

Finally, again using the total cross section for the shielding but now Doppler broadened, one gets

$$G_{\text{tot}} (T=1000\text{K}) = 0.393,$$

a value accidentally close to  $G_{\text{act}} (T=0)$ .

#### 4. Conclusion

- The use of SAND-II group structure results in no considerable changes in integral quantities.
- Doppler broadening of resonances and a more detailed investigation of the selfshielding effect is necessary if one aims at uncertainties below 3-4 %.



References:

- [1] W.L. Zijp: "Review of Activation methods for the Determination of Neutron Flux Density Spectra, " Reactor Centrum Nederland, Report: RCN-241 (1976)
- [2] K.H. Beckurts and K. Wirtz: "Neutron Physics", Springer Verlag, Berlin, Göttingen, Heidelberg, New York 1964.
- [3] S. Pearlstein and E.V. Weinstock: "Scattering and Self-Shielding Corrections ...", Nucl. Sci. Eng. 29, 28 (1967)
- [4] O. Ozer: "The Program RESEND", National Neutron Cross Section Center, Brookhaven National Laboratory, Report BNL-17134 (1972).
- [5] D. Garber: "ENDF-201, ENDF/B Summary Documentation" National Neutron Cross Section Center, Brookhaven National Laboratory, Report: BNL 17541 (1975)
- [6] B.A. Magurno: "ENDF/B-IV Dosimetry file".  
National Neutron Cross Section Center, Brookhaven National Laboratory, Report: BNL-NCS-50446 (1975).
- [7] W.N. McElroy, S. Berg, T. Crockett, R.G. Hawkins: "A Computer-automated iterative Method for Neutron Flux Spectra Determination by Foil Activation", Air Force Weapons Laboratory, Report AFWLR-TR 67-41 Vol. I and Vol. II (1967).

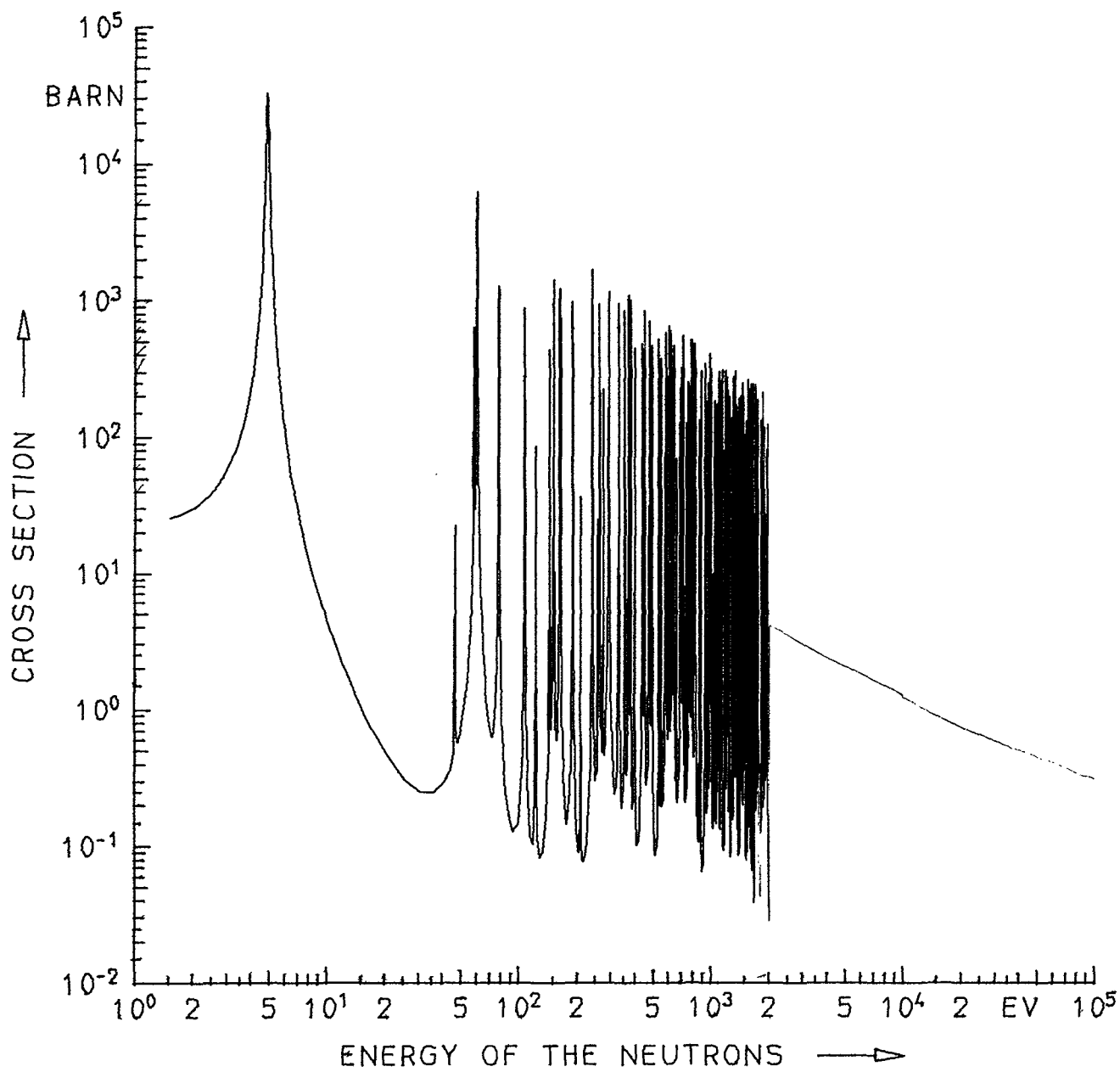


Fig. 1 CROSS SECTION OF AU197(N,G) MAT=1283  
 ERROR FROM RESEND: < 0.3%

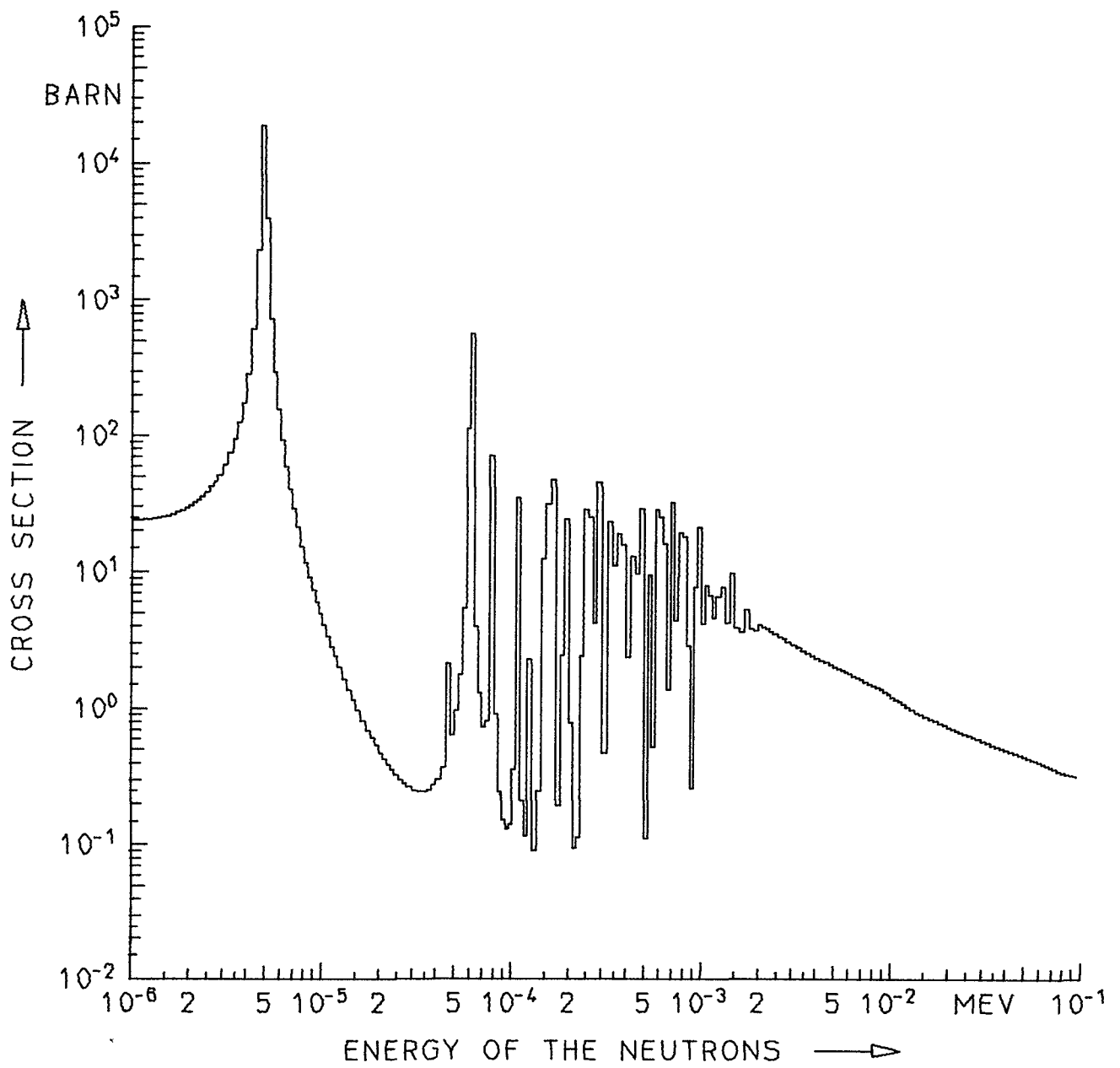


Fig. 2 CROSS SECTION OF AU197(N,G) MAT=1283  
SAND-II GROUP STRUCTURE

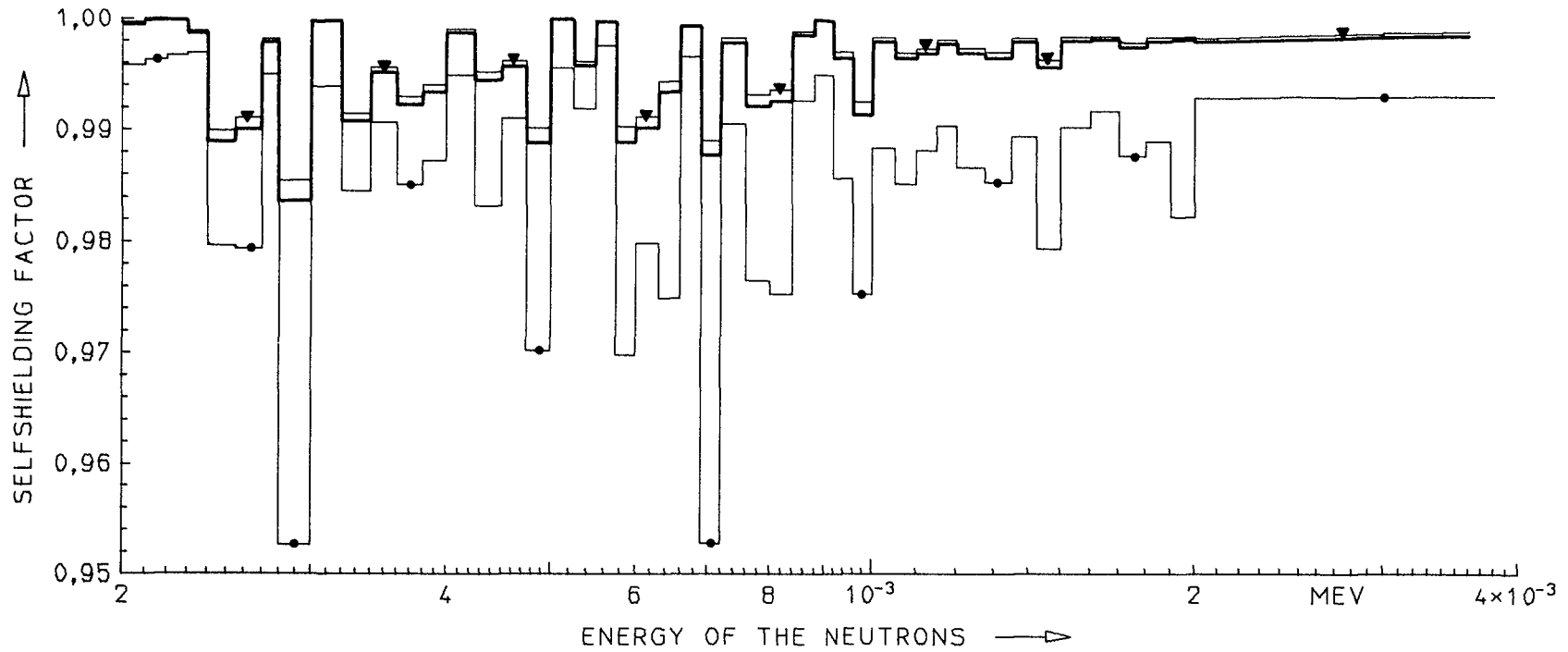


Fig. 3 SELFSHIELDING FACTOR OF A GOLD FOIL  
 $D=20.0E-4$  CM

●	AU197(N,G)AU198	,SELFSHIELDING,(ONLY SIGTOT USED),	D= 0.20000E-02 CM
▼	AU197(N,G)AU198	,SELFSHIELDING,(TOTAL AND SCATTERING),	D= 0.20000E-02 CM
—	AU197(N,G)AU198	,SELFSHIELDING,(ONLY SIGACT USED),	D= 0.20000E-02 CM

SUMMARY AND CONCLUSIONS OF IAEA TECHNICAL COMMITTEE MEETING ON  
CURRENT STATUS OF NEUTRON SPECTRUM UNFOLDING

The importance of accurate and well-documented unfolding procedures is widely recognized. The procedures affect safety analysis, as well as economic aspects of reactors. The techniques needed to accomplish unfolding have undergone gradual improvement with time, and the present conference served to disseminate the latest information and allow discussion and evaluation of the latest techniques. The conference was highly successful in accomplishing such dissemination, discussion, and evaluation, as a number of quite informative and interesting papers were presented. An account of the papers and of some of the discussions follows.

The opening paper, by Frank Kam, gave an account of the current status of the older LWR pressure vessels and their RPV embrittlement surveillance. The pertinent parts of the applicable nuclear regulatory regulations were discussed. The geometry of the locations of surveillance specimens and associated dosimetry sets was detailed, and an insight was given of the dosimetry and damage function problems associated with prediction of safe operating lifetimes of pressure vessels of currently operating and planned LWR reactors. This paper laid out one of the major areas of applied problems of spectrum and damage function unfolding.

Several papers reviewed the details of the uses, comparative advantages, reliability, consistency, and possible difficulties associated with the available unfolding codes.

Clarence Oster reviewed unfolding methods currently in use, gave some details of the algorithms, and suggested methods for testing the codes for their ability to give non-conflicting and reliable results. Use of mathematical benchmark problems was recommended.

W. L. Zijp presented actual plots of outputs of SAND-II, CRYSTAL BALL, and RFSP-JUL. The codes were compared on the basis of smoothness of output, tendency to generate spectral modification in regions of scanty data, and the value of the energy dependent improvement ratio. This latter item is the ratio of normal deviation of input to that of the output in the case where the codes were used in a type of Monte Carlo application.

Operating speeds of modified SAND-II-like codes were reviewed in a paper by L. J. M. Kuijpers, presented by Dr. Zijp. The modifications, tested on High Energy Neutron Spectrum unfolding problems, did not materially decrease the operating time as compared to the standard version of SAND-II. Dr. Zijp also presented a paper wherein he regrouped the terms in the modifying

factors in SAND-II. These factors are the quantities which are used to change the flux amplitudes in the individual energy groups. By regrouping the terms, Dr. Zijp isolated the contribution to the modifying factors on a foil-by-foil basis, so that for a given foil it was possible to observe the spectral nature and magnitude of the contribution of a particular foil to the total modifying factor which was applied in going from one iteration to the next.

Errors in damage function analysis and the use of window functions in Multiple Foil Dosimetry were discussed in papers presented by W. R. Burrus and F. W. Stallmann. The two papers covered some common ground from two different viewpoints. Dr. Burrus discussed errors in general and covered some of the commonalities and differences of codes similar to SAND-II or CRYSTAL BALL when compared to the recently developed STAY'SL code of Francis Perey. An important point that emerged was that the uncertainty of important integral quantities, such as degradation of a particular property, is likely to be much less than the errors in the spectral shape or in the damage function. It was pointed out that in the actual final calculation of a degraded property, the important item is usually a ratio where the damage function appears both in the numerator and denominator, although not always in a cleanly algebraically factorable form. A similar situation applied in the case of the spectral shape and its contribution to the relevant integral quantities. The general problem of unfolding was rather precisely stated and comments were made on the approaches and philosophies of STAY'SL and other codes.

Dr. Stallmann showed in some detail how the advantages mentioned by Dr. Burrus could be realized by window functions. By the use of linear combinations of foil activations, Dr. Stallmann showed that it was possible to correlate foil activations directly to property degradations or other internal properties whose magnitude was desired. This technique can in some cases bypass some of the unfolding problems and reduce the resulting errors.

In a somewhat related paper, J. Dorlet showed how linear programming techniques could be used to find two separate linear combinations of foil activation cross sections to place upper and lower bounds on damage functions.

Several papers discussed particular application techniques in foil dosimetry. A paper by Dr. Zijp presented a preliminary investigation of various models for calculation of shielding corrections. The results indicated that for some cases involving moderately thick ( $\approx 1$  mm or greater) B or Cd covers, care should be taken to do the self-shielding calculations under

realistic assumptions of angular distribution of the flux. Assumptions of parallel beam flux lead to small but significant errors. Use of Cd or Boron covers has not been of major importance to date in fast reactor dosimetry in the United States. Dr. Matzke commented that the self-shielding factor for gold changed by ~ 5% when the Doppler broadening at 1000° was taken into account.

A paper by H. J. Nolthenius presented some new and updated cross section library data in the SAND-II format for 49 separate detector isotopes and three possible cover materials in 620 energy groups.

W. L. Zijp presented a quadruple foil technique for increasing the sensitivity of foil dosimetry. The technique involved the comparison of a shielded foil in a three-part sandwich with the activation of a similar, but unsandwiched, foil.

E. D. McGarry described several benchmark neutron spectrum facilities at the National Bureau of Standards. These included  $^{252}\text{Cf}$  (fission spectrum) standard field facilities and the ISNF facility which produces a spectrum similar to that of a fast breeder reactor.

The required features of a benchmark facility were stated, and the advantages and uses of such facilities were presented. It was pointed out that a standard or reference benchmark neutron field can be used to provide certified fluence irradiations to test calculated total fluence and the unfolded spectrum. An alternate and sometimes preferred method of evaluation is to compare those integral quantities and their ratios that can be accurately measured relative to benchmark fields against comparable quantities derivable from unfolded spectra. Benchmark fields can also be used effectively to calibrate input data and determine corrections for foil self-shielding or stacked-foil and container flux perturbations.

Dr. Roussin presented a review of the CSEWG-IWGRRM task force report on reactor dosimetry and distributed the minutes thereof. He then reported on the anticipated release of the ENDF/B version V dosimetry file which has the following schedule: (A) Evaluations to Brookhaven by late November; (B) Phase I review completed by mid-January; (C) Version V files released in early April, 1978. All the above dates are approximate.

Francis Perey presented a paper giving some of the philosophy and details of his unfolding code STAY'SL. This work generated considerable interest and was the subject of exhaustive discussions. The paper was entitled "Least Squares Method for Dosimetry Unfolding." A least squares method was presented where the uncertainties in the input data, the activations,

and the input trial spectrum are in the form of covariance matrices describing the joint density function of these three types of data. The solution, the spectrum and its covariance matrix, is only a function of the input data and reflects all of the information in the input data including the uncertainties. This code is noticeably different from other unfolding codes now commonly in use. STAY'SL puts the supplied input spectrum on the same footing as the foil activation data. Both are regarded as necessary input data, along with the foil activation cross-section spectral information. These data must all be accompanied by uncertainty information in the form of covariance matrices. The program then calculates the values of the output spectrum which results in a minimum value of chi-squared for the total data set.

The interest generated by the paper by Perey resulted in a panel discussion where the members of the panel were F. Perey, C. Oster, and F. W. Stallmann. A reaction panel was appointed to comment on the panel discussion. This reaction panel consisted of W. R. Burrus, V. R. R. Uppuluri, and N. B. Gove. However, the discussion soon included all members present at the conference.

W. R. Burrus opened the discussion by reacting as follows.

"In hearing the various proponents of various unfolding methods defend their respective methods, it is very clear that the discussion is greatly obscured by mixing several distinct problems together in ways that cannot be easily understood. For example, various problems usually jointly addressed include: dosimetric and radiation damage considerations, solution of undetermined linear equations, heuristic techniques to describe uncertainties in experimental functions (e.g., cross sections) where exact knowledge of covariance matrix is computationally and experimentally unfeasible at present (and at any time in the foreseeable future), and special problems of benchmark reconciliation. There is little hope of mutual agreement among different groups until the key problems are isolated."

Dr. Burrus pointed out that if it was agreed that Dr. Perey had stated the problem in a manner satisfactory to all participants (if we agree that it is a least squares problem with the trial spectrum, activities, cross sections, and all covariance matrices regarded as input data), then the Perey solution was the correct solution. As a consequence, then all other solutions which deviated noticeably from that solution would necessarily have to be regarded as incorrect.

However, he stated that he felt it would be unreasonable to label the output of another code as being "bad" if the alternate code produced only a



slightly higher value of chi-square and if all the output quantities differed from those of the Perey code by amounts that were less than the statistical uncertainties calculated by STAY'SL.

Several participants expressed concern about the lack of availability of the required covariance matrices for the foil activation cross sections. W. Zijp questioned whether there could be covariance matrices for all cross sections in ENDF/B-V and whether such a requirement would hold up the release of this cross-section file. C. R. Weisbin, chairman of the Cross Section Evaluation Working Group (CSEWG) Data Testing Subcommittee stated that covariance matrices would be generated for each file. Evaluators have been asked to supply the necessary uncertainties; however, data are coming in very slowly. F. Perey, chairman of the Covariance Data Subcommittee, stated that he has the responsibility to collect the uncertainty data and generate the covariance matrices. He stated that he would supply his own uncertainties to generate the covariance matrices if the requested input is too slow coming to him.

Several participants noted that the Perey program cannot attain widespread application unless all the users are capable of generating the covariance matrices associated with the trial spectrum. C. R. Weisbin and others suggested some references that dealt with such a problem, including papers by Peelle, Perey, Weisbin, and Hale. Dr. Perey stated that the codes presently in use already have some implied covariance matrix off-diagonal elements of the input spectrum buried in the algorithm. This situation arises as the result of the smoothing feature which smooths the output spectrum. He felt that all users could gain the required expertise in generating satisfactory covariance matrices for the input spectrum with a minimum of practice and offered some comments on typical values of off diagonal elements and the significance thereof.

Dr. Lippincott stated that he was pleased to have Dr. Perey's code available and intended to test it, but would be very interested to see how sensitive the output was to changes in the values of the elements in the input covariance matrices. He wanted to judge this sensitivity in terms of the uncertainty which would exist in the values of the elements of the input covariance matrices.

At the conclusion of the discussion, there was widespread agreement on several points. It was good to have a clear mathematical statement of the problem at hand. If one agreed that least squares techniques applied and that the input spectrum and the required covariance matrices for  $\phi$ ,  $\sigma$ , and the activations could all be regarded as input data, then the Perey approach

or something equivalent was the correct way to approach the problem. The Perey code is a welcome addition to our set of tools and should be given some sort of mathematical benchmark testing. It was also agreed that the codes now in use could legitimately be given continued use, especially in areas where they have received extensive testing.

The conference has been extremely useful to the participants, especially as a forum for disseminating information about STAY'SL and discussing the implications in its use. The conference also served as a useful vehicle for the dissemination of information about general problems in unfolding theory, status and use of benchmark fields and advances in techniques of constructing and using dosimetry packages. The enthusiasm and attentiveness of the attendees was well outside the 3-sigma limit on the high side, a fact that was obvious from the constant alert attendance and participation of all members of the conference.

## LIST OF PARTICIPANTS

W. R. Burrus  
Tennecomp Systems  
Oak Ridge, Tennessee 37830, USA

V. Chernyshev  
IAEA  
Vienna, Austria

J. D. Dorlet  
CEA, DE, RDE  
Montrouge Cedex, France

N. B. Gove  
Oak Ridge National Laboratory  
Oak Ridge, Tennessee 37830, USA

L. Greenwood  
Argonne National Laboratory  
Argonne, Illinois 60439, USA

G. Guthrie  
Westinghouse Hanford Co.  
Richland, Washington 99352, USA

F. B. K. Kam  
Oak Ridge National Laboratory  
Oak Ridge, Tennessee 37830, USA

E. P. Lippincott  
Westinghouse Hanford Co.  
Richland, Washington 99352, USA

M. Matzke  
Physikal. Techn. Bundesanstalt  
Braunschweig, FR Germany

E. D. McGarry  
National Bureau of Standards  
Washington, D.C. 20234, USA

H. J. Nolthenius  
ECN  
Petten, The Netherlands

C. A. Oster  
Battelle Pacific Northwest Laboratory  
Richland, Washington 99352, USA

F. G. Perey  
Oak Ridge National Laboratory  
Oak Ridge, Tennessee 37830, USA

F. J. Rahn  
Electric Power Research Institute  
Palo Alto, California 94303, USA

F. W. Stallmann  
University of Tennessee  
Knoxville, Tennessee 37916, USA

V. R. R. Uppuluri  
Oak Ridge National Laboratory  
Oak Ridge, Tennessee 37830, USA

C. R. Weisbin  
Oak Ridge National Laboratory  
Oak Ridge, Tennessee 37830, USA

W. L. Zijp  
ECN  
Petten, The Netherlands

B. F. Maskewitz  
B. L. McGill  
R. W. Roussin  
D. K. Trubey  
RSIC, Oak Ridge National Laboratory  
Oak Ridge, Tennessee 37830, USA

### Part-time Observers:

J. A. Cox  
F. C. Maienschein  
Oak Ridge National Laboratory

### Local Secretariat:

C. M. Anthony  
M. W. Landay  
RSIC, Oak Ridge National Laboratory